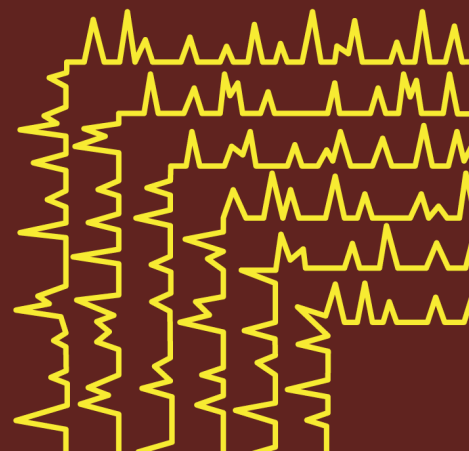
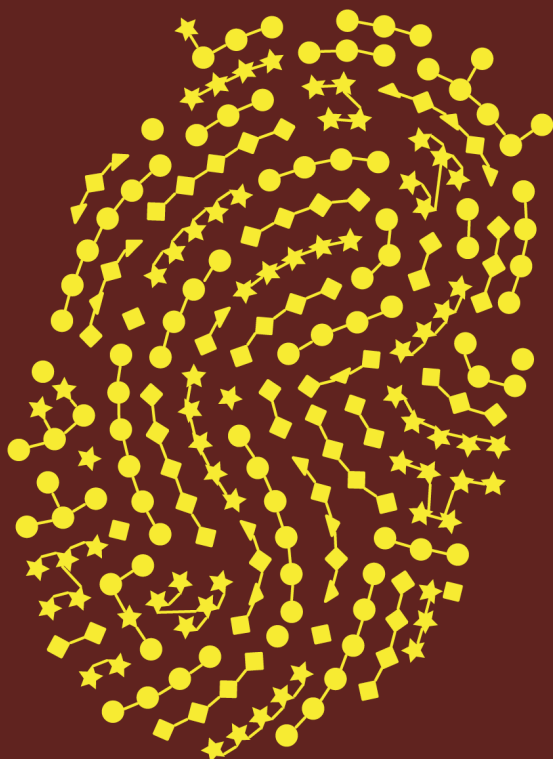


Non-enzymatic approaches to depolymerize polysaccharides into oligosaccharides for polysaccharides fingerprinting



Carolina O. Pandeirada

Propositions

1. The power of chemical approaches to obtain polysaccharide structure-informative oligosaccharides is underestimated.
(this thesis)
2. Accurate structural characterization of polysaccharides is only reached by combining old established chemical methods with novel analytical methods.
(this thesis)
3. Dealing with the temporary frustration of not making progress is an integral part of the path towards growing into a critical, independent, and knowledgeable scientist.
(based on Tim Ferris, Tools of Titans)
4. Online meetings are ineffective to fairly judge people's characters.
5. Science unrelated to aerospace and/or to clinical research is undervalued.
6. A healthy diet routine depends on the perceived workload.

Propositions belonging to the thesis, entitled
"Non-enzymatic approaches to depolymerize polysaccharides into
oligosaccharides for polysaccharides fingerprinting"

Carolina O. Pandeirada
Wageningen, 8 June 2022

**Non-enzymatic approaches to depolymerize
polysaccharides into oligosaccharides for
polysaccharides fingerprinting**

Carolina O. Pandeirada

Thesis committee

Promotor

Prof. Dr H.A. Schols
Personal chair at the Laboratory of Food Chemistry
Wageningen University & Research

Co-promotors

Prof. Dr H.-G. Janssen
Special professor Recognition Based Analytical Chemistry
Wageningen University & Research

Dr Y. Westphal
Global Technical Program Leader
Unilever Foods Innovation Centre, Wageningen

Other members

Prof. Dr M.A.J.S. van Boekel, Wageningen University & Research
Prof. Dr L. Nyström, ETH Zurich, Switzerland
Prof. Dr M. Wuhler, University of Leiden
Dr A. Gargano, University of Amsterdam

This research was conducted under the auspices of the Graduate School VLAG (Advanced studies in Food Technology, Agrobiotechnology, Nutrition and Health Sciences).

Non-enzymatic approaches to depolymerize polysaccharides into oligosaccharides for polysaccharides fingerprinting

Carolina O. Pandeirada

Thesis

submitted in fulfilment of the requirements for the degree of doctor
at Wageningen University

by the authority of the Rector Magnificus,

Prof. Dr A.P.J. Mol,

in the presence of the

Thesis Committee appointed by the Academic Board

to be defended in public

on Wednesday 8 June 2022

at 4 p.m. in the Omnia Auditorium

Carolina O. Pandeirada

Non-enzymatic approaches to depolymerize polysaccharides into oligosaccharides for polysaccharides fingerprinting

202 pages.

PhD thesis, Wageningen University, Wageningen, The Netherlands (2022)

With references, with summary in English and in Portuguese

ISBN 978-94-6447-166-3

DOI <https://doi.org/10.18174/567613>

To my family and friends

“Põe quanto és no mínimo que fazes.”

Ricardo Reis, in Odes

Abstract

Plant polysaccharides are the most abundant biomacromolecules found in nature and frequently used in foods. Despite this, detailed characterization of their structures remains challenging. A method often used to characterize and recognize polysaccharides in full detail relies on the enzymatic digestion of polysaccharides to structure-informative oligosaccharides (enzymatic fingerprinting), prior to full analysis of these oligomers with LC and MS approaches. However, the enzyme-polysaccharide specificity hampers the use of this method as universal polysaccharide depolymerization approach for polysaccharides fingerprinting. In this thesis, various chemical-induced polysaccharide depolymerization approaches were investigated to reach a generic fingerprinting of polysaccharides.

A polysaccharide depolymerization method based on TEMPO-oxidation and partial acid-hydrolysis was investigated for the fingerprinting of arabinoxylans (AXs), the main cereal hemicellulose components. TEMPO:NaClO₂:NaOCl oxidation of AXs selectively oxidized the arabinose side chains of AXs into arabinuronic acid, resulting in an arabinuronoxylan with a xylan structure having a substitution pattern mostly resembling the parental AX. Subsequently, three structurally different AXs were TEMPO-oxidized, partially acid-hydrolysed and reduced, releasing arabinurono-xylo-oligomer alditols (AUXOS-A). Ultra-high performance liquid chromatography-mass spectrometry (UHPLC-MS) with a stationary phase of porous-graphitized carbon (PGC) allowed the separation and identification of various isomeric AUXOS-A. AX-specific UHPLC-PGC-MS profiles of AUXOS-A were obtained, allowing to distinguish different AXs. Additionally, tandem MS analysis of individual AUXOS-A enabled tentative and conclusive characterization of their structures, which allowed us to substantiate the main structural differences among the AXs investigated.

Periodate oxidation of plant polysaccharides with and without subsequent autoclave (AC) thermal treatment was a second approach investigated to reach a generic fingerprinting of plant polysaccharides. After periodate oxidation and AC treatment, all investigated plant polysaccharides, except xyloglucan, and mixes thereof released oligosaccharides. These oligosaccharides had highly complex structures, comprising intact sugar units, and oxidized sugars in the form of dialdehydes, hemialdals, and remnants of oxidized sugars. This high structural complexity resulted in clusters of oxidized oligosaccharides that were polysaccharide structure-dependent, giving unique ESI-Ion trap-MS and MALDI-TOF MS oligosaccharide profiles per polysaccharide. These findings allowed us to distinguish individual plant polysaccharides, within and between polysaccharide classes, and identify the polysaccharide classes present in a polysaccharide mix by their oligosaccharides fingerprint.

Thus, partial acid-hydrolysis of TEMPO-oxidized AXs, and thermal treatment of periodate-oxidized plant polysaccharides have potential to more generically recognize AXs and plant polysaccharides, respectively, by oligosaccharides fingerprinting. This can be of high interest for the food industry to study the carbohydrate fraction of a food product.

Table of contents

Chapter 1	General Introduction	1
Chapter 2	TEMPO/NaClO ₂ /NaOCl oxidation of arabinoxylans	35
Chapter 3	Partial acid-hydrolysis of TEMPO-oxidized arabinoxylans generates arabinoxylan-structure resembling oligosaccharides	59
Chapter 4	Periodate oxidation of plant polysaccharides provides polysaccharide-specific oligosaccharides	95
Chapter 5	Recognition of plant polysaccharides through MALDI-TOF MS fingerprinting after periodate oxidation and thermal depolymerization	129
Chapter 6	General Discussion	163
Summary		187
Acknowledgements		195
About the author		199

Chapter 1

General Introduction



Research project outline

Polysaccharides are macromolecules of interest for the food industry due to their ability to modulate the physical properties of food products or to provide health benefits. The functionalities of polysaccharides are highly dependent on their chemical structure, which can be very diverse and complex. The polysaccharide chemical structures can vary in sugar and linkage composition, anomeric configuration, size, and they can also comprise non-sugar substituents. In addition, substituents can vary over the polymer backbone in level, type, and distribution. Detailed characterization of polysaccharide chemical structures is often achieved by enzymatic digestion of single polysaccharides to structure-informative (diagnostic) oligosaccharides followed by (chromatography –) mass spectrometry (MS) analysis of the formed oligosaccharides. However, such an enzymatic digestion is highly polysaccharide-specific, and developed approaches can hardly be used as a generic polysaccharide characterization method.

The present PhD research focused on investigating chemical polysaccharide depolymerization approaches that can form diagnostic oligosaccharides that allow fingerprinting in a generic manner. This will contribute to a faster recognition of the type of polysaccharides present for example in food products.

1. Polysaccharides used in the food sector

Polysaccharides from plant sources are the most abundant biomacromolecules found in nature and are frequently used as ingredients in foods [1, 2]. Plant polysaccharides are very diverse and have highly complex structures, making their characterization challenging. Non-plant polysaccharides have also emerged in food industry. Among the non-plant polysaccharides, the most commonly ones used in foods are carrageenans, alginate, chitin, chitosan, and xanthan [3-5]. In this PhD thesis, mainly plant polysaccharides were studied, since these are mostly used in food industry.

1.1. Plant polysaccharides

The main plant polysaccharides are starch (Fig. 1), a storage polysaccharide, cellulose, hemicelluloses, and pectins, which are present in the cell wall (Fig. 2) [1, 6]. The structural features of these polysaccharide classes are described in the following paragraphs.

Starch

The main sources of commercial starch are (waxy) maize, potatoes, wheat, and cassava [6, 7]. Starch is composed of two glucose (Glc)-based polymers, amylose, and amylopectin. Amylose is a linear polysaccharide composed of α -(1→4)-Glc units, whereas in amylopectin the α -(1→4)-Glc backbone is branched at the position *O*-6 of Glc with α -(1→4)-Glc units (Fig. 1). Amylose and amylopectin content and characteristics depend on the source of starch [7]. Overall, amylose is smaller than amylopectin. Amylose has a molecular weight (*M_w*) as high as 97 kDa, whereas amylopectin has a *M_w* ranging from 50 – 500 x 10³ kDa [8]. The main fraction of starch in cereals, tuber and roots is amylopectin (> 70 %), and the amylopectin content can reach 100 % for waxy starches [7, 9].

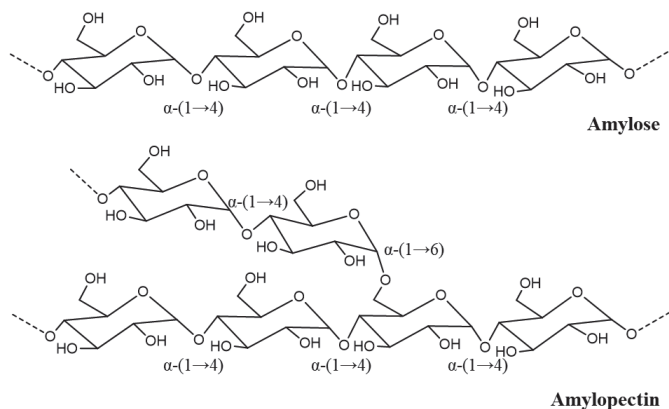


Figure 1. Amylose and amylopectin structures.

Cellulose

Cellulose, the most abundant biopolymer on earth, can be found not only in plants, wood, and algae, but also in bacteria or fungi [10]. Cellulose is a linear polysaccharide composed of β -(1 \rightarrow 4)-linked Glc units (Fig. 2). Cellulose chains in higher plants have a DP ranging from 2000-6000, and its chains can aggregate via hydrogen bonds and van der Waals forces to form microfibrils [10, 11]. The structure of cellulose comprises both crystalline (high order) and amorphous (low order) regions. The native cellulose crystal structure (cellulose I) has cellulose chains parallelly oriented [10]. Among the other crystal structures (cellulose II, III, and IV), cellulose II has the most (thermodynamically) stable structure with antiparallel cellulose chains [12]. Cellulose II can be formed from cellulose I by mercerization or regeneration, and it is the most relevant structure for technical uses.

Hemicelluloses

Hemicelluloses are a heterogenous class of polysaccharides that can be linear or branched pentose- or hexose-based polymers, or a mixture of both type of sugars. Hemicelluloses can also comprise uronic acids and non-sugar substituents. Depending on the plant species and tissue, hemicellulose components may differ in content and structure. Hemicelluloses are normally divided into four groups, xylans, mannans, xyloglucans, and mixed-linked glucans [13, 14]. A summary of the hemicellulose chemical structures is shown in Fig. 2.

◆ *Xylans*

Xylans are a diverse group of polysaccharides that can be grouped into various xylan classes, including homoxylans, arabinoxylans (AXs), glucuronoxylans (GXs), glucuronoarabinoxylans (GAXs) (Fig. 2), and other heteroxylans [13]. Different plant species have different xylan components. For example, AXs are mainly found in cereals, such as wheat, rye, oat, and maize [15, 16], whereas GXs are mainly present in hardwoods, like beech and birch [13]. All xylans consist of a linear backbone of β -(1 \rightarrow 4)-xylose (Xyl) residues, which can be substituted with single α -L-arabinofuranosyl (Araf) residues at the *O*-3 and/or *O*-2 positions (AX), with (4-*O*-methyl)-glucuronic acid (GlcA) residues at



the *O*-2 position of Xyl (GX), or simultaneously substituted with Ara and (4-*O*-Me-)GlcA units (GAX) [13, 15, 17]. Xylans can also be acetylated at *O*-2 and/or *O*-3 positions of the Xyl unit. Additionally, presence of hydroxycinnamic acids, such as ferulic and *p*-coumaric acids, has also been reported for AXs via ester-linkage at C-5 position of the Ara side chains [18-20].

◆ *Mannans*

Mannans, which are often present as seed storage compounds, include galactomannans, glucomannans, and galactoglucomannans. Galactomannans are composed of a linear backbone of β -(1 \rightarrow 4)-mannose (Man) residues that is substituted with single α -Galactose (Gal) residues at the *O*-6 position (Fig. 2) [21, 22]. The main galactomannan sources used in food industry are locust bean- (or carob), guar-, and tara-gums [23]. Depending on the source, the Man:Gal ratio varies, with locust bean-, guar-, and tara-gums having a Man:Gal ratio of 4:1, 2:1, and 3:1, respectively [13, 24]. This Man:Gal ratio value is rather constant for each specie, as it is genetically controlled [22], although variation in distribution of Gal residues over the backbone exist [24].

Glucomannans and galactoglucomannans are mainly present in the secondary cell wall of softwood, but also in seeds and olives [25]. Unlike galactomannans, glucomannans are composed of a backbone of both β -(1 \rightarrow 4)-Man and β -(1 \rightarrow 4)-Glc residues, whereas galactoglucomannans additionally hold Gal side chains attached at *O*-6 position of the Man and/or Glc units (Fig. 2) [13, 17]. In addition, both glucomannans and galactoglucomannans can be partially acetylated [17, 26, 27].

◆ *Xyloglucans*

Xyloglucans (XGs) are the major hemicelluloses found in dicotyls and are also found in some seeds, such as tamarind [13, 14, 28]. XG contain a β -(1 \rightarrow 4)-glucan backbone that is heavily branched at *O*-6 position with α -Xyl units. Some of the Xyl units can be further substituted at *O*-2 position with β -Gal, α -Fuc-(1 \rightarrow 2)- β -Gal(1 \rightarrow or α -Araf. Additionally, Gal, Glc, and Ara units can be acetylated (Fig. 2) [29]. XGs have a rather regular and organized structure, which led to the introduction of a one-letter code for the differently-substituted β -D-Glc units [30]. Unbranched Glc unit is coded with **G**, a branched Glc unit with: **1**) α -Xyl unit is coded with **X**; **2**) β -Gal(1 \rightarrow 2)- α -Xyl-(1 \rightarrow is coded with **L**; **3**) α -Fuc-(1 \rightarrow 2)- β -Gal(1 \rightarrow 2)- α -Xyl-(1 \rightarrow is coded with **F**; and **4**) α -Araf-(1 \rightarrow 2)- α -Xyl-(1 \rightarrow is coded with **S**. XGs are made up of repeating substituted backbone units, which can be classified in two main types, XXXG-type and XXGG-type [13, 30], having three and two unsubstituted Glc residues in the repeat, respectively.

Pectins

As for hemicelluloses, pectins represent a heterogeneous group of polysaccharides that comprise homogalacturonan (HG), rhamnogalacturonan I (RG-I) and II (RG-II) as main structural elements. Other substituted galacturonans can also be found within the pectin class, such as xylogalacturonans (XGAs), which have a HG backbone partially substituted with β -Xylp(1 \rightarrow 3) units (Fig. 2) [36-38].

◆ *Homogalacturonan*

HG is composed of a α -(1 \rightarrow 4)-galacturonic acid (GalA) backbone that can be methyl-esterified at position C6 and/or acetylated at *O*-2 and/or *O*-3 positions of GalA (Fig. 2) [39]. The degree of methyl-esterification (DM) and acetylation (DA), and the distribution of esters along the HG backbone depends on the plant source, environment and on the developmental stage [40, 41]. Generally, commercially available HGs are extracted from citrus peel and apple pomace, which can have a DM ranging from 30-75 %, and normally display a low DA (<5 %) [42, 43].

◆ *Rhamnogalacturonan I*

RG-I has a backbone composed of the repeating disaccharide unit [\rightarrow 4)- α -D-GalA-(1 \rightarrow 2)- α -L-rhamnopyranose (Rhap)-(1 \rightarrow)_n (Fig. 2), where *n* can be as high as 100 [38, 44]. RG-I is often acetylated at the *O*-2 and/or *O*-3 positions of GalA, whereas methyl-esterification of RG-I is rare [39, 44, 45]. RG-I can comprise neutral sugar side chains composed of Gal (galactans), Ara (arabinans), and/or both Gal and Ara units (arabinogalactans type I and/or II; AG-I AG-II) (Fig. 2) that are linked at position *O*-4 of the Rha residues [37, 39, 44]. Galactans are composed of β -(1 \rightarrow 4)-Gal units and arabinans have an α -(1 \rightarrow 5)-Araf/backbone that can be substituted with one or more α -Ara units at the *O*-2 and/or *O*-3 position [36]. It should be noted that the proportion and length of these side chains have many variations depending on the plant source [46]. For example, potato RG-I is rich in galactan side chains (~67 %) [47, 48], whereas the RG-I backbone from sugar beet pectin is mainly substituted with arabinans [39].

◆ *Rhamnogalacturonan II*

RG-II is one of the most conserved pectic polysaccharides found in nature. It has a HG backbone that is branched with four complex oligosaccharide side chains (A, B, C, and D side chains, Fig. 3). These side chains comprise 12 monosaccharides, including some rare sugars, such as 2-*O*-methyl-Fucose (2-Me-Fuc), 2-*O*-methyl-Xylose (2-Me-Xyl), apiose (Api), aceric acid (AceA, 3-C-carboxyl-5-deoxy-L-xylose), 3-deoxy-D-lyxo-2-heptulosaric acid (Dha), and 3-deoxy-D-manno-2-octulosonic acid (Kdo) [37, 49].



polysaccharide functional groups, such as methyl-esters and acetyl groups of pectins [64, 65]. Nonetheless, significant overlap in the fingerprint region makes analysis complex and difficult if polysaccharides are not purified before analysis.

In summary, the above discussion shows that a reliable characterization of polysaccharides requires the use of several methods simultaneously, which is very laborious and tedious. Thus, there is a need for a more rapid and generic characterization and recognition of polysaccharides in the food sector. This is important for the food industry because identification and a good characterization of the polysaccharides present in food raw materials will allow a better utilization of these materials. This will enable e.g. reducing food waste, preparing healthier products by increasing the dietary fibres content, and preparing products with an improved mouthfeel. A possible approach to reach a more rapid and generic characterization and recognition of polysaccharides consists of the depolymerization of polysaccharides to structure-informative low molecular weight (LMw) fragments, also known as diagnostic oligosaccharides [40, 66]. LMw compounds with a DP ranging from 2-20 are amenable for (liquid chromatography -) mass spectrometry (MS) analysis [67, 68], contrary to polysaccharides. The high MS sensitivity and ability of tandem MS to characterize mass-to-charge (m/z) ratios in detail will allow the characterization of the generated diagnostic oligosaccharides. This will subsequently allow the recognition of polysaccharides in a higher throughput manner. Hereby, a suitable approach to depolymerize polysaccharides into oligosaccharides that comprise the structural features of the native polysaccharide is crucial to achieve a reliable polysaccharide characterization and/or identification.

3. Approaches to depolymerize polysaccharides into oligosaccharides

Depolymerization of polysaccharides can be reached using various approaches, including the use of enzymes (section 3.1.), chemicals (section 3.2.), and thermo-mechanical processes like ultrasound, microwave irradiations, and ball-milling [69-74]. In this section, enzymatic and chemical approaches are discussed in detail to investigate their potential to depolymerize polysaccharides into diagnostic oligosaccharides.

3.1. Enzymatic digestion

Diagnostic oligosaccharides are majorly obtained by enzymatic digestion of polysaccharides. Enzymes that degrade, modify, and/or create glycosidic bonds are called Carbohydrate-Active enZYmes (CAZymes) and they are described in the CAZy database [75]. The main enzyme families involved in the hydrolysis of polysaccharides are classified into **1**) glycoside hydrolases (GHs), which cleave glycosidic bonds, **2**) carbohydrate esterases (CEs), which are specific towards carbohydrate ester bonds, and **3**) polysaccharide lyases (PLs), which cleave uronic acid-containing polysaccharide chains via a β -elimination mechanism to generate an unsaturated hexuronic acid residue at the non-reducing end and create a new reducing end [76]. To generate diagnostic oligosaccharides, the enzymes used should be active towards glycosidic linkages (GHs and PLs) within the polymer backbone, in an endo-acting manner [77]. A summary of the main enzymes involved in the digestion of plant polysaccharides to yield diagnostic oligosaccharides is given in Table 1.



(Arabino)xylans are mostly digested with endo-xylanases I and III (GH family 10 and 11) [16, 78-80], releasing arabino-xylo-oligomers (AXOS). These AXOS can be used to speculate about the distribution patterns of substituents along the xylan backbone. For example, Tian et al. [16] proposed that in oat AXs the distribution of Ara f side chains is contiguous, whereas in wheat and barley AXs it is random or clustered [80, 81].

Insights into the structure of galactomannans is reached by enzymatic digestion with endo- β -(1 \rightarrow 4)-mannanase [24], releasing galactomanno-oligomers that can be used to understand the distribution of Gal side chains over the mannan backbone. This enabled e.g., to show that guar gums have a blockwise distribution of Gal units, whereas locust bean gum has random, blockwise, and ordered distributions of Gal units [24].

Pectins are digested with a combination of various pure and highly specific pectolytic enzymes, mostly endo-polygalacturonase (PG) and pectin lyase (PEL), with or without combination with pectin methyl-esterases (PME), to obtain diagnostic oligosaccharides for structural characterization [40, 82-87]. Analysis of these oligosaccharides allows the determination of various pectin descriptive parameters, which are the absolute degree of blockiness (DB_{abs}), degree of hydrolysis by PG (DH_{PG}), and degree of hydrolysis by PEL (DH_{PEL}).

Recently, a new family of enzymes involved in the degradation of polysaccharides has been created and included in the CAZy database [75], named auxiliary activities (AA). This family includes lytic polysaccharide monooxygenases (LMPOs), which are enzymes capable of cleaving recalcitrant polysaccharides using an oxidative mechanism [88]. Although LMPOs have not been used to structurally characterize plant polysaccharides, they are able to oxidatively cleave xylan and glucans, forming oxidized xylo- and gluco-oligomers, respectively [89, 90]. This opens the potential utility of LMPOs to yield diagnostic oligosaccharides for polysaccharide structure elucidation besides GHs and PLs.

The above studies show that the oligosaccharide fragments, e.g., AXOS, galactomanno-oligomers, and pectin-oligomers, derived from digestion of polysaccharides using endo-acting enzymes comprise information about the structural features of the original polysaccharide. This allows characterization of the native polysaccharide structure. However, from Table 1 and the studies mentioned herein, it is clear that enzymatic digestion of plant polysaccharides to obtain diagnostic oligosaccharides requires the use of various enzymes per structurally different polysaccharide. Additionally, only few pure and well-characterized enzymes are commercially available, and production, extraction, purification, and characterization of enzymes is laborious [91, 92]. This makes enzymatic digestion of polysaccharides unsuitable as a generic polysaccharide depolymerization method.



Table 1. Overview of the main endo-enzymes used to obtain oligosaccharides from plant polysaccharides, enzyme families according to CAZy [75].

Substrate(s)	Enzyme(s)	Enzyme specificity	Ref(s)
Starch	α (β)-amylase (GH13, 57, 119, 126)	Hydrolysis of α -D-(1 \rightarrow 4)-glucosidic linkages.	[93]
Cellulose	Endo- β -(1 \rightarrow 4)-glucanase (GH7)	Hydrolysis of β -D-(1 \rightarrow 4)-glucosidic linkages.	[94]
Xylans	Endo- β -(1 \rightarrow 4)-xylanase type I (GH10) Endo- β -(1 \rightarrow 4)-xylanase type III (GH11)	Hydrolysis of β -D-(1 \rightarrow 4)-xylosidic linkages.	[95-97]
Mannans	endo- β -(1 \rightarrow 4)-mannanase (GH26)	Hydrolysis of β -D-(1 \rightarrow 4)-mannosidic linkages.	[24, 75, 77]
XG	XG specific endo-glucanase (GH5)	Hydrolysis between the non-substituted β -D-(1 \rightarrow 4)-glucosidic linkage and the neighboring substituted glucose unit.	[98]
β -(1 \rightarrow 3,1 \rightarrow 4)-glucan	Endo- β -(1 \rightarrow 4)-glucanase (GH7) Endo- β -(1 \rightarrow 4)-glucanase (GH7)	Hydrolysis of β -D-(1 \rightarrow 4)-glucosidic linkages. Hydrolysis of β -D-(1 \rightarrow 4)-glucosidic linkages.	[94]
	Endo- β -(1 \rightarrow 3, 1 \rightarrow 4)-glucanase (Lichenase, GH9, 26)	Hydrolysis of β -D-(1 \rightarrow 4)-glucosidic linkages in β -glucans containing (1 \rightarrow 3)- and (1 \rightarrow 4)-bonds. Hydrolysis of (1 \rightarrow 4)-linkages in β -glucans when the Glc residue whose reducing group is involved in the linkage to be hydrolyzed is itself substituted at C-3	[16, 75, 99]
HG	Endo-polygalacturonase (endo-PG; GH28) Pectin lyase (PEL; PL1)	Hydrolysis between two non-esterified α -D-(1 \rightarrow 4)-GalA units. Hydrolysis between two methyl-esterified α -D-(1 \rightarrow 4)-GalA units with the release of an unsaturated GalA-oligomer with a 4-deoxy-(6- <i>O</i> -methyl)- α -D-galact-4-enuronosyl groups at the non-reducing end.	[100, 101]; [102, 103]; [104]
	Pectate lyase (PLY; PL1, 3, 9)	Hydrolysis between two non-esterified α -D-(1 \rightarrow 4)-GalA units with the release of an unsaturated GalA-oligomer with a 4-deoxy- α -D-galact-4-enuronosyl groups at the non-reducing end.	
RG-I	Rhamnogalacturonan hydrolase (GH28)	Hydrolysis of α -D-GalA-(1 \rightarrow 2)- α -L-Rha glycosidic linkage releasing oligosaccharides with β -D-GalA at the reducing end.	[105, 106]; [105, 107];
	Rhamnogalacturonan lyase (PL4 and 11)	Hydrolysis of α -L-Rhap-(1 \rightarrow 4)- α -D-GalA linkages by β -elimination releasing oligosaccharides with Rha at the reducing end and unsaturated GalA at the non-reducing end.	[108, 109]; [110, 111]
Arabinan	Endo-arabinanase (GH43)	Hydrolysis of α -(1 \rightarrow 5)-arabinofuranosidic linkages.	
Galactan	Endo-galactanase (GH53)	Hydrolysis of β -(1 \rightarrow 3)- and β -(1 \rightarrow 4)-linked Gal units.	
Xylogalacturonan	Xylogalacturonan hydrolase (GH28)	Hydrolysis of α -D-(1 \rightarrow 4)-linked GalA units that are substituted with β -(1 \rightarrow 3)-Xyl units.	[112, 113]

Enzymatic fingerprinting of polysaccharides based on the oligosaccharide profiles

Although specific enzymes are needed per structurally different polysaccharide, the enzymatically released oligosaccharides can be efficiently identified, characterized and quantified using various analytical methods, such as high-performance anion-exchange chromatography (HPAEC), LC-MS, Matrix-Assisted Laser Desorption Ionization Time-Of-Flight (MALDI-TOF) MS, and NMR [16, 24, 80, 84, 114-116]. Enzymatic digestion of polysaccharides results in oligosaccharide profiles that are polysaccharide structure-dependent, which is reflected in e.g. HPAEC [24] and LC-MS [84] elution patterns and MALDI-TOF mass spectra [16, 117], specific per polysaccharide sample. This allows distinction and/or recognition of polysaccharide samples based on oligosaccharides profiles (fingerprinting). For example, oligomers of structurally different galactomannans analyzed by HPAEC resulted in different oligosaccharide profiles, allowing recognition of different galactomannan samples [24, 118]. Analysis of a complex mixture of oligosaccharides derived from enzymatic digestion of plant polysaccharides (arabinan, xylan, mannan, galactan, xyloglucan, homogalacturonan of low DM, RG-I, and xylogalacturonan) using porous graphitic carbon (PGC-)UHPLC-MS also gave structure-dependent oligosaccharide profiles [116, 119]. This technique allows characterization of neutral and charged oligomers, as well as oligomers carrying non-sugar substituents, and it has more recently been used to characterize oxidized cello-oligomers [120, 121]. In addition, HPAEC chromatographic and MALDI-TOF MS data of depolymerized polysaccharides have been subjected to multivariate analysis techniques (principal component analysis; PCA) to study similarities/differences between polysaccharide samples [66, 99, 122].

Overall, enzymatic digestion of polysaccharides is not only suitable to obtain insights into the polysaccharide chemical structures, but also to screen and identify polysaccharide types based on the oligosaccharides fingerprinting. A remark to the enzymatic digestion of polysaccharides composed of isomeric sugar units, like arabinoxylans and galactomannans, is that isomeric oligosaccharides are released, which are rather difficult to characterize by MS due to the inability of MS to distinguish isomers [123]. Moreover, the enzyme-polysaccharide specificity hampers to have a generic method to depolymerize polysaccharides into diagnostic oligosaccharides. Thus, a polysaccharide depolymerization approach that overcomes these limitations is still needed to structurally characterize and identify polysaccharides in a more generic and accessible manner.

3.2. Chemical-induced depolymerization approaches

Chemical approaches might provide possible solutions to reach a controlled, more generic, and accessible depolymerization of polysaccharides into diagnostic oligosaccharides in comparison to enzymes. The main chemical approaches leading to polysaccharide depolymerization are based on partial acid- and/or alkaline-hydrolysis, on oxidative reactions (Periodate oxidation and Fenton reaction), and on β -elimination. As we knew beforehand that an alkaline treatment removes alkali-labile esterified components of polysaccharides [124], this approach will not be included in this overview. In this section, selected chemical approaches are discussed in detail to verify their potential to release (diagnostic) oligosaccharides from polysaccharides.



3.2.1. Partial acid-hydrolysis

Partial acid-hydrolysis is a simple and inexpensive polysaccharide depolymerization approach that can easily be controlled. The temperature (normally above 60 °C), time of hydrolysis, and concentration of acid are normally optimized per polysaccharide sample to reach oligosaccharides with variable Mw and structural features [125-127]. The most common acids used to perform partial acid-hydrolysis are trifluoroacetic acid (TFA), sulfuric acid (H₂SO₄), and hydrochloric acid (HCl) [128]. Besides TFA, other weaker organic acids have been used to depolymerize polysaccharides, such as oxalic, maleic, citric, and acetic acids [129, 130]. The low boiling point of TFA compared to other (mineral) acids allows its easy removal from the reaction medium by evaporation [128]. This enables simple purification of the degradation products for posterior analysis.

Although partial acid-hydrolysis is considered a non-specific polysaccharide degradation approach, unlike enzymes, it shows some hydrolysis preferences depending on the sugar anomeric configuration, type, ring, and size, and on the glycosidic linkages [131]. For example, α -linkages between sugars are less resistant to acid hydrolysis than β -linkages, and deoxy sugars, furanosyl rings (e.g., Ara_f) and aldopentoses are known for being acid labile [126, 128, 131]. Additionally, polysaccharides containing uronic acids are rather resistant to acid hydrolysis, which might be attributed to the glycosidic linkages of aldobiouronic acids (uronic acid→neutral sugar) being more resistant to acid degradation than the linkage between neutral sugars [131-134].

Examples of partial acid-hydrolysis conditions applied to various plant polysaccharides, the type of products released, and main findings are described in Table 2. MALDI-TOF-MS of the partially acid-hydrolyzed glucuronoxylans extracted from olive pulp and olive seed hull showed long blocks of neutral (DP≤18) and acidic (DP≤16) xylo-oligosaccharides (XOS), which suggested that acidic units were irregularly distributed along the xylan backbone [135]. This study also showed that, despite acting randomly, partial acid-hydrolysis of structurally different polysaccharides gave oligosaccharide profiles that are polysaccharide structure-dependent.

Lin et al. [130] partially acid-hydrolyzed xylans and described that despite comprising 15 to 20 % (w/w) of Ara, only XOS were identified after partial acid-hydrolysis of these xylans. This highlights the low acid stability of Ara units in xylans, hindering detailed structural characterization of the (arabino)xylan native structure based on the oligosaccharides' characterization. The preferential and rapid release of Ara residues upon partial acid-hydrolysis of AXs was also seen by others [136-139]. Yet, identification of feruloylated AXOS released after partial acid-hydrolysis (0.05 M TFA, 100 °C, 2 h) of heteroxylans from the maize bran and perennial cereal grains still allowed identification of their structures as feruloylated AXs [138, 139].

Table 2. Examples of partial acid-hydrolysis applied to various plant polysaccharides, type of partially acid-released products, and main findings.

Polysaccharide(s)	Hydrolysis condition	Type of products released	Main Finding(s)	Ref(s)
Glucuronoxylans (GX) (Olive pulp and seed)	0.05 M TFA, 100 °C, 45 min	Neutral (DP<18) and acidic (DP<16) XOS. Xyl _n MeGlcA, Xyl _n GlcA and Xyl _n GlcA ₂	Acidic units were irregularly distributed along the xylan backbone	[135]
GX (Olive seed hull)	0.05 M TFA, 100 °C, 45 min	Neutral and acidic XOS (DP7, 10, 14, 17)	One GlcA unit per 14 contiguously linked Xyl units (regular structure)	[140]
GX (Soft- and hardwood)	Variable [TFA], temperatures and times	Neutral XOS (DP<18) and acidic XOS with MeGlcA units	Regular distribution of acidic units over the xylan backbone in softwood GX and irregular distribution in hardwood GX	[141-143]
Arabinoxylans	Various acids, temperatures and times.	Ara XOS Feruloylated AXOS	Rapid release of the Ara substituents	[130, 137-139]
Heteroxylans (Hardwood – from bast and core kenaf, <i>Hibiscus cannabinus</i>)	2.0 M TFA, 120 °C, 30 min	Aldo- to aldotetrauronic acids (4- <i>O</i> -Me-GlcA-Xyl _{1,3} and GlcA-Xyl _{1,3}); 4- <i>O</i> -(α -D-GalAp)-D-Xyl	Presence (galacturono)glucuronoxylans of	[144]
Galactomannan (<i>M. indica</i> seeds)	0.05 M H ₂ SO ₄ , 95°C, 12 h	Monosaccharides β -Man(1 \rightarrow 2/4)-Man; α -Gal(1 \rightarrow 6)-Man; α -Gal(1 \rightarrow 4)-Gal; α -Gal(1 \rightarrow 6)- β -Man-(1 \rightarrow 4)-Man.	(1 \rightarrow 4)- and (1 \rightarrow 2)-mannan backbone branched at position <i>O</i> -6 with single Gal units, and minorly with a disaccharide of (1 \rightarrow 4)-linked Gal, and a trisaccharide of (1 \rightarrow 4)-linked Man attached at position <i>O</i> -4 of a Gal unit.	[145]
Galactomannans (Seeds of <i>Schizolobium</i> species and <i>Cassia fastuosa</i>)	0.025 M H ₂ SO ₄ , 5h	Monosaccharides Galactomanno-oligosaccharides with DP2-6	β -(1 \rightarrow 4)-mannan backbone substituted with single α -Gal units at position <i>O</i> -6. Galactomanno-oligosaccharides with DP2-6 were similar between <i>Schizolobium</i> species but different from <i>C. fastuosa</i>	[146]
(Galacto)glucomannan (Seeds of <i>Artemisia sphaerocephala</i>)	0.1 M TFA, 100 °C, 0.5-3.5 h	Quick release of Ara (side chains). Increase release of Gal and Man with increasing hydrolysis time (backbone sugars).	Backbone consisted of (1 \rightarrow 4)-linked D-Manp and (1 \rightarrow 4)-linked D-Glcp in a molar ratio of 1:1.3	[126]
Xyloglucan (Tamarind seed)	0.1 M HCl, 100 °C, 4 h	Removal of some side chain units (Xyl and Gal). Release of XGXG, XXGG, GGXG, GXXG, and XGGG (with variations containing Gal).	Hydrolysis of XXXG, XLXG, XXLG and XLLG into smaller fragments and monosaccharides	[147]

Table 2. Continuation.

Polysaccharide(s)	Hydrolysis condition	Type of products released	Main Finding(s)	Ref(s)
RG-I (Sugar beet pulp)	0.05 or 0.1 M TFA, 100 °C, 1 h	Presence of feruloyl groups. Ara, Gal and Rha monomers. (1→3,5)-Ara, and (1→4)- and (1→3,4)-Gal oligomers	Ara side chains were more degraded than Gal side chains. The non-reducing Ara terminal units were cleaved faster than the inner bonds.	[148]
RG-II (citrus and <i>Arabidopsis</i>)	M TFA, 40 °C, 16 h (+ 1 h hydrolysis at 60, 80, and 100 °C)	Intact A side-chain. Intact B side-chain. Intact C side-chain. Intact D side-chain (hardly detected). Oligosaccharides from partial degradation of B side-chains (lacking Ara and terminal Rha units). GalA ₄ to GalA ₆ .	Preferable hydrolysis of the acid-labile Kdo, Dha, and Api at the branchpoint between A, B, C and D side-chains and the backbone. Quick Dha and Ara degradation during acid hydrolysis (D side-chain).	[149]
(De-esterified) Pectins (Apple, citrus, and beet)	0.1 M HCl, 80 °C, up to 72 h	Neutral sugars derived from galactans and arabinogalactans (< 5 h hydrolysis). (Rha-GalA) _n segments. GalA units (24 to 72 h hydrolysis)	Firstly, rapid release and hydrolysis of arabinan and arabinogalactan side chains. Secondly, hydrolysis of linkages between Rha and GalA units: Release of HG sequences. Thirdly, hydrolysis of linkages between GalA units.	[150]

Various studies have also been carried out on mannans, XGs, and pectic polysaccharides (Table 2). Differences in the galactomannan fine structures between the galactomannans of *Schizolobium* species and *Cassia fastuosa* could be inferred from the different proportion of galactomanno-oligosaccharides formed after their partial acid-hydrolysis [146]. From the partial acid-hydrolysis of XG it was noted that the hydrolysis randomly removed Xyl and Gal units, generating oligo-XG fragments no longer representing the XG native structure [147]. Moreover, partial acid-hydrolysis of various pectins resulted in a quick degradation of Ara chains, emphasizing the high acid lability of Ara_f units [148-151]. Studies on XG and pectins further highlight that neutral sugar side chains, in particular Ara units, are rapidly released from the polymer backbone after partial acid-hydrolysis.

Some studies have taken advantage of the high acid resistance of aldobiouronic acids to investigate the structure of pectic polysaccharides [132, 150]. For example, by reduction of the methyl-esterified GalA units to Gal units and selective cleavage of the glycosidic linkage of the resulting Gal residues by partial acid-hydrolysis using hydrogen fluoride (HF) solvolysis, it was possible to study the distribution of contiguous non-esterified GalA units in pectins [132]. This study underlines that selective polysaccharide modification before hydrolysis can be wisely used to generate diagnostic oligosaccharides.

Polysaccharide modification before mild acid-hydrolysis could be of particular interest for AXs to avoid the rapid release of the acid labile Ara_f units. Considering that the glycosidic linkage of an aldobiouronic acid is more resistant to acid hydrolysis than the bond of a neutral disaccharide [133], selective oxidation of Ara to arabinuronic acid (AraA_f) would yield an arabinuronoxylan that comprises aldobiouronic acids (AraA→Xyl) in its structure. This might avoid the quick release of the Ara(A) substituent during partial acid-hydrolysis, allowing to produce diagnostic arabinurono-xylo-oligomers (AUXOS) [152].

Partial acid-hydrolysis of modified polysaccharides by 2,2,6,6-tetramethylpiperidine-1-oxyl radical (TEMPO)-oxidation

Selective oxidation of primary hydroxyl groups of neutral sugars of polysaccharides into carboxylic acids can be reached using a 2,2,6,6-tetramethylpiperidine-1-oxyl radical (TEMPO)-mediated oxidation [153]. TEMPO, a secondary amine nitrogen oxide (nitroxyl radical), is present in various species (nitrosonium ion, hydroxylamine, and TEMPO; Fig. 4) during the oxidation reaction. TEMPO is normally used as an oxidation catalyst in presence of other oxidizing agents. The nitrosonium ion derived from TEMPO is the reactive species that initiates the reaction by oxidizing a primary alcohol into an aldehyde, being itself reduced to the corresponding hydroxylamine form (Fig. 4). The aldehyde group is further oxidized to a carboxyl group, either by another nitrosonium ion or by the primary catalyst present in the reaction medium, normally sodium hypochlorite (NaOCl). The nitrosonium ion can be continuously regenerated throughout the reaction by oxidation of the hydroxylamine by the primary oxidant at both alkaline and acid pH (Fig. 4).

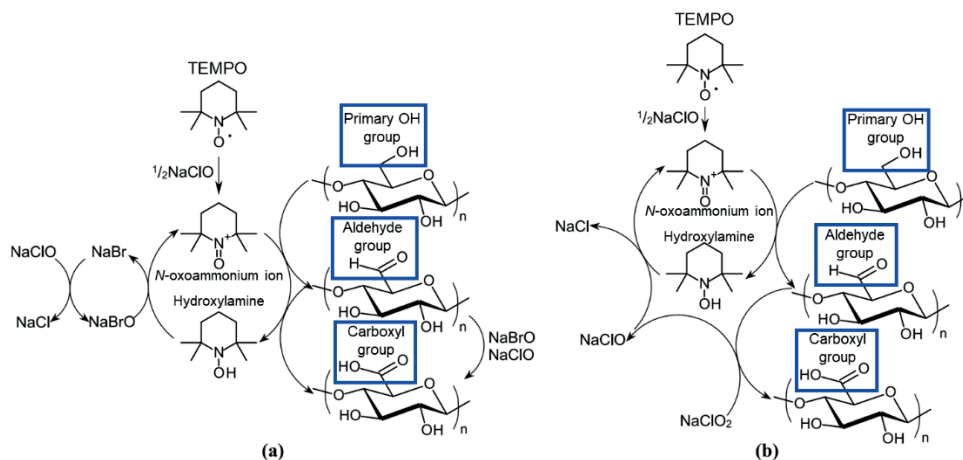


Figure 4. Oxidation of the C6 primary hydroxyls to carboxylates by the (a) TEMPO/NaOCl/NaBr system in water at alkaline pH and (b) TEMPO/NaOCl/NaClO₂ system under neutral or weakly acidic conditions, adapted from Nechporchuk et al. [154].

A TEMPO/NaOCl/NaBr system at pH 10 (Fig. 4a) was the first oxidation system used to convert C6 primary hydroxyls of neutral sugars to carboxyl groups in starch and inulin [155], and it is still the condition mostly used to oxidize polysaccharides [153]. The alkaline medium used in the TEMPO/NaOCl/NaBr system can lead to polysaccharide depolymerization [156]. However, the alkaline medium will also remove alkali-labile esterified substituents of polysaccharides [124], which is undesirable for a reliable structural characterization of polysaccharides. Other TEMPO-oxidation systems that do not require the use of an alkaline medium, such as TEMPO/bis(acetoxy)iodobenzene (BAIB) in an acetonitrile-aqueous buffer mixture [157-159] or TEMPO/NaOCl/NaClO₂ (sodium chlorite) in a mild acidic (pH 3.5 to 6.8) medium (Fig. 4b) [160-162], showed also to be effective in converting primary hydroxyl groups of neutral sugars of polysaccharides into carboxylic acids.

TEMPO-oxidation has been mostly performed on neutral polysaccharides composed of hexoses, such as cellulose, starch, and galactomannans [163-166]. Only ter Haar et al. [166] have subjected TEMPO-oxidized hexosans (starch) to (mild) acid-hydrolysis and analyzed the released oligosaccharides to study the structure of the TEMPO-oxidized starch. These authors not only verified the presence of blocks of GlcA units in the oxidized starch, but also of clusters of aldehydes close to carboxyl groups. Furthermore, they observed that the α -(1→4)-GlcA-GlcA linkage was more resistant to acid hydrolysis than the α -(1→4)-GlcA-Glc and the α -(1→4)-Glc-Glc, respectively.

Not many studies have been performed on TEMPO-oxidation of pentosans. Among pentosans, AXs are an ideal substrate to obtain a polyuronide carrying negative charges exclusively in the side chains, as only the Ara_f units display primary hydroxyl groups [15]. Oxidation of AXs using a Laccase/TEMPO and a TEMPO/BAIB system, respectively, led to preferable conversion of Ara_f to the aldehyde rather than to the uronic acid [157, 167]. This shows that depending on the TEMPO-oxidation system used, oxidation products other than uronic acids can be formed during TEMPO-oxidation. Bowman et al. [152] oxidized AXs from birch, wheat, and switchgrass using a 4-Acetamido-TEMPO/NaOCl/NaBr system in alkaline medium. After partial acid-hydrolysis of the TEMPO-oxidized AXs and HILIC-MS analysis of the released fragments, these authors observed the presence

of XOS carrying AraAf units, proving the presence of AraAf as an oxidized product derived from AraF. Therefore, TEMPO-oxidation of AXs before partial acid-hydrolysis seems to be a promising approach to obtain AXs with increased resistance to acid hydrolysis and to obtain diagnostic oligosaccharides. Nonetheless, attention to the TEMPO-oxidation conditions must be paid to obtain an arabinuronoxylan fully resembling the native AX structure.

3.2.2. Periodate oxidation

Periodate (IO_4^-) oxidation is a reaction that leads to specific oxidation of free vicinal diols to aldehydes with cleavage of the carbon chain (Fig. 5) [168, 169]. One molecule of periodate is consumed per vicinal diol. When there are three vicinal hydroxyl groups at C2, C3, and C4, two molecules of periodate will attack the three groups, releasing a molecule of formic acid including the C3, and forming aldehyde groups at C2 and C4 positions [169, 170]. The rate of oxidation depends on the conformation of the sugar units. For the oxidation of diols to take place, the hydroxyl groups must be oriented in an equatorial (*eq.*-*eq.*) or axial (*ax.*-*eq.*) positions. The rigid *ax.*-*ax.* position does not make a complex with IO_4^- and therefore oxidation cannot occur [168]. Sugar units containing *cis*-hydroxyl groups (e.g. Ara, Gal, and Man) are oxidized quicker than sugars containing *trans*-hydroxyl groups (e.g. Glc and Xyl) [170]. Additionally, the rate of oxidation also depends on the pH, being maximum in the pH range from 4 to 5 and low in alkaline medium [169]. The reaction should be performed in the dark at low temperatures ($\leq 30^\circ\text{C}$), as periodate is unstable to light.

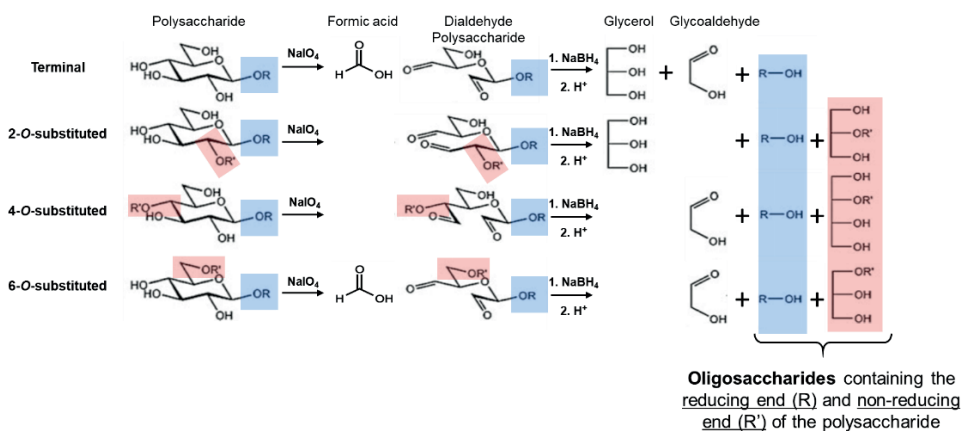


Figure 5. Type of products formed from a terminal, a 2-*O*-, a 4-*O*-, and a 6-*O*-Glc unit after periodate (NaIO_4) oxidation, and reduction (NaBH_4) followed by mild acid-hydrolysis (H^+) (Smith degradation approach). Adapted from Stenutz [171].

Periodate oxidation has emerged as a polysaccharide modification approach to create materials with new/improved functionalities by introducing dialdehyde functionalities [168, 172-174]. NaIO_4 is a key factor in determining the aldehyde content of dialdehyde polysaccharides. The aldehyde content increases when the NaIO_4 is used in an excessive amount relatively to the monomeric unit of the polysaccharide [175]. It should be mentioned that the aldehyde groups of polysaccharides in aqueous medium can be present in a masked form, leading to a decrease in the apparent dialdehyde content. In

such a masked form, free aldehydes have reacted with neighboring hydroxyl groups, forming intra- and/or inter-hemiacetal bonds, or with water, forming hemialdals or hydrated aldehydes [176-179], as described for cellulose (Fig. 6). Increasing the reaction temperature and the amount of periodate can increase the oxidation rate, therefore decreasing the reaction time needed, which might prevent side oxidation reactions [180, 181]. Furthermore, some studies have shown that periodate oxidation of polysaccharides can be accompanied by polysaccharide depolymerization, e.g. for carboxymethyl cellulose, chitosan, xyloglucan, 4-*O*-methylglucuronoxylans, and pectins [172-174, 182-184]. Polysaccharide depolymerization normally increases when there is a rise in the NaIO₄ concentration [175, 185], temperature (>30 °C) [180, 186], and reaction time [174], or when the pH is outside the range from 3 to 5 [168, 186]. This suggests that by subjecting polysaccharides to more extreme periodate oxidation conditions, oligosaccharides might be obtained directly. No studies have used periodate oxidation to depolymerize polysaccharides into oligosaccharides for structural characterization of polysaccharides, and only few studies have used MS to study the structure of periodate-oxidized oligosaccharides [187].

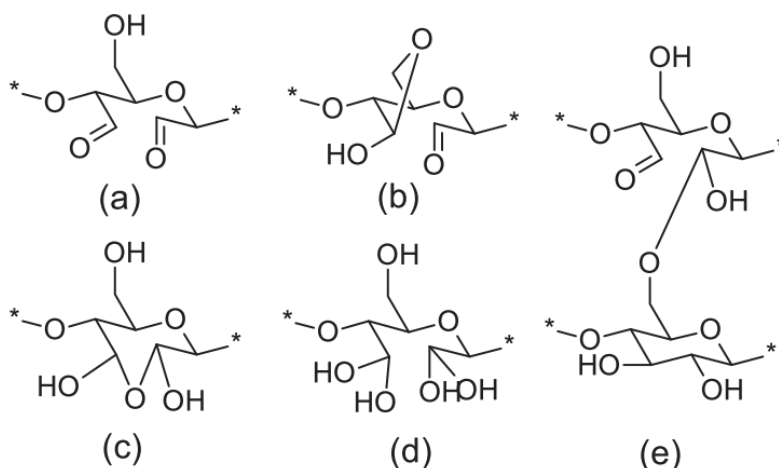


Figure 6. Possible structures that can be formed after periodate oxidation of cellulose in aqueous medium: (a) free aldehyde, (b) intramolecular hemiacetal, (c) hemialdal, (d) hydrated aldehydes, and (e) intermolecular hemiacetal [176]. * - extension of the cellulose chain.

Periodate oxidation followed by mild acid-hydrolysis (Smith degradation)

Periodate oxidation has long been used to characterize the structure of complex polysaccharides for number and type of branches in an approach called Smith degradation [188]. This approach consists of periodate oxidation of the polysaccharide, followed by dialdehyde reduction to alcohol, and by mild acid-hydrolysis to cleave the acid sensitive acyclic acetal linkage and release mono- and/or oligosaccharides (Fig. 5). The products released are generally analyzed by GC-MS and NMR and, based on the characterization of these products, it is possible to study the native polysaccharide structure [189-192]. Smith degradation oligosaccharides comprising the terminal non-reducing end of the parental polysaccharide have a sugar-glycerol (three carbons) or sugar-erythritol (four carbons) located at the other end of the oligosaccharide chain (Fig. 5) [169].



Based on the periodate specificity (Fig. 5), it is possible to determine the linkage position of a sugar unit from the Smith degradation products. For example, in AXs, (1→4)-linked Xyl residues in the polymer backbone that are 2-*O*- and/or 3-*O*-substituted cannot be oxidized by periodate because there are no vicinal diols, allowing to determine branching points. The main Smith degradation products of a rye-flour AX were 2-*O*-β-D-Xylp-glycerol, xylobiosyl-glycerol, and xylotriosyl-glycerol in the molar ratio of 7.5:2.2:1 [193]. This shows that the Ara units were randomly distributed along the xylan backbone, since the Xyl units in the released fragments corresponded to substituted units and glycerol to a (1→4)-linked Xyl unit. Many more studies have used Smith degradation as an approach to study the structural features of AXs [62, 191, 192, 194-198]. It should be mentioned that although Smith degradation allows identification of branched Xyl units in AXs, the mild acid-hydrolysis step used in this approach might rapidly remove the (oxidized and reduced) Ara side chains, as mentioned in section 3.2.1. This hampers the production of diagnostic oligosaccharides for structural characterization, as it is not possible to determine if the Ara side chain was linked at the position *O*-2 and/or *O*-3 of the Xyl unit of AXs.

The (1→3)-linked residues in the backbone of polymers cannot be oxidized by periodate (Fig. 5), which allows to study the proportion of (1→4):(1→3) linkages in β-glucans by Smith degradation. In β-glucans, 2-*O*-β-D-glycosyl-D-erythritol and D-erythritol are the major Smith degradation products [199]. A high amount of D-erythritol indicates a high amount of adjacent (1→4)-linked Glc units. This approach also enables identification of consecutive (1→3)-linked Glc units in the polymer backbone, which is seen by the presence of 2-*O*-β-D-[laminarisaccharide]₂₋₅-D-erythritol series [199-201].

Furthermore, the structure of pectins and the location of acetyl groups in the galactan side chains can also be studied by Smith degradation [190, 202]. Tomoda et al. [202] verified the complete oxidation of GalA units, whereas Rha, Ara, and Gal were only partly oxidized. Rha and Ara oxidation survival was due to the existence of branching points, whereas Gal survived due to acetyl substitution.

The above studies show that Smith degradation is helpful to study the structure of AXs, β-glucans and pectins, especially to determine branching positions. This is due to the different sensitivities of the polysaccharide sugar units to periodate oxidation. It should be mentioned that for polysaccharides composed of sugar units where all the sugar moieties are sensitive to periodate oxidation, it is rather difficult to pinpoint branching positions by Smith degradation. For example, in galactomannans all sugar units are available for oxidation, which leads to the release of glycerol and erythritol as main Smith degradation products [145, 203, 204]. Interestingly, Gupta et al. [204] found besides glycerol and erythritol, also mannose as a Smith degradation product of GM, showing that Gal side chains are more rapidly oxidized by periodate than Man units. Thus, despite being a long time and widely used polysaccharide characterization approach, Smith degradation might be a valuable strategy to study polysaccharide structures due to the periodate oxidation reaction specificity. However, attention must be paid to the release of acid-labile sugar residues during the mild acid-hydrolysis step.

Periodate oxidation followed by alkaline or thermal hydrolysis

Aldehyde groups in the dialdehyde polysaccharides after periodate oxidation are quite sensitive to alkaline degradation by β-elimination [205, 206]. β-elimination of a dialdehyde sugar unit within a dialdehyde polysaccharide could result in chain scission (Fig. 7), allowing the production of oligosaccharides. This could be a faster hydrolysis method to obtain structure-informative

oligosaccharides compared to the mild acid-hydrolysis commonly used in the Smith degradation because a reduction step could be skipped. Unfortunately, considering that various plant polysaccharides contain alkali-labile esterified substituents, such as methyl and acetyl esters [124], alkaline degradation of periodate-oxidized polysaccharides would lead to loss of important structural features, which is undesirable for generic structure elucidation purposes.

Veelaert et al. [205] studied the stability of periodate-oxidized starches in aqueous suspensions upon heating at variable pH. These authors observed that the Mw of a periodate-oxidized starch decreased upon heating (90 °C, 15 min) at acidic pH (pH 3 and 5) or even at neutral pH. The decrease in Mw could be due to acid hydrolysis or possibly β -elimination. This shows that periodate oxidation of polysaccharides, followed by a thermal treatment could also release oligosaccharides. This would not only be a faster approach to obtain oligosaccharides in comparison to Smith degradation due to the absence of a reduction step, but it would also avoid the use of acids, which can lead to undesirable removal of acid-labile sugar side chains. Thus, periodate oxidation of polysaccharides, as well as periodate oxidation of polysaccharides followed by a thermal treatment can be promising approaches to depolymerize polysaccharides into diagnostic oligosaccharides, given the high periodate specificity towards vicinal diol groups.

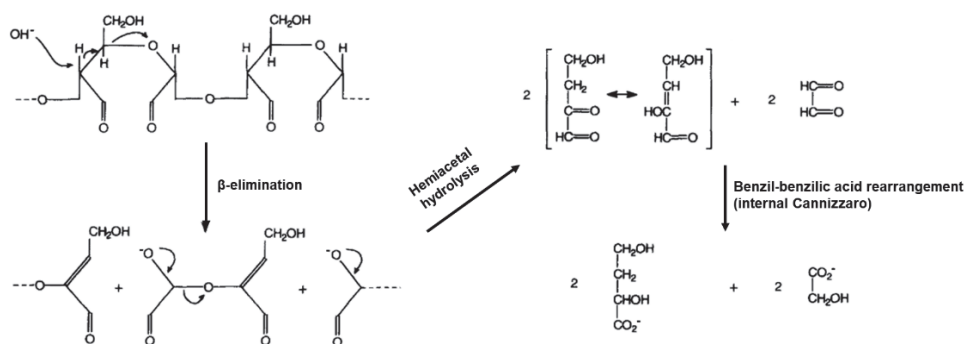


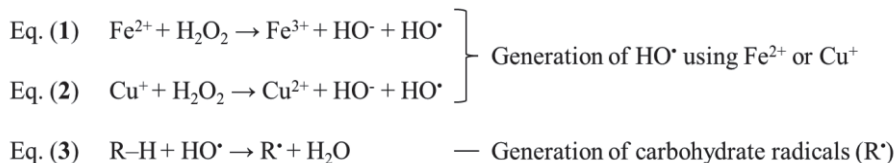
Figure 7. β -Elimination, hemiacetal hydrolysis and benzil-benzilic acid rearrangement of dialdehyde starch in alkaline medium [205].

3.2.3. Fenton reaction

In biological processes, polysaccharides can undergo scission *via* non-enzymatic strategies. Particularly, hydroxyl radicals (HO^\bullet) are involved in the oxidative scission of polysaccharides [207]. HO^\bullet can be formed by decomposition of H_2O_2 in the presence of a reduced transition metal ion (Fenton reaction), such as Fe^{2+} (Eq. (1)) and Cu^+ (Eq. (2)) [208, 209], being the latter more reactive [210]. HO^\bullet abstract hydrogen atoms from a C-H bond of carbohydrates (R-H, Eq. (3)), creating carbohydrate radicals (R^\bullet) [211]. These R^\bullet , especially when formed at the carbons involved in the glycosidic linkage, can cause backbone scission [212, 213]. Nonetheless, HO^\bullet can abstract hydrogens from any C-H bond of carbohydrates, being therefore a rather non-specific abstraction of hydrogens. Additionally, during carbohydrate oxidation induced by HO^\bullet , not only polysaccharide scission can take place, but also modification of the chemical structure of the sugar units. This might be due to, for example, extraction of hydrogen atoms, oxidation of functional groups and scission of C-C bonds [213-215]. Tudella et al.



[216] showed that galactomannosyl and mannosyl (GalMan₂ and Man₃) trisaccharides subjected to Fenton reaction (Fe²⁺/H₂O₂) gave a wide range of oxidation products, including hexuronic, hexonic, pentonic and erythronic acids, and neutral oligosaccharides with hydroperoxy, hydrated carbonyl residues, and residues resulting from pyranosyl ring cleavage.



Various plant polysaccharides have been degraded using various Fenton reaction systems (Table 3). Guilloux et al. [217] verified that the Mw of AX decreased when the H₂O₂ concentration increased. These authors did not observe a change in the carbohydrate composition of the obtained oligosaccharides, suggesting that the AXOS had a degree of Ara substitution close to the native structure. This indicates that subjecting AXs to the Fenton reaction has potential to release diagnostic oligosaccharides. Nonetheless, for β -glucans, polymer degradation was accompanied by formation of lactones, carboxylic acids, ketones, and aldehydes [214] (Table 3). The formation of these oxidation products changes the structure of the native polysaccharide significantly, making interpretation of the original polysaccharide structure rather complex. Additionally, as these oxidation products have a relatively low stability, their analysis is quite challenging. For pectins, although polymer degradation induced by HO[•] did release oligogalacturonides, polymer degradation was accompanied by the loss of methyl-esters and acetyl groups [218] (Table 3). This loss is undesirable for structural elucidation purposes. Thus, Fenton reaction can lead to depolymerization of polysaccharides with formation of oligosaccharides. Nonetheless, the loss of e.g., pectic structural features, formation of oxidation products and the absence of radical reaction specificity might hinder the use of Fenton reaction as a generic polysaccharide depolymerization approach to obtain oligosaccharides.

Table 3. Overview of plant polysaccharides degraded using Fenton reaction systems, effect on the molecular weight (Mw), and type of products formed upon Fenton reaction of polysaccharides.

Polysaccharide	Fenton reaction system	Effect on Mw	Type of end products and Main findings	Ref(s)
XG	Ascorbate/O ₂ /Cu ²⁺ Ascorbate/H ₂ O ₂ .	↓ Mw (↓ viscosity)*	Introduction of ester bonds within the XG backbone.	[207, 219]
Birch wood xylan (Feruloylated) AX	Chatecol/Fe ³⁺ /H ₂ O ₂ . Ascorbate/ Fe ²⁺ /H ₂ O ₂ Cu(CO ₂ CH ₃) ₂ /H ₂ O ₂ .	↓ Mw (↑ Reducing sugars)* ↓ Mw (↓ viscosity)* ↓ from 1001 * 10 ³ to 1.9 * 10 ³ Da (HPLC)*	- AXOS	[220] [217, 221, 222]
β-glucans	Ascorbate/Fe ²⁺ /H ₂ O ₂ Ascorbate/Fe ²⁺ H ₂ O ₂ .	↓ Mw (↓ viscosity)* (HPSEC-MALLS)*	Degradation with formation of peroxy radicals and new oxidized functional groups (lactones, carboxyl groups, ketones and aldehydes). β-(1→3)-linkages more easily attacked by HO• than β-(1→4)-linkages.	[207, 214, 215, 223, 224]
Polygalacturonic acid. Pectin.	Cu ²⁺ /H ₂ O ₂ Fe ²⁺ /H ₂ O ₂ (+ultrasound)	↓ from 500 kDa to 10 kDa. ↓ from 500 kDa to 20 or 5 kDa.	Oligogalacturonides (DP<6). Preferable cleavage of the homogalacturonan region. Decrease in the DM and DA content.	[218, 225]

* Approach/technique used to access the effect of Fenton reaction on the Mw of the polysaccharide.

3.2.4. β -elimination of esterified polysaccharides at neutral pH

β -elimination has been mainly used to study the structure of pectin samples [226-229]. The first step of the β -elimination reaction requires the presence of an ester group in the GalA unit, so that abstraction of H-5 of the GalA residue can occur [228]. This will result in specific splitting of the glycosidic linkage next to the esterified GalA unit, releasing an oligosaccharide comprising an unsaturated GalA ($\Delta^{4,5}$ GalA) at the non-reducing end (Fig. 8). Due to this specific splitting, β -elimination can be used to determine segments of methyl-esters along the pectin backbone [229].

Upon selective esterification of the 4-linked GalA_p residues of branched RG-I, β -elimination (0.2 M sodium borate pH 7.3, 120-125 °C, 2.5-3 h) selectively cleaves the Rha_p-(1→4)- α -GalA_p linkages. This releases an oligosaccharide composed of a disaccharide of β -L- $\Delta^{4,5}$ GalA_p(1→2)-L-Rha_p derived from the RG-I backbone, where the Rha unit carries a single side chain (Fig. 8), which allows studying the structure of branched RG-I [226, 227]. When performing β -elimination, two main aspects must be considered: **1)** β -elimination can lead to hydrolysis of, for example, methyl-esters, resulting in incomplete degradation, and formation of side products e.g. vinyl and/or keto groups [227]; and **2)** despite more extensive β -elimination fragmentation is reached at temperatures > 125 °C, also more side reactions occur at higher temperatures, which might be undesirable for structure elucidation purposes. In sum, although being a very valuable approach to characterize esterified polysaccharides, β -elimination is not suitable to characterize polysaccharides lacking (esterified) uronic acid residues (neutral polysaccharides). Therefore, its use as generic polysaccharide depolymerization approach is very difficult to achieve.

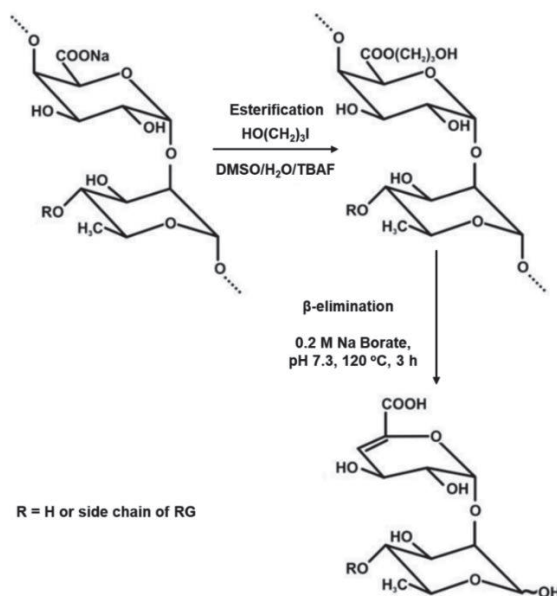


Figure 8. 3-Hydroxypropyl esterification and β -elimination of RG-I to release intact side chains (-R), adapted from Deng et al. [226].



4. Aim and thesis outline

The aim of this thesis was to seek for chemical-induced depolymerization approaches that can release oligosaccharides from food plant polysaccharides for recognition and structural characterization of polysaccharides in a generic manner. Such search for chemical degradation methods was desired because the traditional enzymatic depolymerization approaches used are polysaccharide-specific and therefore not suitable for a *generic* characterization of polysaccharides. Based on the literature described in **Chapter 1**, two chemical approaches are investigated on various model plant polysaccharides.

The influence of various TEMPO/NaClO₂/NaOCl oxidation conditions on the oxidation of arabinoxylans is described in **Chapter 2**. The TEMPO/NaClO₂/NaOCl oxidation condition that yielded an arabinuronoxylan, with a structure closely related to the native arabinoxylan, was selected to oxidize several other arabinoxylans. Partial acid-hydrolysis of these TEMPO-oxidized arabinoxylans was studied for the release of diagnostic oligosaccharides, which was monitored by UHPLC-PGC-MS as described in **Chapter 3**.

The influence of various periodate oxidation conditions on the chemical structure of several plant polysaccharides is described in **Chapter 4**. The mildest periodate oxidation condition tested was selected to oxidize a wide range of plant polysaccharides to avoid the loss of the structural features of polysaccharides. Thermal hydrolysis of these periodate-oxidized plant polysaccharides was investigated for the generic formation of oligosaccharides that are polysaccharide structure-dependent, which was studied by MALDI-TOF MS as described in **Chapter 5**. In addition, the collected MALDI-TOF MS data was analyzed using chemometric tools to unambiguously classify polysaccharides, as described in **Chapter 5**.

In **Chapter 6** the main findings obtained in this PhD thesis are discussed and reflected upon. Remaining challenges faced in this thesis and promising approaches to solve them are also discussed. In addition, we discuss and compare the results obtained in this thesis against the typical enzymatic approaches used to study the structure of polysaccharides. Our results are also discussed against recently developed non-enzymatic polysaccharide depolymerization approaches used for polysaccharides fingerprinting. Moreover, the implications of our results for future research on the application of these non-enzymatic depolymerization approaches on other food polysaccharides and/or food products are discussed.



References

- [1] Harris, P.J. and B.G. Smith. Plant cell walls and cell-wall polysaccharides: Structures, properties and uses in food products. *International Journal of Food Science and Technology*. **2006**, 41, 129-143.
- [2] Saha, A., S. Tyagi, R.K. Gupta, and Y.K. Tyagi. Natural gums of plant origin as edible coatings for food industry applications. *Critical Reviews in Biotechnology*. **2017**, 37, 959-973.
- [3] Muxika, A., A. Etxabide, J. Uranga, P. Guerrero, and K. de la Caba. Chitosan as a bioactive polymer: Processing, properties and applications. *International Journal of Biological Macromolecules*. **2017**, 105, 1358-1368.
- [4] Habibi, H. and K. Khosravi-Darani. Effective variables on production and structure of xanthan gum and its food applications: A review. *Biocatalysis and Agricultural Biotechnology*. **2017**, 10, 130-140.
- [5] Liao, Y.C., C.C. Chang, D. Nagarajan, C.Y. Chen, and J.S. Chang. Algae-derived hydrocolloids in foods: applications and health-related issues. *Bioengineered*. **2021**, 12, 3787-3801.
- [6] Perin, D. and E. Murano. Starch polysaccharides in the human diet: Effect of the different source and processing on its absorption. *Natural Product Communications*. **2017**, 12, 837-853.
- [7] Swinkels, J.J.M. Composition and Properties of Commercial Native Starches. *Starch - Stärke*. **1985**, 37, 1-5.
- [8] Pérez, S., P.M. Baldwin, and D.J. Gallant, Chapter 5 - Structural Features of Starch Granules I, in *Starch (Third Edition)*, J. BeMiller and R. Whistler, Editors. **2009**, Academic Press: San Diego. 149-192.
- [9] Wang, S., C. Li, L. Copeland, Q. Niu, and S. Wang. Starch Retrogradation: A Comprehensive Review. *Comprehensive Reviews in Food Science and Food Safety*. **2015**, 14, 568-585.
- [10] Klemm, D., B. Heublein, H.P. Fink, and A. Bohn. Cellulose: Fascinating biopolymer and sustainable raw material. *Angewandte Chemie - International Edition*. **2005**, 44, 3358-3393.
- [11] Nishiyama, Y., P. Langan, and H. Chanzy. Crystal structure and hydrogen-bonding system in cellulose I β from synchrotron X-ray and neutron fiber diffraction. *Journal of the American Chemical Society*. **2002**, 124, 9074-9082.
- [12] Langan, P., Y. Nishiyama, and H. Chanzy. X-ray Structure of Mercerized Cellulose II at 1 Å Resolution. *Biomacromolecules*. **2001**, 2, 410-416.
- [13] Ebringerová, A. Structural diversity and application potential of hemicelluloses. *Macromolecular Symposia*. **2006**, 232, 1-12.
- [14] Scheller, H.V. and P. Ulvskov. Hemicelluloses. *Annual Review of Plant Biology*. **2010**, 61, 263-289.
- [15] Izydorczyk, M.S., 23 - Arabinoxylans, in *Handbook of Hydrocolloids (Second Edition)*, G.O. Phillips and P.A. Williams, Editors. **2009**, Woodhead Publishing. 653-692.
- [16] Tian, L., H. Gruppen, and H.A. Schols. Characterization of (Glucurono)arabinoxylans from Oats Using Enzymatic Fingerprinting. *Journal of Agricultural and Food Chemistry*. **2015**, 63, 10822-10830.
- [17] Girio, F.M., C. Fonseca, F. Carneiro, L.C. Duarte, S. Marques, and R. Bogel-Lukaszik. Hemicelluloses for fuel ethanol: A review. *Bioresource Technology*. **2010**, 101, 4775-4800.
- [18] Niño-Medina, G., E. Carvajal-Millan, A. Rascon-Chu, J.A. Marquez-Escalante, V. Guerrero, and E. Salas-Muñoz. Feruloylated arabinoxylans and arabinoxylan gels: Structure, sources and applications. *Phytochemistry Reviews*. **2010**, 9, 111-120.
- [19] Saulnier, L., C. Marot, E. Chanliaud, and J.F. Thibault. Cell wall polysaccharide interactions in maize bran. *Carbohydrate Polymers*. **1995**, 26, 279-287.
- [20] Smith, M.M. and R.D. Hartley. Occurrence and nature of ferulic acid substitution of cell-wall polysaccharides in graminaceous plants. *Carbohydrate Research*. **1983**, 118, 65-80.
- [21] Dey, P.M., *Biochemistry of plant galactomannans*, in *Advances in Carbohydrate Chemistry and Biochemistry*. 1978. p. 341-376.
- [22] Mulimani, V.H. and S.J. Prashanth. Investigating plant galactomannans. *Biochemistry and Molecular Biology Education*. **2002**, 30, 101-103.
- [23] Prajapati, V.D., G.K. Jani, N.G. Moradiya, N.P. Randeria, B.J. Nagar, N.N. Naikwadi, and B.C. Variya. Galactomannan: A versatile biodegradable seed polysaccharide. *International Journal of Biological Macromolecules*. **2013**, 60, 83-92.
- [24] Daas, P.J.H., H.A. Schols, and H.H.J. de Jongh. On the galactosyl distribution of commercial galactomannans. *Carbohydrate Research*. **2000**, 329, 609-619.
- [25] Pereira, H., J. Graca, and J.C. Rodrigues. Wood Chemistry in Relation to Quality. *ChemInform*. **2004**, 35, 53-86.
- [26] Lundqvist, J., A. Teleman, L. Junel, G. Zacchi, O. Dahlman, F. Tjerneld, and H. Stålbrand. Isolation and characterization of galactoglucomannan from spruce (*Picea abies*). *Carbohydrate Polymers*. **2002**, 48, 29-39.
- [27] Zhang, H., M. Yoshimura, K. Nishinari, M.A.K. Williams, T.J. Foster, and I.T. Norton. Gelation behaviour of konjac glucomannan with different molecular weights. *Biopolymers*. **2001**, 59, 38-50.



- [28] Mishra, A. and A.V. Malhotra. Tamarind xyloglucan: A polysaccharide with versatile application potential. *Journal of Materials Chemistry*. **2009**, 19, 8528-8536.
- [29] Maruyama, K., C. Goto, M. Numata, T. Suzuki, Y. Nakagawa, T. Hoshino, and T. Uchiyama. O-acetylated xyloglucan in extracellular polysaccharides from cell-suspension cultures of *Mentha*. *Phytochemistry*. **1996**, 41, 1309-1314.
- [30] Fry, S.C., W.S. York, P. Albersheim, and A. Darvill. An unambiguous nomenclature for xyloglucan-derived oligosaccharides. *PHYSIOLOGIA PLANTARUM*. **1993**, 89, 1-3.
- [31] Hilz, H., *Characterisation of cell wall polysaccharides in Bilberries and Black Currants*, in *Voragen, prof.dr.ir. A.G.J. (promotor); Schols, dr. H.A. (co-promotor); Wageningen Universiteit, 2007, ISBN 90-8504-624-6*. 2007. p. 158.
- [32] Fry, S.C., B.H.W.A. Nesselrode, J.G. Miller, and B.R. Mewburn. Mixed-linkage (1→3,1→4)-β-D-glucan is a major hemicellulose of *Equisetum* (horsetail) cell walls. *New Phytologist*. **2008**, 179, 104-115.
- [33] Mikkelsen, M.S., B.M. Jespersen, F.H. Larsen, A. Blennow, and S.B. Engelsen. Molecular structure of large-scale extracted β-glucan from barley and oat: Identification of a significantly changed block structure in a high β-glucan barley mutant. *Food Chemistry*. **2013**, 136, 130-138.
- [34] Wood, P.J. Cereal β-glucans in diet and health. *Journal of Cereal Science*. **2007**, 46, 230-238.
- [35] Cui, W., P.J. Wood, B. Blackwell, and J. Nikiforuk. Physicochemical properties and structural characterization by two-dimensional NMR spectroscopy of wheat β-D-glucan—comparison with other cereal β-D-glucans. *Carbohydrate Polymers*. **2000**, 41, 249-258.
- [36] Atmodjo, M.A., Z. Hao, and D. Mohnen, *Evolving views of pectin biosynthesis*, in *Annual Review of Plant Biology*. 2013. p. 747-779.
- [37] Ridley, B.L., M.A. O'Neill, and D. Mohnen. Pectins: structure, biosynthesis, and oligogalacturonide-related signaling. *Phytochemistry*. **2001**, 57, 929-967.
- [38] Schols, H.A. and A.G.J. Voragen, Complex Pectins: Structure elucidation using enzymes, in *Progress in Biotechnology*, J. Visser and A.G.J. Voragen, Editors. **1996**, Elsevier. 3-19.
- [39] Voragen, A.G.J., G.-J. Coenen, R.P. Verhoef, and H.A. Schols. Pectin, a versatile polysaccharide present in plant cell walls. *Structural Chemistry*. **2009**, 20, 263-275.
- [40] Ralet, M.C., M.J. Crépeau, and E. Bonnin. Evidence for a blockwise distribution of acetyl groups onto homogalacturonans from a commercial sugar beet (*Beta vulgaris*) pectin. *Phytochemistry*. **2008**, 69, 1903-1909.
- [41] Willats, W.G.T., C. Orfila, G. Limberg, H.C. Buchholt, G.J.W.M. Van Alebeek, A.G.J. Voragen, S.E. Marcus, T.M.I.E. Christensen, J.D. Mikkelsen, B.S. Murray, and J.P. Knox. Modulation of the degree and pattern of methyl-esterification of pectic homogalacturonan in plant cell walls: Implications for pectin methyl esterase action, matrix properties, and cell adhesion. *Journal of Biological Chemistry*. **2001**, 276, 19404-19413.
- [42] Kaya, M., A.G. Sousa, M.J. Crépeau, S.O. Sorensen, and M.C. Ralet. Characterization of citrus pectin samples extracted under different conditions: Influence of acid type and pH of extraction. *Annals of Botany*. **2014**, 114, 1319-1326.
- [43] Maxwell, E.G., N.J. Belshaw, K.W. Waldron, and V.J. Morris. Pectin – An emerging new bioactive food polysaccharide. *Trends in Food Science & Technology*. **2012**, 24, 64-73.
- [44] McNeil, M., A.G. Darvill, and P. Albersheim. Structure of Plant Cell Walls: X. RHAMNOGALACTURONAN I, A STRUCTURALLY COMPLEX PECTIC POLYSACCHARIDE IN THE WALLS OF SUSPENSION-CULTURED SYCAMORE CELLS I. *Plant Physiology*. **1980**, 66, 1128-1134.
- [45] Quémener, B., J.C. Cabrera Pino, M.C. Ralet, E. Bonnin, and J. Thibault. Assignment of acetyl groups to O-2 and/or O-3 of pectic oligogalacturonides using negative electrospray ionization ion trap mass spectrometry. *Journal of Mass Spectrometry*. **2003**, 38, 641-648.
- [46] Lerouge, P., M.A. O'Neill, A.G. Darvill, and P. Albersheim. Structural characterization of endoglycanase-generated oligoglycosyl side chains of rhamnogalacturonan I. *Carbohydrate Research*. **1993**, 243, 359-371.
- [47] Oomen, R.J.F.J., C.H.L. Doeswijk-Voragen, M.S. Bush, J.P. Vincken, B. Borkhardt, L.A.M. Van Den Broek, J. Corsar, P. Ulvskov, A.G.J. Voragen, M.C. McCann, and R.G.F. Visser. In muro fragmentation of the rhamnogalacturonan I backbone in potato (*Solanum tuberosum* L.) results in a reduction and altered location of the galactan and arabinan side-chains and abnormal periderm development. *Plant Journal*. **2002**, 30, 403-413.
- [48] Schols, H.A., M.A. Posthumus, and A.G.J. Voragen. Structural features of hairy regions of pectins isolated from apple juice produced by the liquefaction process. *Carbohydrate Research*. **1990**, 206, 117-129.
- [49] O'Neill, M.A., D. Warrenfeltz, K. Kates, P. Pellerin, T. Doco, A.G. Darvill, and P. Albersheim. Rhamnogalacturonan-II, a pectic polysaccharide in the walls of growing plant cell, forms a dimer that is covalently cross-linked by a borate ester. In vitro conditions for the formation and hydrolysis of the dimer. *Journal of Biological Chemistry*. **1996**, 271, 22923-22930.
- [50] Peterson, G. Gas-chromatographic analysis of sugars and related hydroxy acids as acyclic oxime and ester trimethylsilyl derivatives. *Carbohydrate Research*. **1974**, 33, 47-61.

- [51] Ruiz-Matute, A.I., O. Hernández-Hernández, S. Rodríguez-Sánchez, M.L. Sanz, and I. Martínez-Castro. Derivatization of carbohydrates for GC and GC-MS analyses. *Journal of Chromatography B: Analytical Technologies in the Biomedical and Life Sciences*. **2011**, 879, 1226-1240.
- [52] De Ruiter, G.A., H.A. Schols, A.G.J. Voragen, and F.M. Rombouts. Carbohydrate analysis of water-soluble uronic acid-containing polysaccharides with high-performance anion-exchange chromatography using methanolysis combined with TFA hydrolysis is superior to four other methods. *Analytical Biochemistry*. **1992**, 207, 176-185.
- [53] De Souza, A.C., T. Rietkerk, C.G.M. Selin, and P.P. Lankhorst. A robust and universal NMR method for the compositional analysis of polysaccharides. *Carbohydrate Polymers*. **2013**, 95, 657-663.
- [54] Beaugrand, J., G. Chambat, V.W.K. Wong, F. Goubet, C. Rémond, G. Paës, S. Benamrouche, P. Debeire, M. O'Donohue, and B. Chabbert. Impact and efficiency of GH10 and GH11 thermostable endoxylanases on wheat bran and alkali-extractable arabinoxylans. *Carbohydrate Research*. **2004**, 339, 2529-2540.
- [55] Huisman, M.M.H., A. Oosterveld, and H.A. Schols. Fast determination of the degree of methyl esterification of pectins by head-space GC. *Food Hydrocolloids*. **2004**, 18, 665-668.
- [56] Dourado, F., S.M. Cardoso, A.M.S. Silva, F.M. Gama, and M.A. Coimbra. NMR structural elucidation of the arabinan from *Prunus dulcis* immunobiological active pectic polysaccharides. *Carbohydrate Polymers*. **2006**, 66, 27-33.
- [57] Rondeau-Mouro, C., R. Ying, J. Ruellet, and L. Saulnier. Structure and organization within films of arabinoxylans extracted from wheat flour as revealed by various NMR spectroscopic methods. *Magnetic Resonance in Chemistry*. **2011**, 49, S85-S92.
- [58] Perrone, P., C.M. Hewage, A.R. Thomson, K. Bailey, I.H. Sadler, and S.C. Fry. Patterns of methyl and O-acetyl esterification in spinach pectins: new complexity. *Phytochemistry*. **2002**, 60, 67-77.
- [59] Silva Elipse, M.V. Advantages and disadvantages of nuclear magnetic resonance spectroscopy as a hyphenated technique. *Analytica Chimica Acta*. **2003**, 497, 1-25.
- [60] Winning, H., N. Viereck, L. Nørgaard, J. Larsen, and S.B. Engelsen. Quantification of the degree of blockiness in pectins using ¹H NMR spectroscopy and chemometrics. *Food Hydrocolloids*. **2007**, 21, 256-266.
- [61] Andersen, A.K., B. Larsen, and H. Grasdalen. Sequential structure by ¹H NMR as a direct assay for pectinesterase activity. *Carbohydrate Research*. **1995**, 273, 93-98.
- [62] Revanappa, S.B., C.D. Nandini, and P.V. Salimath. Structural characterisation of pentosans from hemicellulose B of wheat varieties with varying chapati-making quality. *Food Chemistry*. **2010**, 119, 27-33.
- [63] Kacuráková, M., P. Capek, V. Sasinková, N. Wellner, and A. Ebringerová. FT-IR study of plant cell wall model compounds: Pectic polysaccharides and hemicelluloses. *Carbohydrate Polymers*. **2000**, 43, 195-203.
- [64] Guo, Q., S.W. Cui, J. Kang, H. Ding, Q. Wang, and C. Wang. Non-starch polysaccharides from American ginseng: Physicochemical investigation and structural characterization. *Food Hydrocolloids*. **2015**, 44, 320-327.
- [65] Singthong, J., S. Ningsanond, S.W. Cui, and H. Douglas Goff. Extraction and physicochemical characterization of Krueo Ma Noy pectin. *Food Hydrocolloids*. **2005**, 19, 793-801.
- [66] Westphal, Y., H.A. Schols, A.G.J. Voragen, and H. Gruppen. MALDI-TOF MS and CE-LIF fingerprinting of plant cell wall polysaccharide digests as a screening tool for arabidopsis cell wall mutants. *Journal of Agricultural and Food Chemistry*. **2010**, 58, 4644-4652.
- [67] Bauer, S. Mass Spectrometry for Characterizing Plant Cell Wall Polysaccharides. *Frontiers in Plant Science*. **2012**, 3, 1-6.
- [68] Ruhaak, L.R., A.M. Deelder, and M. Wuhrer. Oligosaccharide analysis by graphitized carbon liquid chromatography-mass spectrometry. *Analytical and Bioanalytical Chemistry*. **2009**, 394, 163-174.
- [69] Singh, V., R. Sethi, A. Tewari, V. Srivastava, and R. Sanghi. Hydrolysis of plant seed gums by microwave irradiation. *Carbohydrate Polymers*. **2003**, 54, 523-525.
- [70] Singh, V. and A. Tiwari. Hydrolytic fragmentation of seed gums under microwave irradiation. *International Journal of Biological Macromolecules*. **2009**, 44, 186-189.
- [71] Prajapat, A.L. and P.R. Gogate. Depolymerization of guar gum solution using different approaches based on ultrasound and microwave irradiations. *Chemical Engineering and Processing: Process Intensification*. **2015**, 88, 1-9.
- [72] Van Craeyveld, V., U. Holopainen, E. Selinheimo, K. Poutanen, J.A. Delcour, and C.M. Courtin. Extensive dry ball milling of wheat and rye bran leads to in situ production of arabinoxylan oligosaccharides through nanoscale fragmentation. *Journal of Agricultural and Food Chemistry*. **2009**, 57, 8467-8473.
- [73] Li, L., S. Ma, L. Fan, C. Zhang, X. Pu, X. Zheng, and X. Wang. The influence of ultrasonic modification on arabinoxylans properties obtained from wheat bran. *International Journal of Food Science and Technology*. **2016**, 51, 2338-2344.
- [74] Ogutu, F.O. and T.-H. Mu. Ultrasonic degradation of sweet potato pectin and its antioxidant activity. *Ultrasonics Sonochemistry*. **2017**, 38, 726-734.



- [75] Lombard, V., H. Golaconda Ramulu, E. Drula, P.M. Coutinho, and B. Henrissat. The carbohydrate-active enzymes database (CAZy) in 2013. *Nucleic Acids Research*. **2014**, 42, D490-D495.
- [76] Lombard, V., T. Bernard, C. Rancurel, H. Brumer, P.M. Coutinho, and B. Henrissat. A hierarchical classification of polysaccharide lyases for glycogenomics. *Biochem J*. **2010**, 432, 437-44.
- [77] Bauer, S., P. Vasu, S. Persson, A.J. Mort, and C.R. Somerville. Development and Application of a Suite of Polysaccharide-Degrading Enzymes for Analyzing Plant Cell Walls. *Proceedings of the National Academy of Sciences of the United States of America*. **2006**, 103, 11417-11422.
- [78] Murciano Martínez, P., M.A. Kabel, and H. Gruppen. Delignification outperforms alkaline extraction for xylan fingerprinting of oil palm empty fruit bunch. *Carbohydrate Polymers*. **2016**, 153, 356-363.
- [79] McCleary, B.V., V.A. McKie, A. Draga, E. Rooney, D. Mangan, and J. Larkin. Hydrolysis of wheat flour arabinoxylan, acid-debranched wheat flour arabinoxylan and arabino-xylo-oligosaccharides by β -xylanase, α -L-arabinofuranosidase and β -xylosidase. *Carbohydrate Research*. **2015**, 407, 79-96.
- [80] Kormelink, F.J.M., R.A. Hoffmann, H. Gruppen, A.G.J. Voragen, J.P. Kamerling, and J.F.G. Vliegenthart. Characterisation by ¹H NMR spectroscopy of oligosaccharides derived from alkali-extractable wheat-flour arabinoxylan by digestion with endo-(1 \rightarrow 4)- β -D-xylanase III from *Aspergillus awamori*. *Carbohydrate Research*. **1993**, 249, 369-382.
- [81] Viëtor, R.J., F.J.M. Kormelink, S.A.G.F. Angelino, and A.G.J. Voragen. Substitution patterns of water-unextractable arabinoxylans from barley and malt. *Carbohydrate Polymers*. **1994**, 24, 113-118.
- [82] Remoroza, C., S. Broxterman, H. Gruppen, and H.A. Schols. Two-step enzymatic fingerprinting of sugar beet pectin. *Carbohydrate Polymers*. **2014**, 108, 338-347.
- [83] Remoroza, C., H.C. Buchholt, H. Gruppen, and H.A. Schols. Descriptive parameters for revealing substitution patterns of sugar beet pectins using pectolytic enzymes. *Carbohydrate Polymers*. **2014**, 101, 1205-1215.
- [84] Remoroza, C., S. Cord-Landwehr, A.G.M. Leijdekkers, B.M. Moerschbacher, H.A. Schols, and H. Gruppen. Combined HILIC-ELSD/ESI-MS n enables the separation, identification and quantification of sugar beet pectin derived oligomers. *Carbohydrate Polymers*. **2012**, 90, 41-48.
- [85] Ognyanov, M., C. Remoroza, H.A. Schols, Y. Georgiev, M. Kratchanova, and C. Kratchanov. Isolation and structure elucidation of pectic polysaccharide from rose hip fruits (*Rosa canina* L.). *Carbohydrate Polymers*. **2016**, 151, 803-811.
- [86] Leijdekkers, A.G.M., J.H. Huang, E.J. Bakx, H. Gruppen, and H.A. Schols. Identification of novel isomeric pectic oligosaccharides using hydrophilic interaction chromatography coupled to traveling-wave ion mobility mass spectrometry. *Carbohydrate Research*. **2015**, 404, 1-8.
- [87] Leijdekkers, A.G.M., M.G. Sanders, H.A. Schols, and H. Gruppen. Characterizing plant cell wall derived oligosaccharides using hydrophilic interaction chromatography with mass spectrometry detection. *Journal of Chromatography A*. **2011**, 1218, 9227-9235.
- [88] Hemsforth, G.R., B. Henrissat, G.J. Davies, and P.H. Walton. Discovery and characterization of a new family of lytic polysaccharide monoxygenases. *Nature chemical biology*. **2014**, 10, 122-126.
- [89] Frommhagen, M., S. Sforza, A.H. Westphal, J. Visser, S.W.A. Hinz, M.J. Koetsier, W.J.H. van Berkel, H. Gruppen, and M.A. Kabel. Discovery of the combined oxidative cleavage of plant xylan and cellulose by a new fungal polysaccharide monoxygenase. *Biotechnology for Biofuels*. **2015**, 8, 101.
- [90] Frommhagen, M., M.J. Koetsier, A.H. Westphal, J. Visser, S.W.A. Hinz, J.-P. Vincken, W.J.H. van Berkel, M.A. Kabel, and H. Gruppen. Lytic polysaccharide monoxygenases from *Myceliophthora thermophila* C1 differ in substrate preference and reducing agent specificity. *Biotechnology for Biofuels*. **2016**, 9, 186.
- [91] Kormelink, F.J.M., M.J.F. Searle-Van Leeuwen, T.M. Wood, and A.G.J. Voragen. Purification and characterization of three endo-(1,4)- β -xylanases and one β -xylosidase from *Aspergillus awamori*. *Journal of Biotechnology*. **1993**, 27, 249-265.
- [92] van Gool, M.P., G.C.J. van Muiswinkel, S.W.A. Hinz, H.A. Schols, A.P. Sinitzyn, and H. Gruppen. Two novel GH11 endo-xylanases from *Myceliophthora thermophila* C1 act differently toward soluble and insoluble xylans. *Enzyme and Microbial Technology*. **2013**, 53, 25-32.
- [93] Möller, M.S. and B. Svensson. Structural biology of starch-degrading enzymes and their regulation. *Current Opinion in Structural Biology*. **2016**, 40, 33-42.
- [94] Beldman, G., M.F. Searle-Van Leeuwen, F.M. Rombouts, and F.G. Voragen. The cellulase of *Trichoderma viride*. Purification, characterization and comparison of all detectable endoglucanases, exoglucanases and beta-glucohydrolases. *European journal of biochemistry*. **1985**, 146, 301-308.
- [95] Biely, P., M. Vršanská, M. Tenkanen, and D. Kluepfel. Endo- β -1,4-xylanase families: Differences in catalytic properties. *Journal of Biotechnology*. **1997**, 57, 151-166.
- [96] Paës, G., J.G. Berrin, and J. Beaugrand. GH11 xylanases: Structure/function/properties relationships and applications. *Biotechnology Advances*. **2012**, 30, 564-592.

- [97] Pell, G., E.J. Taylor, T.M. Gloster, J.P. Turkenburg, C.M.G.A. Fontes, L.M.A. Ferreira, T. Nagy, S.J. Clark, G.J. Davies, and H.J. Gilbert. The Mechanisms by Which Family 10 Glycoside Hydrolases Bind Decorated Substrates. *Journal of Biological Chemistry*. **2004**, 279, 9597-9605.
- [98] Pauly, M., L.N. Andersen, S. Kauppinen, L.V. Kofod, W.S. York, P. Albersheim, and A. Darvill. A xyloglucan-specific endo-beta-1,4-glucanase from *Aspergillus aculeatus*: expression cloning in yeast, purification and characterization of the recombinant enzyme. *Glycobiology*. **1999**, 9, 93-100.
- [99] Rakha, A., L. Saulnier, P. Man, and R. Andersson. Enzymatic fingerprinting of arabinoxylan and β -glucan in triticale, barley and tritordeum grains. *Carbohydrate Polymers*. **2012**, 90, 1226-1234.
- [100] Mill, P.J. and R. Tuttobello. The pectic enzymes of *Aspergillus niger*. 2. Endopolygalacturonase. *The Biochemical journal*. **1961**, 79, 57-64.
- [101] Pařenicova, L., H.C.M. Kester, J.A.E. Benen, and J. Visser. Characterization of a novel endopolygalacturonase from *Aspergillus niger* with unique kinetic properties. *FEBS Letters*. **2000**, 467, 333-336.
- [102] Mutenda, K.E., R. Korner, T.M.I.E. Christensen, J. Mikkelsen, and P. Roepstorff. Application of mass spectrometry to determine the activity and specificity of pectin lyase A. *Carbohydrate Research*. **2002**, 337, 1217-1227.
- [103] Kester, H.C.M. and J. Visser. Purification and characterization of pectin lyase B, a novel pectinolytic enzyme from *Aspergillus niger*. *FEMS Microbiology Letters*. **1994**, 120, 63-67.
- [104] Roy, C., H. Kester, J. Visser, V. Shevchik, N. Hugouvieux-Cotte-Pattat, J. Robert-Baudouy, and J. Benen. Modes of action of five different endopectate lyases from *Erwinia chrysanthemi* 3937. *Journal of Bacteriology*. **1999**, 181, 3705-3709.
- [105] Mutter, M., C.M.G.C. Renard, G. Beldman, H.A. Schols, and A.G.J. Voragen. Mode of action of RG-hydrolase and RG-lyase toward rhamnogalacturonan oligomers. Characterization of degradation products using RG-rhamnohydrolase and RG-galacturonohydrolase. *Carbohydrate Research*. **1998**, 311, 155-164.
- [106] Schols, H.A., C.C.J.M. Geraeds, M.F. Searle-van Leeuwen, F.J.M. Kormelink, and A.G.J. Voragen. Rhamnogalacturonase: a novel enzyme that degrades the hairy regions of pectins. *Carbohydrate Research*. **1990**, 206, 105-115.
- [107] Mutter, M., L.J. Colquhoun, G. Beldman, H.A. Schols, E.J. Bakx, and A.G.J. Voragen. Characterization of recombinant rhamnogalacturonan α -L-rhamnopyranosyl-(1,4)- α -D-galactopyranosyluronide lyase from *Aspergillus aculeatus*: An enzyme that fragments rhamnogalacturonan I regions of pectin. *Plant Physiology*. **1998**, 117, 141-152.
- [108] Leal, T.F. and I.d. Sa-Nogueira. Purification, characterization and functional analysis of an endo-arabinanase (AbnA) from *Bacillus subtilis*. *FEMS Microbiology Letters*. **2004**, 241, 41-48.
- [109] Kuhnel, S., S.W.A. Hinz, L. Pouvreau, J. Wery, H.A. Schols, and H. Gruppen. *Chrysosporium lucknowense* arabinohydrolases effectively degrade sugar beet arabinan. *Bioresource Technology*. **2010**, 101, 8300-8307.
- [110] Kotake, T., N. Hirata, Y. Degi, M. Ishiguro, K. Kitazawa, R. Takata, H. Ichinose, S. Kaneko, K. Igarashi, M. Samejima, and Y. Tsumuraya. Endo- β -1,3-galactanase from winter mushroom *Flammulina velutipes*. *Journal of Biological Chemistry*. **2011**, 286, 27848-27854.
- [111] Labavitch, J.M., L.E. Freeman, and P. Albersheim. Structure of plant cell walls. Purification and characterization of a β 1,4 galactanase which degrades a structural component of the primary cell walls of dicots. *Journal of Biological Chemistry*. **1976**, 251, 5904-5910.
- [112] Beldman, G., J.P. Vincken, H.A. Schols, P.J.A. Meeuwssen, M. Herweijer, and A.G.J. Voragen. Degradation of Differently Substituted Xylogalacturonans by Endoxylogalacturonan Hydrolase and Endopolygalacturonases. *Biocatalysis and Biotransformation*. **2003**, 21, 189-198.
- [113] Zandleven, J., G. Beldman, M. Bosveld, J. Benen, and A. Voragen. Mode of action of xylogalacturonan hydrolase towards xylogalacturonan and xylogalacturonan oligosaccharides. *The Biochemical journal*. **2005**, 387, 719-725.
- [114] Limberg, G., R. Korner, H.C. Buchholt, T.M.I.E. Christensen, P. Roepstorff, and J.D. Mikkelsen. Analysis of different de-esterification mechanisms for pectin by enzymatic fingerprinting using endopectin lyase and endopolygalacturonase II from *A. Niger*. *Carbohydrate Research*. **2000**, 327, 293-307.
- [115] Broxterman, S.E., P. Picouet, and H.A. Schols. Acetylated pectins in raw and heat processed carrots. *Carbohydrate Polymers*. **2017**, 177, 58-66.
- [116] Westphal, Y., H.A. Schols, A.G.J. Voragen, and H. Gruppen. Introducing porous graphitized carbon liquid chromatography with evaporative light scattering and mass spectrometry detection into cell wall oligosaccharide analysis. *Journal of Chromatography A*. **2010**, 1217, 689-695.
- [117] Lerouxel, O., T.S. Choo, M. Seveno, B.r. Usadel, L.c. Faye, P. Lerouge, and M. Pauly. Rapid Structural Phenotyping of Plant Cell Wall Mutants by Enzymatic Oligosaccharide Fingerprinting. *Plant Physiology*. **2002**, 130, 1754-1763.

- [118] Grün, C.H., P. Sanders, M. Van Der Burg, E. Schuurbijs, L. Van Adrichem, E.J.J. Van Velzen, N. De Roo, K. Brunt, Y. Westphal, and H.A. Schols. Strategy to identify and quantify polysaccharide gums in gelled food concentrates. *Food Chemistry*. **2015**, 166, 42-49.
- [119] Westphal, Y., S. Kühnel, H.A. Schols, A.G.J. Voragen, and H. Gruppen. LC/CE-MS tools for the analysis of complex arabino-oligosaccharides. *Carbohydrate Research*. **2010**, 345, 2239-2251.
- [120] Westereng, B., J.W. Agger, S.J. Horn, G. Vaaje-Kolstad, F.L. Aachmann, Y.H. Stenstrom, and V.G.H. Eijssink. Efficient separation of oxidized cello-oligosaccharides generated by cellulose degrading lytic polysaccharide monooxygenases. *Journal of Chromatography A*. **2013**, 1271, 144-152.
- [121] Westereng, B., M.Ø. Arntzen, F.L. Aachmann, A. Várnai, V.G.H. Eijssink, and J.W. Agger. Simultaneous analysis of C1 and C4 oxidized oligosaccharides, the products of lytic polysaccharide monooxygenases acting on cellulose. *Journal of Chromatography A*. **2016**, 1445, 46-54.
- [122] Ordaz-Ortiz, J.J., M.F. Devaux, and L. Saulnier. Classification of wheat varieties based on structural features of arabinoxylans as revealed by endoxylanase treatment of flour and grain. *Journal of Agricultural and Food Chemistry*. **2005**, 53, 8349-8356.
- [123] Gross, J.R.H., *Mass spectrometry : a textbook*. 2017, Cham, Switzerland: Springer.
- [124] Ralet, M.-C., J.C. Cabrera, E. Bonnin, B. Quémener, P. Hellin, and J.-F. Thibault. Mapping sugar beet pectin acetylation pattern. *Phytochemistry*. **2005**, 66, 1832-1843.
- [125] Yu, G., H. Guan, A.S. Ioanoviciu, S.A. Sikkander, C. Thanawiroon, J.K. Tobacman, T. Toida, and R.J. Linhardt. Structural studies on κ -carrageenan derived oligosaccharides. *Carbohydrate Research*. **2002**, 337, 433-440.
- [126] Guo, Q., S.W. Cui, Q. Wang, X. Hu, J. Kang, and R.Y. Yada. Structural characterization of a low-molecular-weight heteropolysaccharide (glucomannan) isolated from *Artemisia sphaerocephala* Krasch. *Carbohydrate Research*. **2012**, 350, 31-39.
- [127] Cao, J., C. Wen, J. Lu, N. Teng, S. Song, and B. Zhu. Characterization of acidic polysaccharides from the mollusks through acid hydrolysis. *Carbohydrate Polymers*. **2015**, 130, 268-274.
- [128] Biermann, C.J., *Hydrolysis and other Cleavages of Glycosidic Linkages in Polysaccharides*, in *Advances in Carbohydrate Chemistry and Biochemistry*. 1988. p. 251-271.
- [129] Yang, B., G. Yu, X. Zhao, G. Jiao, S. Ren, and W. Chai. Mechanism of mild acid hydrolysis of galactan polysaccharides with highly ordered disaccharide repeats leading to a complete series of exclusively odd-numbered oligosaccharides. *FEBS Journal*. **2009**, 276, 2125-2137.
- [130] Lin, Q., H. Li, J. Ren, A. Deng, W. Li, C. Liu, and R. Sun. Production of xylooligosaccharides by microwave-induced, organic acid-catalyzed hydrolysis of different xylan-type hemicelluloses: Optimization by response surface methodology. *Carbohydrate Polymers*. **2017**, 157, 214-225.
- [131] Bemiller, J.N., *Acid-Catalyzed Hydrolysis of Glycosides*, in *Advances in Carbohydrate Chemistry*, M.L. Wolfrom and R.S. Tipson, Editors. **1967**, Academic Press. 25-108.
- [132] Mort, A.J., F. Qiu, and N.O. Maness. Determination of the pattern of methyl esterification in pectin. Distribution of contiguous nonesterified residues. *Carbohydrate Research*. **1993**, 247, 21-35.
- [133] De, K.K. and T.E. Timell. The acid hydrolysis of glycosides: IV. Hydrolysis of aldobiouronic acids. *Carbohydrate Research*. **1967**, 4, 177-181.
- [134] Garna, H., N. Mabon, K. Nott, B. Wathelet, and M. Paquot. Kinetic of the hydrolysis of pectin galacturonic acid chains and quantification by ionic chromatography. *Food Chemistry*. **2006**, 96, 477-484.
- [135] Reis, A., M.R.M. Domingues, A.J. Ferrer-Correia, and M.A. Coimbra. Structural characterisation by MALDI-MS of olive xylo-oligosaccharides obtained by partial acid hydrolysis. *Carbohydrate Polymers*. **2003**, 53, 101-107.
- [136] Van Craeyveld, V., J.A. Delcour, and C.M. Courtin. Extractability and chemical and enzymic degradation of psyllium (*Plantago ovata* Forsk) seed husk arabinoxylans. *Food Chemistry*. **2009**, 112, 812-819.
- [137] Whistler, R.L. and W.M. Corbett. Oligosaccharides from Partial Acid Hydrolysis of Corn Fiber Hemicellulose. *Journal of the American Chemical Society*. **1955**, 77, 6328-6330.
- [138] Saulnier, L., J. Vigouroux, and J.-F. Thibault. Isolation and partial characterization of feruloylated oligosaccharides from maize bran. *Carbohydrate Research*. **1995**, 272, 241-253.
- [139] Schendel, R.R., A. Becker, C.E. Tyl, and M. Bunzel. Isolation and characterization of feruloylated arabinoxylan oligosaccharides from the perennial cereal grain intermediate wheat grass (*Thinopyrum intermedium*). *Carbohydrate Research*. **2015**, 407, 16-25.
- [140] Coimbra, M.A., K.W. Waldron, and R.R. Selvendran. Isolation and characterisation of cell wall polymers from the heavily lignified tissues of olive (*Olea europaea*) seed hull. *Carbohydrate Polymers*. **1995**, 27, 285-294.
- [141] Havlicek, J. and O. Samuelson. Chromatography of oligosaccharides from xylan by various techniques. *Carbohydrate Research*. **1972**, 22, 307-316.
- [142] Jacobs, A., P.T. Larsson, and O. Dahlman. Distribution of uronic acids in xylans from various species of soft- and hardwood as determined by MALDI Mass spectrometry. *Biomacromolecules*. **2001**, 2, 979-990.

- [143] Shimizu, K., M. Hashi, and K. Sakurai. Isolation from a softwood xylan of oligosaccharides containing two 4-O-methyl-d-glucuronic acid residues. *Carbohydrate Research*. **1978**, 62, 117-126.
- [144] Komiyama, H., A. Kato, H. Aimi, J. Ogihara, and K. Shimizu. Chemical structure of kenaf xylan. *Carbohydrate Polymers*. **2008**, 72, 638-645.
- [145] Gupta, A.K. and S. Bose. Structure of the d-galacto-d-mannan isolated from the seeds of *Melilotus indica* All. *Carbohydrate Research*. **1986**, 153, 69-77.
- [146] Petkowicz, C.L.O., M.R. Sierakowski, J.L.M.S. Ganter, and F. Reicher. Galactomannans and arabinans from seeds of caesalpiniaaceae. *Phytochemistry*. **1998**, 49, 737-743.
- [147] Marry, M., D.M. Cavalier, J.K. Schnurr, J. Netland, Z. Yang, V. Pezeshk, W.S. York, M. Pauly, and A.R. White. Structural characterization of chemically and enzymatically derived standard oligosaccharides isolated from partially purified tamarind xyloglucan. *Carbohydrate Polymers*. **2002**, 51, 347-356.
- [148] Guillon, F. and J.F. Thibault. Methylation analysis and mild acid hydrolysis of the "hairy" fragments of sugar-beet pectins. *Carbohydrate Research*. **1989**, 190, 85-96.
- [149] Séveno, M., A. Voxel, C. Rihouey, A.-m. Wu, T. Ishii, C. Chevalier, M.C. Ralet, A. Driouich, A. Marchant, and P. Lerouge. Structural characterisation of the pectic polysaccharide rhamnogalacturonan II using an acidic fingerprinting methodology: An International Journal of Plant Biology. *Planta*. **2009**, 230, 947-57.
- [150] Thibault, J.F., C.M.G.C. Renard, M.A.V. Axelos, P. Roger, and M.J. Crépeau. Studies of the length of homogalacturonic regions in pectins by acid hydrolysis. *Carbohydrate Research*. **1993**, 238, 271-286.
- [151] Round, A.N., N.M. Rigby, A.J. MacDougall, and V.J. Morris. A new view of pectin structure revealed by acid hydrolysis and atomic force microscopy. *Carbohydrate Research*. **2010**, 345, 487-497.
- [152] Bowman, M.J., B.S. Dien, P.J. O'Bryan, G. Sarath, and M.A. Cotta. Selective chemical oxidation and depolymerization of (*Panicum virgatum* L.) xylan with switchgrass oligosaccharide product analysis by mass spectrometry. *Rapid Communications in Mass Spectrometry*. **2011**, 25, 941-950.
- [153] Pierre, G., C. Punta, C. Delattre, L. Melone, P. Dubessay, A. Fiorati, N. Pastori, Y.M. Galante, and P. Michaud. TEMPO-mediated oxidation of polysaccharides: An ongoing story. *Carbohydrate Polymers*. **2017**, 165, 71-85.
- [154] Nechyporchuk, O., M.N. Belgacem, and J. Bras. Production of cellulose nanofibrils: A review of recent advances. *Industrial Crops and Products*. **2016**, 93, 2-25.
- [155] de Nooy, A.E.J., A.C. Besemer, and H. van Bekkum. Highly selective tempo mediated oxidation of primary alcohol groups in polysaccharides. *Recueil des Travaux Chimiques des Pays-Bas*. **1994**, 113, 165-166.
- [156] Spier, V.C., M.R. Sierakowski, W.F. Reed, and R.A. de Freitas. Polysaccharide depolymerization from TEMPO-catalysis: Effect of TEMPO concentration. *Carbohydrate Polymers*. **2017**, 170, 140-147.
- [157] Börjesson, M. and G. Westman. Branching of hemicelluloses through an azetidinium salt ring-opening reaction. *Carbohydrate Research*. **2016**, 428, 23-30.
- [158] Chatterjee, D., T. Halder, N.P. Pathak, A. Paul, Rajkamal, and S. Yadav. DAIB/TEMPO mediated synthesis of anomeric lactones from anomeric hydroxides. *Tetrahedron Letters*. **2017**, 58, 1943-1946.
- [159] Tojo, G. and M. Fernández. *Oxidation of primary alcohols to carboxylic acids : a guide to current common practice*. 2007, Springer: New York.
- [160] Saito, T., M. Hirota, N. Tamura, and A. Isogai. Oxidation of bleached wood pulp by TEMPO/NaClO/NaClO₂ system: Effect of the oxidation conditions on carboxylate content and degree of polymerization. *Journal of Wood Science*. **2010**, 56, 227-232.
- [161] Tamura, N., M. Hirota, T. Saito, and A. Isogai. Oxidation of curdlan and other polysaccharides by 4-acetamide-TEMPO/NaClO/NaClO₂ under acid conditions. *Carbohydrate Polymers*. **2010**, 81, 592-598.
- [162] Tanaka, R., T. Saito, and A. Isogai. Cellulose nanofibrils prepared from softwood cellulose by TEMPO/NaClO/NaClO₂ systems in water at pH 4.8 or 6.8. *International Journal of Biological Macromolecules*. **2012**, 51, 228-234.
- [163] Meng, Q., S. Fu, and L.A. Lucia. The role of heteropolysaccharides in developing oxidized cellulose nanofibrils. *Carbohydrate Polymers*. **2016**, 144, 187-195.
- [164] Hao, J., J. Lu, N. Xu, R.J. Linhardt, and Z. Zhang. Specific oxidation pattern of soluble starch with TEMPO-NaBr-NaClO system. *Carbohydrate Polymers*. **2016**, 146, 238-244.
- [165] Sakakibara, C.N., M.R. Sierakowski, N. Lucyszyn, and R.A. de Freitas. TEMPO-mediated oxidation on galactomannan: Gal/Man ratio and chain flexibility dependence. *Carbohydrate Polymers*. **2016**, 153, 371-378.
- [166] ter Haar, R., J.W. Timmermans, T.M. Slaghek, F.E.M. Van Dongen, H.A. Schols, and H. Gruppen. TEMPO oxidation of gelatinized potato starch results in acid resistant blocks of glucuronic acid moieties. *Carbohydrate Polymers*. **2010**, 81, 830-838.
- [167] Parikka, K., I. Nikkilä, L. Pitkänen, A. Ghafar, T. Sontag-Strohm, and M. Tenkanen. Laccase/TEMPO oxidation in the production of mechanically strong arabinoxylan and glucomannan aerogels. *Carbohydrate Polymers*. **2017**, 175, 377-386.
- [168] Kristiansen, K.A., A. Potthast, and B.E. Christensen. Periodate oxidation of polysaccharides for modification of chemical and physical properties. *Carbohydrate Research*. **2010**, 345, 1264-1271.



- [169] Perlin, A.S. Glycol-Cleavage Oxidation. *Advances in Carbohydrate Chemistry and Biochemistry*. **2006**, 60, 183-250.
- [170] Halsall, T.G., E.L. Hirst, and J.K.N. Jones. Oxidation of carbohydrates by the periodate ion. *Journal of the Chemical Society (Resumed)*. **1947**. 1427-1432.
- [171] Stenutz, R. *A practical guide to structural analysis of carbohydrates - Smith (periodate) degradation*. 2013. Available from: <http://www.stenutz.eu/sop/sop101.html>.
- [172] Chemin, M., A. Rakotovelofy, F. Ham-Pichavant, G. Chollet, D. Da Silva Perez, M. Petit-Conil, H. Cramail, and S. Grelier. Synthesis and characterization of functionalized 4-O-methylglucuronoxylan derivatives. *Holzforschung*. **2015**, 69, 713-720.
- [173] Chetouani, A., N. Follain, S. Marais, C. Rihouey, M. Elkolli, M. Bounekhel, D. Benachour, and D. Le Cerf. Physicochemical properties and biological activities of novel blend films using oxidized pectin/chitosan. *International Journal of Biological Macromolecules*. **2017**, 97, 348-356.
- [174] Kochumalayil, J.J., Q. Zhou, W. Kasai, and L.A. Berglund. Regioselective modification of a xyloglucan hemicellulose for high-performance biopolymer barrier films. *Carbohydrate Polymers*. **2013**, 93, 466-472.
- [175] Ding, W., J. Zhou, Y. Zeng, Y.N. Wang, and B. Shi. Preparation of oxidized sodium alginate with different molecular weights and its application for crosslinking collagen fiber. *Carbohydrate Polymers*. **2017**, 157, 1650-1656.
- [176] Sirviö, J.A., H. Liimatainen, M. Visanko, and J. Niinimäki. Optimization of dicarboxylic acid cellulose synthesis: Reaction stoichiometry and role of hypochlorite scavengers. *Carbohydrate Polymers*. **2014**, 114, 73-77.
- [177] Spedding, H. 628. Infrared spectra of periodate-oxidised cellulose. *Journal of the Chemical Society (Resumed)*. **1960**. 3147-3152.
- [178] Sulaeva, I., K.M. Klinger, H. Amer, U. Henniges, T. Rosenau, and A. Potthast. Determination of molar mass distributions of highly oxidized dialdehyde cellulose by size exclusion chromatography and asymmetric flow field-flow fractionation. *Cellulose*. **2015**, 22, 3569-3581.
- [179] Amer, H., T. Nypelö, I. Sulaeva, M. Bacher, U. Henniges, A. Potthast, and T. Rosenau. Synthesis and Characterization of Periodate-Oxidized Polysaccharides: Dialdehyde Xylan (DAX). *Biomacromolecules*. **2016**, 17, 2972-2980.
- [180] Gupta, B., M. Tummalapalli, B.L. Deopura, and M.S. Alam. Functionalization of pectin by periodate oxidation. *Carbohydrate Polymers*. **2013**, 98, 1160-1165.
- [181] Sirvio, J., U. Hyvakkö, H. Liimatainen, J. Niinimäki, and O. Hormi. Periodate oxidation of cellulose at elevated temperatures using metal salts as cellulose activators. *Carbohydrate Polymers*. **2011**, 83, 1293-1297.
- [182] Li, H., B. Wu, C. Mu, and W. Lin. Concomitant degradation in periodate oxidation of carboxymethyl cellulose. *Carbohydrate Polymers*. **2011**, 84, 881-886.
- [183] Simi, C.K. and T.E. Abraham. Transparent xyloglucan-chitosan complex hydrogels for different applications. *Food Hydrocolloids*. **2010**, 24, 72-80.
- [184] Vold, I.M.N. and B.E. Christensen. Periodate oxidation of chitosans with different chemical compositions. *Carbohydrate Research*. **2005**, 340, 679-684.
- [185] Chemin, M., A. Rakotovelofy, F. Ham-Pichavant, G. Chollet, D. Da Silva Perez, M. Petit-Conil, H. Cramail, and S. Grelier. Periodate oxidation of 4-O-methylglucuronoxylans: Influence of the reaction conditions. *Carbohydrate Polymers*. **2016**, 142, 45-50.
- [186] Kholiya, F., J.P. Chaudhary, N. Vadodariya, and R. Meena. Synthesis of bio-based aldehyde from seaweed polysaccharide and its interaction with bovine serum albumin. *Carbohydrate Polymers*. **2016**, 150, 278-285.
- [187] Morelle, W., J. Lemoine, and G. Strecker. Structural analysis of O-linked oligosaccharide-alditols by electrospray-tandem mass spectrometry after mild periodate oxidation and derivatization with 2-aminopyridine. *Analytical Biochemistry*. **1998**, 259, 16-27.
- [188] Goldstein, I.J. Controlled degradation of polysaccharides by periodate oxidation, reduction, and hydrolysis. *Methods in Carbohydrate Chemistry*. **1965**, 5, 361-370.
- [189] Ai, L., Q. Guo, H. Ding, B. Guo, W. Chen, and S.W. Cui. Structure characterization of exopolysaccharides from *Lactobacillus casei* LC2W from skim milk. *Food Hydrocolloids*. **2016**, 56, 134-143.
- [190] Duan, J., Y. Zheng, Q. Dong, and J. Fang. Structural analysis of a pectic polysaccharide from the leaves of *Diospyros kaki*. *Phytochemistry*. **2004**, 65, 609-615.
- [191] Höjje, A., C. Sandström, J.P. Roubroeks, R. Andersson, S. Gohil, and P. Gatenholm. Evidence of the presence of 2-O-β-d-xylopyranosyl-α-l-arabinofuranose side chains in barley husk arabinoxylan. *Carbohydrate Research*. **2006**, 341, 2959-2966.
- [192] Rao, R.S.P. and G. Muralikrishna. Structural characteristics of water-soluble feruloyl arabinoxylans from rice (*Oryza sativa*) and ragi (finger millet, *Eleusine coracana*): Variations upon malting. *Food Chemistry*. **2007**, 104, 1160-1170.
- [193] Aspinall, G.O. and K.M. Ross. The degradation of two periodate-oxidised arabinoxylans. *Journal of the Chemical Society (Resumed)*. **1963**. 1676-1680.

- [194] Gruppen, H., F.J.M. Kornelink, and A.G.J. Voragen. Water-unextractable Cell Wall Material from Wheat Flour. 3. A Structural Model for Arabinoxylans. *Journal of Cereal Science*. **1993**, 18, 111-128.
- [195] Revanappa, S.B., C.D. Nandini, and P.V. Salimath. Structural variations of arabinoxylans extracted from different wheat (*Triticum aestivum*) cultivars in relation to chapati-quality. *Food Hydrocolloids*. **2015**, 43, 736-742.
- [196] Aman, P. and S. Bengtsson. Periodate oxidation and degradation studies on the major water-soluble arabinoxylan in rye grain. *Carbohydrate Polymers*. **1991**, 15, 405-414.
- [197] Dervilly-Pinel, G., V. Tran, and L. Saulnier. Investigation of the distribution of arabinose residues on the xylan backbone of water-soluble arabinoxylans from wheat flour. *Carbohydrate Polymers*. **2004**, 55, 171-177.
- [198] Ebringerová, A., Z. Hromádková, E. Petráková, and M. Hricovini. Structural features of a water-soluble l-arabino-d-xylan from rye bran. *Carbohydrate Research*. **1990**, 198, 57-66.
- [199] Woodward, J.R., G.B. Fincher, and B.A. Stone. Water-soluble (1→3), (1→4)- β -D-glucans from barley (*Hordeum vulgare*) endosperm. II. Fine structure. *Carbohydrate Polymers*. **1983**, 3, 207-225.
- [200] Rodge, A.B., V.D. Pawar, and G.M. Machewad. ISOLATION, PURIFICATION AND CHARACTERIZATION OF β -GLUCANS FROM INDIAN BARLEY. *Journal of Food Processing and Preservation*. **2010**, 34, 666-679.
- [201] Fleming, M. and K. Kawakami. Studies of the fine structure of β -d-glucans of barleys extracted at different temperatures. *Carbohydrate Research*. **1977**, 57, 15-23.
- [202] Tomoda, M., N. Shimizu, and R. Gonda. Pectic Substances. II. The Location of O-Acetyl Groups and the Smith Degradation of Zizyphus-Pectin A. *Chemical and Pharmaceutical Bulletin*. **1985**, 33, 4017-4020.
- [203] Hu, C., Q. Kong, D. Yang, and Y. Pan. Isolation and structural characterization of a novel galactomannan from *Eremurus anisopterus* (Ker. et Kir) Regel roots. *Carbohydrate Polymers*. **2011**, 84, 402-406.
- [204] Gupta, D.S., B. Jann, K.S. Bajpai, and S.C. Sharma. Structure of a galactomannan from *Cassia alata* seed. *Carbohydrate Research*. **1987**, 162, 271-276.
- [205] Veelaert, S., D. de Wit, K.F. Gottlieb, and R. Verhé. Chemical and physical transitions of periodate oxidized potato starch in water. *Carbohydrate Polymers*. **1997**, 33, 153-162.
- [206] Whistler, R.L., P.K. Chang, and G.N. Richards. Alkaline Degradation of Periodate-oxidized Starch I. *Journal of the American Chemical Society*. **1959**, 81, 3133-3136.
- [207] Fry, S.C. Oxidative scission of plant cell wall polysaccharides by ascorbate-induced hydroxyl radicals. *Biochemical Journal*. **1998**, 332, 507-515.
- [208] Crescenzi, V., M. Belardinelli, and C. Rinaldi. Polysaccharides depolymerization via hydroxyl radicals attack in dilute aqueous solution. *Journal of Carbohydrate Chemistry*. **1997**, 16, 561-572.
- [209] Uchiyama, H., Y. Dobashi, K. Ohkouchi, and K. Nagasawa. Chemical change involved in the oxidative reductive depolymerization of hyaluronic acid. *J Biol Chem*. **1990**, 265, 7753-7759.
- [210] Halliwell, B. and J.M. Gutteridge. Role of free radicals and catalytic metal ions in human disease: an overview. *Methods Enzymol*. **1990**, 186, 1-85.
- [211] Isbell, H.S. and H.L. Frush. Mechanisms for hydroperoxide degradation of disaccharides and related compounds. *Carbohydrate Research*. **1987**, 161, 181-193.
- [212] Schuchmann, M.N. and C. von Sonntag. The effect of oxygen on the OH-radical-induced scission of the glycosidic linkage of cellobiose. *Int J Radiat Biol Relat Stud Phys Chem Med*. **1978**, 34, 397-400.
- [213] Šoltés, L., R. Mendichi, G. Kogan, J. Schiller, M. Stankovská, and J. Arnhold. Degradative action of reactive oxygen species on hyaluronan. *Biomacromolecules*. **2006**, 7, 659-668.
- [214] Faure, A.M., A. Sánchez-Ferrer, A. Zabara, M.L. Andersen, and L. Nyström. Modulating the structural properties of β -d-glucan degradation products by alternative reaction pathways. *Carbohydrate Polymers*. **2014**, 99, 679-686.
- [215] Kivelä, R., U. Henniges, T. Sontag-Strohm, and A. Potthast. Oxidation of oat β -glucan in aqueous solutions during processing. *Carbohydrate Polymers*. **2012**, 87, 589-597.
- [216] Tudella, J., F.M. Nunes, R. Paradela, D.V. Evtuguin, P. Domingues, F. Amado, M.A. Coimbra, A.I.R.N.A. Barros, and M.R.M. Domingues. Oxidation of mannosyl oligosaccharides by hydroxyl radicals as assessed by electrospray mass spectrometry. *Carbohydrate Research*. **2011**, 346, 2603-2611.
- [217] Guilloux, K., I. Gaillard, J. Courtois, B. Courtois, and E. Petit. Production of arabinoxylan-oligosaccharides from flaxseed (*Linum usitatissimum*). *Journal of Agricultural and Food Chemistry*. **2009**, 57, 11308-11313.
- [218] Zhi, Z., J. Chen, S. Li, W. Wang, R. Huang, D. Liu, T. Ding, R.J. Linhardt, S. Chen, and X. Ye. Fast preparation of RG-I enriched ultra-low molecular weight pectin by an ultrasound accelerated Fenton process. *Scientific Reports*. **2017**, 7, 541.
- [219] Miller, J.G. and S.C. Fry. Characteristics of xyloglucan after attack by hydroxyl radicals. *Carbohydrate Research*. **2001**, 332, 389-403.
- [220] Arantes, V. and A.M.F. Milagres. Degradation of cellulosic and hemicellulosic substrates using a chelator-mediated Fenton reaction. *Journal of Chemical Technology and Biotechnology*. **2006**, 81, 413-419.



- [221] Bagdi, A., S. Tömösközi, and L. Nyström. Hydroxyl radical oxidation of feruloylated arabinoxylan. *Carbohydrate Polymers*. **2016**, 152, 263-270.
- [222] Bagdi, A., S. Tömösközi, and L. Nyström. Structural and functional characterization of oxidized feruloylated arabinoxylan from wheat. *Food Hydrocolloids*. **2017**, 63, 219-225.
- [223] Faure, A.M., M.L. Andersen, and L. Nyström. Ascorbic acid induced degradation of beta-glucan: Hydroxyl radicals as intermediates studied by spin trapping and electron spin resonance spectroscopy. *Carbohydrate Polymers*. **2012**, 87, 2160-2168.
- [224] Faure, A.M., J. Werder, and L. Nyström. Reactive oxygen species responsible for beta-glucan degradation. *Food Chemistry*. **2013**, 141, 589-596.
- [225] Elboutachfati, R., C. Delattre, P. Michaud, B. Courtois, and J. Courtois. Oligogalacturonans production by free radical depolymerization of polygalacturonan. *International Journal of Biological Macromolecules*. **2008**, 43, 257-261.
- [226] Deng, C., M.A. O'Neill, M.G. Hahn, and W.S. York. Improved procedures for the selective chemical fragmentation of rhamnogalacturonans. *Carbohydrate Research*. **2009**, 344, 1852-1857.
- [227] Deng, C., M.A. O'Neill, and W.S. York. Selective chemical depolymerization of rhamnogalacturonans. *Carbohydrate Research*. **2006**, 341, 474-484.
- [228] Keijbets, M.J.H. and W. Pilnik. β -Elimination of pectin in the presence of anions and cations. *Carbohydrate Research*. **1974**, 33, 359-362.
- [229] Kravtchenko, T.P., I. Arnould, A.G.J. Voragen, and W. Pilnik. Improvement of the selective depolymerization of pectic substances by chemical β -elimination in aqueous solution. *Carbohydrate Polymers*. **1992**, 19, 237-242.

Chapter 2

TEMPO/NaClO₂/NaOCl oxidation of arabinoxylans

Published as: Pandeirada, C.O., D.W.H. Merx, H.-G. Janssen, Y. Westphal, and H.A. Schols.
Carbohydrate Polymers. **2021**, 259, 117781.



Abstract

TEMPO-oxidation of neutral polysaccharides has been used to obtain polyuronides displaying improved functional properties. Although arabinoxylans (AX) from different sources may yield polyuronides with diverse properties due to their variable arabinose (Araf) substitution patterns, information of the TEMPO-oxidation of AX on its structure remains scarce. We oxidized AX using various TEMPO:NaClO₂:NaOCl ratios. A TEMPO:NaClO₂:NaOCl ratio of 1.0:2.6:0.4 per mol of Ara gave an oxidized-AX with high molecular weight, minimal effect on xylose appearance, and comprising charged side chains. Although NMR analyses unveiled arabinuronic acid (AraA) as the only oxidation product in the oxidized-AX, accurate AraA quantification is still challenging. Linkage analysis showed that > 75 % of the β -(1→4)-xylan backbone remained single substituted at position O-3 of Xyl similarly to native AX. TEMPO-oxidation of AX can be considered a promising approach to obtain arabinuronoxylans with a substitution pattern resembling its parental AX.



1. Introduction

Modification of neutral polysaccharides to anionic polymers by the generation of polyuronides may lead to improved/unique functional properties of the polymer [1]. For example, these polyuronides can show thickening and gelling properties, similarly to pectin, a naturally occurring polyuronide [2]. Additionally, conversion of neutral polysaccharides to polyuronides has also enabled the production of nano-fibres [3, 4] compatible with biomedical applications [5].

2,2,6,6-tetramethylpiperidine-1-oxyl radical (TEMPO)-mediated oxidation is one of the major approaches used to selectively oxidize primary hydroxyl groups of neutral polysaccharides into carboxylic acids to obtain polyuronides [1, 6-10]. A TEMPO/NaOCl/NaBr system at pH 10 was the first system used to convert C6 primary hydroxyls to carboxyl groups in the neutral polysaccharides starch and inulin [11], and it is still the most used condition set to oxidize polysaccharides [1]. However, the alkaline medium used in the TEMPO/NaOCl/NaBr system can lead to undesirable polysaccharide depolymerization [12]. This depolymerization can be overcome by using alternative systems that do not require the use of an alkaline medium, such as TEMPO/bis(acetoxy)iodobenzene (BAIB) in an acetonitrile-aqueous buffer mixture [13-15] or TEMPO/NaOCl/NaClO₂ (sodium chlorite) in a mild acidic (pH 3.5 to 6.8) medium [8, 9, 16-18].

TEMPO-oxidation has been mostly performed on neutral polysaccharides composed of hexoses, such as cellulose [4, 19], starch [9], galactomannans [20, 21], and curdlan [17]. Although not many studies have been performed on TEMPO-oxidation of pentose-based polysaccharides (pentosans), arabinoxylan (AX), a major hemicellulose of the cereal cell walls [22], is a promising pentosan to obtain polyuronides. Arabinoxylans are composed of a linear β -(1 \rightarrow 4)-xylan backbone mainly substituted with single α -L-Araf units, which are attached at positions *O*-3 and/or *O*-2 of the β -D-Xylp unit [23]. As the primary hydroxyl groups in the AX structure are only shown in the C5 position of the Araf units [24], TEMPO-oxidation of an AX would selectively oxidize the Araf side chains to arabinuronic acid (AraAf), keeping the β -(1 \rightarrow 4)-xylan backbone intact and creating a polyuronide (arabinuronoxytan) carrying negative charged sugar residues as side chains. As the level and distribution of the Araf side chains along the xylan backbone can differ among arabinoxylans from different sources [25], TEMPO-oxidation of various arabinoxylans might yield arabinuronoxytans with a wide range of different properties, which can be valuable for food and/or biomedical applications.

Parikka et al. [26] and Börjesson and Westman [13] oxidized an AX using a Laccase/TEMPO and a TEMPO/BAIB system, respectively, to improve the functional properties of the native AX. Both studies observed the preferred conversion of Araf to the aldehyde form rather than the uronic acid form. Therefore, attention must be paid to oxidized products other than uronic acids when TEMPO-oxidizing polysaccharides. Additionally, Bowman et al. [27] oxidized AX from birch, wheat and switchgrass (SG) using a 4-Acetamido-TEMPO/NaOCl/NaBr system to distinguish the isomers Ara and Xyl, by selectively oxidizing Araf to AraAf. These authors observed an increment of 14 Da in oxidized-oligosaccharides comparatively to non-oxidized ones in hydrophilic interaction liquid chromatography (HILIC-LC)-MS analysis of the partially-acid depolymerized oxidized SG AX, proving the presence of AraAf as an oxidized product derived from Araf. However, this study did not indicate whether the native AX structure was kept after oxidation, by solely converting the Ara side chains into an AraA residue, or even arabinose removal, degradation or formation of side oxidation products.



Our study aims to investigate if TEMPO-oxidation of an AX will selectively oxidize the Ara f side chains to Ara f without major changes in the native AX structure, allowing us to obtain a polyuronide with a substitution pattern closely related to its parental arabinoxylan. For this, TEMPO/NaClO₂/NaOCl system at pH 4.6, with various TEMPO:NaClO₂:NaOCl ratios, was selected to oxidize an AX. The TEMPO oxidized-AX structure was characterized in terms of molecular weight distribution, sugar and linkage composition, and identification of oxidized compounds by NMR spectroscopy.

2. Materials and methods

2.1. Materials

The polysaccharide substrate used to perform the TEMPO-mediated oxidation was a commercial wheat arabinoxylan (AX) of medium viscosity (Ara:Xyl=38:62, Purity > 95 %, Megazyme, Wicklow, Ireland). L-(+)-Arabinose (Ara) (99 %), Maleic acid (98 %), sodium borodeuteride (NaBD₄, 98 %, 41.86 g/mol), trifluoroacetic acid (TFA, 99 %), HCl in dried methanol (3 M), deuterium oxide (D₂O, 99.9 %), and sodium nitrate (NaNO₃, > 99 %, 84.99 g/mol) were purchased from Sigma-Aldrich (St. Louis, MO, USA). D-(+)-Xylose (Xyl) (> 99 %), 2,2,6,6-tetramethylpiperidine-1-oxyl radical (TEMPO, 98 %, 156.25 g/mol), NaClO₂ (80 %, 90.44 g/mol), sodium hypochlorite solution (6-14 % active chlorine NaOCl), N-Cyclo-N'-[2-(N-methylmorpholino)-ethyl]-carbodiimide 4-toluolsulfonate, and sodium acetate (NaOAc) anhydrous were purchased from Merck (Darmstadt, Germany). Methyl iodide (CH₃I) was obtained from VWR (Rue Carnot, France), lithium aluminum deuteride (LiAlD₄, > 98 %, 41.99 g/mol) was obtained from BOC Sciences (NY, USA), and acetonitrile from Biosolve (Valkenswaard, The Netherlands). All water was purified in a Milli-Q system from Millipore (Molsheim, France), unless otherwise mentioned.

2.2. Oxidation of arabinoxylan

Various TEMPO-oxidation systems were preliminarily screened to oxidize AX, namely TEMPO/NaClO₂/NaOCl and TEMPO/NaOCl systems at pH 4.6 (24 h at 35 °C) [16-18], and TEMPO/BAIB (1:9 mol equivalent of Ara) and TEMPO/BAIB/NaOCl (1:9:1.5 mol equivalent of Ara) in Acetonitrile:Water (3:1, v/v) for 2 h at 0 °C followed by 4 h at room temperature (RT) [13, 15]. TEMPO/NaClO₂/NaOCl and TEMPO/NaOCl systems were also tested in Acetonitrile:Water (3:1, v/v) and at pH 4.6 for 2 h at 0 °C followed by 4 h at RT. TEMPO/NaClO₂/NaOCl system at pH 4.6 for 24 h at 35 °C using a TEMPO/NaClO₂/NaOCl ratio of 0.2:2.6:0.4 (per mol equivalent of Ara) was the system that gave more promising results. Based on this, TEMPO/NaClO₂/NaOCl oxidation of AX was selected to be further investigated in this study by testing various TEMPO/NaClO₂/NaOCl ratios (Table 1). TEMPO and NaOCl were tested in two levels, 0.2 and 1.0, and 0.4 and 1.5 mol equivalent of Ara, respectively, and NaClO₂ was kept constant (Table 1).

Oxidation of the wheat AX was done using the TEMPO/NaClO₂/NaOCl system at pH 4.6 using a protocol adapted from Tamura et al. [17]. TEMPO/NaClO₂/NaOCl mixtures were tested in three different mol ratios per mol of primary OH group (C5-OH of Ara) (Table 1). 200 mg of AX in a final



reaction volume of 40 mL, comprising 0.2 M NaOAc buffer pH 4.6, and TEMPO, NaClO₂ and NaOCl solutions as listed in Table 1 was used to perform the reaction.

AX powder was completely solubilized in 0.2 M NaOAc buffer at pH 4.6 (different volumes of buffer were added depending on the oxidation condition described in Table 1) under magnetic stirring in a glass flask. Stock solutions of TEMPO and NaClO₂ were prepared in 0.2 M NaOAc buffer to a final concentration of 0.05 mmol/mL and 0.40 mmol/mL, respectively. The required volume of 0.05 mmol/mL TEMPO and 0.40 mmol/mL NaClO₂ to reach the desired concentration in the final reaction volume (Table 1) were mixed and incubated under magnetic stirring for 10 min at RT. Thereafter, the pre-incubated TEMPO/NaClO₂ solution was added to the flask containing the AX solution in buffer. Then, variable volumes of 6-14 % NaOCl solution to be added to each oxidation condition to have the desired final NaOCl concentration was added at once to the flask to start the reaction. The flask was closed, and the reaction was carried out in an incubator for 24 h at 35 °C under shaking (100 rpm). The reaction was quenched by adding cold ethanol (96 % v/v) to a final concentration of 70 % (v/v) to the solution, followed by stirring for 1 h at RT. The precipitate formed containing the oxidized (ox-) AX was recovered by centrifugation (11 571 g, 15 °C, 30 min), washed with 70 % (v/v) EtOH by stirring for 1 h at RT, and collected by centrifugation as mentioned above. Afterwards, the ox-AX was re-suspended in demi-water, dialyzed (cut-off 12-14 kDa, Medicell Membranes Ltd, London, UK) against demi-water, and freeze-dried to obtain homogeneous dried material, yielding the final ox-AX samples. Native AX and ox-AX samples were further characterized.

Table 1. Sample identification and reaction conditions used to TEMPO-oxidize arabinoxylans. Reactions were performed in 0.2 M NaOAc buffer pH 4.6 for 24 h at 35 °C with variable molar ratios of TEMPO:NaClO₂:NaOCl. Final concentrations of AX in mg/mL, and TEMPO, NaClO₂, and NaOCl in mM used during oxidation reaction are mentioned. Values within parentheses correspond to the TEMPO:NaClO₂:NaOCl ratio per mol of C5-OH.

Sample name ^a	C _{AX} (mg/mL)	C _{TEMPO} (mM)	C _{NaClO₂} (mM)	C _{NaOCl} (mM)
ox-AX ^{1.0:2.6:1.5}	5.0	14 (1.0)	38 (2.6)	22 (1.5)
ox-AX ^{0.2:2.6:1.5}	5.0	3 (0.2)	38 (2.6)	22 (1.5)
ox-AX ^{1.0:2.6:0.4}	5.0	14 (1.0)	38 (2.6)	6 (0.4)

^a - ox-AX^b refers to the oxidized wheat arabinoxylan (ox-AX) obtained with a ^b TEMPO:NaClO₂:NaOCl ratio per mol of C5-OH.

2.3. Molecular weight distribution of polysaccharides

The molecular weight (Mw) was determined by high performance size exclusion chromatography (HPSEC). HPSEC analysis was carried out on an Ultimate 3000 system (Dionex, Sunnyvale, CA, USA) coupled to a Shodex RI-101 detector (Showa Denko K.K., Tokyo, Japan). The system was equipped with a set of three TSK-Gel Super columns 4000AW, 3000AW, and 2500AW (6 mm ID × 150 mm per column, 6 μm) connected in series preceded by a TSK Super AW-L guard column (4.6 mm ID × 35 mm, 7 μm), all from Tosoh Bioscience (Tokyo, Japan). The column oven temperature was maintained at 55 °C during analysis. Standards and samples were dissolved in water to a concentration of 1.0 mg/mL. 10 μL of sample was injected onto the system and eluted with 0.2 M NaNO₃ solution at a flow rate of 0.6 mL/min. Although the final oxidized products are negatively charged, calibration of the SEC columns was done with pullulan standards (0.180–708 kDa; Polymer



Laboratories, Church Stretton, UK) since the parental AX is neutral and ox-AX moderately charged. Calibrating the columns with available pectin standards would provide incorrect Mw values for the AX and also not give accurate results for ox-AX either, as pectins might be heavily charged. The retention times of the monodisperse pullulan standards were used to obtain the calibration curve to determine the apparent Mw of the samples. The collected data was analyzed using Chromeleon 7.2 software (Dionex Corporation).

2.4. Monosaccharide composition analysis by HPAEC-PAD

(ox-)AX samples were methanolysed using 2.0 M HCl in dried methanol for 16 h at 80 °C, and the released methyl-glycosides were converted to their non-methylated form via TFA acid hydrolysis in accordance with De Ruiter et al. [28] and ter Haar et al. [29]. Hydrolysates were diluted with water to about 25 µg/mL and the sugars released were analyzed by High-Performance Anion-Exchange Chromatography with Pulsed Amperometric Detection (HPAEC-PAD). An ICS-5000 HPLC system (Dionex, Sunnyvale, CA, USA) equipped with a CarboPac PA1 guard column (2 mm ID × 50 mm) and a CarboPac PA-1 column (2 mm ID × 250 mm; both from Dionex) was used for this analysis. Detection of the eluted compounds was performed by an ED40 EC-detector running in the PAD mode (Dionex). 10 µL of the diluted hydrolysate was injected on the system. Mobile phases used to elute the compounds were kept under helium flushing and the column temperature was 20 °C. A flow rate of 0.4 mL/min was used with the following gradient of 0.1 M sodium hydroxide (NaOH: A) and 1.0 M NaOAc in 0.1 M NaOH (B): 0-35 min, 100 % milli-Q water; 35.1 min, 100 % A; 35.2-50 min, 0-40 % B; 50.1-55 min, 100 % B; 55.1-63.0 min, 100% A; 63.1-78.0 min, 100 % milli-Q water. A post-column alkali addition (0.5 M NaOH; 0.1 mL/min) was used from 0.0-34.9 min and from 68.1-78.0 min. All samples were analyzed in duplicate. Standards of Ara and Xyl in a concentration range of 1.0-150 µg/mL were used for quantification. The collected data was analyzed using Chromeleon 7.2 software (Dionex Corporation).

2.5. Purification of oxidized compounds from the ox-AX^{1.0:2.6:0.4} hydrolysate by SPE

To isolate the oxidized compounds present in the ox-AX^{1.0:2.6:0.4} hydrolysate (section 2.4.), the sample was fractionated using solid phase extraction (SPE) as described by Sun et al. [30] with some modifications. About 100 µg of hydrolysate was dissolved in water and loaded onto a SupelcleanTM ENVI-CarbTM column (3.0 mL, Sigma-Aldrich), which was activated with 1.5 mL acetonitrile:water (80:20; v/v) containing 0.1 % (v/v) TFA, and water (3 x 1.5 mL). Neutral monosaccharides were eluted from the column with water (4 x 1.5 mL), whereas retained oxidized compounds were eluted with three times 1.5 mL of acetonitrile:water (60:40; v/v) containing 0.05 % (v/v) TFA. Water and acetonitrile:water:TFA fractions were dried under a stream of nitrogen at RT, yielding the fractions Hydr_ox-AX^{1.0:2.6:0.4}_H₂O and Hydr_ox-AX^{1.0:2.6:0.4}_TFA, respectively. Fractions were analyzed by ¹H-NMR (section 2.6.) and Hydr_ox-AX^{1.0:2.6:0.4}_TFA was further analyzed by 2D-NMR COSY (section 2.6.).



2.6. Analysis by ¹H-NMR and ¹H-¹H COSY

Dried hydrolysates of the native AX and ox-AX^{1.0:2.6:0.4} samples, and the Hydr_ox-AX^{1.0:2.6:0.4}_H₂O and Hydr_ox-AX^{1.0:2.6:0.4}_TFA fractions collected from SPE were re-suspended in D₂O and freeze-dried to exchange the free -OH groups by -OD. Samples were subsequently dissolved in D₂O to approximately 0.2 mg/mL containing 0.2 mg/mL maleic acid (internal standard, IS). Additionally, dried AX and ox-AX^{1.0:2.6:0.4} samples were dissolved in D₂O to approximately 3.7 mg/mL containing 0.2 mg/mL IS. All samples were analyzed by ¹H-NMR and the Hydr_ox-AX^{1.0:2.6:0.4}_TFA fraction was further analyzed by homonuclear ¹H-¹H correlation (COSY) to identify AraA and assign ¹H-NMR signals. Both ¹H-NMR and COSY-NMR experiments were carried out on a 600 MHz (14.1 T) Bruker Avance III NMR spectrometer (Bruker BioSpin, Switzerland) equipped with a 5-mm cryoprobe at 298 K. The 1D ¹H-NMR spectra were recorded with a noesygppld pulse sequence. The size of the FID was 65k. In total, 256-512 scans were collected with a relaxation time of 1 s and an acquisition time of 4 s. Low power water suppression (16 Hz) was applied for 0.1 s. The 90° pulse length (~7.6 μs) and receiver gain were determined automatically. The data was processed with Bruker TopSpin 4.0.7 software. Fourier transformation with exponential window function and a line broadening factor of 0.3 Hz were applied, followed by automatic phase- and baseline correction. The 2D ¹H-¹H COSY experiments were recorded with a cosygpqrq pulse sequence. The spectral widths were 4 ppm in both dimensions, with the O1 at 4.7 ppm to centre around the aromatic region. The number of scans was 128 with 16 dummy scans. 256 increments were collected in F1, and 1024 increments in F2. The recycle delay was 2 s.

A relative monosaccharide quantification for AX and ox-AX^{1.0:2.6:0.4} was performed based on the sum of the ¹H-NMR signal integrals derived from each identified sugar (I_{sugar} (Eq. (1)) [31, 32].

$$(1) \quad \text{Sugar (\%)} = \frac{I_{\text{sugar}}}{\sum (I_{\text{Ara}} + I_{\text{Xyl}} + I_{\text{AraA}})}$$

I_{sugar} corresponds to either Ara (I_{Ara}), Xyl (I_{Xyl}), or AraA (I_{AraA}) and is the sum of the α - and β -signal integrals of the anomeric proton of Ara, Xyl and AraA, respectively.

2.7. Glycosidic linkage and substitution analysis

Carboxyl groups of the uronic acids present in the ox-AX^{1.0:2.6:0.4} sample were reduced to neutral monosaccharides using two different methods. The uronic acids present on the polysaccharide were twice reduced with Carbodiimide/NaBD₄ prior to linkage analysis in accordance with Taylor and Conrad [33], or alternatively were reduced with LiAlD₄ upon per-methylation of the polysaccharide as described by Pandeirada et al. [34]. Carboxyl-reduced and non-reduced ox-AX^{1.0:2.6:0.4}, and AX samples were subjected to per-methylation analysis to access the glycosidic linkage patterns. Per-methylation was performed with a modification to the method described by Nunes et al. [35] and Pandeirada et al. [34], by replacing the argon atmosphere by nitrogen. Partially methylated polysaccharide samples were converted into their partially methylated alditol acetate (PMAA) forms by hydrolysis, reduction and acetylation [34], and then analyzed by gas chromatography coupled to



mass spectrometry (GC-MS). PMAA samples were analyzed using a GC (Trace GC Ultra™, Thermo Scientific) with a split injector equipped with a 30 m DB 35MS column (Restek, Bellefonte, PA, USA) with diameter and film thickness of 0.25 mm and 0.25 μm, respectively, and connected to a Dual Stage Quadrupole (DSQII, Thermo Scientific) mass selective detector. 1.0 μL of sample was injected in the PTV split mode with the injector operating at an initial temperature of 190 °C, ramped to 275 °C at 14.5 °C/min, holding for 1.0 min. The GC oven temperature program was set to an initial temperature of 120 °C, raised to 250 °C at 2.5 °C/min, holding for 5 min. The pressure of the carrier gas (He) was set at 100 kPa. The mass spectrometer was operated in the electron impact mode (EI) at 70 eV scanning the range 50–450 m/z, in full scan acquisition mode. The collected data was analyzed using Xcalibur 4.1 software (Thermo Scientific) and chromatographic peaks were identified comparing all mass spectra with a laboratory made database of PMAAs. As reduction of the ox-AX^{1.0:2.6:0.4} sample with carbodiimide/NaBD₄ prior to per-methylation gave more reliable results, only these results will be shown.

3. Results and discussion

In this study, oxidation of arabinoxylan (AX) using a TEMPO/NaClO₂/NaOCl system at pH 4.6 was performed to investigate if the TEMPO-oxidation will selectively oxidize the Ara_f side chains of an AX to arabinuronic acid (Ara_{Af}), allowing us to yield a polyuronide type structure (arabinuronoxyylan) with a structure resembling the parental AX structure. A preliminary oxidation study on wheat AX indicated that a TEMPO/NaClO₂/NaOCl oxidation system using a ratio of 0.2:2.6:0.4 (per mol equivalent of Ara) gave preferential results with an oxidized-AX with an apparent molecular weight (M_w) identical to the native AX (Fig. S1) and a degree of Ara oxidation of about 54 (w/w) % (Table S1), based on the Ara content decrease. Consequently, TEMPO and NaOCl were tested in variable ratios and in higher amounts, 1.0 and 1.5 mol equivalent of Ara (Table 1), respectively, when compared to the preliminary condition to ensure that all available primary OH groups would be oxidized to aldehydes and further oxidized to carboxylic groups by NaO₂Cl. NaO₂Cl was kept constant, as it was being used in an amount that should ensure full conversion of aldehydes to carboxyl groups during reaction, as it is the primary oxidant [7, 15, 36]. From these AX oxidations with variable TEMPO:NaClO₂:NaOCl ratios per mol of primary hydroxyl group of Ara (C5-OH), three oxidized (ox-)AX samples, ox-AX^{1.0:2.6:1.5}, ox-AX^{0.2:2.6:1.5}, and ox-AX^{1.0:2.6:0.4} were obtained.

3.1. Molecular weight distribution of TEMPO-oxidized AX samples

To monitor if the TEMPO-oxidation reaction would lead to AX degradation, the M_w distribution of the native and ox-AX samples was analyzed by HPSEC (Fig. 1). The apparent M_w of wheat AX was determined by using the retention time of the maximum value of the peak, which gave a M_w value for AX of around 400 kDa, in accordance with previous reports (200-700 kDa) [22, 37-39]. Compared to AX, the apparent M_w of the three ox-AX samples decreased and it was noted that the ox-AX samples were more polydisperse, as observed by the broad peaks in Fig. 1. This can be due to the charge effect due to polymer oxidation, or due to polymer degradation. Furthermore, compared to the preliminary ox-AX^{0.2:2.6:0.4}, whose apparent M_w was similar to the M_w of the native AX (Fig. S1A), these results



suggest that increasing the amount of TEMPO and/or NaOCl (from 0.2 to 1.0, and from 0.4 to 1.5 mol eq. of C5-OH, respectively, Table 1) might favor polymer degradation. The smallest decrease in the apparent Mw was obtained for ox-AX^{1.0:2.6:0.4} (175 kDa), followed by ox-AX^{0.2:2.6:1.5} (124 kDa) and ox-AX^{1.0:2.6:1.5} (106 kDa). These results indicate that, within the conditions tested in our work, NaOCl used at 1.5 mol equivalent of C5-OH potentiates polymer degradation, especially when TEMPO was only present at low level. This suggests that TEMPO can protect against polymer degradation, as reported before [12]. Furthermore, the polymer degradation likely boosted by an elevated amount of NaOCl is probably be due to non-selective oxidation of vicinal secondary hydroxyl groups at C-2 and/or C-3 of Ara and/or Xyl to carbonyl groups triggered by NaOCl [40], which probably caused instability and degradation of the xylan backbone. Despite the decrease in the Mw, the still high Mw of the ox-AX samples indicates that the AX native structure could be largely conserved. This result agrees with literature suggesting that a TEMPO/NaClO₂/NaOCl approach only leads to minimal polysaccharide depolymerization [8, 16-18].

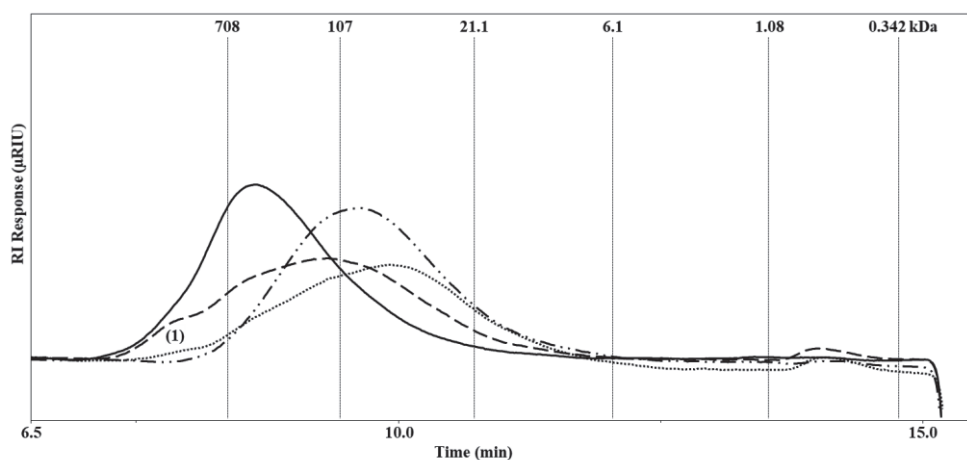


Figure 1. HPSEC elution patterns of the native AX (—), and of the TEMPO-oxidized AX samples ox-AX^{1.0:2.6:1.5} (.....), ox-AX^{0.2:2.6:1.5} (-.-.-), and ox-AX^{1.0:2.6:0.4} (----). Pullulan standards were used to calibrate the system. Population (1) present in ox-AX^{1.0:2.6:1.5} and ox-AX^{1.0:2.6:0.4}.

Interestingly, within the ox-AX samples, the oxidized samples obtained with the highest amount of TEMPO (ox-AX^{1.0:2.6:1.5} and ox-AX^{1.0:2.6:0.4}) displayed a second population being more shifted to the left in the HPSEC elution pattern (population (1) in Fig. 1). This population has an apparent Mw higher than 400 kDa and is especially present when higher amounts of TEMPO and lower amounts of NaOCl were used (ox-AX^{1.0:2.6:0.4}, Fig. 1). The presence of this population suggests that part of the ox-AX^{1.0:2.6:0.4} molecules have an increased hydrodynamic volume, probably due to an increase in repulsing anionic groups on the polymer formed during TEMPO oxidation [41]. This phenomenon was seen before by ter Haar et al. [29] studying TEMPO/NaBr/NaOCl oxidized starches with different degrees of oxidation (DO). Thus all together, it can be speculated that among the various ox-AX samples, ox-AX^{1.0:2.6:0.4} is the most oxidized AX, followed by ox-AX^{1.0:2.6:1.5} and ox-AX^{0.2:2.6:1.5}. Moreover, this suggests that TEMPO is key in the oxidation reaction, and that increasing the NaOCl does not lead to an increase in the oxidation level but preferably boosts polymer degradation. Although



working at a different pH, this agrees with the findings that in alkaline medium, NaOCl can lead to more depolymerization [42, 43], while it also has been reported that increasing the NaOCl in a TEMPO:NaBr:NaOCl system at alkaline pH leads to a higher content in carboxyl groups [42, 44].

3.2. Sugar composition of TEMPO-oxidized AX samples

The sugar composition of the native and TEMPO ox-AX samples is shown in Table 2. AX was composed of Xyl (58.9 %, w/w) and Ara (31.6 %, w/w) with a molar Ara:Xyl ratio of approximately 0.5, which is in accordance with literature for wheat AX [22, 39, 45, 46]. Regarding the ox-AX samples, ox-AX^{1.0:2.6:1.5} was composed of 57.5 % (w/w) Xyl, and both ox-AX^{0.2:2.6:1.5} and ox-AX^{1.0:2.6:0.4} were composed of 53.9 % (w/w) Xyl (Table 2). This showed that Xyl was largely recovered (> 80 %) in all ox-AX samples. The high recovery of Xyl indicates that none or minor changes of the xylan backbone have occurred during TEMPO oxidation, as expected, since TEMPO preferable oxidizes primary alcohols with minimal effect on secondary alcohols, as those present in Xylp units [27, 47, 48].

Table 2. Yields, sugar composition and recovery of the native AX, and of the oxidized AX (ox-AX) samples using various ratios of TEMPO:NaClO₂:NaOCl.

Sample	Yield ^a (%, w/w)	Carbohydrate composition (%, w/w) ^b			Ox- Product	Sugar Recovery (%, w/w) ^c
		Ara	Xyl	Total		
AX	-	31.6 ± 0.1	58.9 ± 0.5	90.5 ± 0.6	-	-
ox-AX ^{1.0:2.6:1.5}	97	0.9 ± 0.0	56.5 ± 0.6	57.5 ± 0.6	+	55.7 ± 0.6
ox-AX ^{0.2:2.6:1.5}	98	9.5 ± 0.2	53.9 ± 0.4	63.4 ± 0.6	+	62.1 ± 0.6
ox-AX ^{1.0:2.6:0.4}	91	2.1 ± 0.1	53.9 ± 1.9	55.9 ± 1.9	+	50.1 ± 1.8

ox-AX^b: oxidized arabinoxylan (ox-AX) obtained with a ^b TEMPO:NaClO₂:NaOCl ratio per mol of C5-OH of Ara.

^a Yield in weight % relative to the native AX.

^b Results are expressed as average (n=2) weight % of sample. Presence of the oxidized product formed during TEMPO-oxidation reaction is indicated with +, and absence with -.

^c Results are expressed as average (n=2) weight % of native AX. ox-Product is not accounted in the sugar recovery of ox-AX samples.

Contrarily, the Ara content in the ox-AX samples abruptly decreased comparatively to the parental AX sample (31.6 %, w/w). ox-AX^{1.0:2.6:1.5}, ox-AX^{0.2:2.6:1.5} and ox-AX^{1.0:2.6:0.4} were respectively composed of 0.9 %, 9.5 % and 2.1 % (w/w) of Ara (Table 2), explaining the very low recovery yield of Ara (approximately 3 %, 30 % and 6 % for ox-AX^{1.0:2.6:1.5}, ox-AX^{0.2:2.6:1.5} and ox-AX^{1.0:2.6:0.4}, respectively). This shows that Ara was preferentially TEMPO-oxidized, as expected since only the primary alcohols of Ara units are susceptible to oxidation [12, 15, 16, 27]. The large decrease in Ara suggests a degree of Ara oxidation higher than 90 % for ox-AX^{1.0:2.6:1.5} and ox-AX^{1.0:2.6:0.4}, and 70 % for ox-AX^{0.2:2.6:1.5}. These values agree with HPSEC results suggesting that ox-AX^{1.0:2.6:0.4} and ox-AX^{1.0:2.6:1.5} had the highest DO, followed by ox-AX^{0.2:2.6:1.5}. Connected to the decrease in Ara_f, a new compound (coded ox-Product in Table 2) was detected in the HPAEC elution pattern of the ox-AX hydrolysates (Supplementary Material, Fig. S2). This novel compound, which eluted at retention times commonly found for uronic acids (results not shown), might be derived from the oxidation of Ara into

its uronic acid form (arabinuronic acid, AraA). Due to the lack of standards, the identification and quantification of this new compound as AraA_f could not be ascertained by HPAEC. Accordingly, the sugar recovery was calculated for all ox-AX samples considering only Ara and Xyl, which led to an expected low sugar recovery ranging from 50.1-62.1 % (w/w) (Table 2).

3.3. Characterization of ox-AX^{1.0:2.6:0.4} by 1D- and 2D-NMR

Together, the sugar composition and the Mw distribution of the ox-AX samples suggested that ox-AX^{1.0:2.6:0.4} had the highest DO of Ara and was least degraded. Therefore, this sample was chosen to be further characterized to elucidate the structure of the ox-product recognized by HPAEC. The ¹H-NMR spectra of the anomeric region of the monosaccharides present in the hydrolysates of the AX and ox-AX^{1.0:2.6:0.4} samples are shown in Fig. 2. Full ¹H-NMR spectra and signal integrals are shown in supplementary material (Fig. S3). For AX hydrolysate (Fig. 2, line A), the doublets at δ 5.15 ppm and δ 4.48 ppm correspond to the α-anomeric proton derived from Xyl and Ara, respectively, whereas the doublets at δ 4.53 ppm and δ 5.20 ppm are derived from the β-anomeric proton of Xyl and Ara, respectively, according to Benesi et al. [49].

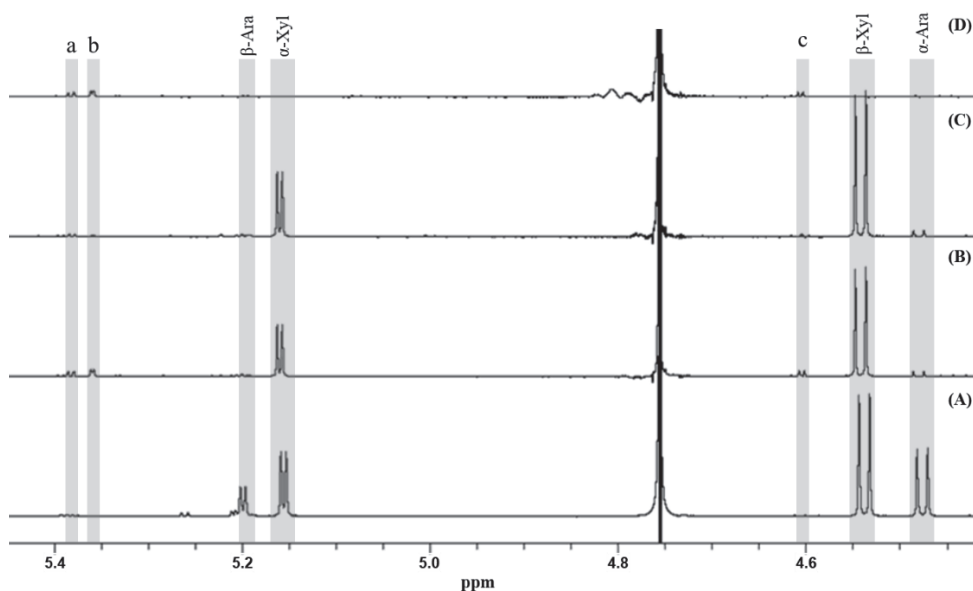


Figure 2. ¹H-NMR spectra (600 MHz) of the anomeric region of the monosaccharides present in the hydrolysates of the native AX (A), and ox-AX^{1.0:2.6:0.4} (B), and of the fractions Hydr_ox-AX^{1.0:2.6:0.4}_H₂O (C) and Hydr_ox-AX^{1.0:2.6:0.4}_TFA (D) obtained from SPE of the hydrolysate of the ox-AX^{1.0:2.6:0.4} sample with water and acetonitrile:water (60:40; v/v) containing 0.05 % (v/v) TFA, respectively. α- and β-anomeric proton signals of Xyl and Ara, and additional chemical shifts arising in the anomeric region (a, b, and c) of the ox-AX^{1.0:2.6:0.4} sample compared to the native AX are highlighted in grey boxes.

The α/β-anomeric proton signal intensities derived from Xyl in the ¹H-NMR spectrum of both AX and ox-AX^{1.0:2.6:0.4} hydrolysates (Fig. 2, line A and B, respectively) were comparable. Contrarily, the α/β-anomeric proton signal intensities derived from Ara largely decreased in the ox-AX^{1.0:2.6:0.4}



hydrolysate (Fig. 2, line B) relatively to the ones derived from AX (Fig. 2, line A). These observations agree with the results obtained by HPAEC. Additionally, the $^1\text{H-NMR}$ spectrum of the ox-AX^{1.0:2.6:0.4} hydrolysate exhibited three new doublets, one at around δ 4.60 ppm (peak c, Fig. 2, line B) and two between δ 5.3-5.4 ppm (peaks b and a, Fig. 2, line B), in comparison to AX hydrolysate. Considering that TEMPO oxidizes Ara to AraA, the doublets of the α/β -anomeric protons of AraA should be less protected than the respective doublets of Ara, due to the presence of a carboxyl group in the AraA structure, as observed for e.g. GalA comparatively to Gal [32, 50]. Thus, two out of the three new observed doublets that appear in the anomeric region in Fig. 2 (signals a, b, and c) might be derived from the H-1 of α/β -AraA.

To assign the new doublets that appear in the anomeric region of the $^1\text{H-NMR}$ spectrum (signals a, b, and c in Fig. 2, line B) of the ox-AX^{1.0:2.6:0.4} hydrolysate to their corresponding protons and to unveil the structure of the ox-product present in this sample, the ox-AX^{1.0:2.6:0.4} hydrolysate was fractionated by SPE. This yielded a neutral Hydr_ox-AX^{1.0:2.6:0.4}_H₂O fraction retaining the Ara and Xyl residues (still present (Fig. 2, line C), and an acidic Hydr_ox-AX^{1.0:2.6:0.4}_TFA fraction containing the ox-product (Fig. 2, line D). Consequently, this fraction was further analyzed by homonuclear $^1\text{H-}^1\text{H}$ correlation (COSY) (Fig. 3) to reveal the structure of the ox-product.

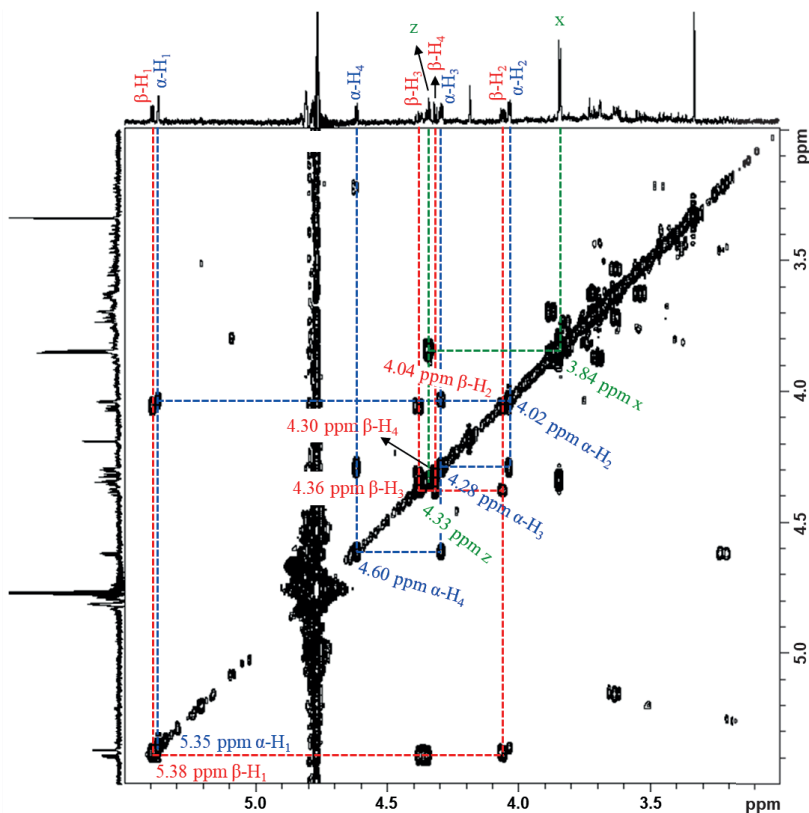


Figure 3. The 2D $^1\text{H-}^1\text{H}$ COSY spectrum of the Hydr_ox-AX^{1.0:2.6:0.4}_TFA fraction in D₂O. Signal assignments of the α - and β -conformation protons of AraA_f are shown in blue and red, respectively. Signal at δ 4.8 ppm and at δ 3.33 ppm are due to residual H₂O and methanol, respectively.



The 2D ¹H-¹H COSY spectrum enabled identification of the α- and β-conformations of the H-1, H-2, H-3, and H-4 signals of AraA (Fig. 3 and table 3), which appeared from the least to the most shielded chemical shift signal as follows: β-H1 (5.38 ppm) > α-H1 > α-H4 > β-H3 > β-H4 > α-H3 > β-H2 > α-H2 (4.02 ppm). This chemical shift sequence and the ¹H-¹H coupling constants obtained in our study for AraA (Table 3) are similar to the ones observed by Wu and Serianni [51], who oxidized Ara to AraA via methyl glycosidation of Ara, followed by oxidation of methyl-AraA to methyl-AraAf using platinum oxide, and hydrolysis of the methyl-AraAf to AraAf before analysis by ¹H-NMR spectroscopy. These authors verified that the H-1 of the α- and β-conformation of AraA were only δ 0.03 ppm separated from each other, which was also seen in our work (δ β-H1 - δ α-H1 = δ 0.03 ppm). The 2D-NMR results proved that part of the Ara was selectively oxidized to AraA, resulting in an anionic polymer (arabinuronoxylan), which has potential to be further explored for its polyuronides properties [1]. Additionally, 2D-NMR also allowed us to unveil the three new doublets that appeared in the ¹H-NMR spectrum of the ox-AX^{1.0:2.6:0.4} hydrolysate. The doublets at δ 5.38 ppm and δ 5.35 ppm (signal a and b, respectively, Fig. 2, lines B and D) are the H-1 signals of the β-AraA and α-AraA, respectively, whereas the doublet at δ 4.6 ppm (signal c, Fig. 2, lines B and D) is the H-4 signal of the α-AraA. Considering only the anomeric signal integrals (Supplementary Material, Fig. S3) derived from the α/β-forms of AraA, Ara, and Xyl in the ¹H-NMR spectrum, the relative content of AraA in the ox-AX^{1.0:2.6:0.4} sample was approximately 7 % (mol/mol), with 4 % and 89 % (mol/mol) accounting for Ara and Xyl, respectively. This relative AraA content is rather low when compared to the Ara content (35 %, mol/mol). Consequently, from these results, some AX debranching cannot be ruled out during TEMPO-oxidation.

Apart from AraA chemical shifts, other signals were seen in the 2D-NMR spectrum of the Hydr_ox-AX^{1.0:2.6:0.4}_TFA fraction. The doublet at δ 3.84 ppm (X in Fig. 3 and Table 3) and the triplet at δ 4.33 ppm (Z in Fig. 3 and Table 3) had vicinal coupling (³J_{HH} of 4.1 Hz). As the chemical shift at δ 4.33 ppm (Z) is a triplet, it must have two coupling partner protons, meaning that the doublet at δ 3.84 ppm (X) must be composed of two proton nuclei, which couple identically with proton Z. This would explain the double signal intensity obtained for the doublet X in comparison to the triplet Z (Supplementary Material, Fig. S3), since the signal integral is proportional to the number of nuclei contributing to the signal [31]. Hence, the compound comprising the X and Z signals was putatively assigned to arabinaric acid (Table 3), the aldaric acid form of arabinose (arabinaric acid structure is shown in Supplementary Material, Fig. S3), which can explain the relatively low AraA level in the ox-AX^{1.0:2.6:0.4} hydrolysate. Besides X and Z signals, other chemical shifts were seen in the 2D-NMR spectrum of the Hydr_ox-AX^{1.0:2.6:0.4}_TFA fraction (singlet at δ 4.18 ppm; signals between δ 3.5-3.8 ppm) (Fig. 3), but the corresponding unknown compounds could not be identified.



Table 3. ^1H chemical shifts (ppm) of the protons assigned to α - and β -AraA by 2D ^1H - ^1H COSY, values of the $^3J_{\text{HH}}$ coupling constant of these protons in Hz, and type of signal of each proton.

Compound	Chemical Shift (ppm)	Proton	$^3J_{\text{HH}}$ Coupled nuclei	$^3J_{\text{HH}}$ Coupling constant (Hz)	Type of signal
α -D-Arabinuronic acid	5.35	H1	H1-H2	1.8	Doublet
	4.02	H2	H2-H1	1.8	Double doublet
			H2-H3	2.9	
	4.28	H3	H3-H2	2.9	Double doublet
H3-H4			4.1		
4.6	H4	H4-H3	4.1	Doublet	
β -D-Arabinuronic acid	5.38	H1	H1-H2	4.3	Doublet
	4.04	H2	H2-H1	4.3	Double doublet
			H2-H3	6.4	
	4.36	H3	H3-H2	6.5	Double doublet
H3-H4			5.7		
4.30	H4	H4-H3	5.7	Doublet	
Tentative compound assigned to δ 3.84 ppm and δ 4.33 ppm					
Arabinaric acid	3.84	X	H2-H3	4.1	Doublet
			(H2, H4)		
	4.33	Z	H3-H2	4.1	Triplet
			(H3)		

To verify if the proposed arabinaric acid and the other unknown chemical shifts were derived from side oxidation reactions of Ara during TEMPO reaction, NMR analyses were performed on the non-hydrolysed AX and ox-AX^{1.0:2.6:0.4} samples. Only chemical shifts assigned to (residual) α -Ara, α -AraA, and β -Xyl were seen in the anomeric region of the ^1H -NMR spectrum of the non-hydrolysed ox-AX^{1.0:2.6:0.4} (Fig. 4, full NMR spectra are shown in Fig. S4). Signals **a'**, **b'**, and **c'** in Figure 4 were attributed to the H-1 of α -AraA based on our NMR results of ox-AX^{1.0:2.6:0.4} hydrolysate (Fig. 2 and 3), and on literature showing that H-1 signals of t-GlcA in glucurono-arabinoxylans falls within the δ 5.0-5.6 ppm range [52, 53]. Hence, these results indicate that the proposed arabinaric acid was likely formed from oxidation of the released AraA_f during methanolysis and TFA hydrolysis of ox-AX^{1.0:2.6:0.4}, and that no other oxidation products than AraA are formed during TEMPO oxidation of AX. Generally, aldaric acids are produced by nitric acid oxidation of aldoses or by oxidation of the C1 terminal aldehyde group of an uronic acid [54, 55], although it has never been reported for the acid hydrolysis conditions used in our study.

Relatively low AraA signal intensities were noted in the ^1H -NMR spectrum of ox-AX^{1.0:2.6:0.4} (Fig. 4B) in comparison to the corresponding Ara signal intensities in the ^1H -NMR spectrum of AX (Fig. 4A). However, accurate AraA quantitation could not be performed using these ^1H -NMR results due to the high viscosity of the ox-AX in comparison to AX.

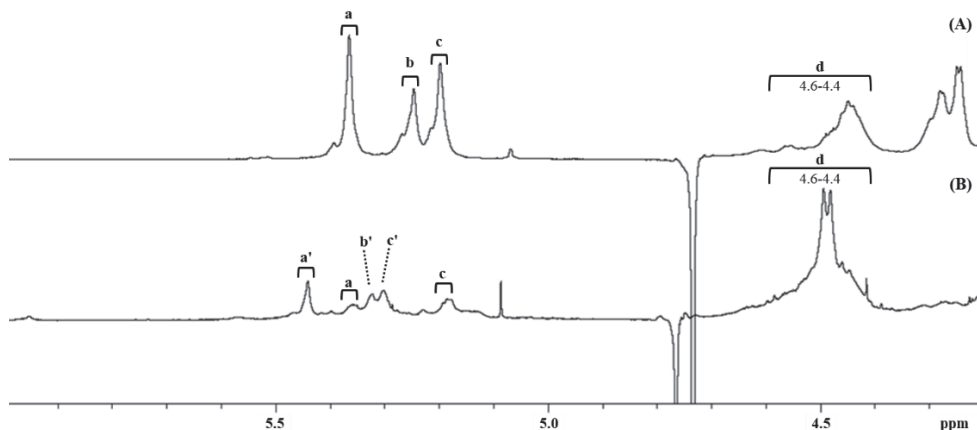


Figure 4. ¹H-NMR spectra (600 MHz) of the anomeric region of the native AX (A) and ox-AX^{1.0:2.6:0.4} (B) samples. H-1 signals of the α-Ara linked at positions *O*-3 of 3,4-Xyl (a), *O*-3 of 2,3,4-Xyl (b), and *O*-2 of 2,3,4-Xyl (c). a', b', and c' are assumed to be the corresponding signals derived from α-AraA, as the H-1 signals of t-GlcA in glucurono-arabinoxylans also falls within δ 5.0-5.6 ppm [52, 53]. d corresponds to the chemical shift range of the H-1 of the β-Xyl. Ara and Xyl-derived signal assignments were performed using previously published data [56-59]. Chemical shift range between δ 4.7-4.8 ppm is due to residual H₂O.

3.4. Glycosidic linkages pattern of AX and ox-AX^{1.0:2.6:0.4}

GC-MS analyses of the partially-methylated alditol acetate (PMAA) forms derived from AX and carbodiimide/NaBD₄ carboxyl-reduced ox-AX^{1.0:2.6:0.4} were performed to compare the substitution pattern over the xylan backbone between AX and ox-AX^{1.0:2.6:0.4} samples. About 65.7 % (mol/mol) (4-Xyl_p, mol/mol % of all Xyl residues in Table 4) of the β-(1→4)-xylan backbone in native AX was unsubstituted. Substitution of the xylan backbone occurred preferably as single-substitution at position *O*-3 of Xyl (24.7 %), but low amounts of double substitution at both *O*-2 and *O*-3 Xyl positions (5.8 %) and minor single-substitution at position *O*-2 of Xyl (2.3 %) also occurred in AX. These results are in agreement with previous studies [22, 39, 45, 60].

Similar relative terminal-Xyl_p amounts were found for AX and red-ox-AX^{1.0:2.6:0.4} (Table 4), next to an increase of 1.8 % (mol/mol) in the relative amount of 2,4-linked Xyl_p, likely due to debranching at position *O*-3 of the 2,3,4-Xyl_p unit. The relative 4- and 3,4-Xyl_p amounts present in the red-ox-AX^{1.0:2.6:0.4} sample decreased 7.9 % and 8.6 %, respectively, whereas the 2,3,4-Xyl_p amount concomitantly increased 14.9 % (mol/mol). This suggests that ox-AX^{1.0:2.6:0.4} underwent undermethylation, which is substantiated by the increased 2,3,4-Xyl_p content. Even though no conclusions can be drawn on the double substitution Xyl pattern due to undermethylation, still 20.2 % out of 27.0 % (mol/mol) expected single-substituted Xyl units (2,4- and 3,4-Xyl_p) are present in the ox-AX^{1.0:2.6:0.4}. This suggests a DO of Ara higher than 75 % as derived from single-substituted xylan segments only. From this 75 %, 60 % correspond to *O*-3 substituted Xyl, showing that ox-AX^{1.0:2.6:0.4} was still mainly single-substituted at position *O*-3 of Xyl, similarly to AX. Considering that this 75 % single-substituted xylan segments should still be corrected for undermethylation, our results suggest that no major changes in the substitution pattern of the xylan backbone occurred.



Table 4. Glycosidic linkage patterns of the native wheat AX and of the carboxyl-reduced ox-AX^{1.0:2.6:0.4} (red-ox-AX^{1.0:2.6:0.4}) determined by methylation analysis.

Glycosidic linkage	% (mol/mol)	
	AX	Red-ox-AX ^{1.0:2.6:0.4 a}
t-Xylp	1.0 (1.4)	1.2 (1.4)
4-Xylp	45.4 (65.7)	50.6 (57.8)
3,4-Xylp	17.1 (24.7)	14.1 (16.1)
2,4-Xylp	1.6 (2.3)	3.6 (4.1)
2,3,4-Xylp	4.0 (5.8)	18.1 (20.7)
Total Xyl	69.1 (65)*	87.7 (85)*
t-Araf	29.6	0.0
2-Araf	0.8	0.0
3-Araf	0.1	0.1
5-Araf	0.4	0.1
3,5-Araf	0.0	0.0
2,3,5-Araf	0.0	0.0
Total Ara	30.9 (35)*	0.2 (-)*
t-AraAf ^b	-	9.3 ^b
2-AraAf ^b	-	0.6 ^b
2,3,5-AraAf ^b	-	2.1 ^b
Total AraAf	-	12.0 (15)*
Degree of branching (DB) ^c	38.6	61.6
t-Ara(A)/Xyl _{subst}	1.1	0.2

() values represent a relative mol % considering only Xyl residues.

()* values represent the relative mol % of sugar determined by HPAEC analysis of the hydrolysates.

^a red-ox-AX^{1.0:2.6:0.4} – ox-AX^{1.0:2.6:0.4} was carboxyl-reduced with carbodiimide/NaBD₄ before being subjected to methylation.

^b AraA moieties were measured as Ara but identified as AraA due to an increment of 2 in the m/z value of the EI-mass spectrum of Ara.

^c DB was calculated as $[Xyl_{subst}/Xyl_{total}]$, where Xyl_{subst} is the sum of (2,4-Xyl + 3,4-Xyl + 2*2,3,4-Xyl) [61].

Regarding Ara, this sugar was mainly found as t-Araf (29.6 %, mol/mol) in AX (Table 4), indicating that the xylan backbone is mainly branched with single Ara units. Only low levels (< 0.8 %) of substituted Araf residues (2-, 5-, and 3-Araf) were observed, showing the presence of few oligomeric-Ara side chains in the AX native structure, which was also reported before [22, 60]. Similarly, the carbodiimide/NaBD₄ carboxyl-reduced ox-AX^{1.0:2.6:0.4} sample also displayed t-Araf as main Ara derived residue. However, this residue was identified as t-AraAf instead of t-Araf due to an increment of 2 in the m/z value relative to the PMAA derived from Ara, as a result of the AraA reduction to Ara with carbodiimide/NaBD₄ [33, 62]. Carboxyl-reduced ox-AX^{1.0:2.6:0.4} contained 9.3 % (mol/mol) of t-AraAf and low amounts of 2,3,5- and 2-AraAf moieties (2.1 and 0.6 %, respectively) (Table 4). Although the absolute Ara amount initially present in the ox-AX^{1.0:2.6:0.4} sample increased from 2.1 % (w/w) (Table 2) to 9.7 % (w/w) (Table S1) in the carboxyl-reduced ox-AX^{1.0:2.6:0.4} sample, the carboxyl-reduced ox-AX^{1.0:2.6:0.4} still contained AraA (Fig. S2), demonstrating incomplete



reduction of ox-AX^{1.0:2.6:0.4}. To reach complete reduction of ox-AX^{1.0:2.6:0.4} and to obtain more accurate results, more than two reduction treatments using carbodiimide/NaBD₄ might be needed [62, 63]. Even though having incomplete reduction of ox-AX^{1.0:2.6:0.4} and having noted some undermethylation of ox-AX^{1.0:2.6:0.4}, these results show that the single-substitution pattern of the xylan backbone of AX was basically conserved in ox-AX^{1.0:2.6:0.4}. This suggests that ox-AX^{1.0:2.6:0.4} has a structure closely related to its native AX by comprising AraA side chains in place of Ara mainly at positions O-3 and/or O-2 of Xyl.

4. Conclusions

TEMPO:NaClO₂:NaOCl in a ratio of 1.0:2.6:0.4 per mol of C5-OH of Ara was the condition that allowed us to oxidize AX to an anionic polymer (arabinuronoxylan) with low level of polymer degradation, with minor effect on the xylan backbone and displaying charged side chains. These acidic side chains were identified to be arabinuronic acid (AraA) by COSY-NMR analysis of its monomeric oxidized-products, conferring an anionic nature to the polymer. Although an accurate AraA quantification could not be reached in our study and a low amount of Ara_f was lost during oxidation, the conversion of Ara_f towards AraA is rather complete. The glycosidic linkage analysis showed that >>75 % of the single-substituted β-(1→4)-xylan backbone was conserved in the ox-AX structure. Therefore, our results indicate that the ox-AX is an arabinuronoxylan mostly comprising AraA side chains, with a substituent distribution intimately related to its parental AX structure. This finding is rather interesting for structure elucidation of arabinoxylans by MS since AraA is heavier than the isomers Ara and Xyl, facilitating distinction of the Ara(A) side chains from the Xyl units by MS. Moreover, as AX are easily extracted and purified from cereals, and their level and pattern of branching with Ara can vary among AX from different sources, TEMPO-oxidation of various AX may yield arabinuronoxylans that display different functional properties, which is particularly valuable for further exploitation for food and/or biomedical applications.



References

- [1] Pierre, G., C. Punta, C. Delattre, L. Melone, P. Dubessay, A. Fiorati, N. Pastori, Y.M. Galante, and P. Michaud. TEMPO-mediated oxidation of polysaccharides: An ongoing story. *Carbohydrate Polymers*. **2017**, 165, 71-85.
- [2] Sundar Raj, A.A., S. Rubila, R. Jayabalan, and T.V. Ranganathan. A Review on Pectin: Chemistry due to General Properties of Pectin and its Pharmaceutical Uses. *Open Access Scientific Reports*. **2012**, 1, 1-4.
- [3] Habibi, Y. Key advances in the chemical modification of nanocelluloses. *Chemical Society Reviews*. **2014**, 43, 1519-1542.
- [4] Meng, Q., S. Fu, and L.A. Lucia. The role of heteropolysaccharides in developing oxidized cellulose nanofibrils. *Carbohydrate Polymers*. **2016**, 144, 187-195.
- [5] Chao, F.-C., M.-H. Wu, L.-C. Chen, H.-L. Lin, D.-Z. Liu, H.-O. Ho, and M.-T. Sheu. Preparation and Characterization of Chemically TEMPO-oxidized and Mechanically Disintegrated Sacchachitin Nanofibers (SCNF) for Enhanced Diabetic Wound Healing. *Carbohydrate Polymers*. **2020**, 229, 115507.
- [6] Bragdt, P.L., H. Van Bekkum, and A.C. Besemer. TEMPO-mediated oxidation of polysaccharides: Survey of methods and applications. *Topics in Catalysis*. **2004**, 27, 49-66.
- [7] Isogai, A., T. Hänninen, S. Fujisawa, and T. Saito. Review: Catalytic oxidation of cellulose with nitroxyl radicals under aqueous conditions. *Progress in Polymer Science*. **2018**, 86, 122-148.
- [8] Tamura, N., M. Wada, and A. Isogai. TEMPO-mediated oxidation of (1→3)-β-d-glucans. *Carbohydrate Polymers*. **2009**, 77, 300-305.
- [9] Hao, J., F. Wu, R. Tang, Y. Sun, D. Liu, and Z. Zhang. Preparation of 1,4-linked α-D-glucuronans from starch with 4-acetamide-TEMPO/NaClO₂/NaClO system. *International Journal of Biological Macromolecules*. **2020**, 151, 740-746.
- [10] de Nooy, A.E.J., A.C. Besemer, and H. van Bekkum. Selective oxidation of primary alcohols mediated by nitroxyl radical in aqueous solution. Kinetics and mechanism. *Tetrahedron*. **1995**, 51, 8023-8032.
- [11] de Nooy, A.E.J., A.C. Besemer, and H. van Bekkum. Highly selective tempo mediated oxidation of primary alcohol groups in polysaccharides. *Recueil des Travaux Chimiques des Pays-Bas*. **1994**, 113, 165-166.
- [12] Spier, V.C., M.R. Sierakowski, W.F. Reed, and R.A. de Freitas. Polysaccharide depolymerization from TEMPO-catalysis: Effect of TEMPO concentration. *Carbohydrate Polymers*. **2017**, 170, 140-147.
- [13] Börjesson, M. and G. Westman. Branching of hemicelluloses through an azetidinium salt ring-opening reaction. *Carbohydrate Research*. **2016**, 428, 23-30.
- [14] Chatterjee, D., T. Halder, N.P. Pathak, A. Paul, Rajkamal, and S. Yadav. DAIB/TEMPO mediated synthesis of anomeric lactones from anomeric hydroxides. *Tetrahedron Letters*. **2017**, 58, 1943-1946.
- [15] Tojo, G. and M. Fernández, *Oxidation of primary alcohols to carboxylic acids : a guide to current common practice*. 2007, Springer: New York.
- [16] Saito, T., M. Hirota, N. Tamura, and A. Isogai. Oxidation of bleached wood pulp by TEMPO/NaClO/NaClO₂ system: Effect of the oxidation conditions on carboxylate content and degree of polymerization. *Journal of Wood Science*. **2010**, 56, 227-232.
- [17] Tamura, N., M. Hirota, T. Saito, and A. Isogai. Oxidation of curdlan and other polysaccharides by 4-acetamide-TEMPO/NaClO/NaClO₂ under acid conditions. *Carbohydrate Polymers*. **2010**, 81, 592-598.
- [18] Tanaka, R., T. Saito, and A. Isogai. Cellulose nanofibrils prepared from softwood cellulose by TEMPO/NaClO/NaClO₂ systems in water at pH 4.8 or 6.8. *International Journal of Biological Macromolecules*. **2012**, 51, 228-234.
- [19] Mendoza, D.J., C. Browne, V.S. Raghuvanshi, G.P. Simon, and G. Garnier. One-shot TEMPO-periodate oxidation of native cellulose. *Carbohydrate Polymers*. **2019**, 226, 115292.
- [20] Sakakibara, C.N., M.R. Sierakowski, N. Lucyszyn, and R.A. de Freitas. TEMPO-mediated oxidation on galactomannan: Gal/Man ratio and chain flexibility dependence. *Carbohydrate Polymers*. **2016**, 153, 371-378.
- [21] Sierakowski, M.R., M. Milas, J. Desbrières, and M. Rinaudo. Specific modifications of galactomannans. *Carbohydrate Polymers*. **2000**, 42, 51-57.
- [22] Izydorezyk, M.S., 23 - Arabinoxylans, in *Handbook of Hydrocolloids (Second Edition)*, G.O. Phillips and P.A. Williams, Editors. **2009**, Woodhead Publishing, 653-692.
- [23] Perlin, A.S. Structure of the soluble pentosans of wheat flours. *Cereal Chem*. **1951**, 28, 382-393.
- [24] Perez, S. Symbolic Representation of Monosaccharides in the Age of Glycobiology. **2018**. Available from: <http://www.glycopedia.eu/e-chapters/symbolic-representation-of-monosaccharides-in-the-age-of-glycobiology/article/abstract>.
- [25] Izydorezyk, M.S. and C.G. Biliaderis. Cereal arabinoxylans: advances in structure and physicochemical properties. *Carbohydrate Polymers*. **1995**, 28, 33-48.



- [26] Parikka, K., I. Nikkilä, L. Pitkänen, A. Ghafar, T. Sontag-Strohm, and M. Tenkanen. Laccase/TEMPO oxidation in the production of mechanically strong arabinoxylan and glucomannan aerogels. *Carbohydrate Polymers*. **2017**, 175, 377-386.
- [27] Bowman, M.J., B.S. Dien, P.J. O'Bryan, G. Sarath, and M.A. Cotta. Selective chemical oxidation and depolymerization of (*Panicum virgatum* L.) xylan with switchgrass oligosaccharide product analysis by mass spectrometry. *Rapid Communications in Mass Spectrometry*. **2011**, 25, 941-950.
- [28] De Ruiter, G.A., H.A. Schols, A.G.J. Voragen, and F.M. Rombouts. Carbohydrate analysis of water-soluble uronic acid-containing polysaccharides with high-performance anion-exchange chromatography using methanolysis combined with TFA hydrolysis is superior to four other methods. *Analytical Biochemistry*. **1992**, 207, 176-185.
- [29] ter Haar, R., J.W. Timmermans, T.M. Slaghek, F.E.M. Van Dongen, H.A. Schols, and H. Gruppen. TEMPO oxidation of gelatinized potato starch results in acid resistant blocks of glucuronic acid moieties. *Carbohydrate Polymers*. **2010**, 81, 830-838.
- [30] Sun, P., M. Frommhagen, M. Kleine Haar, G. van Erven, E.J. Bakx, W.J.H. van Berkel, and M.A. Kabel. Mass spectrometric fragmentation patterns discriminate C1- and C4-oxidised cello-oligosaccharides from their non-oxidised and reduced forms. *Carbohydrate Polymers*. **2020**, 234, 115917.
- [31] Malz, F. and H. Jancke. Validation of quantitative NMR. *Journal of Pharmaceutical and Biomedical Analysis*. **2005**, 38, 813-823.
- [32] Merx, D.W.H., Y. Westphal, E.J.J. van Velzen, K.V. Thakoer, N. de Roo, and J.P.M. van Duynhoven. Quantification of food polysaccharide mixtures by ¹H NMR. *Carbohydrate Polymers*. **2018**, 179, 379-385.
- [33] Taylor, R.L. and H.E. Conrad. Stoichiometric depolymerization of polyuronides and glycosaminoglycuronans to monosaccharides following reduction of their carbodiimide-activated carboxyl group. *Biochemistry*. **1972**, 11, 1383-1388.
- [34] Pandeirada, C.O., É. Maricato, S.S. Ferreira, V.G. Correia, B.A. Pinheiro, D.V. Evtuguin, A.S. Palma, A. Correia, M. Vilanova, M.A. Coimbra, and C. Nunes. Structural analysis and potential immunostimulatory activity of *Nannochloropsis oculata* polysaccharides. *Carbohydrate Polymers*. **2019**, 222, 114962.
- [35] Nunes, C., L. Silva, A.P. Fernandes, R.P.F. Guiné, M.R.M. Domingues, and M.A. Coimbra. Occurrence of cellobiose residues directly linked to galacturonic acid in pectic polysaccharides. *Carbohydrate Polymers*. **2012**, 87, 620-626.
- [36] Brückner, C., Nitroxide-Catalyzed Alcohol Oxidations in Organic Synthesis, in *Stable Radicals: Fundamentals and Applied Aspects of Odd-Electron Compounds*. **2010**, John Wiley and Sons. 433-460.
- [37] Dervilly, G., L. Saulnier, P. Roger, and J.F. Thibault. Isolation of Homogeneous Fractions from Wheat Water-Soluble Arabinoxylans. Influence of the Structure on Their Macromolecular Characteristics. *Journal of Agricultural and Food Chemistry*. **2000**, 48, 270-278.
- [38] Dervilly-Pinel, G., J.F. Thibault, and L. Saulnier. Experimental evidence for a semi-flexible conformation for arabinoxylans. *Carbohydrate Research*. **2001**, 330, 365-372.
- [39] Saulnier, L., P.-E. Sado, G. Branlard, G. Charmet, and F. Guillon. Wheat arabinoxylans: Exploiting variation in amount and composition to develop enhanced varieties. *Journal of Cereal Science*. **2007**, 46, 261-281.
- [40] Rejzek, M., B. Mukhopadhyay, C.Q. Wenzel, J.S. Lam, and R.A. Field. Direct oxidation of sugar nucleotides to the corresponding uronic acids: TEMPO and platinum-based procedures. *Carbohydrate Research*. **2007**, 342, 460-466.
- [41] Guo, Q., L. Ai, and S.W. Cui, *Methodology for structural analysis of polysaccharides*. 2018, Springer: Cham, Switzerland.
- [42] Lin, C., T. Zeng, Q. Wang, L. Huang, Y. Ni, F. Huang, X. Ma, and S. Cao. Effects of the conditions of the TEMPO/NaBr/NaClO System on carboxyl groups, degree of polymerization, and yield of the oxidized cellulose. *BioResources*. **2019**, 13, 5965-5975.
- [43] Shibata, I. and A. Isogai. Depolymerization of cellouronic acid during TEMPO-mediated oxidation. *Cellulose*. **2003**, 10, 151-158.
- [44] Huang, J., W.-w. Chen, S. Hu, J.-Y. Gong, H.-W. Lai, P. Liu, L.-h. Mei, and J.-w. Mao. Biochemical activities of 6-carboxy β-chitin derived from squid pens. *Carbohydrate Polymers*. **2013**, 91, 191-197.
- [45] Gruppen, H., R.J. Hamer, and A.G.J. Voragen. Water-unextractable cell wall material from wheat flour. 2. Fractionation of alkali-extracted polymers and comparison with water-extractable arabinoxylans. *Journal of Cereal Science*. **1992**, 16, 53-67.
- [46] Izydorczyk, M.S. and C.G. Biliaderis. Structural heterogeneity of wheat endosperm arabinoxylans. *Cereal Chemistry*. **1993**, 70, 641-646.
- [47] Davis, N.J. and S.L. Flitsch. Selective oxidation of monosaccharide derivatives to uronic acids. *Tetrahedron Letters*. **1993**, 34, 1181-1184.
- [48] Takeda, T., J.G. Miller, and S.C. Fry. Anionic derivatives of xyloglucan function as acceptor but not donor substrates for xyloglucan endotransglucosylase activity. *Planta*. **2008**, 227, 893-905.



- [49] Benesi, A.J., C.J. Falzone, S. Banerjee, and G.K. Farber. NMR assignments for the aldopentoses. *Carbohydrate Research*. **1994**, 258, 27-33.
- [50] Kiemle, D.J., A.J. Stipanovic, and K.E. Mayo, *Proton NMR methods in the compositional characterization of polysaccharides*, in *ACS Symposium Series*, P. Gatenholm and M. Tenkanen, Editors. 2004. p. 122-139.
- [51] Wu, J. and A.S. Serianni. d-Penturonic acids: solution studies of stable-isotopically enriched compounds by ¹H- and ¹³C-n.m.r. spectroscopy. *Carbohydrate Research*. **1991**, 210, 51-70.
- [52] Munk, L., J. Muschiol, K. Li, M. Liu, A. Perzon, S. Meier, P. Ulvskov, and A.S. Meyer. Selective Enzymatic Release and Gel Formation by Cross-Linking of Feruloylated Glucurono-Arabinoxylan from Corn Bran. *ACS Sustainable Chemistry & Engineering*. **2020**, 8, 8164-8174.
- [53] Yin, J.Y., H.X. Lin, S.P. Nie, S.W. Cui, and M.Y. Xie. Methylation and 2D NMR analysis of arabinoxylan from the seeds of *Plantago asiatica* L. *Carbohydrate Polymers*. **2012**, 88, 1395-1401.
- [54] Hinton, M.R., M. Manley-Harris, K.I. Hardcastle, and D.E. Kiely. Pentic acids and derivatives from nitric acid-oxidized pentoses. *Journal of Carbohydrate Chemistry*. **2013**, 32, 68-85.
- [55] Mehtiö, T., M. Toivari, M.G. Wiebe, A. Harlin, M. Penttilä, and A. Koivula. Production and applications of carbohydrate-derived sugar acids as generic biobased chemicals. *Critical Reviews in Biotechnology*. **2016**, 36, 904-916.
- [56] Bengtsson, S., R. Andersson, E. Westerlund, and P. Åman. Content, structure and viscosity of soluble arabinoxylans in rye grain from several countries. *Journal of the Science of Food and Agriculture*. **1992**, 58, 331-337.
- [57] Gruppen, H., R.A. Hoffmaann, F.J.M. Kormelink, A.G.J. Voragen, J.P. Kamerlin, and J.F.G. Vliegthart. Characterisation by ¹H NMR spectroscopy of enzymically derived oligosaccharides from alkaline-extractable wheat-flour arabinoxylan. *Carbohydrate Research*. **1992**, 233, 45-64.
- [58] Guo, R., Z. Xu, S. Wu, X. Li, J. Li, H. Hu, Y. Wu, and L. Ai. Molecular properties and structural characterization of an alkaline extractable arabinoxylan from hull-less barley bran. *Carbohydrate Polymers*. **2019**, 218, 250-260.
- [59] Rondeau-Mouro, C., R. Ying, J. Ruellet, and L. Saulnier. Structure and organization within films of arabinoxylans extracted from wheat flour as revealed by various NMR spectroscopic methods. *Magnetic Resonance in Chemistry*. **2011**, 49, S85-S92.
- [60] Kormelink, F.J.M. and A.G.J. Voragen. Degradation of different [(glucurono)arabino]xylans by a combination of purified xylan-degrading enzymes. *Applied Microbiology and Biotechnology*. **1993**, 38, 688-695.
- [61] Coelho, E., M.A.M. Rocha, A.S.P. Moreira, M.R.M. Domingues, and M.A. Coimbra. Revisiting the structural features of arabinoxylans from brewers' spent grain. *Carbohydrate Polymers*. **2016**, 139, 167-176.
- [62] Sims, I.M., S.M. Carnachan, T.J. Bell, and S.F.R. Hinkley. Methylation analysis of polysaccharides: Technical advice. *Carbohydrate Polymers*. **2018**, 188, 1-7.
- [63] Kamerling, J.P. and G.J. Gerwig, 2.01 - Strategies for the Structural Analysis of Carbohydrates, in *Comprehensive Glycoscience*, H. Kamerling, Editor. **2007**, Elsevier: Oxford. 1-68.



Supplementary data

Molecular weight distribution by HPSEC

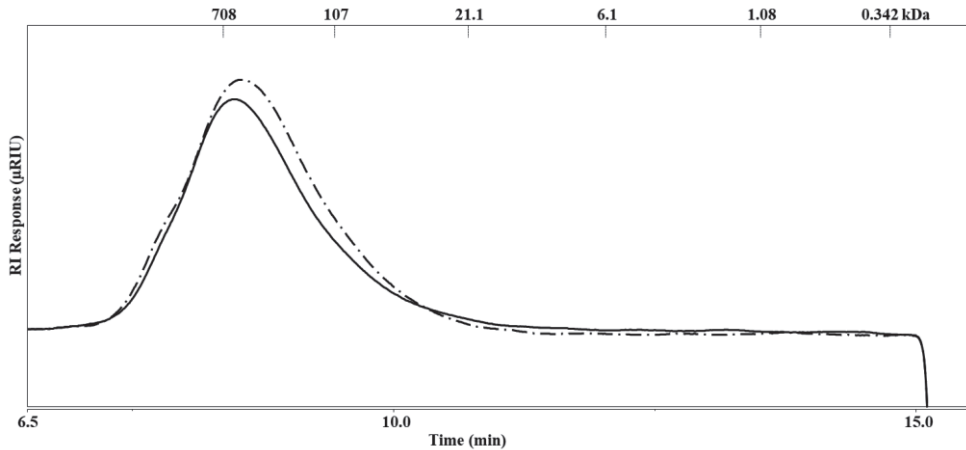


Figure S 1. HPSEC elution patterns of the native AX (—) and of the preliminary TEMPO-oxidized AX sample (ox-AX^{0.2:2.6:0.4}, - - -). Pullulan standards were used to calibrate the system.

Sugar composition profile ascertained by HPAEC

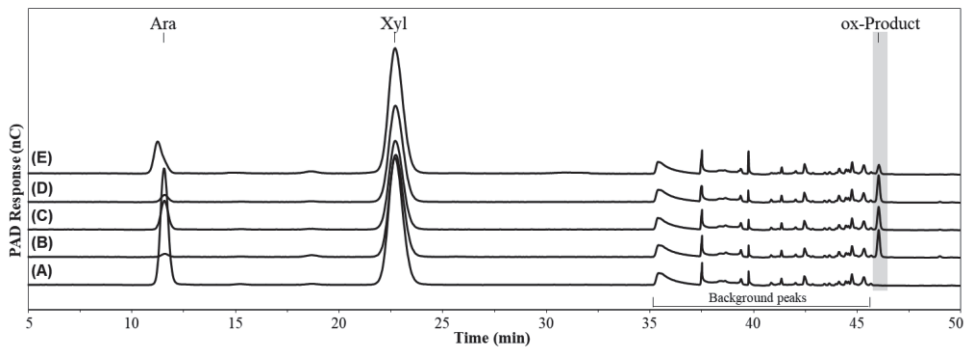


Figure S 2. HPAEC elution profile of the hydrolysates of the native AX (A), ox-AX^{1.0:2.6:1.5} (B), ox-AX^{0.2:2.6:1.5} (C), ox-AX^{1.0:2.6:0.4} (D), and carboxyl-reduced ox-AX^{1.0:2.6:0.4} with carbodiimide/NaBD4 (E) samples. Ara, arabinose; Xyl, xylose; ox-Product, oxidized product (arabinuronic acid, AraAf) is highlighted with a grey box. Elution of uronic acids occurs in the time range between 40 and 50 min. ox-AX^b refers to the oxidized wheat arabinoxylan (ox-AX) obtained with a ^b TEMPO:NaClO₂:NaOCl ratio per mol of C5-OH of Ara.



Table S 1. Yields, and sugar composition and recovery of the native wheat AX, of the oxidized AX (ox-AX) samples using various ratios of TEMPO:NaClO₂:NaOCl per mol of C5-OH, and of the carboxyl-reduced ox-AX^{1.0:2.6:0.4} (red-ox-AX^{1.0:2.6:0.4}) with carbodiimide/NaBD₄.

Sample	Yield (%, w/w)	Carbohydrate composition (%, w/w) ^c			Ox- Product	Sugar Recovery (%, w/w)
		Ara	Xyl	Total		
AX	-	31.6 ± 0.1 (34.9 ± 0.1)	58.9 ± 0.5 (65.1 ± 0.1)	90.5 ± 0.6	-	-
ox-AX ^{0.2:2.6:0.4}	88 ^a	16.6 ± 0.3 (20.6 ± 0.1)	63.8 ± 1.9 (79.4 ± 0.1)	80.4 ± 2.2	+	70.5 ± 1.9
ox-AX ^{1.0:2.6:1.5}	97 ^a	0.9 ± 0.0 (1.6 ± 0.0)	56.5 ± 0.6 (98.4 ± 0.0)	57.5 ± 0.6	+	55.7 ± 0.6 ^d
ox-AX ^{0.2:2.6:1.5}	98 ^a	9.5 ± 0.2 (15.0 ± 0.2)	53.9 ± 0.4 (85.0 ± 0.2)	63.4 ± 0.6	+	62.1 ± 0.6 ^d
ox-AX ^{1.0:2.6:0.4}	91 ^a	2.1 ± 0.1 (3.7 ± 0.0)	53.9 ± 1.9 (96.3 ± 0.0)	55.9 ± 1.9	+	50.1 ± 1.8 ^d
Red-ox- AX ^{1.0:2.6:0.4}	68 ^b	9.7 ± 0.1 (15.1 ± 0.0)	54.6 ± 0.2 (84.9 ± 0.0)	64.3 ± 0.3	+	39.8 ± 0.2 ^e

^a Yield in weight % relative to the native AX.

^b Yield in weight % relative to the oxidized polysaccharide.

^c Results are expressed as average (n=2) weight % of sample. Results in brackets refer to a relative mol percentage (%) considering only Ara and Xyl sugar residues. Presence of the oxidized product (AraAf) formed during TEMPO-oxidation reaction is indicated with +, and absence with -.

^d Results are expressed as average (n=2) weight % of native AX. ox-Product (arabinuronic acid, AraAf) is not accounted in the sugar recovery of ox-AX.

^e Results are expressed as average (n=2) weight % of oxidized polysaccharide (ox-AX^{1.0:2.6:0.4}). ox-Product (AraAf) is not accounted in the sugar recovery of ox-AX.

ox-AX^b refers to the oxidized wheat arabinoxylan (ox-AX) obtained with a ^b TEMPO:NaClO₂:NaOCl ratio per mol of C5-OH of Ara.

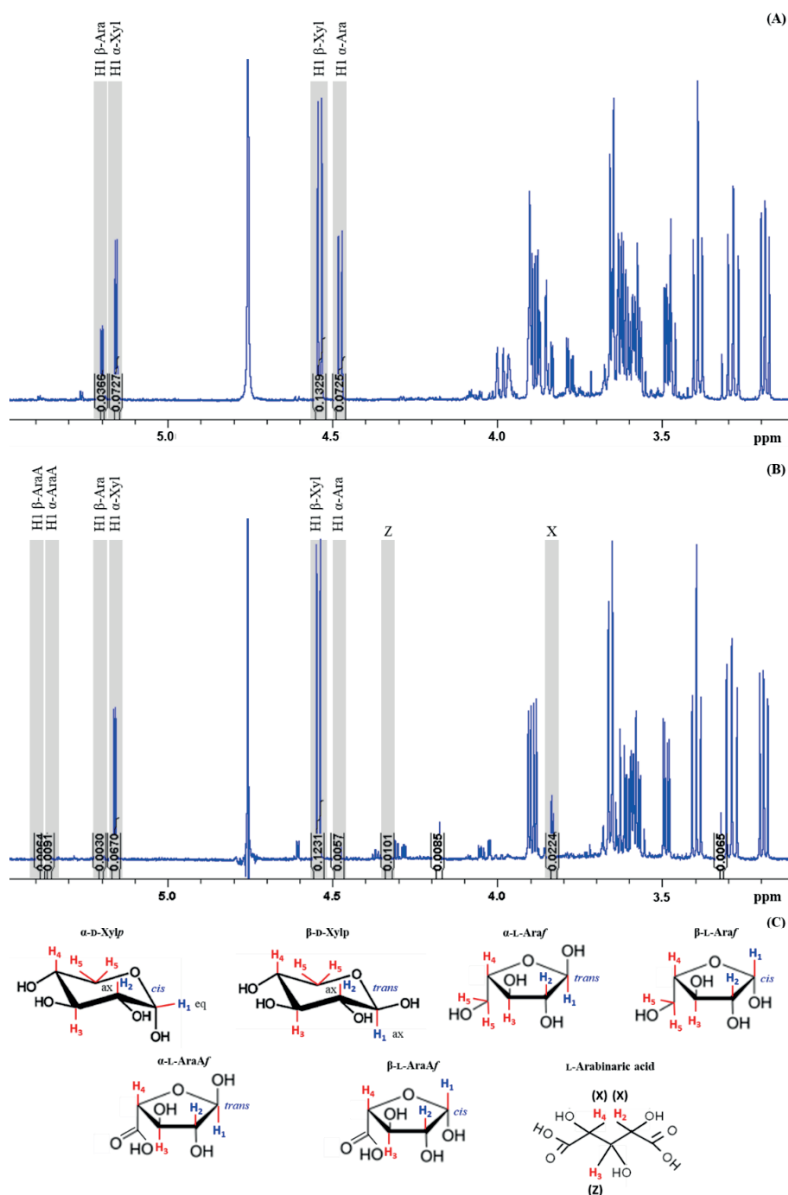
**¹H-NMR spectra of the AX and ox-AX^{1.0:2.6:0.4} hydrolysates**

Figure S 3. ¹H-NMR spectra (600 MHz) of the monosaccharides present in the hydrolysates of the native AX (A) and ox-AX^{1.0:2.6:0.4} (B) samples. H1 signals of the α- and β-conformations of Xyl, Ara and AraA, and chemical shifts Z and X of tentative compounds derived from AraA ascertained by 2D-NMR are highlighted in grey boxes. Relative integrals of each highlighted signal relative to the integral of the internal standard (Maleic acid), which was set to 1.0, are depicted. Corresponding identified monosaccharide and tentatively assigned oxidized sugar-derived compound structures are shown (C). *cis* and *trans* positions of the H1 and H2 of the cyclic sugars are depicted. ax, axial; eq, equatorial.

$^1\text{H-NMR}$ spectra of AX and ox-AX^{1.0:2.6:0.4}

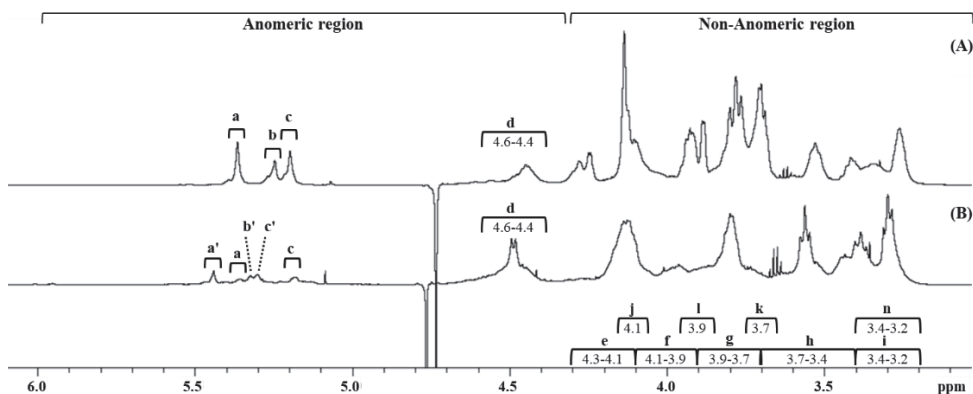


Figure S 4. $^1\text{H-NMR}$ spectra (600 MHz) of the native AX (A) and ox-AX^{1.0:2.6:0.4} (B) samples. H1 signals of the α -Ara linked at positions *O*-3 of 3,4-Xyl (a), *O*-3 of 2,3,4-Xyl (b), and *O*-2 of 2,3,4-Xyl (c). a', b', and c' are assumed to be the corresponding signals derived from α -AraA, as the H1 signals of t-GlcA in glucurono-arabinoxylans also falls within δ 5.0-5.6 ppm [1, 2]. d corresponds to the chemical shift range of the H1 of the β -Xyl. Ara and Xyl-derived signal assignments (e-m) were performed using previously published data [3-6]. Chemical shift range between δ 4.7-4.8 ppm is due to residual H_2O .

- [1] Munk, L., J. Muschiol, K. Li, M. Liu, A. Perzon, S. Meier, P. Ulvskov, and A.S. Meyer. Selective Enzymatic Release and Gel Formation by Cross-Linking of Feruloylated Glucurono-Arabinoxylan from Corn Bran. *ACS Sustainable Chemistry & Engineering*. **2020**, 8, 8164-8174.
- [2] Yin, J.Y., H.X. Lin, S.P. Nie, S.W. Cui, and M.Y. Xie. Methylation and 2D NMR analysis of arabinoxylan from the seeds of *Plantago asiatica* L. *Carbohydrate Polymers*. **2012**, 88, 1395-1401.
- [3] Bengtsson, S., R. Andersson, E. Westerlund, and P. Åman. Content, structure and viscosity of soluble arabinoxylans in rye grain from several countries. *Journal of the Science of Food and Agriculture*. **1992**, 58, 331-337.
- [4] Gruppen, H., R.A. Hoffmaann, F.J.M. Kormelink, A.G.J. Voragen, J.P. Kamerlin, and J.F.G. Vliegthart. Characterisation by ^1H NMR spectroscopy of enzymically derived oligosaccharides from alkali-extractable wheat-flour arabinoxylan. *Carbohydrate Research*. **1992**, 233, 45-64.
- [5] Guo, R., Z. Xu, S. Wu, X. Li, J. Li, H. Hu, Y. Wu, and L. Ai. Molecular properties and structural characterization of an alkaline extractable arabinoxylan from hull-less barley bran. *Carbohydrate Polymers*. **2019**, 218, 250-260.
- [6] Rondeau-Mouro, C., R. Ying, J. Ruellet, and L. Saulnier. Structure and organization within films of arabinoxylans extracted from wheat flour as revealed by various NMR spectroscopic methods. *Magnetic Resonance in Chemistry*. **2011**, 49, S85-S92.

Chapter 3

Partial acid-hydrolysis of TEMPO-oxidized arabinoxylans generates arabinoxylan-structure resembling oligosaccharides

Published as: Pandeirada, C.O., S. Speranza, E. Bakx, Y. Westphal, H.-G. Janssen, and H.A. Schols. *Carbohydrate Polymers*. **2022**, 276, 118795.



Abstract

Arabinoxylans (AXs) display biological activities that depend on their chemical structures. To structurally characterize and distinguish AXs using a non-enzymatic approach, various TEMPO-oxidized AXs were partially acid-hydrolysed to obtain diagnostic oligosaccharides (OS). Arabinuronoxyloligomer alditols (AUXOS-A) with degree of polymerization 2–5, comprising one and two arabinuronic acid (AraA) substituents were identified in the UHPLC-PGC-MS profiles of three TEMPO-oxidized AXs, namely wheat (ox-WAX), partially-debranched WAX (ox-pD-WAX), and rye (ox-RAX). Characterization of these AUXOS-A highlighted that single-substitution of the Xyl unit preferably occurs at position *O*-3 for these samples, and that ox-WAX has both more single substituted and more double-substituted xylose residues in its backbone than the other AXs. Characteristic UHPLC-PGC-MS OS profiles, differing in OS abundance and composition, were obtained for each AX. Thus, partial acid-hydrolysis of TEMPO-oxidized AXs with analysis of the released OS by UHPLC-PGC-MS is a promising novel non-enzymatic approach to distinguish AXs and obtain insights into their structures.



1. Introduction

There is a high interest in dietary fibres due to their associated health benefits [1]. Cereals, such as wheat, rye, oat, and maize, are amongst the main sources of dietary fibre, and their bran can be added to food systems to increase the dietary fibre content [1, 2]. Arabinoxylans (AXs) are the major dietary fibres found in cereals. Their biological activities are highly dependent on the chemical fine structure of the AX [3]. In terms of chemical structure AX consists of a linear β -(1 \rightarrow 4)-D-xylan backbone that is substituted with single α -L-arabinofuranosyl (Araf) attached to positions O-3 and/or O-2 of the β -D-xylopiranosyl (Xylp) unit [4]. The substitution pattern along the xylan backbone with Araf can vary, depending on the cellular origin or source [5]. For example, pericarp AXs from wheat are reported to have the highest degree of double-substituted Xyl units [6], and water extractable AXs (WEAX) from rye have a higher degree of single-substituted Xyl units than the corresponding WEAX from wheat [7, 8]. More complex structures have been reported, especially for rice, sorghum, and maize, comprising for example 4-O-methylglucopyranosyluronic acid, acetyl and feruloyl groups as substituents [5].

The structure of AXs can be accessed through their enzymatic depolymerization into (arabino-)xylo-oligosaccharides (AXOS) with detailed analysis of these products using various methods, such as liquid chromatography - mass spectrometry (LC-MS) and NMR [9-11]. An advantage of using pure and well characterized enzymes to depolymerize AXs from various sources is that specific (diagnostic) OS are obtained for structurally different AXs due to the enzyme's substrate specificity [12]. The enzymatic depolymerization approach results in characteristic chromatographic oligosaccharide profiles for each type of AX, enabling a quick distinction among them. A drawback of the enzymatic approach is that it requires pure and highly specific enzymes, which are not always available [13]. As an alternative to enzymatic hydrolysis, partial acid-hydrolysis is an easy and more accessible approach to degrade polysaccharides (PS) into OS [14]. However, opposite to the enzymatic approach, partial acid-hydrolysis of AXs to polymer structure-representative OS is hindered by the low acid stability of the Ara substituents [15], leading to the formation of Ara and Xyl monomers and XOS as main depolymerization products, no longer representing the polymer's structural features.

The Ara residues of AXs can be selectively oxidized to arabinuronic acid (AraA) using a TEMPO-mediated reaction [16, 17], yielding an arabinuronoxylan that comprises aldobiuronic acids (AraA \rightarrow Xyl) in its structure. The selective oxidation of Ara to AraA is due to the high selectivity of 2,2,6,6-tetramethylpiperidine-1-oxyl (TEMPO) to oxidize primary hydroxyls, as those present at C5 of Araf in AX, to carboxyl groups when the right co-oxidant is present [18-20]. The glycosidic linkage of aldobiuronic acids is more resistant to acid degradation than the linkage between neutral sugars [21-23]. Hence, the AraA side chains of arabinuronoxylans are expected to be more resistant to acid treatments than the Ara side chains in AX. This might allow the production of diagnostic arabinuronoxyloligomers (AUXOS) upon partial acid-hydrolysis [16].

Among the various chromatographic methods used to characterize OS, such as high performance anion-exchange chromatography (HPAEC) and hydrophilic interaction liquid chromatography (HILIC) [10, 24, 25], porous graphitic carbon (PGC) chromatography has shown the ability to successfully separate neutral and acidic oligosaccharide isomers [26-29]. Due to the retention mechanism of the PGC column, where the size, type of linkage, the conformational structure and planarity of OS determine the interaction with the stationary phase [30]. Additionally, PGC ultra-high-



performance liquid chromatography (UHPLC) is highly compatible with MS, enabling in-depth characterization of OS by (tandem) MS experiments [26, 30].

In this study, a non-enzymatic approach consisting of partial acid-hydrolysis of various TEMPO-oxidized (ox-)AXs followed by analysis of the released fragments using UHPLC-PGC-MS is proposed to obtain characteristic chromatographic OS profiles for ox-AX structure investigation. Three AXs with different structures, wheat AX, partial acid-debranched wheat AX, and rye AX are studied. Structural characterization of the released OS is used to obtain an insight into the structure of the native AX.

2. Materials and methods

2.1. Materials

The arabinoxylans (AXs) studied were a wheat flour AX (WAX) of medium viscosity (Ara:Xyl=38:62, Purity > 95 %), a rye flour AX (RAX, Ara:Xyl=38:62, Purity ~ 90 %), and a partially acid-debranched WAX (pD-WAX, Ara:Xyl=22:78, Purity > 94 %). All samples were purchased from Megazyme (Wicklow, Ireland). β -(1 \rightarrow 4)-linked xylo-oligomer (XOS) standards with a degree of polymerization (DP) from 2 to 5 were also purchased from Megazyme. Sodium borodeuteride (NaBD₄, 98 %) was purchased from Sigma Aldrich (St. Louis, MO, USA). 2,2,6,6-tetramethylpiperidine-1-oxyl radical (TEMPO, 98 %), NaClO₂ (80 %), and sodium hypochlorite solution (6-14 % active chlorine NaOCl) were purchased from Merck (Darmstadt, Germany). Methyl iodide (CH₃I) was obtained from VWR (Rue Carnot, France). Acetonitrile, isopropanol (IPA), formic acid, and ULC-MS water were of UHPLC-grade (Biosolve, Valkenswaard, The Netherlands). All water was purified in a Milli-Q system from Millipore (Molsheim, France), unless otherwise mentioned.

2.2. TEMPO/NaClO₂/NaOCl oxidation of polysaccharides

A TEMPO/NaClO₂/NaOCl system at pH 4.6 was used to oxidize WAX, pD-WAX, and RAX. TEMPO/NaClO₂/NaOCl oxidation was performed as described previously [17]. To have one uniform TEMPO-oxidation reaction for the three AXs, a TEMPO:NaO₂Cl:NaOCl ratio of 1.0:2.6:0.4 per mol of C5-OH in WAX or RAX was selected to perform the reaction, as both WAX and RAX have the same Xyl:Ara ratio. A polysaccharide concentration of 5.0 mg/mL was used for the reaction and polysaccharide oxidation was performed in duplicate. All oxidized (ox-)AXs were characterized and further subjected to a partial acid-hydrolysis (section 2.6) to create OS.

2.3. Sugar composition analysis by HPAEC-PAD

Monosaccharides composition was determined in accordance with Pandeirada et al. [17]. After methanolysis (2.0 M HCl in dried methanol, 16 h, 80 °C) of the (ox-)AXs and acid hydrolysis using TFA (2.0 M, 1 h, 121 °C), the released monosaccharides were analyzed by High-Performance Anion-Exchange Chromatography with Pulsed Amperometric Detection (HPAEC-PAD). An ICS-5000 HPLC system (Dionex, Sunnyvale, CA, USA) equipped with a CarboPac PA1 guard column (2 mm ID \times 50 mm) and a CarboPac PA-1 column (2 mm \times 250 mm; Dionex) was used for this analysis. Detection of the eluted compounds was performed by an ED40 EC-detector (Dionex) running in the PAD mode. 10



μL of the diluted hydrolysates (25 $\mu\text{g}/\text{mL}$) was injected on the system. Mobile phases used to elute the compounds were kept under helium flushing and the column temperature was 20 $^{\circ}\text{C}$. A flow rate of 0.4 mL/min was used with the following gradient of 0.1 M sodium hydroxide (NaOH: A) and 1.0 M sodium acetate (NaOAc) in 0.1 M NaOH (B): 0-35 min, 100 % milli-Q water; 35.1 min, 100 % A; 35.2-50 min, 0-40 % B; 50.1-55 min, 100 % B; 55.1-63.0 min, 100% A; 63.1-78.0 min, 100 % milli-Q water. A post-column alkali addition step (0.5 M NaOH; 0.1 mL/min) was used from 0.0-34.9 min and from 68.1-78.0 min. All samples were analyzed in duplicate. Standards of Ara and Xyl (0-150 $\mu\text{g}/\text{mL}$) were used for quantification. Due to absence of a commercially available AraA standard, the presence of this monomeric sugar was identified without quantification. The collected data was analyzed using Chromeleon 7.2 software (Dionex).

2.4. Glycosidic linkage analysis

WAX, pD-WAX, and RAX were subjected to per-methylation analysis to study the glycosidic linkage patterns. Partially methylated polysaccharides were converted into their partially methylated alditol acetate (PMAA) forms by hydrolysis, reduction, and acetylation, and further analyzed by gas-chromatography coupled to mass spectrometry (GC-MS) as described elsewhere [17]. The collected data was analyzed using Xcalibur 4.1 software (Thermo Scientific) and chromatographic peaks were identified comparing all mass spectra with a laboratory made database of PMAA forms. The degree of branching (DB) was calculated as $[\text{Xyl}_{\text{subst}}/\text{Xyl}_{\text{total}}]$, where $\text{Xyl}_{\text{subst}}$ is the sum of (2,4-Xyl + 3,4-Xyl + 2*2,3,4-Xyl), and $\text{Xyl}_{\text{total}}$ is the sum of (t-Xyl + 4-Xyl + 2,4-Xyl + 3,4-Xyl + 2*2,3,4-Xyl) [31].

2.5. Molecular weight distribution by HPSEC-RI

The average molecular weight (Mw) was determined by high performance size exclusion chromatography (HPSEC). HPSEC analysis was carried out on an Ultimate 3000 system (Dionex, Sunnyvale, CA, USA) coupled to a Shodex RI-101 detector (Showa Denko K.K., Tokyo, Japan). The system was equipped with a set of three TSK-Gel Super columns 4000AW, 3000AW, and 2500AW connected in series preceded by a TSK Super AW-L guard column (4.6 mm ID \times 35 mm, 7 μm), all from Tosoh Bioscience (Tokyo, Japan). Standards and samples (1.0 mg/mL) were eluted from the system as described by Pandeirada et al. [17]. Pullulan standards (0.180–708 kDa; Polymer Laboratories, Church Stretton, UK) were used to calibrate the SEC columns and used to estimate the Mw distribution. The collected data was analyzed using Chromeleon 7.2 software (Dionex Corporation). The extent of polysaccharide depolymerization after TFA partial acid-hydrolysis into various degree of polymerization (DP; DP<2, 2<DP<20, DP>20; % Released DP_x) was calculated using the area under the peak with a retention time (Rt)>14.7 min for DP<2, the area between 12.7 min<Rt<14.7 min for 2<DP<20, and the area with a Rt<12.7 min for DP>20 as percentage of the area of the non-hydrolysed arabinoxylan.



2.6. Depolymerization of (ox-)AX samples using TFA partial acid-hydrolysis

Native and ox-AX samples (2.0 mg) were partially acid-hydrolysed with 0.2 M TFA (4.0 mL) in a closed glass tube for 2 h at 90 °C [32, 33]. All polysaccharides were hydrolysed in duplicate. Afterwards, the hydrolysates were concentrated under N₂ at room temperature (RT), and diluted in milli-Q water for further characterization.

2.7. Oligosaccharides profile and characterization by UHPLC-PGC-MS

Prior to analysis, the reducing-end residue of the OS obtained from partial acid-hydrolysis was converted into an alditol by reduction to improve LC separation and to facilitate structure characterization by MS [34]. Briefly, 200 µL of 2.0 mg/mL of partially acid-hydrolysed native and ox-AX samples or standard mixture composed of Ara, Xyl, and XOS (DP2-5) was incubated with freshly prepared 0.5 M NaBD₄ (200 µL) for 20 h at 20 °C. Reduced samples and standards were cleaned-up by SPE using Supelclean™ ENVICarb™ columns (3 mL, Sigma-Aldrich). Collected NaBD₄-reduced OS-alditols, named (AU)XOS-A, from the SPE column were dried under a stream of N₂ at RT and dissolved in Milli-Q water to a final concentration of 0.25 mg/mL for AX and 0.05 mg/mL for XOS standards.

(AU)XOS-A were separated and analyzed by ultra-high performance liquid chromatography (UHPLC) using a porous-graphitized carbon (PGC) as the stationary phase coupled to electron spray ionization (ESI) mass spectrometry (MS). Liquid chromatography was carried out on a Vanquish UHPLC system (Thermo Scientific, Waltham, MA, USA) equipped with a Hypercarb PGC column (150 x 2.1 mm; 3 µm particle size; Thermo Scientific) in combination with a Hypercarb guard column (10 x 2.1 mm, 3 µm particle size; Thermo Scientific). The column oven temperature was set at 70 °C and the flow rate at 0.3 mL/min; injection volume was 5.0 µL. Various elution conditions and organic modifiers were tested, namely methanol, acetonitrile and acetonitrile:isopropanol (50 %, v/v), all containing 0.1 % formic acid. Elution of OS using the strongest organic mobile phase (acetonitrile:isopropanol (50 %, v/v) containing 0.1 % formic acid) eluted OS with higher DP compared to the other organic mobile phases (data not shown). Water (A) and 50 % (v/v) acetonitrile:isopropanol (B), both containing 0.1 % (v/v) formic acid were used as mobile phases. The following gradient was used: 0-13.3 min, 3-15 % B; 13.3-40 min, 15-40 % B; 40-41 min, 40-100 % B; 41-46.3 min, 100 % B; 46.3-47.3 min, 100-3 % B; and 47.3-53.3 min, 3 % B. The mass-to-charge ratio (m/z) of the separated OS was detected by an LTQ-VelosPro mass spectrometer (Thermo Scientific) equipped with a heated ESI probe. MS data were obtained in negative ion mode with the following settings: source heater temperature 413 °C, capillary temperature 256 °C, sheath gas flow 48 units, source voltage 2.5 kV and m/z range 125-2000. As MS^{2/3} settings, CID with a normalized collision energy of 35 %, with a minimum signal threshold of 500 counts at an activation Q of 0.25 and activation time of 10 ms were used. Mass spectrometric data were processed by using Xcalibur 4.1 software (Thermo Scientific). Peak areas of the identified (AU)XOS-A within a DP2-7 as extracted from the MS signal were used for relative quantification.



3. Results and discussion

A TEMPO/NaO₂Cl/NaOCl system was used to oxidize the Ara substituents of three arabinoxylans (AXs) having different substitution levels and patterns, namely a wheat AX (WAX), a partially acid-debranched WAX (pD-WAX), and a rye AX (RAX), to arabinuronic acid (AraA). The oxidized (ox-)AXs were partially acid-hydrolysed to obtain arabinurono-xylo-oligosaccharides (AUXOS) that allow characterization of AX structures by analysis of the generated AUXOS by MS. Furthermore, the obtained oligosaccharide chromatographic profiles among AXs were used to distinguish the three AXs.

3.1. Sugar (linkage) composition of parental and TEMPO-oxidized arabinoxylans

We have recently characterized the chemical structure of native and ox-WAX samples [17]. WAX and RAX had an identical molar Ara:Xyl ratio of 35:65 mol/mol %, in agreement with previous works [9, 35-38]. Although having an identical Ara:Xyl ratio, RAX displayed a higher degree of branching (DB) than WAX (47 % and 39 %, respectively, Table 1), which is due to different levels of single- and double-substitution of the Xyl units between samples. RAX has more single-substituted (1→4)-xylose residues at position *O*-3 (39 mol % of total Xyl units) than WAX (25 %). RAX has only minor single substitution at position *O*-2 of Xyl (3 %) or double substitution at *O*-2 and *O*-3 position of Xyl. These results are in agreement with literature for RAX showing that approximately half of the Xyl units are single-substituted with Ara at position *O*-3 of the Xyl unit, and that about 2 % of the Xyl units are double-substituted [7, 8, 35].

Partial acid-hydrolysis of WAX led to removal of the Ara substitutes present mainly at position *O*-3 of Xyl, yielding pD-WAX with a molar Ara:Xyl ratio of 0.3 (Table 1). This was inferred from the decrease in the 1,3,4- and 1,2,3,4-linked Xyl units with a concomitant increase in the 1,4- and 1,2,4-linked Xyl units, when comparing pD-WAX to WAX (Table 1).



Table 1. Yield, sugar recovery, sugar composition and glycosidic linkage patterns, and degree of branching (DB) of the native and of the oxidized (ox-) arabinoxyln samples (WAX, pD-WAX, and RAX) with TEMPO/NaO₂Cl/NaOCl.

	WAX	ox-WAX	pD-WAX	ox-pD-WAX	RAX	ox-RAX
Yield (w/w %)^a	-	91	-	82	-	84
Ara + Xyl Recovery (w/w %)^b		50.1 ± 1.8 (83.3 ± 2.9)		59.5 ± 4.9 (81.6 ± 6.8)		41.8 ± 0.1 (80.2 ± 0.1)
Carbohydrate composition (w/w %)^c						
Ara^f	31.6 ± 0.1 (34.9 ± 0.1)	2.1 ± 0.1 (3.7 ± 0.0)	21.4 ± 0.4 (23.2 ± 0.1)	1.8 ± 0.1 (2.5 ± 0.1)	27.1 ± 0.3 (34.8 ± 0.3)	1.3 ± 0.1 (2.6 ± 0.2)
AraA	-	+	-	+	-	+
Xyl	58.9 ± 0.5 (65.1 ± 0.1)	53.9 ± 1.9 (96.3 ± 0.0)	70.9 ± 1.1 (76.8 ± 0.1)	70.6 ± 5.9 (97.5 ± 0.1)	50.8 ± 1.2 (65.2 ± 0.3)	48.5 ± 0.1 (97.4 ± 0.2)
Total	90.5 ± 0.6	55.9 ± 1.9	92.3 ± 1.5	72.4 ± 6.0	77.9 ± 1.4	49.8 ± 0.2
Glycosidic linkage^d (mol %)						
t-Xylp	1.4	n.d.	2.1	n.d.	0.7	n.d.
4-Xylp	65.7	n.d.	78.7	n.d.	55.2	n.d.
3,4-Xylp	24.7	n.d.	12.0	n.d.	39.0	n.d.
2,4-Xylp	2.3	n.d.	5.2	n.d.	2.6	n.d.
2,3,4-Xylp	5.8	n.d.	2.1	n.d.	2.7	n.d.
DB^e	38.6		21.3		46.8	

n.d. – not determined.

^a Yield in weight % relative to the parental AX sample.

^b Results are expressed as average (n=2) weight % of native polysaccharide (AX). AraA is not accounted in the sugar recovery of ox-AX samples. Results in parentheses are the Xyl-recovery yield in % of weight Xyl per weight of native polysaccharide.

^c Results are expressed as average (n=2) weight % of sample. Results in parentheses are the relative mol percentage (%) considering only Ara and Xyl residues.

^d Results are expressed in relative % (mol/mol) of all Xyl residues.

^e DB was calculated as $[Xyl_{\text{subst}}/Xyl_{\text{total}}]$, where Xyl_{subst} is the sum of (2,4-Xyl + 3,4-Xyl + 2*(2,3,4-Xyl)) [31].

^f Ara was mainly found as terminal-linked Ara units (data not shown).



Due to Ara oxidation, the molar Ara:Xyl ratio of all TEMPO-oxidized AXs substantially decreased by appr. 90% (Table 1). AraA was identified as the oxidation product derived from Ara in all ox-AXs by HPAEC (data not shown). Additionally, most of the Xyl was recovered for all ox-AX samples (Table 1), indicating an almost unchanged xylan backbone. This result was expected since TEMPO/NaClO₂/NaOCl preferentially oxidizes primary alcohol groups [39], which only appear in the Ara side chains of AX. These results show that all native AXs indeed have a different structure, and that, upon TEMPO-oxidation, the Ara side chains of AXs are the main sugar residues to undergo modification. This indicates that three differently modified xylans were obtained.

3.2. Partially acid-hydrolysed TEMPO-oxidized AXs have larger fragmentation products than the parental AX

Native and TEMPO-oxidized AXs were partially acid-hydrolysed with TFA to yield oligosaccharides (OS) and the polysaccharide depolymerization of the native and ox-AXs before and after partial acid hydrolysis was monitored by HPSEC (Fig. 1). Results showed that native WAX is slightly smaller (400 kDa) than RAX (414 kDa), in accordance with literature [7, 40]. The apparent Mw of ox-WAX (175 kDa) and ox-RAX (213 kDa) decreased in comparison to WAX (Fig. 1A) and RAX (Fig. 1C), respectively, and both ox-AXs were more polydisperse than the respective parental AX. The increase in polydispersity can be due to the presence of repulsing anionic groups arising from polymer oxidation and/or degradation. Similarly, ox-pD-WAX was also more polydisperse than the respective native sample, and it was observed that some of the molecules of ox-pD-WAX eluted earlier than the ones of pD-WAX (42 kDa, Fig. 1B) [17].

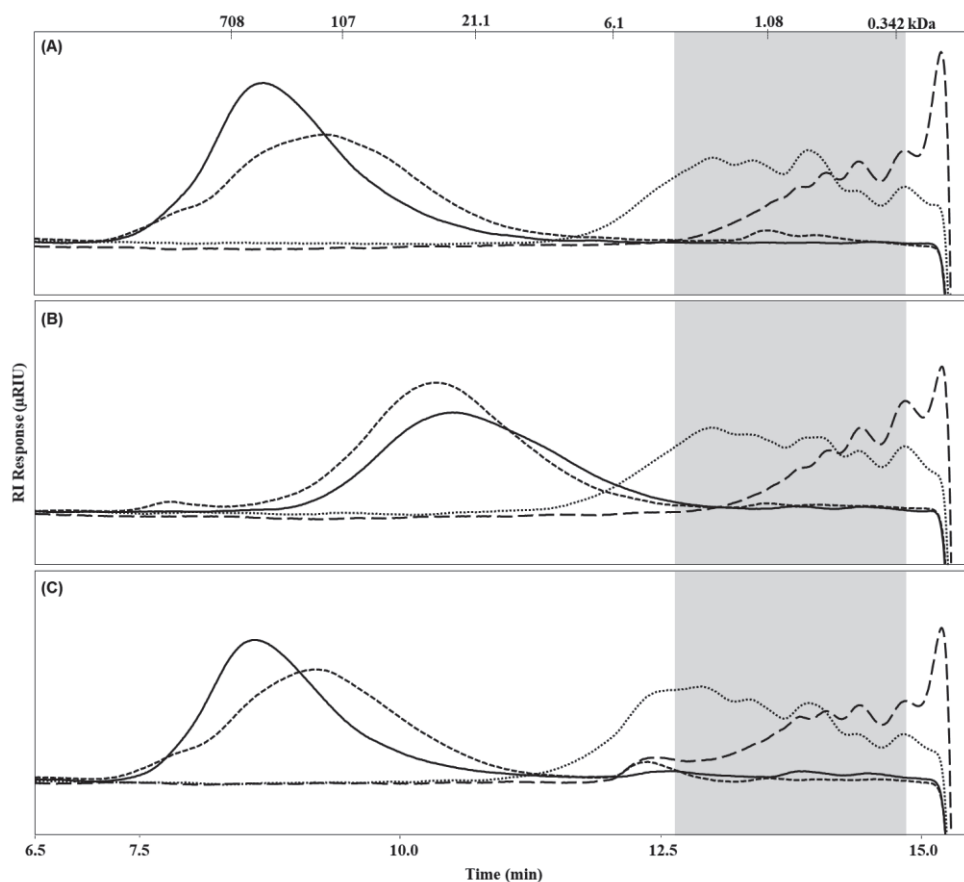


Figure 1. HPSEC elution patterns of the native (—) and oxidized (---) AXs, and of the TFA partially-acid hydrolysed native (— — —) and oxidized (·····) AXs. **A:** wheat arabinoxylan, **B:** partial acid-debranched wheat arabinoxylan and **C:** rye arabinoxylan. Pullulan standards were used to estimate the Mw (kDa). Grey box indicates the time range corresponding to an apparent degree of polymerization between 2 and 20 (Pullulan).

Upon 0.2 M TFA partial acid-hydrolysis, all samples were broken down to lower molecular weights (Fig. 1). About 57 %, 84 % and 65 % of the partially acid-hydrolysed ox-WAX, ox-pD-WAX and ox-RAX samples, respectively, had a degree of polymerization (DP) between 2 and 20 (grey boxes in Fig. 1, Table S1), with still some degradation products with a DP>20 (16 %, 14 % and 31 % for ox-WAX, ox-pD-WAX and ox-RAX, respectively). TFA hydrolysis of native WAX, pD-WAX, and RAX samples led predominantly to 2<DP<20 degradation products (40 %, 42 %, and 49 %, respectively), but also to major amounts of degradation products of around 200 Da, illustrating the release of monomers. Thus, our results indicate that TEMPO-oxidation of AX creates an oxidized-polymer with increased resistance to acid hydrolysis, due to the conversion of Ara to AraA within the polysaccharide, whose linkage is more resistant to acid hydrolysis than the neutral Ara→Xyl linkage [21]. Additionally, most of the fragments present in the partially acid-hydrolysed ox-AXs had a 2<DP<20, a suitable DP range for OS characterization by LC-MS [24, 25, 41].



3.3. Analysis of the released fragments upon TFA partial acid-hydrolysis of TEMPO-oxidized AXs by UHPLC-PGC-MS

UHPLC-PGC-MS analysis of the partially acid-hydrolysed ox-AXs was used with three main purposes. Firstly, to confirm that the released OS indeed comprised AUXOS; secondly, to elucidate AUXOS structures to obtain insights into the native AX structure; and thirdly, to distinguish AXs by characteristic AUXOS chromatographic patterns. Prior to UHPLC-PGC-MS analysis, the reducing-end of the partially acid-hydrolysed ox-AXs was converted into an alditol by reduction with NaBD₄ [34], yielding (AU)XOS alditols that were designated (AU)XOS-A.

3.3.1. *Hydrolysates of TEMPO-oxidized AXs comprise (AU)XOS*

The PGC column and MS detector allowed us to recognize the presence of pentose-oligomers with a DP2-7 (Fig. 2). These pentose-oligomers were assigned to xylo-oligomers (XOS) by linear XOS standards. Besides XOS, also isomeric singly- and doubly-AraA-substituted XOS with a DP2-5 were identified in the UHPLC-PGC-MS profile (Fig. 2). In total, 18 AUXOS-A were identified in the UHPLC-PGC-MS profile, which are indicated in Fig. 2 by alphabet letters from a_n-g_n. Identical letters with a different subscript number indicates the presence of isomeric AUXOS-A. Identification of these oligomers can be performed based on of their *m/z* values to AUXOS-A because AraA is 14 Da heavier than the isomers Xyl and Ara [16, 42]. This result confirms the oxidation of AX to arabinuronoxylan [17] and corroborates the resistance of the AraA→Xyl linkage to acid hydrolysis under the conditions used (0.2 M TFA, 90 °C, 2 h) [21-23, 43].

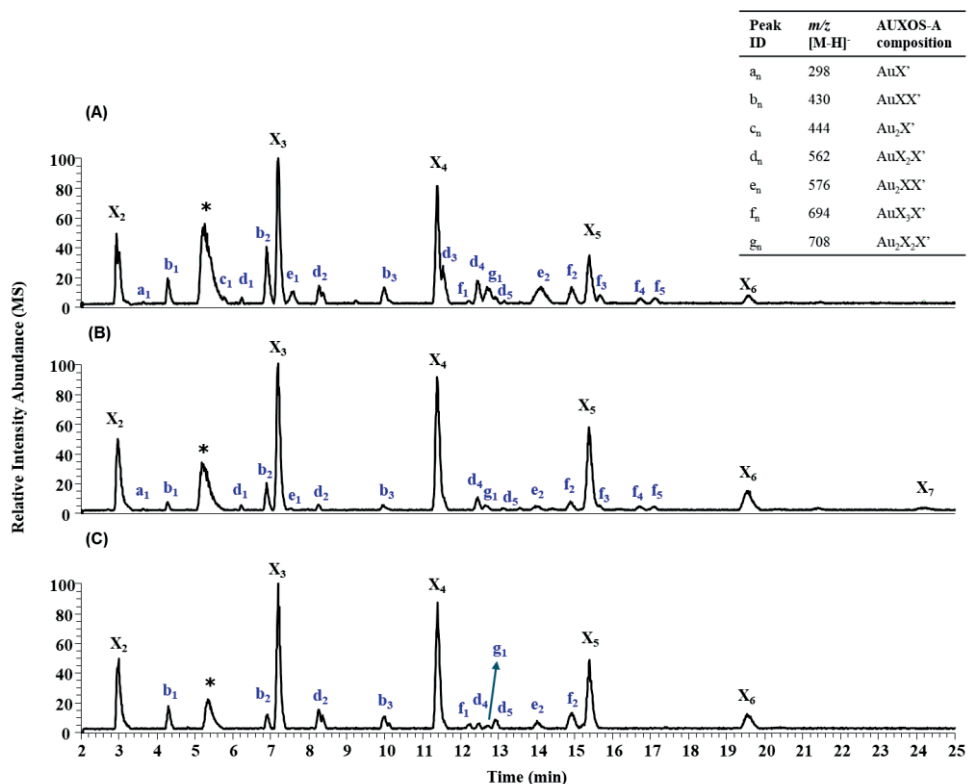


Figure 2. UHPLC-PGC-MS base peak elution patterns (2-25 min) of the NaBD₄-reduced TFA partially acid-hydrolysed ox-WAX (A), ox-pD-WAX (B), and ox-RAX (C). AUXOS-A are identified by alphabet letters (a-g), identical letters with different subscript numbers are isomeric AUXOS-A. AUXOS-A composition is given in the table inserted. Au_mX_nX[']: m - number of AraA; n - number of xyloses; X['] - terminal xylitol. * Background peak.

3.3.2. Characterization of AUXOS-A using UHPLC-PGC-MS

To obtain more detailed insights in the chemical structures of the formed AUXOS-A, tandem MS was performed on the identified AUXOS-A in the UHPLC-PGC-MS profiles (Fig. 2). The fragmentation patterns of the AUXOS-A with DP3 composed of AuXX['] (m/z 430 [M-H]⁻), and DP4 composed of Au₂XX['] (m/z 576 [M-H]⁻) is discussed in detail below.

Characterization of the DP3 AuXX['] isomers b_1 , b_2 , and b_3

Fragmentation patterns of the singly-AraA-substituted XOS with DP3, isomers b_1 , b_2 and b_3 (m/z 430 [M-H]⁻) are shown in Fig. 3A-C. Fragment ions are described in accordance with the nomenclature of Domon and Costello [44]. The parent ion with m/z 430 [AuXX[']-H]⁻ had m/z 284 as dominant fragment ion in the MS² fragmentation spectra of all isomeric structures (Fig. 3A-C). The latter ion derives from removal of the AraA side chain during fragmentation. This AraA removal during fragmentation hampers structure elucidation of the OS. Fortunately, although in low abundances, diagnostic fragment ions were seen in the fragmentation spectra as well. The fragment ion m/z 236



($^{0,2}X_1$) present in the spectrum of isomer **b**₁ (Fig. 3A) resulting from a cross-ring fragmentation at the non-reducing end Xyl, indicates that AraA is linked at position *O*-3 of this Xyl unit. This indicates that isomer **b**₁ has the following structure: AraA(1→3)Xyl(1→4)Xyl.

For isomer **b**₂ (Fig. 3B), the fragment ion *m/z* 298 (*Y*₁) originating from glycosidic cleavage of the xylan-backbone indicates that AraA is linked at the xylitol residue. However, whether it is linked at position *O*-2 or *O*-3 is difficult to ascertain. The low presence of the fragment ion *m/z* 368, resulting from a loss of *m/z* 62, can be derived from C2-C3 cleavage of a substituted xylitol unit at position *O*-3, or from AraA fragmentation/rearrangement (see Fig. S1). Furthermore, WAX and RAX are mostly substituted at position *O*-3 than at position *O*-2 of Xyl (ratio *O*-3:*O*-2 of 25:2 and 39:3 for WAX and RAX, respectively), as shown in this study and reported in literature [5, 7, 8, 35]. Consequently, AraA is most likely linked at position *O*-3 of the xylitol residue, giving the following structure for isomer **b**₂: Xyl(1→4)[AraA(1→3)]Xyl.

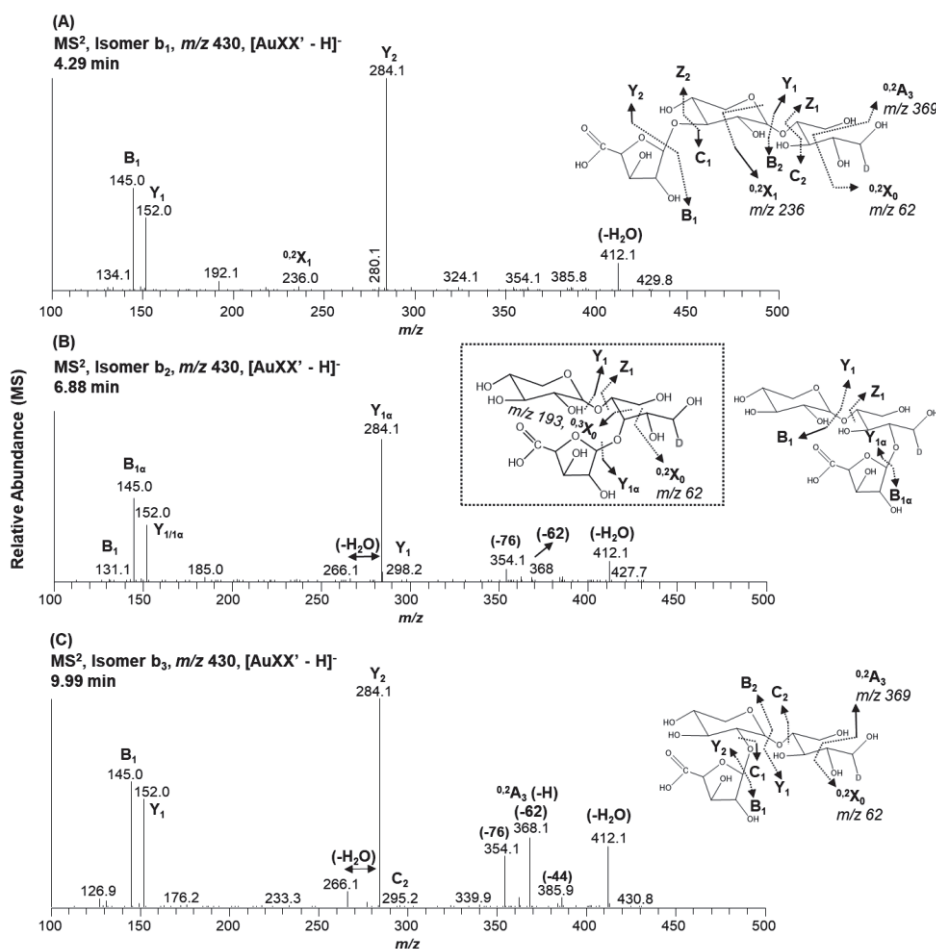


Figure 3. Fragmentation spectra (ESI-MS²) in negative mode of the AUXOS-A with DP3 (parent ion [AuXX'-H]⁻ with *m/z* 430) that eluted at 4.29 min (A), 6.88 min (B), and 9.99 min (C) in the PGC elution profile shown in Figure 2. Tentatively oligosaccharide structures are depicted. Fragment ions are described in accordance with Domon and Costello [44]. More likely AUXOS-A structures are surrounded by a box.



The presence of the C_2 fragment with m/z 295 in the mass spectrum of isomer **b₃** (Fig. 3C), which is derived from glycosidic cleavage of the oligomeric xylan-backbone, shows that AraA is present at the non-reducing end Xyl unit. This result together with the fact that isomer **b₁** was verified to have AraA linked at the position *O*-3 of the non-reducing end Xyl allows us to assign the structure of isomer **b₃** as AraA(1→2)Xyl(1→4)Xyl. Additionally, a relatively high intensity of the fragment ion with m/z 368 ($^{0.2}A_3$, Fig. 3C) was seen in the MS² fragmentation spectrum of isomer **b₃**, which is likely derived from intra-cleavage of the xylitol residue corresponding to the reducing-end Xyl unit. This suggests that substituted Xyl at position *O*-2 induces intra-cleavage of the contiguous reducing-end xylosyl unit, as reported for neutral AXOS with DP3 (AX₂) [45].

Characterization of the DP4 Au₂XX' isomers e₁ and e₂

Fragmentation patterns found for DP3 were used to reveal DP4 structures comprising two AraA units. The fragmentation patterns of DP4 isomers **e₁** and **e₂** composed of Au₂XX' with m/z 576 ([M-H]⁻) are shown in Fig. 4. As observed for the DP3 isomers **b₁**, **b₂** and **b₃** (m/z 430 [M-H]⁻), also the fragment ion derived from the loss of an AraA unit during fragmentation of the parent ion with m/z 576 was the dominant fragment ion (m/z 430 in Fig. 4A and B). Notably, for isomer **e₁**, the fragment ion with m/z 444 (Y₁, Fig. 4A) was present in high abundance. This fragment ion corresponds to a xylitol unit double substituted with AraA units, suggesting that isomer **e₁** has the following structure: Xyl(1→4)[AraA(1→3), AraA(1→2)]Xyl. Although the minor fragment with m/z 277 may point to the presence of a B₂ ion composed of a pentose (Xyl) and an AraA, suggesting that isomer **e₁** could be composed of two consecutive single substituted Xyl units with AraA, the structure highlighted by the fragment ion with m/z 444 is most dominant. This shows that isomer **e₁**, more present in ox-WAX than in the two other AX (Fig. 2), has a double-substituted Xyl unit, confirming that WAX has the highest degree of double-substituted Xyl units (Table 1).

To obtain structural information about isomer **e₂**, both MS² and MS³ experiments were needed. The presence of the fragment ion m/z 152 (Y₁, Fig. 4B₁) derived from the fragment ion m/z 430 in the MS² spectrum (Fig. 4B) indicates that one of the two AraA is present at the non-reducing end Xyl unit. Considering that this MS³ spectrum (Fig. 4B₁) is identical to the MS² spectrum of isomer **b₃** (Fig. 3C), it is assumed that one AraA in isomer **e₂** is linked at position *O*-2 of the non-reducing end Xyl.

Although the minor presence of the m/z 368 may indicate a $^{0.2}A_3$ ion (Fig. 4B), resulting from intra-cleavage of a xylitol unit substituted with AraA at the position *O*-2 in the MS² spectrum of isomer **e₂**, the fragment ion with m/z 514 was more predominant. The m/z 514 suggests that the position *O*-2 of the xylitol unit is free. Comparing these results with the expected amount of double-substituted Xyl units from the glycosidic linkages analysis (Table 1), it is speculated that the second AraA is also linked at the non-reducing end Xyl. This would indicate that isomer **e₂** has the following structure: [AraA(1→3), AraA(1→2)]Xyl(1→4)Xyl. However, the possibility of the second AraA located at position *O*-3 and/or *O*-2 of the xylitol unit cannot be fully discarded.

These results indicate that the only DP4 Au₂XX' isomers **e₁** and **e₂** (Fig. 2) consisted of an unsubstituted and a double-substituted Xyl unit. This suggests that contiguous single-substituted Xyl units do not occur in the WAX structure or were not released upon TFA partial acid-hydrolysis. This result is in accordance with the tentative structural models for WAX proposed by Gruppen et al. [46] and Gruppen et al. [47], where consecutive single-substituted Xyl units are seen only in trace amounts



Table 2. Overview of the m/z values of the identified AUXOS-A isomers as [M-H]⁻ on the UHPLC-PGC-MS profile (Fig. 2) of the NaBD₄-reduced TFA partially acid-hydrolysed ox-WAX, ox-pD-WAX, and ox-RAX samples. Oligosaccharides (OS) composition and conclusive or tentative AUXOS-A structures are depicted.

AUXOS-A Isomer ^a (ret time)	m/z [M-H] ⁻	OS Composition ^b	Graphical ^c and Chemical conclusive and tentative AUXOS-A structures	Ox-WAX	Ox-pD-WAX	Ox-RAX
a ₁ (3.65 min)	298	Aux ^c		+	+	-
b ₁ (4.29 min)	430	AuxXX ^c		+	+	+
c ₁ (5.78 min)	444	AuxX ^c		+	-	-
d ₁ (6.23 min)	562	AuxXX ^c	 [AraA(1→3), AraA(1→2)]XyY ^f	+	+	-
b ₂ (6.88 min)	430	AuxXX ^c	 *XyY(1→4)XyY(1→4)[AraA(1→2)]XyY ^f or XyY(1→4)XyY(1→4)[AraA(1→3)]XyY ^f	+	+	+
e ₁ (7.57 min)	576	AuxXX ^c	 *XyY(1→4)[AraA(1→3)]XyY ^f or XyY(1→4)[AraA(1→2)]XyY ^f	+	+	-
d ₂ (8.27 min)	562	AuxXX ^c	 *XyY(1→4)[AraA(1→2), AraA(1→3)]XyY ^f or AraA(1→2)→XyY(1→4)[AraA(1→2)]XyY ^f or AraA(1→2)→XyY(1→4)[AraA(1→3)]XyY ^f or AraA(1→3)→XyY(1→4)[AraA(1→2)]XyY ^f or AraA(1→3)→XyY(1→4)[AraA(1→3)]XyY ^f	+	+	+
b ₃ (9.99 min)	430	AuxXX ^c	 XyY(1→4)[AraA(1→3)]XyY(1→4)XyY ^f	+	+	+
d ₃ (11.53 min)	562	AuxXX ^c	 AraA(1→2)XyY(1→4)XyY ^f	+	-	-
f ₁ (12.21 min)	694	AuxXX ^c	 *XyY(1→4)XyY(1→4)[AraA(1→3)]XyY ^f or XyY(1→4)XyY(1→4)[AraA(1→2)]XyY ^f	+	-	+
d ₄ (12.43 min)	562	AuxXX ^c	 *XyY(1→4)XyY(1→4)XyY(1→4)[AraA(1→2)]XyY ^f or XyY(1→4)XyY(1→4)XyY(1→4)[AraA(1→3)]XyY ^f	+	+	+

Table 2. Continuation.

AUXOS-A Isomer ^a (ret time)	m/z [M-H] ⁻	OS Composition ^b	Graphical ^c and Chemical conclusive and tentative AUXOS-A structures	Ox-WAX	Ox-pd-WAX	Ox-RAX
g ₁ (12.7 min)	708	AuxXX ^c	 *AraA(1→3)Xy(1→4)Xy(1→4)[AraA(1→5)]Xy ^d or AraA(1→2)Xy(1→4)Xy(1→4)[AraA(1→3)]Xy ^d or Xy(1→4)[AraA(1→2)]Xy(1→4)[AraA(1→3)]Xy ^d or Xy(1→4)[AraA(1→3)]Xy(1→4)[AraA(1→3)]Xy ^d	+	+	+
d ₁ (13.15 min)	562	AuxXX ^c	 Xy(1→4)[AraA(1→2)]Xy(1→4)Xy ^d	+	+	+
e ₁ (13.9 min)	576	AuxXX ^c	 *AraA(1→2), AraA(1→3)Xy(1→4)Xy ^d or AraA(1→2)Xy(1→4)[AraA(1→3)]Xy ^d or AraA(1→2)Xy(1→4)[AraA(1→2)]Xy ^d	+	+	+
f ₁ (14.9 min)	694	AuxXX ^c	 Xy(1→4)Xy(1→4)[AraA(1→3)]Xy(1→4)Xy ^d	+	+	+
f ₁ (15.67 min)	694	AuxXX ^c	 *Xy(1→4)[AraA(1→3)]Xy(1→4)Xy(1→4)Xy ^d or Xy(1→4)[AraA(1→2)]Xy(1→4)Xy(1→4)Xy ^d	+	+	-
f ₁ (16.73 min)	694	AuxXX ^c	 *Xy(1→4)Xy(1→4)[AraA(1→2)]Xy(1→4)Xy ^d or Xy(1→4)[AraA(1→3)]Xy(1→4)Xy(1→4)Xy ^d or Xy(1→4)[AraA(1→2)]Xy(1→4)Xy(1→4)Xy ^d	+	+	-
f ₁ (17.11 min)	694	AuxXX ^c	 *Xy(1→4)[AraA(1→2)]Xy(1→4)Xy(1→4)Xy ^d or Xy(1→4)[AraA(1→3)]Xy(1→4)Xy(1→4)Xy ^d	+	+	-

^a - Alphabet letters (a-g) are identified AUXOS-A, identical letters with a different subscript number are isomeric AUXOS-A.

^b - Abbreviations in accordance with Fauré et al. [48]. Au, arabinuronic acid; X, xylose; X', xylitol; subscript number indicates the amount of each sugar in the OS.

^c - Symbolic representation in accordance with Perez [49], including conclusively and tentatively characterized AUXOS-A: orange star, Xy^d; dark red star, AraA. * - More likely AUXOS-A structure based on comparison with glycosidic linkage analysis and on the most dominant fragment ions present in the fragmentation spectrum.

+ , indicates presence of OS; -, indicates absence of OS.



3.3.3. *Distinctive UHPLC-PGC-MS AUXOS-A profiles among partially acid-hydrolysed TEMPO-oxidized AXs*

Knowledge on the type of AUXOS-A structures originating from each TEMPO-oxidized AX was essential to understand individual AX structural features, and to recognize similarities and/or differences among samples. Partially acid-hydrolysed ox-WAX comprised of about 55 % XOS-A (DP2-7) and 45 % AUXOS-A (DP2-5), with X₂ (11 %), X₃ (20 %), and X₄ (15 %) as most predominant unsubstituted XOS-A (Table S2). Tandem MS allowed us to (tentatively) assign the structure of the most abundant AUXOS-A of ox-WAX, namely **b₂**, **e₂**, **d₃**, **d₄**, **b₁**, and **g₁** (Fig. 5 and Table 2). This result demonstrated that single-substitution mainly occurred at position *O*-3 of the Xyl unit (isomers **b₂** > **d₃** > **d₄** > **b₁** = **g₁**), representing 29 % of all identified OS, and that 9 % were AUXOS-A containing *O*-2,3 double-substituted Xyl units (isomers **c₁**, **e₁**, and **e₂**). Both values agree nicely with the glycosidic linkage composition of WAX (Table 1). These results show that in ox-WAX unsubstituted xylan regions are mainly intercepted by single- or double-AraA-substituted short Xyl segments with mainly 2 and 3 Xyl units. This suggests that the substituted Xyl units tend to appear in isolated clusters of single- and double-substituted residues, and that there is an alternation between less dense branched and highly-branched regions, which agrees with the model proposed for WAX by Gruppen et al. [47].

ox-pD-WAX (Fig. 2B) was mainly composed of unsubstituted XOS-A (83 %, Table S2), with a high proportion of X₂ (14 %), X₃ (22 %), and X₄ (28 %). 15 % of all identified OS in ox-pD-WAX were AUXOS-A containing single-substituted Xyl units (Table S2), with minor substitution occurring simultaneously at *O*-2 and *O*-3 positions of the Xyl unit (2 %, **e₁** and **e₂** isomers), coinciding with the glycosidic linkage analysis of pD-WAX (Table 1). Single-substitution of the (1→4)-Xyl in AUXOS-A occurred mainly at position *O*-3 (11 %), as represented by the three most abundant structures Xyl(1→4)[AraA(1→3)]Xyl' (**b₂**, 3 %), AraA(1→3)Xyl(1→4)Xyl(1→4)Xyl' (**d₄**), and Xyl(1→4)Xyl(1→4)[AraA(1→3)]Xyl(1→4)Xyl' (**f₂**) (Fig. 5). These results emphasize that (ox-)pD-WAX has more contiguous unsubstituted Xyl regions than (ox-)WAX, and that these regions are preferably interlinked by single-AraA-substituted XOS-A, illustrating a low level of xylan substitution, as expected. Furthermore, the sum of the singly-substituted AUXOS-A isomers **f₃**, **f₄**, and **f₅** (Table 2) accounted 8 and 14 % of the total AUXOS-A of ox-WAX and ox-pD-WAX (Fig. 5), respectively. This result also indicates that AUXOS-A comprising longer xylose sequences were majorly present in ox-pD-WAX.

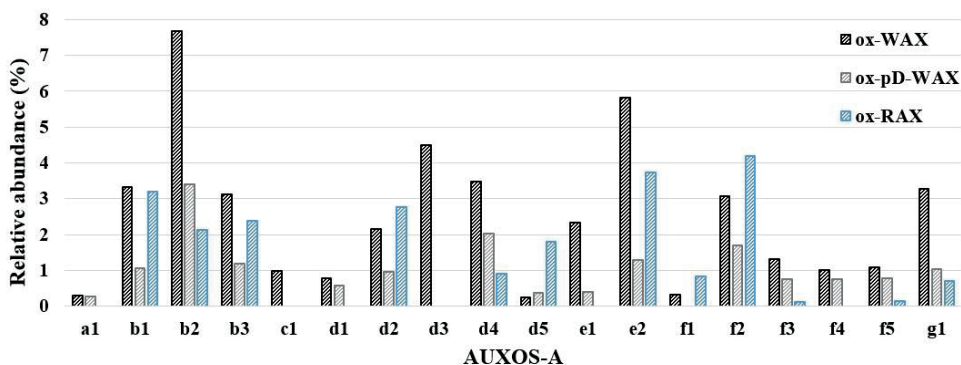


Figure 5. Relative abundance (%) of arabinurono-xylo-oligomer alditols (AUXOS-A) present in the NaBD₄-reduced partially acid-hydrolysed TEMPO-oxidized AX samples (ox-WAX, ox-pD-WAX, and ox-RAX). AUXOS-A are identified by alphabet letters (a-g), identical letters with a different number are isomeric AUXOS-A. AUXOS-A composition and structure, as based on the UHPLC-PGC-MS profile (Fig. 2) is given in Table 2. Peak areas of the identified XOS-A and AUXOS-A within a DP2-7 as extracted from the MS signal were used for relative quantification (%).

Similarly to ox-pD-WAX, also ox-RAX was mainly composed of XOS-A (77 %, Table S2), with a high proportion of X₂ (14 %), X₃ (23 %) and X₄ (22 %), demonstrating a low level of xylan substitution. Although this result was expected for (ox-)pD-WAX based on our glycosidic linkage analysis, it disagrees for ox-RAX, since RAX displayed the highest level of branching among the studied AXs (Table 1) [7, 8, 35]. This result suggests that RAX has been partially debranched during TEMPO-oxidation and/or partial acid-hydrolysis.

Despite the possible occurrence of debranching, diagnostic AUXOS-A were still obtained for ox-RAX upon partial acid-hydrolysis. Ox-RAX mostly comprised AUXOS-A containing single-substituted Xyl units (19 %, Table S2), with e₂ being the only AUXOS-A comprising double-substituted Xyl units (4 %, Fig. 5 and Table 2). Single-substitution of Xyl was predominant at position O-3 (14 %, Table S2) with f₂ (4 %), b₁, and d₂ (3 %) (Table 2) as the three most abundant AUXOS-A (Fig. 5). The relative amount of O-3 substitution in the identified AUXOS-A of ox-RAX is 25 % lower than the corresponding O-3 substitution of RAX ascertained by linkage analysis, proposing that the noted partial debranching of RAX mainly occurred at position O-3 of Xyl.

Regardless the fact that partial debranching of the AX can occur during TEMPO-oxidation and/or partial acid-hydrolysis, important compositional AUXOS-A differences were seen among samples. This highlights that sample dependent-AUXOS-A profiles were successfully obtained for each studied AX. For example, isomer e₁ (Xyl(1→4)[AraA(1→2),AraA(1→3)]Xyl') was majorly present in ox-WAX, scarcely present in ox-pD-WAX, and absent in ox-RAX (Fig. 5). Accordingly, isomer e₁ can be considered a diagnostic AUXOS-A of ox-WAX. Additionally, isomer d₃ (Xyl(1→4)Xyl(1→4)[AraA(1→3)]Xyl') was also considered a diagnostic AUXOS-A of ox-WAX, as it was exclusively found in the UHPLC-PGC-MS profile of ox-WAX (Fig. 2A and Fig. 5). Thus, this indicates that both ox-pD-WAX and ox-RAX can be distinguished from ox-WAX because e₁ and d₃ were marker AUXOS-A found for ox-WAX.

Regarding ox-pD-WAX and ox-RAX, also these samples differed in AUXOS-A composition. Specifically, ox-RAX (Fig. 2C) can be distinguished from ox-pD-WAX (Fig. 2B) due to the absence



in **d**₁ and scarcity in isomers **f**₃-**f**₅ (Table 2 and Fig. 5), together with an elevated amount in **e**₂ and **f**₂ (Table 2 and Fig. 5). This highlights that the obtained UHPLC-PGC-MS AUXOS-A patterns within a DP2-5 are AX-structure dependent since it varied in OS abundance and composition among AXs. Therefore, our results indicate that TEMPO-oxidation of AXs followed by partial acid-hydrolysis and analysis of the released OS by UHPLC-PGC-MS is a promising non-enzymatic approach to obtain insight in their oligosaccharide structures and to distinguish AXs by characteristic (AU)XOS-A profiles.

4. Conclusions

In this study, a non-enzymatic approach consisting of TEMPO-oxidation of arabinoxylans (AXs) followed by TFA partial acid-hydrolysis was investigated to obtain diagnostic oligosaccharides (OS) that allow us to characterize and distinguish various AX samples. Our results showed that partial acid-hydrolysis of TEMPO/NaClO₂/NaOCl oxidized AXs with different structural features (wheat AX (WAX), rye AX (RAX), and partial acid-debranched (pD-)WAX) yields xylo-oligomers (XOS) carrying arabinuronic acid (AraA) side chains (AUXOS), besides XOS. Furthermore, an UHPLC-PGC-MS method that allows distinction between AUXOS-alditol (AUXOS-A) isomers has been developed and, to the best of our knowledge, this is the first time that UHPLC-PGC-MS was used to study XOS carrying side chains that are not obtained from enzymatic hydrolysis of AXs.

UHPLC-PGC-MS analyses of the NaBD₄-reduced hydrolysates of ox-AXs resulted in OS profiles that were AX-structure dependent. This result is rather interesting because the generated OS profile can work as a polysaccharide fingerprint for sample identification. Furthermore, other types of AXs, e.g. glucuronoAX, acetylated AX, and feruloylated AX, are also expected to undergo TEMPO-oxidation at the unsubstituted Ara side chains and, upon partial acid-hydrolysis of the ox-AX, generate independent (AU)XOS-A profiles. This would be due to differences in the degree of branching and the presence of substituents besides AraA units. Thus, partial acid-hydrolysis of TEMPO-oxidized AXs followed by analysis of the generated (AU)XOS-A by UHPLC-PGC-MS is a promising non-enzymatic approach to distinguish AXs, cereal dietary fibres of high interest, and to obtain insight in their structures.



References

- [1] Stephen, A.M., M.M.J. Champ, S.J. Cloran, M. Fleith, L. Van Lieshout, H. Mejbom, and V.J. Burley. Dietary fibre in Europe: Current state of knowledge on definitions, sources, recommendations, intakes and relationships to health. *Nutrition Research Reviews*. **2017**, 30, 149-190.
- [2] Roye, C., K. Bulckaen, Y. De Bondt, I. Liberloo, D. Van De Walle, K. Dewettinck, and C.M. Courtin. Side-by-side comparison of composition and structural properties of wheat, rye, oat, and maize bran and their impact on in vitro fermentability. *Cereal Chemistry*. **2020**, 97, 20-33.
- [3] Wang, J., J. Bai, M. Fan, T. Li, Y. Li, H. Qian, L. Wang, H. Zhang, X. Qi, and Z. Rao. Cereal-derived arabinoxylans: Structural features and structure-activity correlations. *Trends in Food Science & Technology*. **2020**, 96, 157-165.
- [4] Perlin, A.S. Structure of the soluble pentosans of wheat flours. *Cereal Chem.* **1951**, 28, 382-393.
- [5] Izydorczyk, M.S., 23 - Arabinoxylans, in *Handbook of Hydrocolloids (Second Edition)*, G.O. Phillips and P.A. Williams, Editors. **2009**, Woodhead Publishing. 653-692.
- [6] Maes, C. and J.A. Delcour. Structural characterisation of water-extractable and water-unextractable arabinoxylans in wheat bran. *Journal of Cereal Science*. **2002**, 35, 315-326.
- [7] Buksa, K., W. Praznik, R. Loepfert, and A. Nowotna. Characterization of water and alkali extractable arabinoxylan from wheat and rye under standardized conditions. *Journal of Food Science and Technology*. **2016**, 53, 1389-1398.
- [8] Migliori, M. and D. Gabriele. Effect of pentosan addition on dough rheological properties. *Food Research International*. **2010**, 43, 2315-2320.
- [9] Makaravicius, T., L. Basinskiene, G. Juodeikiene, M.P. Van Gool, and H.A. Schols. Production of oligosaccharides from extruded wheat and rye biomass using enzymatic treatment. *Catalysis Today*. **2012**, 196, 16-25.
- [10] Van Gool, M.P., I. Vancsó, H.A. Schols, K. Toth, G. Szakacs, and H. Gruppen. Screening for distinct xylan degrading enzymes in complex shake flask fermentation supernatants. *Bioresource Technology*. **2011**, 102, 6039-6047.
- [11] Hoffmann, R.A., T. Geijtenbeek, J.P. Kamerling, and J.F.G. Vliegthart. ¹H-N.m.r. study of enzymically generated wheat-endosperm arabinoxylan oligosaccharides: structures of hepta- to tetradecasaccharides containing two or three branched xylose residues. *Carbohydrate Research*. **1992**, 223, 19-44.
- [12] Trogh, I., C.M. Courtin, A.A.M. Andersson, P. Åman, J.F. Sørensen, and J.A. Delcour. The combined use of hull-less barley flour and xylanase as a strategy for wheat/hull-less barley flour breads with increased arabinoxylan and (1→3,1→4)-β-D-glucan levels. *Journal of Cereal Science*. **2004**, 40, 257-267.
- [13] van Gool, M.P., G.C.J. van Muiswinkel, S.W.A. Hinz, H.A. Schols, A.P. Sinitzyn, and H. Gruppen. Two novel GH11 endo-xylanases from *Myceliophthora thermophila* C1 act differently toward soluble and insoluble xylans. *Enzyme and Microbial Technology*. **2013**, 53, 25-32.
- [14] Aspinall, G.O. and K.M. Ross. The degradation of two periodate-oxidised arabinoxylans. *Journal of the Chemical Society (Resumed)*. **1963**. 1676-1680.
- [15] Whistler, R.L. and W.M. Corbett. Oligosaccharides from Partial Acid Hydrolysis of Corn Fiber Hemicellulose. *Journal of the American Chemical Society*. **1955**, 77, 6328-6330.
- [16] Bowman, M.J., B.S. Dien, P.J. O'Bryan, G. Sarath, and M.A. Cotta. Selective chemical oxidation and depolymerization of (*Panicum virgatum* L.) xylan with switchgrass oligosaccharide product analysis by mass spectrometry. *Rapid Communications in Mass Spectrometry*. **2011**, 25, 941-950.
- [17] Pandeirada, C.O., D.W.H. Merkx, H.-G. Janssen, Y. Westphal, and H.A. Schols. TEMPO/NaClO₂/NaOCl oxidation of arabinoxylans. *Carbohydrate Polymers*. **2021**, 259, 117781.
- [18] Bragd, P.L., H. Van Bekkum, and A.C. Besemer. TEMPO-mediated oxidation of polysaccharides: Survey of methods and applications. *Topics in Catalysis*. **2004**, 27, 49-66.
- [19] Isogai, A., T. Hänninen, S. Fujisawa, and T. Saito. Review: Catalytic oxidation of cellulose with nitroxyl radicals under aqueous conditions. *Progress in Polymer Science*. **2018**, 86, 122-148.
- [20] Pierre, G., C. Punta, C. Delattre, L. Melone, P. Dubessay, A. Fiorati, N. Pastori, Y.M. Galante, and P. Michaud. TEMPO-mediated oxidation of polysaccharides: An ongoing story. *Carbohydrate Polymers*. **2017**, 165, 71-85.
- [21] Bemiller, J.N., Acid-Catalyzed Hydrolysis of Glycosides, in *Advances in Carbohydrate Chemistry*, M.L. Wolfrom and R.S. Tipson, Editors. **1967**, Academic Press. 25-108.
- [22] Mort, A.J., F. Qiu, and N.O. Maness. Determination of the pattern of methyl esterification in pectin. Distribution of contiguous nonesterified residues. *Carbohydrate Research*. **1993**, 247, 21-35.
- [23] ter Haar, R., J.W. Timmermans, T.M. Slaghek, F.E.M. Van Dongen, H.A. Schols, and H. Gruppen. TEMPO oxidation of gelatinized potato starch results in acid resistant blocks of glucuronic acid moieties. *Carbohydrate Polymers*. **2010**, 81, 830-838.



- [24] Leijdekkers, A.G.M., M.G. Sanders, H.A. Schols, and H. Gruppen. Characterizing plant cell wall derived oligosaccharides using hydrophilic interaction chromatography with mass spectrometry detection. *Journal of Chromatography A*. **2011**, 1218, 9227-9235.
- [25] Westphal, Y., H.A. Schols, A.G.J. Voragen, and H. Gruppen. Introducing porous graphitized carbon liquid chromatography with evaporative light scattering and mass spectrometry detection into cell wall oligosaccharide analysis. *Journal of Chromatography A*. **2010**, 1217, 689-695.
- [26] Logtenberg, M.J., K.M.H. Donners, J.C.M. Vink, S.S. van Leeuwen, P. de Waard, P. de Vos, and H.A. Schols. Touching the High Complexity of Prebiotic Vivinal Galacto-oligosaccharides Using Porous Graphitic Carbon Ultra-High-Performance Liquid Chromatography Coupled to Mass Spectrometry. *Journal of Agricultural and Food Chemistry*. **2020**, 68, 7800-7808.
- [27] Veillon, L., Y. Huang, W. Peng, X. Dong, B.G. Cho, and Y. Mechref. Characterization of isomeric glycan structures by LC-MS/MS. *Electrophoresis*. **2017**, 38, 2100-2114.
- [28] Borewicz, K., F. Gu, E. Saccenti, I.C.W. Arts, J. Penders, C. Thijs, S.S. van Leeuwen, C. Lindner, A. Nauta, E. van Leusen, H.A. Schols, and H. Smidt. Correlating Infant Fecal Microbiota Composition and Human Milk Oligosaccharide Consumption by Microbiota of 1-Month-Old Breastfed Infants. *Molecular Nutrition and Food Research*. **2019**, 63, 1801214.
- [29] Gu, F., S. Wang, R. Beijers, C. de Weerth, and H.A. Schols. Structure-Specific and Individual-Dependent Metabolization of Human Milk Oligosaccharides in Infants: A Longitudinal Birth Cohort Study. *Journal of Agricultural and Food Chemistry*. **2021**, 69, 6186-6199.
- [30] Ruhaak, L.R., A.M. Deelder, and M. Wuhrer. Oligosaccharide analysis by graphitized carbon liquid chromatography-mass spectrometry. *Analytical and Bioanalytical Chemistry*. **2009**, 394, 163-174.
- [31] Coelho, E., M.A.M. Rocha, A.S.P. Moreira, M.R.M. Domingues, and M.A. Coimbra. Revisiting the structural features of arabinoxylans from brewers' spent grain. *Carbohydrate Polymers*. **2016**, 139, 167-176.
- [32] Guillon, F. and J.F. Thibault. Methylation analysis and mild acid hydrolysis of the "hairy" fragments of sugar-beet pectins. *Carbohydrate Research*. **1989**, 190, 85-96.
- [33] Sun, Y.L., X.H. Gu, F. Shan, J.M. Zhang, and W.W. Cui. Partial acid hydrolytic characteristics and methylation analysis of pentosans from black-grained wheat bran. *Gaodeng Xuexiao Huaxue Xuebao/Chemical Journal of Chinese Universities*. **2012**, 33, 964-968.
- [34] Sun, P., M. Frommhagen, M. Kleine Haar, G. van Erven, E.J. Bakx, W.J.H. van Berkel, and M.A. Kabel. Mass spectrometric fragmentation patterns discriminate C1- and C4-oxidised cello-oligosaccharides from their non-oxidised and reduced forms. *Carbohydrate Polymers*. **2020**, 234, 115917.
- [35] Cyran, M., C.M. Courtin, and J.A. Delcour. Structural features of arabinoxylans extracted with water at different temperatures from two rye flours of diverse breadmaking quality. *Journal of Agricultural and Food Chemistry*. **2003**, 51, 4404-4416.
- [36] Ebringerová, A. and Z. Hromádková. Flow properties of rye bran arabinoxylan dispersions. *Food Hydrocolloids*. **1992**, 6, 437-442.
- [37] Izydorezyk, M.S. and C.G. Biliaderis. Structural heterogeneity of wheat endosperm arabinoxylans. *Cereal Chemistry*. **1993**, 70, 641-646.
- [38] Sárossy, Z., M. Tenkanen, L. Pitkänen, A.B. Bjerre, and D. Plackett. Extraction and chemical characterization of rye arabinoxylan and the effect of β -glucan on the mechanical and barrier properties of cast arabinoxylan films. *Food Hydrocolloids*. **2013**, 30, 206-216.
- [39] Saito, T., M. Hirota, N. Tamura, and A. Isogai. Oxidation of bleached wood pulp by TEMPO/NaClO/NaClO₂ system: Effect of the oxidation conditions on carboxylate content and degree of polymerization. *Journal of Wood Science*. **2010**, 56, 227-232.
- [40] Izydorezyk, M.S. and C.G. Biliaderis. Cereal arabinoxylans: advances in structure and physicochemical properties. *Carbohydrate Polymers*. **1995**, 28, 33-48.
- [41] Westphal, Y., H.A. Schols, A.G.J. Voragen, and H. Gruppen. MALDI-TOF MS and CE-LIF fingerprinting of plant cell wall polysaccharide digests as a screening tool for arabidopsis cell wall mutants. *Journal of Agricultural and Food Chemistry*. **2010**, 58, 4644-4652.
- [42] Hosseini, S. and S.O. Martinez-Chapa. *Principles and mechanism of MALDI-ToF-MS analysis*, in *SpringerBriefs in Applied Sciences and Technology*. 2017, Springer Verlag. p. 1-19.
- [43] De Ruiter, G.A., H.A. Schols, A.G.J. Voragen, and F.M. Rombouts. Carbohydrate analysis of water-soluble uronic acid-containing polysaccharides with high-performance anion-exchange chromatography using methanolysis combined with TFA hydrolysis is superior to four other methods. *Analytical Biochemistry*. **1992**, 207, 176-185.
- [44] Domon, B. and C.E. Costello. A systematic nomenclature for carbohydrate fragmentations in FAB-MS/MS spectra of glycoconjugates. *Glycoconjugate Journal*. **1988**, 5, 397-409.
- [45] Juvenon, M., M. Kotiranta, J. Jokela, P. Tuomainen, and M. Tenkanen. Identification and structural analysis of cereal arabinoxylan-derived oligosaccharides by negative ionization HILIC-MS/MS. *Food Chemistry*. **2019**, 275, 176-185.



- [46] Gruppen, H., R.J. Hamer, and A.G.J. Voragen. Water-unextractable cell wall material from wheat flour. 2. Fractionation of alkali-extracted polymers and comparison with water-extractable arabinoxylans. *Journal of Cereal Science*. **1992**, 16, 53-67.
- [47] Gruppen, H., F.J.M. Kormelink, and A.G.J. Voragen. Water-unextractable Cell Wall Material from Wheat Flour. 3. A Structural Model for Arabinoxylans. *Journal of Cereal Science*. **1993**, 18, 111-128.
- [48] Fauré, R., C.M. Courtin, J.A. Delcour, C. Dumon, C.B. Faulds, G.B. Fincher, S. Fort, S.C. Fry, S. Halila, M.A. Kabel, L. Pouvreau, B. Quemener, A. Rivet, L. Saulnier, H.A. Schols, H. Driguez, and M.J. O'Donohue. A brief and informationally rich naming system for Oligosaccharide motifs of heteroxylans found in plant cell walls. *Australian Journal of Chemistry*. **2009**, 62, 533-537.
- [49] Perez, S. Symbolic Representation of Monosaccharides in the Age of Glycobiology. **2018**. Available from: <http://www.glycopedia.eu/e-chapters/symbolic-representation-of-monosaccharides-in-the-age-of-glycobiology/article/abstract>.



Supplementary data

Extent of polysaccharide depolymerization after TFA partial acid-hydrolysis into various degree of polymerization ascertained by HPSEC

Table S 1. Percentage of polymer depolymerized into various degree of polymerization (DP), with DP<2, between 2<DP<20, and a DP>20, upon TFA partial-acid hydrolysis.

TFA Partially-acid hydrolysed sample	Percentage ^a of depolymerized polymer into various DP		
	2<DP (monomer)	2<DP<20	DP>20
WAX	26.2 ± 0.2	39.7 ± 1.0	0.6 ± 0.4
Ox-WAX	8.9 ± 0.7	57.4 ± 1.9	16.0 ± 0.7
pD-WAX	33.6 ± 0.7	42.3 ± 2.1	0.6 ± 0.6
Ox-pD-WAX	13.8 ± 1.1	84.2 ± 6.4	14.4 ± 7.4
RAX	25.5 ± 1.3	49.4 ± 0.0	6.6 ± 0.2
Ox-RAX	8.7 ± 0.3	65.3 ± 1.3	31.4 ± 3.1

^a Results are expressed as average (n =2) of the area percentage (%) relative to the total area of the respective non-hydrolysed native polysaccharide. 2<DP, integral peak area of the retention time higher than 14.7 min; 2<DP<20, integral peak area between 12.7 and 14.7 min; and DP>20, integral peak area under the retention time lower than 12.7 min.



UHPLC-PGC-mass spectra of the AUXOS-A derived from the partially acid-hydrolysed ox-AX samples

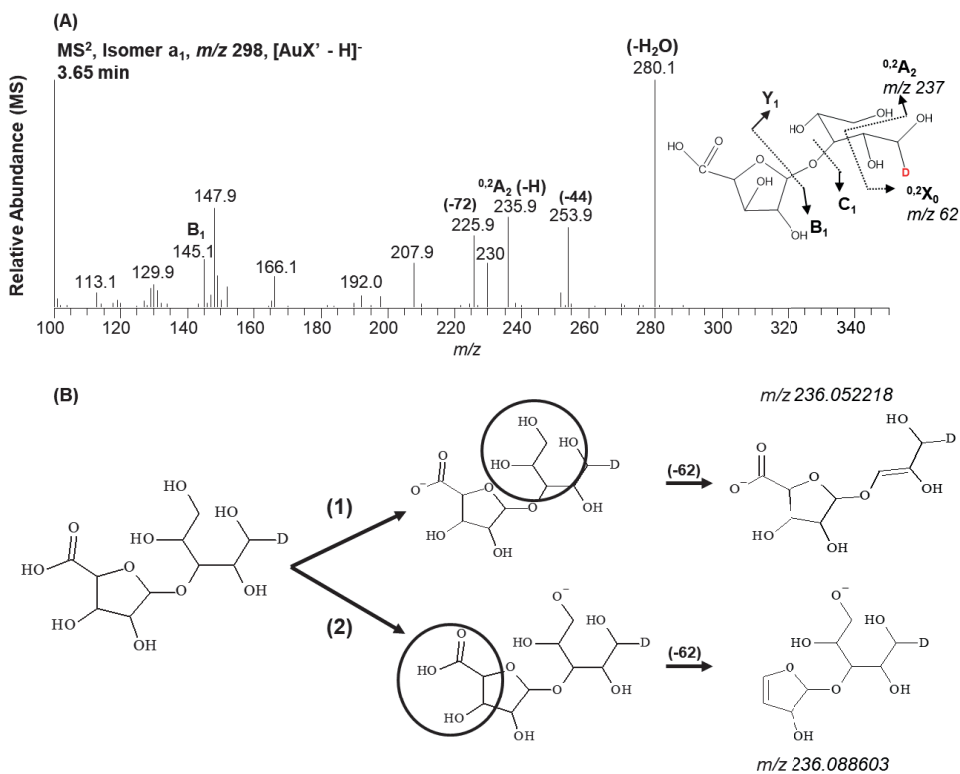


Figure S 1. (A) Fragmentation spectrum (ESI-MS²) in negative mode of the AUXOS-A with DP2 (parent ion [AuX' - H]⁻ with *m/z* 298) that eluted at 3.65 min in the PGC elution profile. Tentative oligosaccharide structure is depicted. (B) Alternative routes (1) and (2) for the loss of *m/z* 62 are indicated. Fragment ions are described in accordance with Domon and Costello [1].

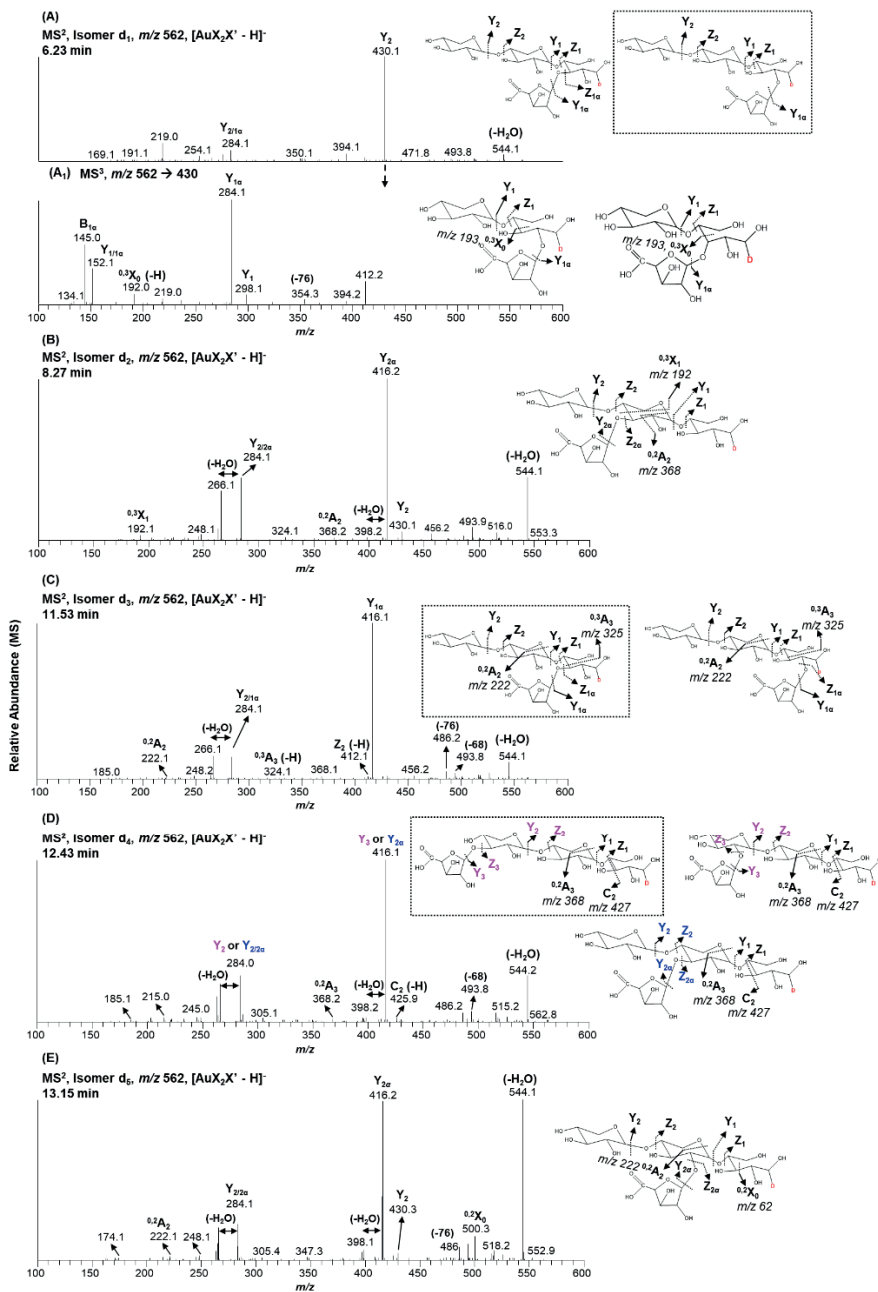


Figure S 2. Fragmentation spectra (ESI-MS²) in negative mode of the AUXOS-A with DP4 (parent ion [AuX₂X' - H] with *m/z* 562) that eluted at 6.23 min (A), 8.27 min (B), 11.53 min (C), 12.43 min (D), and 13.15 min (E) in the PGC elution profile (Fig. 2). ESI-MS³ spectra of the *m/z* 430 derived from the parent ion with *m/z* 562 that eluted at 6.23 min is in (A₁). Tentative oligosaccharide structures are depicted. Fragmentation of isomeric AUXOS-A resulting in different Y and Z ions is highlighted in pink and blue (D). Fragmentation ions are described in accordance with Domon and Costello [1]. More likely AUXOS-A structures are surrounded by a box.

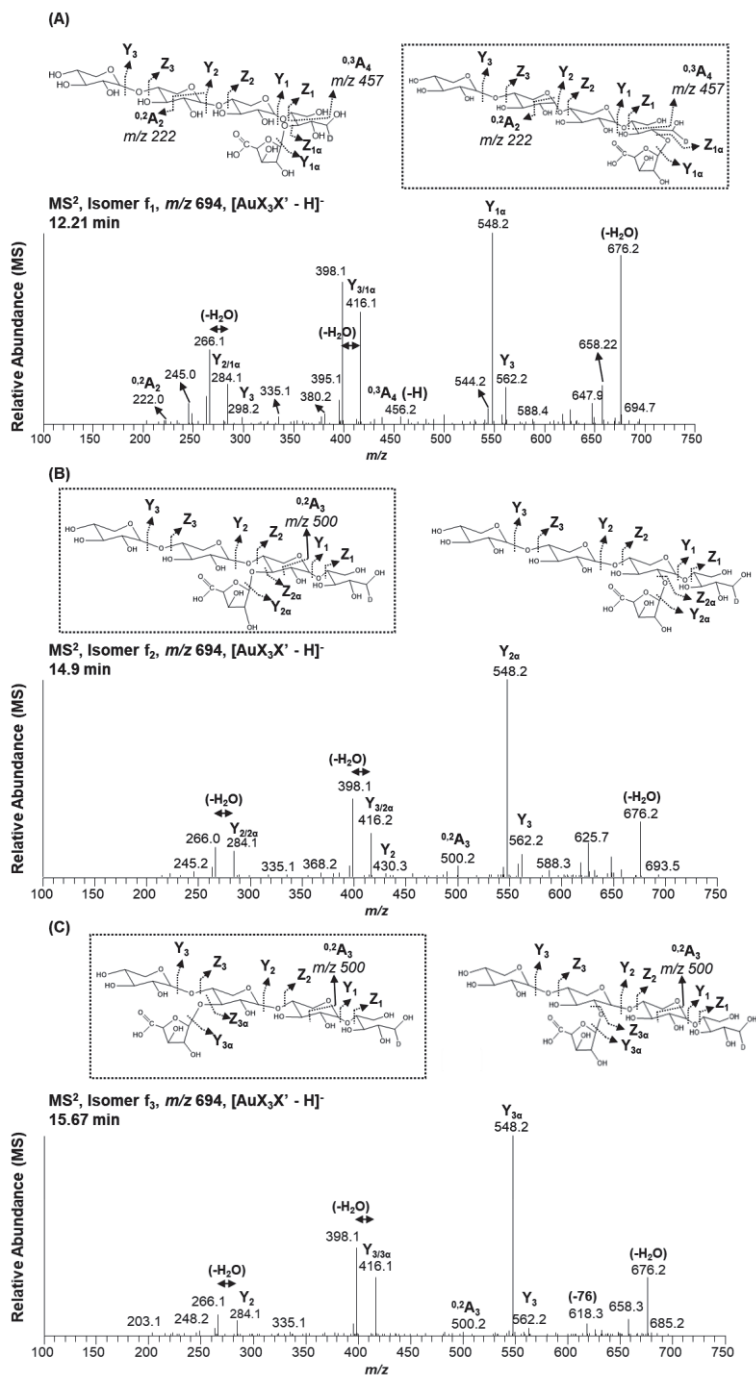


Figure S 3. Fragmentation spectra (ESI-MS²) in negative mode of the AUXOS-A with DP5 (parent ion [AuX₃X' - H]⁻ with *m/z* 694) that eluted at 12.21 min (A), 14.9 min (B), and 15.67 min (C) in the PGC elution profile (Fig. 2). Tentative oligosaccharide structures are depicted. Fragment ions are described in accordance with Domon and Costello [1]. More likely AUXOS-A structures are surrounded by a box.

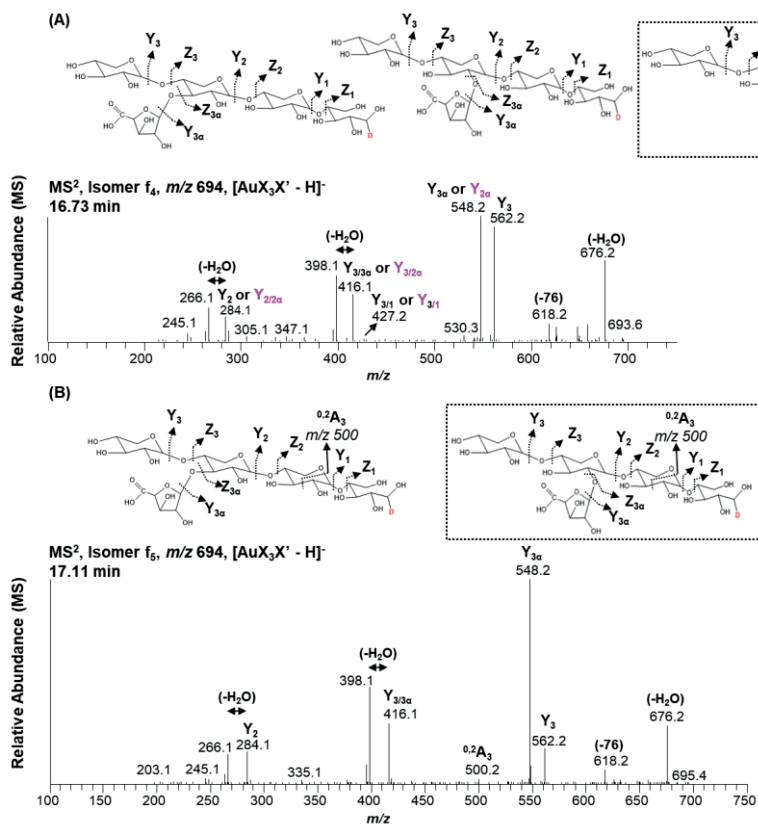


Figure S 4. Fragmentation spectra (ESI-MS²) in negative mode of the AUXOS-A with DP5 (parent ion [AuX₃X' - H]⁻ with *m/z* 694) that eluted at 16.73 min (A), and 17.11 min (B) in the PGC elution profile (Fig. 2). Tentative oligosaccharide structures are depicted. Fragmentation of isomeric AUXOS-A resulting in different Y and Z ions is highlighted in pink (A). Fragment ions are described in accordance with Domon and Costello [1]. More likely AUXOS-A structures are surrounded by a box.

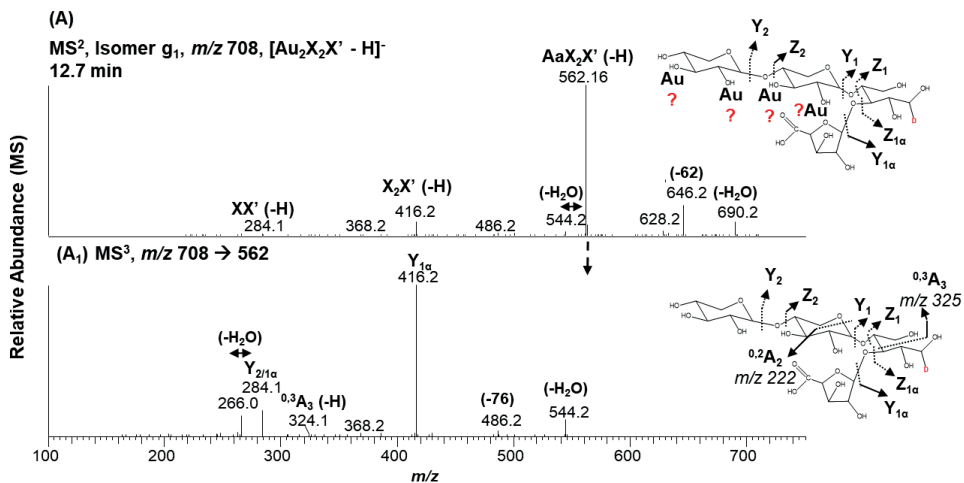


Figure S 5. Fragmentation spectra (ESI-MS²) in negative mode of the AUXOS-A with DP5 (parent ion [Au₂X₂X' - H]⁻ with *m/z* 708) that eluted at 12.7 min in the PGC elution profile (A). ESI-MS³ spectra of the *m/z* 562 derived from the parent ion with *m/z* 708 is shown in (A₁). Tentative oligosaccharide structures are depicted. ? indicates possible positions of the second AraA unit. Fragment ions are described in accordance with Domon and Costello [1].



Table S 2. Overview of UHPLC-PGC-MS identified (AU)XOS-A of NaBD₄-reduced TFA partially acid-hydrolysed (ox-)WAX, pD-WAX, and RAX samples. Oligosaccharide (OS) composition, and conclusive and tentative (AU)XOS-A structures are depicted. Relative abundance of each OS within DP2-7 is mentioned.

(AU)XOS-A (ret time)	OS composition ^a	Conclusive and Tentative (AU)XOS-A structures ^a	Position of AraA in AUXOS-A	Relative abundance (%) ^b of (AU)XOS-A within DP2-7						
				WAX	ox- WAX	pD- WAX	ox- pD-WAX	WAX	ox- WAX	ox- RAX
X₂	XX'	Xyl(1→4)Xyl'	Unsb. Xyl	13.8	10.8	19.3	13.9	13.3	13.4	
a ₁ (3.65min)	AuX'	AraA(1→3)Xyl'	RE	0.0	0.3	0.0	0.3	0.0	0.0	
b ₁ (4.29min)	AuXX'	AraA(1→3)Xyl(1→4)Xyl'	t-	0.0	3.3	0.0	1.1	0.0	3.2	
c ₁ (5.78min)	Au ₂ X'	[AraA(1→3), AraA(1→2)]Xyl'	2*RE	0.0	1.0	0.0	0.0	0.0	0.0	
d ₁ (6.23min)	Au ₂ X ₂ X'	*Xyl(1→4)Xyl(1→4)[AraA(1→2)]Xyl' Xyl(1→4)Xyl(1→4)[AraA(1→3)]Xyl'	RE	0.0	0.8	0.0	0.6	0.0	0.0	
b ₂ (6.88min)	AuXX'	*Xyl(1→4)[AraA(1→3)]Xyl' Xyl(1→4)[AraA(1→2)]Xyl'	RE	0.0	7.7	0.0	3.4	0.0	2.1	
X₃	X₂X'	Xyl(1→4)Xyl(1→4)Xyl'	Unsb. Xyl	21.0	19.6	25.9	22.0	21.1	22.7	
e ₁ (7.57min)	Au ₂ XX'	*Xyl(1→4)[AraA(1→2), AraA(1→3)]Xyl' AraA(1→2)→Xyl(1→4)[AraA(1→3)]Xyl' AraA(1→2)→Xyl(1→4)[AraA(1→2)]Xyl' AraA(1→3)→Xyl(1→4)[AraA(1→3)]Xyl' AraA(1→3)→Xyl(1→4)[AraA(1→2)]Xyl'	2*RE	0.0	2.3	0.0	0.4	0.0	0.0	
d ₂ (8.27min)	Au ₂ X ₂ X'	Xyl(1→4)[AraA(1→3)]Xyl(1→4)Xyl'	-2	0.0	2.2	0.0	1.0	0.0	2.8	



Table S 2. Continuation.

(AU)XOS-A (ret time)	OS composition ^a	Conclusive and Tentative (AU)XOS-A structures ^a	Position of AraA in AUXOS-A	Relative abundance (%) ^b of (AU)XOS-A within DP2-7						
				WAX	ox- WAX	pD- WAX	ox- pD-WAX	RAX	ox- RAX	
b ₃ (9.99min)	AuXX'	AraA(1→2)Xyl(1→4)Xyl'	t-	0.0	3.1	0.0	1.2	0.0	0.0	2.4
X ₄	X ₃ X'	[Xyl(1→4)] ₃ Xyl'	Unsb. Xyl	26.7	14.6	27.7	23.7	25.7	21.9	0.0
d ₃ (11.53min)	AuX ₂ X'	*Xyl(1→4)Xyl(1→4)[AraA(1→3)]Xyl' Xyl(1→4)Xyl(1→4)[AraA(1→2)]Xyl'	RE	0.0	4.5	0.0	0.0	0.0	0.0	0.0
f ₁ (12.21min)	AuX ₃ X'	*Xyl(1→4)Xyl(1→4)Xyl(1→4)[AraA(1→ 2)]Xyl' Xyl(1→4)Xyl(1→4)Xyl(1→4)[AraA(1→3)] Xyl'	RE	0.0	0.3	0.0	0.0	0.0	0.0	0.8
d ₄ (12.43min)	AuX ₂ X'	*AraA(1→3)Xyl(1→4)Xyl(1→4)Xyl' AraA(1→2)Xyl(1→4)Xyl(1→4)Xyl' Xyl(1→4)[AraA(1→3)]Xyl(1→4)Xyl'	t-	0.0	3.5	0.0	2.0	0.0	0.0	0.9
g ₁ (12.70min)	Au ₂ X ₂ X'	*AraA(1→3)Xyl(1→4)Xyl(1→4)[AraA(1 →3)]Xyl' AraA(1→2)Xyl(1→4)Xyl(1→4)[AraA(1 →3)]Xyl' Xyl(1→4)[AraA(1→2)]Xyl(1→4)[AraA(1 →3)]Xyl' Xyl(1→4)[AraA(1→3)]Xyl(1→4)[AraA(1 →3)]Xyl'	RE and t-	0.0	3.3	0.0	1.0	0.0	0.0	0.7



Table S 2. Continuation.

(AU)XOS-A (ret time)	OS	Conclusive and Tentative (AU)XOS-A structures ^a	Position of AraA in AUXOS-A	Relative abundance (%) ^b of (AU)XOS-A within DP2-7						
				WAX	ox- WAX	pD- WAX	ox- pD-WAX	RAX	ox- RAX	
d ₅ (13.15min)	AuX ₂ X'	Xyl(1→4)[AraA(1→2)]Xyl(1→4)Xyl'	-2	0.0	0.2	0.0	0.4	0.0	0.0	1.8
e ₂ (13.90min)	Au ₂ XX'	*[AraA(1→2), AraA(1→3)]Xyl(1→4)Xyl' AraA(1→2)Xyl(1→4)[AraA(1→3)]Xyl' AraA(1→2)Xyl(1→4)[AraA(1→2)]Xyl'	2* ^t	0.0	5.8	0.0	1.3	0.0	0.0	3.7
f ₂ (14.90min)	AuX ₃ X'	Xyl(1→4)Xyl(1→4)[AraA(1→3)]Xyl(1→4)Xyl'	-2	0.0	3.1	0.0	1.7	0.0	0.0	4.2
X₅	X₄X'	[Xyl(1→4)]₄Xyl'	Unsb. Xyl	22.7	8.4	18.4	16.3	22.8	22.8	14.4
f ₃ (15.67min)	AuX ₃ X'	*Xyl(1→4)[AraA(1→3)]Xyl(1→4)Xyl(1→4)Xyl' Xyl(1→4)[AraA(1→2)]Xyl(1→4)Xyl(1→4)Xyl'	-3	0.0	1.3	0.0	0.8	0.0	0.0	0.1
f ₄ (16.73min)	AuX ₃ X'	*Xyl(1→4)Xyl(1→4)[AraA(1→2)]Xyl(1→4)Xyl' Xyl(1→4)[AraA(1→3)]Xyl(1→4)Xyl(1→4)Xyl' Xyl(1→4)[AraA(1→2)]Xyl(1→4)Xyl(1→4)Xyl'	-2	0.0	1.0	0.0	0.8	0.0	0.0	0.0



Table S 2. Continuation.

(AU)XOS-A (ret time)	OS composition ^a	Conclusive and Tentative (AU)XOS-A structures ^a	Position of AraA in						Relative abundance (%) ^b of (AU)XOS-A within DP2-7								
			AUXOS-A	WAX	ox- WAX	pd- WAX	ox- pd-WAX	RAX	ox- WAX	pd- WAX	ox- pd-WAX	RAX					
f ₅ (17.11 min)	AuX ₅ X'	*Xyl(1→4)[AraA(1→2)]Xyl(1→4)Xyl(1→4)Xyl' 4)Xyl'	-3	0.0	1.1	0.0	0.0	0.8	0.0	0.0	0.0	0.1					
		Xyl(1→4)[AraA(1→3)]Xyl(1→4)Xyl(1→4)Xyl' Xyl'															
X₆	X₅X'	[Xyl(1→4)]₅Xyl'	Unsb. Xyl	11.6	1.9	7.5	6.5	12.3	4.8								
X₇	X₆X'	[Xyl(1→4)]₆Xyl'	Unsb. Xyl	3.6	0.0	1.4	1.1	4.9	0.0								
Total relative abundance (%) of (AU)XOS-A within DP2-7																	
		XOS-A		100	55.3	100	83.4	100	77.1								
		AUXOS-A		0	44.8	0	16.6	0	22.9								
		AuX'		0.0	0.3	0.0	0.3	0.0	0.0								
		AuXX'		0.0	14.1	0.0	5.7	0.0	7.7								
		Au ₂ X'		0.0	1.0	0.0	0.0	0.0	0.0								
		AuX ₃ X'		0.0	11.2	0.0	4.0	0.0	5.5								
		Au ₂ XX'		0.0	8.2	0.0	1.7	0.0	3.7								
		AuX ₃ X'		0.0	6.8	0.0	4.0	0.0	5.3								
		Au ₂ X ₂ X'		0.0	3.3	0.0	1.0	0.0	0.7								
Relative mol % present within DP2-7																	
		Ara(A)		0	15.0	0	5.1	0	7.1								
		Xyl		100	85.0	100	94.9	100	92.9								



Table S 2. Continuation.

Relative abundance (%) ^b of (AU)XOS-A within DP2-7					
	WAX	ox- WAX	pD- WAX	ox- pD-WAX	ox- RAX
Relative totals (%) within Xyl units**					
<i>Unsubstituted Xyl</i>					
	100 (67.1)*	55.3	100 (80.8)*	83.4	100 (55.9) *
<i>Single-substituted Xyl</i>					
	- (27.0)*	35.6	- (17.2)*	14.9	- (41.6) *
<i>O-3 Sub. Xyl</i>	- (24.7)*	29.1	- (12.0)*	11.2	- (39.0) *
<i>O-2 Sub. Xyl</i>	- (2.3)*	6.6	- (5.2)*	3.7	- (2.6)*
<i>Double-substituted Xyl</i>					
<i>(O-2 and O-3)</i>	- (5.8)*	9.1	- (2.1)*	1.7	0 (2.7)*
Relative totals (%) of the AraA position along the Xyl backbone of the (AU)XOS-A**					
Unsb. Xyl	100.0	55.3	100.0	83.4	100.0 77.1
RE	0.0	20.8	0.0	5.6	0.0 3.3
-1	0.0	6.5	0.0	3.8	0.0 8.8
-2	0.0	2.4	0.0	1.5	0.0 0.3
t-	0.0	23.2	0.0	7.4	0.0 14.3

^a – Abbreviations in accordance with Fauré et al. [2]. Au, arabinuronic acid; X, xylose; X', xylylitol; subscript number indicates the number of each sugar in the OS.
^b – Determined by integration of peak areas in UHPLC-PGC-MS of all (AU)XOS-A within DP2-7.

* – More likely AUXOS-A structure based on comparison with glycosidic linkage analysis and on the most dominant fragment ions present in the fragmentation spectrum.

Unsb. Xyl – Unsubstituted Xyl; **RE** – Reducing end Xyl; **-1** – 2nd Xyl from RE; **-2** – 3rd Xyl from RE; **t-** terminal non-reducing end Xyl.

** – relative totals (%) were calculated using the most likely AUXOS-A indicated with *.

()* – relative mol percentages obtained from glycosidic linkage analysis was calculated for native AX samples.



- [1] Domon, B. and C.E. Costello. A systematic nomenclature for carbohydrate fragmentations in FAB-MS/MS spectra of glycoconjugates. *Glycoconjugate Journal*. **1988**, 5, 397-409.
- [2] Fauré, R., C.M. Courtin, J.A. Delcour, C. Dumon, C.B. Faulds, G.B. Fincher, S. Fort, S.C. Fry, S. Halila, M.A. Kabel, L. Pouvreau, B. Quemener, A. Rivet, L. Saulnier, H.A. Schols, H. Driguez, and M.J. O'Donohue. A brief and informationally rich naming system for Oligosaccharide motifs of heteroxylans found in plant cell walls. *Australian Journal of Chemistry*. **2009**, 62, 533-537.

Chapter 4

**Periodate oxidation of plant
polysaccharides provides polysaccharide-
specific oligosaccharides**

Submitted for publication as: Carolina O. Pandeirada, Max Achterweust, Hans-Gerd Janssen, Yvonne Westphal, and Henk A. Schols.



Abstract

Although polysaccharides are frequently used in foods, detailed characterization and/or identification of their structures using a single method remains a challenge. We investigated the suitability of periodate oxidation as an approach to depolymerize polysaccharides into oligosaccharides that allow characterization and/or identification of the original polysaccharides. To do this, various periodate oxidation conditions were tested on (arabino)xylan, galactomannan, xyloglucan and homogalacturonan. Each polysaccharide required a different oxidation condition to release a substantial level of oligosaccharides. These oligosaccharides had highly complex structures due to the presence of e.g., dialdehyde sugars, hemialdals, and remnants of (oxidized) sugars, as verified by ESI-MS/MS. Despite these oligosaccharides were highly complex and lost some polysaccharide structural features, each periodate-oxidized sample comprised polysaccharide structure-dependent MS oxidized oligosaccharide profiles. Our findings are a good starting point to find a more generic chemical polysaccharide depolymerization approach based on periodate oxidation to identify polysaccharides by oligosaccharides fingerprinting.



1. Introduction

Plant polysaccharides are the most abundant biomacromolecules in nature and abundantly present in foods [1, 2]. Plant polysaccharides have also been explored as food additives to modulate the functional properties of foods [1]. Although polysaccharides are widely used in food products and involved in a wide variety of functional properties, detailed characterization of their structures remains a challenge.

Characterization of polysaccharides is laborious and often requires the combined use of multiple techniques. Gas chromatography (GC), liquid chromatography (LC) or nuclear magnetic resonance (NMR) spectroscopy can be used to determine the sugar composition after acid hydrolysis [3-6]. The type of glycosidic linkages can be studied by NMR or permethylation analysis [7]. Non-sugar substitution, such as the presence of methyl-esters, acetyl- and hydroxycinnamoyl groups can be assessed through alkaline hydrolysis with GC and high-performance (HP)LC analysis [8, 9]. All these methods are complex and laborious and hence, there remains a need for a more rapid method to characterize and/or identify polysaccharide structures.

Enzymatic depolymerization of polysaccharides into structure-informative (diagnostic) oligosaccharides followed by separation, quantification and characterization of the released oligosaccharides allows a detailed characterization of polysaccharides [10-12]. Although enzymatic digestion is a very powerful strategy to obtain diagnostic oligosaccharides, there is not a universal enzyme able to release oligosaccharides from all polysaccharides. All enzymes are highly polysaccharide-specific. Moreover they are sometimes limited in their action to degrade highly substituted polysaccharides [13].

Periodate (IO_4^-) oxidation of polysaccharides leads to specific oxidation of free vicinal hydroxyl groups to aldehydes with internal ring cleavage [14]. For the reaction to take place, vicinal hydroxyl groups must be oriented in an equatorial (*eq.*)-*eq.* or axial (*ax.*)-*eq.* positions [14]. Periodate oxidation of polysaccharides can be accompanied by polysaccharide depolymerization, which depends on the concentration of NaIO_4 [15, 16], temperature [17, 18], time [19], and pH [18]. Although the periodate oxidation reaction is mostly performed in aqueous systems, in such systems the aldehyde groups in polysaccharides can react with hydroxyl groups, forming inter- and/or intra-hemiacetal bonds, or with water, forming hemialdals or hydrated aldehydes [20-23]. These aldehyde side oxidation reactions might form very complex saccharide chemical structures, which might complicate the analysis of the resulting periodate-oxidized saccharides and consequent characterization of the respective native polysaccharide structure. Yet, given the high specificity of NaIO_4 to oxidize vicinal diols and considering that periodate oxidation can lead to polysaccharide depolymerization, periodate oxidation of polysaccharides might initiate the formation of diagnostic oligosaccharides in a faster and more generic manner than by using enzymes. For example, periodate oxidation of (arabino)xylans allows to determine branching points because the (1→4)-linked xylose (Xyl) residues in the polymer backbone that are 2-*O*- and/or 3-*O*-substituted cannot be oxidized due to absence of vicinal diols [24]. Thus, our study aimed to investigate if periodate oxidation of plant polysaccharides leads to the formation of oligosaccharides that allow characterization and/or identification of polysaccharides. To do this, various periodate oxidation conditions (NaIO_4 concentration, temperature, and time) were tested on five plant polysaccharides (arabinoxylan, xylan, galactomannan, xyloglucan, and homogalacturonan), and the resulting periodate-oxidized polysaccharide products were characterized.



2. Materials and methods

2.1. Materials

Wheat arabinoxylan (AX) of medium viscosity was obtained from Megazyme (arabinose (Ara):Xyl=38:62, Purity > 95 %, Wicklow, Ireland), birch wood xylan (BWX) from Sigma (Darmstadt, Germany), guar galactomannan (GM; mannose (Man): galactose (Gal)=2:1) was from BFGoodrich Diamalt GmbH (Munich, Germany), tamarind seed xyloglucan (XG) from Dainippon Sumitomo Pharma Co. Ltd., (Osaka, Japan), and lemon homogalacturonan (HG) with a high degree of methylesterification was provided by Copenhagen Pectin A/S (Lille Skensved, Denmark). Sodium metaperiodate (NaIO_4 , 98 %) was purchased from Alfa Aesar (Thermo Fisher, Kandel, Germany). Ethylene glycol was from Merck (Darmstadt). Methanol, formic acid, and LC-MS water used in MS experiments were of ultra (U)HPLC-grade (Biosolve, Valkenswaard, The Netherlands). All water was purified in a Milli-Q system from Millipore (Molsheim, France), unless otherwise mentioned.

2.2. Periodate oxidation of polysaccharides

Periodate oxidation of plant polysaccharides was performed adapting the procedure used by Åman and Bengtsson [25]. Wheat AX, BWX, GM, XG, and HG were periodate oxidized using various ratios of $\mu\text{mol NaIO}_4/\text{mg polysaccharide (PS)}$ with two reaction temperatures (room temperature – RT, and 70 °C), and two reaction times (6 and 24 h). The NaIO_4/PS ratios tested were 3.0, 6.0, and 12.0 $\mu\text{mol NaIO}_4/\text{mg PS}$, which should lead to approx. 50 %, 100 % and > 100 % oxidation of all investigated polysaccharides, respectively, except for HG. HG is expected to be fully oxidized already at 3.0 NaIO_4/PS ratio (Table 1). Here, we define 100 % oxidation as oxidation of all sugar units containing free vicinal hydroxyl groups by NaIO_4 with formation of dialdehydes. To calculate these values, we assume that 1 mol of sugar unit containing vicinal diols (unsubstituted Xyl and all Ara units of AX and BWX; all Man units of GM; glucose (Glc) and substituted Xyl units of XG; and all (galacturonic acid) GalA units of HG) would consume 1 mol of NaIO_4 , and that 1 mol of sugar unit containing three vicinal hydroxyl groups (Gal units of GM; and unsubstituted Xyl and Gal units of XG) would consume 2 mol of NaIO_4 .

The reaction volume was set at 40 mL, and 200 mg of PS powder was used in all experiments. Polysaccharides were dissolved in water, and a freshly prepared 250 $\mu\text{mol/mL NaIO}_4$ solution was added to the PS solution to reach the desired $\mu\text{mol NaIO}_4/\text{mg PS}$ ratio (2.4, 4.8, and 9.6 mL of 250 $\mu\text{mol/mL NaIO}_4$ solution to have a $\mu\text{mol NaIO}_4/\text{mg PS}$ ratio of 3.0, 6.0, and 12.0, respectively). The glass reaction flask was protected from light by covering the flask with aluminium foil, and the reaction was carried out for 6 or 24 h at RT under magnetic stirring or at 70 °C in an incubator under shaking. The reaction was quenched by adding 1.6 mL ethylene glycol, and the reaction mixture was dialysed (cut-off for globular proteins: 12-14 kDa, Medicell Membranes Ltd, London) against distilled water. The retentate was freeze-dried, yielding the final periodate-oxidized PS sample, named pOx-PS.



Table 1. Theoretical amount of NaIO₄ (μmol) per mg of PS needed to have full oxidation of arabinoxyylan (AX), birch wood xylan (BWX), galactomannan (GM), xyloglucan (XG), and homogalacturonan (HG).

Theoretical amount of NaIO ₄ /PS needed	Polysaccharides				
	AX	BWX	GM	XG	HG
μmol NaIO ₄ /mg PS	6.3	5.6	6.1	6.8	3.1

2.3. Sugar composition analysis by HPAEC-PAD

Sugar composition of (pOx-)AX, BWX, and HG was determined after methanolysis (2.0 M HCl in dried methanol, 16 h, 80 °C) and TFA acid hydrolysis (2.0 M, 1 h, 121 °C) as described elsewhere [26]. Hydrolysates were diluted in water to ± 25 μg/mL before analysis. Sugar composition of (pOx-)GM and XG samples was accessed after pre-hydrolysis for 15 min at 30 °C in 72 % (w/w) H₂SO₄ followed by hydrolysis for 3 h at 100 °C in 1.0 M H₂SO₄. Sulphuric acid hydrolysates were 100 times diluted with water before analysis. Monosaccharides released were analyzed by High-Performance Anion-Exchange Chromatography with Pulsed Amperometric Detection (HPAEC-PAD). An ICS-5000 HPLC system (Dionex, Sunnyvale, CA, USA) equipped with a CarboPac PA1 guard column (2 mm ID × 50 mm) and a CarboPac PA-1 column (2 mm × 250 mm; both from Dionex) was used for this analysis. Detection of the eluted compounds was performed by an ED40 EC-detector (Dionex) running in the PAD mode. Ten μL of the diluted hydrolysates was injected on the system and compounds were eluted as described by Pandeirada et al. [26]. All samples were analyzed in duplicate. Monosaccharide standards in a concentration range of 1.0-150 μg/mL were used for quantification. The collected data were analyzed using Chromeleon 7.2 software (Dionex). The degree of oxidation (DO) (equation (1)) of samples was calculated based on the decrease in the sugar recovery relative to the respective native PS. The relative DO (DO_{Rel}) (equation (2)) was calculated using the theoretical maximum DO (DO_{Theo}) that each PS can reach and the calculated DO. DO_{Theo} was calculated based on the expected total remaining sugar content, i.e. all sugar units containing vicinal diols are oxidized and not detected as intact sugar anymore.

$$(1) \quad DO (\%, w/w) = 100 - \text{Relative sugar recovery of } pOx - PS$$

$$(2) \quad DO_{Rel} (\%, w/w) = \frac{DO}{DO_{Theo}} \times 100$$

2.4. Uronic acid and Methyl-ester content

The total uronic acid content of (pOx-)BWX and HG was determined using an automated colorimetric *m*-hydroxydiphenyl method [27, 28] after sulphuric acid-hydrolysis as described in section 2.3.

For the determination of the methyl-ester content, (pOx-)HG samples were saponified at 5.0 mg/mL in 0.1 M NaOH for 24 h (1 h at 4 °C followed by 23 h at RT). The methanol released was quantified by gas chromatography (GC) using a method described elsewhere [9]. All analyses were



performed in duplicate. The collected data were analyzed using Xcalibur 4.1 software (Thermo Scientific).

2.5. Molecular weight distribution by HPSEC-RI

The average molecular weight (Mw) was determined by high performance size exclusion chromatography (HPSEC) on an Ultimate 3000 system (Dionex) coupled to Shodex RI-101 detector (Showa Denko K.K., Tokyo, Japan) as described by Pandeirada et al. [26]. Columns were calibrated with pullulan (0.180–708 kDa; Polymer Laboratories, UK) and pectin standards (10–100 kDa, as estimated by viscometry [29]). Standards and samples were analyzed at 1.0 mg/mL. Collected data were analyzed using Chromeleon 7.2 software (Dionex).

2.6. Electrospray ionization mass spectrometry (ESI-MS) and tandem MS

ESI-MS and ESI-MS/MS experiments were carried out on an LTQ-VelosPro mass spectrometer (Thermo Scientific) equipped with a heated ESI probe. MS data were acquired in positive ion mode for pOx-AX, pOx-BWX, pOx-GM, and pOx-XG samples, which were diluted to 2.0 mg/mL in water and introduced into the electrospray source at 20 μ L/min. Spectra were recorded for 2.5 minutes. Instrument settings were: source heater temperature 425 $^{\circ}$ C, capillary temperature 275 $^{\circ}$ C, sheath gas flow 30 units, source voltage 5.0 kV and m/z range 150–1500. The MS data for pOx-HG were obtained in negative ion mode using a sheath gas flow of 50 units, and a source voltage 3.5 kV, with the rest of the parameters being the same as described above. The pOx-HG samples were diluted to 2.0 mg/mL in methanol:water (1:1, v/v) containing 0.1 % (v/v) formic acid and introduced into the electrospray source at 20 μ L/min. MS/MS spectra of all samples were acquired by collision-induced dissociation (CID) using a collision energy set at 32 %, with a minimum signal threshold of 500 counts at an activation Q of 0.25 and activation time of 10 ms were used. MS data were processed using Xcalibur 4.1 software (Thermo Scientific).

3. Results and discussion

Various plant polysaccharides, wheat arabinoxylan (AX), birch wood xylan (BWX), guar galactomannan (GM), tamarind seed xyloglucan (XG), and highly methyl-esterified lemon homogalacturonan (HG), were periodate-oxidized under various conditions. It was investigated whether periodate oxidation of plant polysaccharides could lead to the formation of oligosaccharides that allow structural characterization and/or identification of polysaccharides in a faster and more generic manner than by using enzymes. Two reaction temperatures (room temperature (RT) and 70 $^{\circ}$ C), two reaction times (6 and 24 h), and three different periodate-to-polysaccharide (PS) ratios were tested. The NaIO₄/PS ratios tested were 3.0, 6.0, and 12.0 μ mol NaIO₄/mg PS, which theoretically lead to approx. 50 %, 100 % and >> 100 % oxidation of all investigated polysaccharides, respectively, except for HG. HG is expected to be fully oxidized at 3.0 NaIO₄/PS ratio (Table 1).



3.1. Effect of periodate oxidation on the Mw distribution of polysaccharides

The influence of the various periodate oxidation conditions on the molecular weight (Mw) distribution of polysaccharides was studied by HPSEC. HPSEC profiles of all periodate-oxidized PS (pOx-PS) samples are shown in supplementary material (Fig. S1, AX and BWX; Fig. S2, GM and XG; and Fig. S3, HG). In general, all soluble pOx-PS samples had lower molecular weights than the respective native PS, in agreement with various studies [15, 17, 20, 30, 31]. All pOx-AX and pOx-BWX samples contained molecules within a degree of polymerization (DP) 2-20 (oligosaccharides) or larger. The extent of depolymerization of AX and BWX increased when the NaIO_4/PS ratio was raised from 3.0 to 12.0, in accordance with literature [15], and the highest level of molecules comprising a DP 2-20 were obtained when the reaction was performed at RT for 6 h (Fig. 1A and B).

Regarding GM, XG, and HG samples, polysaccharide depolymerization releasing molecules within the DP 2-20 range mainly occurred when the reaction was performed at 70 °C for 24 h (Fig. 1C, D and E). Maximum GM and XG degradations were reached using a NaIO_4/PS ratio of 6.0 for 24 h at 70 °C. While for HG, maximum degradation was only obtained using a higher NaIO_4/PS ratio of 12.0 at 70 °C for 24 h. Most of the molecules in these samples contained a DP 2-20.

Overall, it can be stated that pentosans are more readily degraded by periodate than hexose- and hexuronic-based polymers. Oligosaccharides were obtained at any periodate oxidation condition for AX and BWX, whereas for GM, XG, and HG, a high level of oligosaccharides was only obtained at 70 °C using a NaIO_4/PS ratio ≥ 6.0 and a long reaction time of 24 h. These results show that periodate oxidation of plant polysaccharides can release oligosaccharides for all polysaccharides. Formation rates depend on the conditions applied and differ per PS structure.

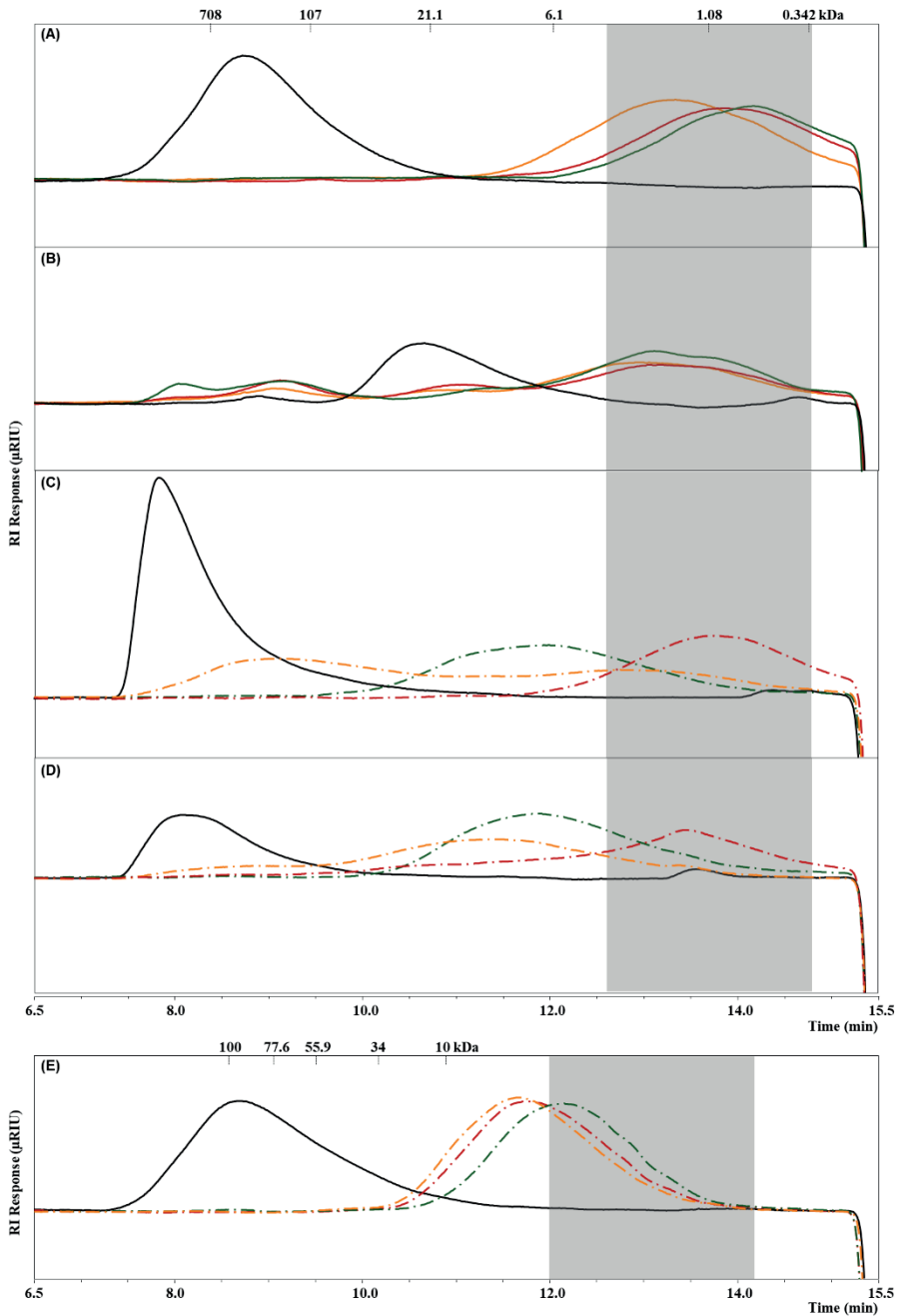


Figure 1. HPSEC elution patterns of the periodate-oxidized AX (A) and BWX (B) samples at room temperature for 6 h, and of the GM (C), XG (D), and HG (E) samples oxidized at 70 °C for 24 h. Native PS samples are shown in black lines, and periodate-oxidized samples with 3.0, 6.0 and 12.0 NaIO₄/PS are shown in orange, red, and green lines, respectively. (—) 6 h reaction; (---) 24 h reaction. Pullulan and pectin standards were used to calibrate the system for neutral polysaccharides and HG, respectively. Grey boxes indicate the time range corresponding to an apparent DP between 2 and 20.



3.2. General composition of periodate-oxidized/degraded polysaccharides

To investigate the influence of the periodate oxidation conditions on the general composition of polysaccharides, the sugar composition of all (pOx-)PS samples, and the methyl-esterification content of pectin samples was investigated. The yield, sugar recovery, and degrees of oxidation (DO and DO_{Rel}) of all pOx-PS samples investigated in this study are shown in Table S1. In general, the sugar recovery of pOx-PS samples relatively to the respective native PS was lower than 75 % (w/w), as expected due to the oxidation process. In the following paragraphs, a detailed description of the composition of the samples containing the highest levels of molecules in the DP2-20 range (based on the HPSEC results, section 3.1.) is given and will be discussed to understand if the oligosaccharides released provide information on the native PS structure.

Arabino(xylan)

pOx-AX samples containing the highest level of molecules in the DP2-20 range were obtained at RT and 6 h reaction time (Fig. 1A). For these samples, the decrease in the Ara and Xyl recoveries increased when the $NaIO_4/PS$ ratio was increased from 3.0 to 12.0 (Fig. 2A). At a $NaIO_4/PS$ ratio of 12.0 at RT and 6 h reaction time, no Ara was detected anymore (Fig. 2A), suggesting complete oxidation and/or degradation of the Ara side chains. At this condition, still 9.7 % (w/w) Xyl was recovered. Retrieval of Xyl and disappearance of Ara at high $NaIO_4$ concentrations is expected because only unsubstituted Xyl units are susceptible to oxidation, whereas all Ara units can be oxidized.

The Xyl recovery of 9.7% is lower than the theoretically value (~20.6 %) that would be obtained if AX is 100 % oxidized (Fig. 2A). This suggests that overoxidation of the pOx-AX at RT for 6 h using a $NaIO_4/PS$ ratio of 12.0 occurred ($DO_{Rel} > 100\%$). This might be due to oxidation and/or degradation of substituted Xyl units, which might have been caused by cleavage of the Ara side chains, leaving new unsubstituted Xyl units available for oxidation. All together this indicates that high $NaIO_4$ concentrations can lead to removal of the PS structural features, in that way hindering the formation of oligosaccharides that can be used for structural characterization of the original PS. Clearly, overoxidation of the polymers should be avoided.

At a $NaIO_4/PS$ ratio of 6.0 for 6 h at RT, pOx-AX recovered minor amounts of Ara (<3.0 %), and Xyl underwent only minor overoxidation and/or degradation (recovered Xyl just slightly below 20.6 %), showing that this pOx-AX was almost completely oxidized (Fig. 2A). This indicates that for AX, the treatment at RT for 6 h using a $NaIO_4/PS$ ratio of 6.0 might provide the highest level of structure-indicative oligosaccharides.

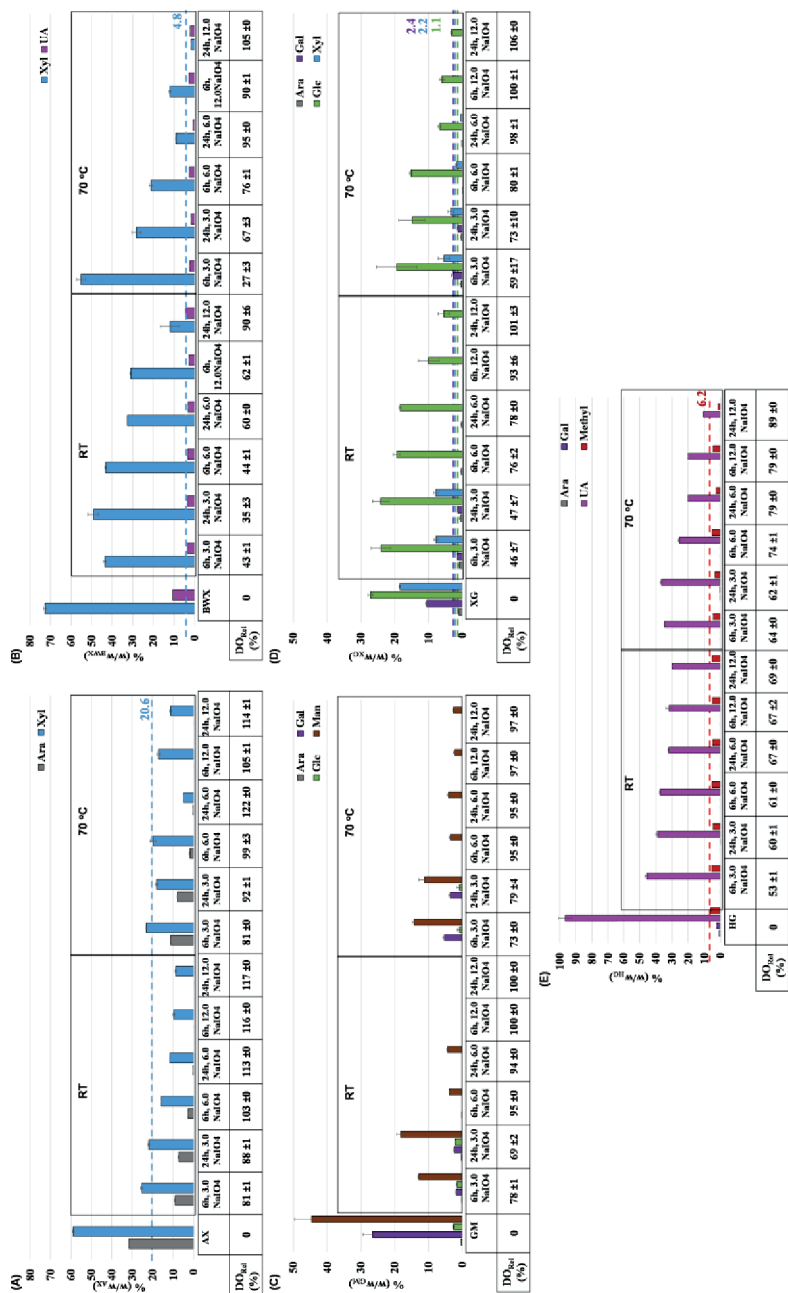


Figure 2. Sugar recovery of the native and periodate-oxidized polysaccharide samples, AX (A), BWX (B), GM (C), XG (D), and HG (E), at room temperature (RT) and at 70 °C, for 6 and 24 h using a $\mu\text{mol NaIO}_4/\text{mg PS}$ ratio of 3.0, 6.0 and 12.0. Uronic acid (UA) recovery of BWX and HG samples, and Methyl-ester methyl-ester (red) that are expected to be obtained at 100 % oxidation. When no dashed line is depicted for a given sugar, it indicates that a minimum amount of 0 can be obtained. Relative degree of oxidation (DO_{rel}) in % is given for each pOx-sample in the table inserted below each graph. DO_{rel} for pOx-HG samples is based on the decrease in the UA recovery.



For BWX, the highest level of molecules in the DP2-20 range was also obtained at RT and 6 h reaction time (Fig. 1B). The decrease in the Xyl and uronic acids (UA) recoveries of pOx-BWX at RT for 6 h was higher at a NaIO₄/PS ratio of 12.0 than at a NaIO₄/PS ratio of 3.0 or 6.0 (Fig. 2B). None of the former oxidation conditions led to complete BWX oxidation. This suggests that a moderately substituted xylan with UA (BWX) is more difficult to oxidize than a highly substituted xylan with Ara units (AX) at RT. This might be due to incomplete solubilization of BWX at RT, or due to easier formation of stable hemiacetal rings in a low substituted xylan, preventing oxidation of the Xyl residues, as suggested by Åman and Bengtsson [25] and Izydorczyk and Biliaderis [32]. Yet, full oxidation of the BWX would completely modify the BWX structure and prevent the formation of diagnostic oligosaccharides. The pOx-BWX samples obtained at RT and 6 h treatment displayed a DO_{Rel} ranging from 43 to 62 % at a NaIO₄/PS ratio of 3.0 and 12.0 (Fig. 2B), and are hence likely to contain BWX structure-informative oligosaccharides.

Galactomannan and Xyloglucan

The pOx-GM and pOx-XG samples that displayed the highest level of molecules with a DP2-20 were obtained using a NaIO₄/PS ratio of 6.0 for 24 h at 70 °C (Fig. 1C and 1D), a condition that theoretically leads to full oxidation of GM and XG (Table 1). Under this condition, pOx-GM and pOx-XG were obtained with a DO_{Rel} of 95 and 98 % (Fig. 2C and 2D), respectively. Minor amounts of Man and Glc (<7.0 %) were recovered in these pOx-GM and pOx-XG samples, respectively. In GM and XG, all sugar units can be periodate-oxidized since all moieties contain vicinal diols. This indicates that in both the GM and XG samples, the sugar side chains were more readily oxidized and/or degraded than the backbone. This agrees with previous studies on periodate oxidation of GM and XG [19, 20, 33, 34]. Thus, if the sugar units in the side chains of GM and XG are oxidized without being removed from the (oxidized) polymer backbone, the released oligosaccharides from the pOx-GM and pOx-XG samples at a NaIO₄/PS ratio of 6.0 for 24 h at 70 °C might be diagnostic.

Homogalacturonan

The pOx-HG obtained using a NaIO₄/PS ratio of 12.0 at 70 °C for 24 h not only had the highest DO_{Rel} (89 %, Fig. 2E), but it also had the highest level of molecules with a DP 2-20 (Fig. 1E). Although this pOx-HG comprised the highest level of oligosaccharides, it was also the pOx-HG sample that had the lowest recovery of methyl-esters (22.3 %, Fig. S4). The removal of methyl-esters indicates that the oligosaccharides obtained for pOx-HG at 70 °C for 24 h using a NaIO₄/PS ratio of 12.0 do not allow detailed characterization of the native HG structure. Although the other pOx-HG samples oxidized at RT, or at 70 °C for 6 h, recovered larger amounts of methyl-esters (72-88 %, Fig. S4), they contained no or only minor levels of oligosaccharides (Fig. S3). Thus, although not fully diagnostic, the oligosaccharides present in pOx-HG (70 °C, 24 h, NaIO₄/PS ratio of 12.0) might still be useful to recognize an HG type structure.

3. 3. ESI-MS analysis of (periodate-oxidized) oligosaccharides

To study the type of oligosaccharides formed upon periodate oxidation, samples containing oligosaccharides were analyzed using electrospray ionization (ESI) mass spectrometry (MS) *via* direct



infusion. The ESI-MS profiles (Fig. 3) obtained for each pOx-PS containing (diagnostic) oligosaccharides are shown and discussed below.

ESI-MS analysis of periodate-oxidized AX and BWX samples

HPSEC and compositional results indicated that pOx-AX at RT for 6 h using a NaIO₄/PS ratio of 6.0 likely had the highest level of diagnostic oligosaccharides. Hence, this sample was selected to be further analyzed by ESI-MS. The selected pOx-AX mostly comprised oxidized oligosaccharides and a negligible level of pentose-oligomers (P_n; Fig. 3A), confirming the high DO of this sample. The released oxidized oligosaccharides had well-defined *m/z* regions, forming DP-clusters of oxidized oligosaccharides (identified as **ox-DP_n** in Fig. 3). These DP-clusters were composed of various sub-oligosaccharide clusters. To better visualize these clusters (**ox-DP_n**), and their respective sub-oligosaccharide clusters, a zoom-in of the *m/z* 650-1000 range is shown in Fig. 3A₁. Each sub-oligosaccharide cluster comprised various *m/z* values that were $\Delta -(16 + n*2)$, $\Delta -(30 + n*2)$, $\Delta -(46 + n*2)$, $\Delta -(62 + n*2)$, and $\Delta -(78 + n*2)$ Da relative to the corresponding DP-oligomer, where $n = 0 - 4$. The $n*2$ present in each sub-oligosaccharide cluster can be due to variable levels (*n*) of dialdehydes (Fig. S5), as a dialdehyde sugar is 2 Da lower than an intact sugar unit.

The sub-oligosaccharide cluster with P_n $\Delta -(30 + n*2)$ Da, with $n = 0, 1, \text{ and } 2$ (Fig. 3A₁) can be attributed to double oxidation of the terminal non-reducing end (NRE-) Xyl, as described in scheme 1. At this Xyl unit, periodate will attack the three vicinal hydroxyl groups at C2, C3, and C4, releasing a molecule of formic acid from C3, and forming aldehyde groups at C2 and C4 positions [35-37]. The sub-oligosaccharide cluster with P_n $\Delta -(60 + n*2)$ Da, with $n = 1 \text{ and } 2$, can be attributed to the oxidation of the reducing end (RE-) Xyl unit. At this unit, oxidation can occur at C1-C2 and C2-C3 bonds, creating an aldehyde in the C3 position, whereas the C1-C2 bond is cleaved off as C₂H₄O₂ (glycolaldehyde; scheme 1) [36-38]. If a dialdehyde Xyl unit in the backbone undergoes intra-molecular cleavage at the C5-O-C1 linkage [39], an oligosaccharide containing a -O-CHOHCHO at the NRE-Xyl will be formed, which is (P_n -74) Da (scheme 1). This intra-molecular cleavage combined with the presence of dialdehydes could explain the sub-oligosaccharide cluster with P_n $\Delta -(74 + n*2)$ Da, with $n = 2, 3 \text{ and } 4$. The other oligosaccharide generated from the intra-molecular cleavage will keep -O-CHCH₂OHCHO at the RE-position, (P_n -60) Da. Thus, these results show that dialdehydes formation can be accompanied by cleavages within the oxidized sugar unit during oxidation.

For BWX, the pOx-BWX at RT for 6 h using a NaIO₄/PS ratio of 3.0 was chosen to be characterized by ESI-MS as it was about 40 % oxidized (Fig. 2B), and it comprised many molecules within the DP 2-20 range (Fig. 1B). In the *m/z* 650-1000 range this pOx-BWX comprised P_n and clusters of oxidized oligosaccharides (Fig. 3B), confirming that this pOx-BWX was partially oxidized. Notably, the ESI-MS profile of pOx-BWX was different from pOx-AX (Fig. 3A₁), confirming that periodate oxidation of structurally different pentose-based polymers indeed generates polysaccharide structure-dependent oxidized oligosaccharides.

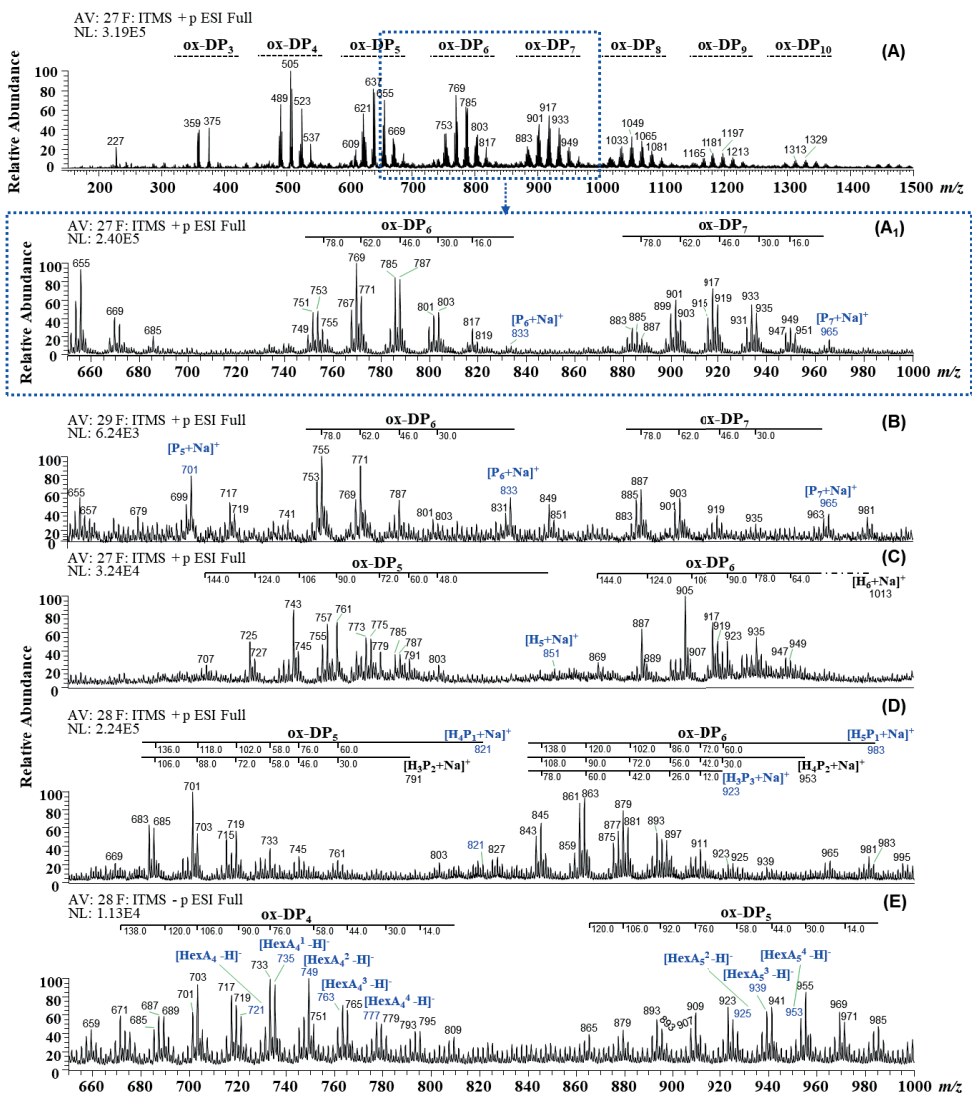
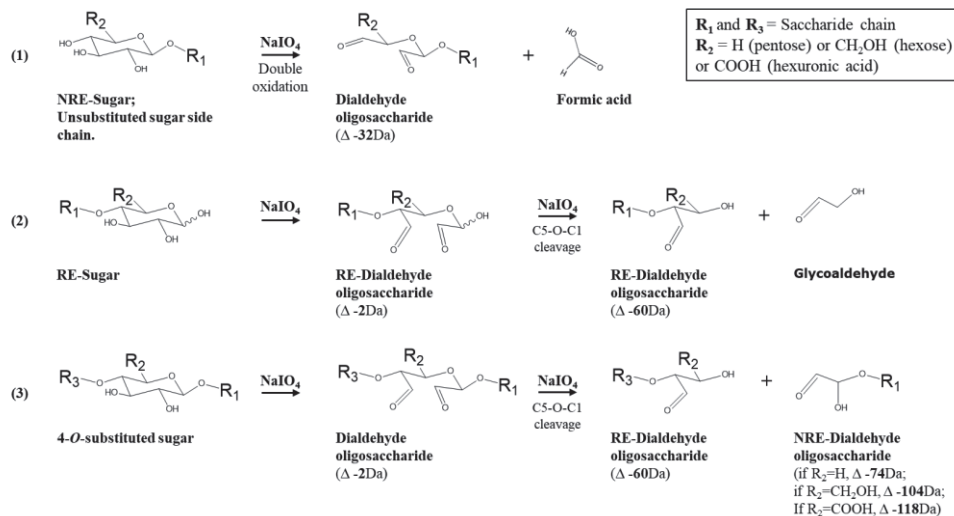


Figure 3. Positive ion mode ESI mass spectrum of the periodate-oxidized (pOx-)AX (RT, 6 h, NaIO₄/PS of 6.0) (A), and a zoom-in of the *m/z* 650-1000 range of pOx-AX (RT, 6 h, NaIO₄/PS of 6.0) (A₁), pOx-BWX (RT, 6 h, NaIO₄/PS of 3.0) (B), pOx-GM (70 °C, 24 h, NaIO₄/PS of 6.0) (C), and pOx-XG (70 °C, 24 h, NaIO₄/PS of 6.0) (D). Negative ion mode ESI mass spectrum (*m/z* 650-1000) of the pOx-HG (70 °C, 24 h, NaIO₄/PS of 12.0) (E). P_n or H_n or H_mP_n – Oligomer composed of *n* pentoses (arabinose or xylose) or *n* hexoses (Gal or Man), or *m* hexoses (Gal or Glc) and *n* pentoses (xylose). HexA_n^m – Oligomer composed of *n* GalA units and *m* methyl-esters. ox-DP_{*n*} – *m/z* region of a cluster of oxidized oligosaccharides potentially with a *n* DP. *m/z* differences from each sub-oligosaccharide cluster with Δ -(*x* + *n**2) Da, with *n* = 0 - 4, to the corresponding non-oxidized DP-oligomer are depicted in (A₁-D). In (E), *m/z* differences from each sub-oligosaccharide cluster with Δ -(*x* + *n**2) Da, with *n* = 0 - 3, are given in relation the highest oxidized *m/z* value detect within each ox-DP_{*n*} cluster. Detected non-oxidized oligomers are highlighted in blue.



Scheme 1. Schematic fragmentations that a dialdehyde sugar unit of a polysaccharide can possibly undergo during periodate (NaIO₄) oxidation. NRE, non-reducing end; RE, reducing end. Δ -#Da, Da difference relative to the corresponding non-oxidized oligosaccharide with the same DP.

ESI-MS analysis of periodate-oxidized GM, XG, and HG samples

Regarding GM, XG, and HG, a high level of oligosaccharides was only obtained at 70 °C for 24 h using a NaIO₄/PS ratio of 6.0 for GM and XG, and a NaIO₄/PS ratio of 12.0 for HG (Fig. 1). The pOx-GM, pOx-XG and pOx-HG samples obtained under these periodate oxidations also mainly comprised clusters of oxidized oligosaccharides within the *m/z* 650-1000 range (ox-DP_n, Fig. 3C, 3D, and 3E). Especially for pOx-HG, still some non-oxidized oligomers were identified, which were composed of galacturonic acid units with and without methyl-esters (Fig. 3E).

As already described for pOx-AX, the oxidized oligosaccharide clusters observed for pOx-GM, pOx-XG, and pOx-HG in Fig. 3 could also derive from the three pathways described in scheme 1, or even from a combination of it: **(1)** release of formic acid with formation of a dialdehyde (Δ -32 Da) at the NRE-sugar units (Man for GM, Glc for XG, and GalA for HG) or at the unsubstituted sugar unit present in the side chain (Gal for GM and XG, and Xyl for XG); **(2)** oxidation of the RE-sugar with formation of an aldehyde at C3 position (Δ -60 Da) and release of C1 and C2 as C₂H₄O₂; and **(3)** intramolecular cleavage of a dialdehyde sugar residue in the middle of the backbone (Man for GM, Glc for XG, and GalA for HG), resulting in two oligosaccharides. One of these oligosaccharides contains the terminal NRE-sugar and is Δ -60 Da relative to the respective non-oxidized DP-oligomer. The other oligosaccharide formed is Δ -104 Da versus the respective non-oxidized DP-oligomer of GM and XG, and Δ -118 Da relative to the respective non-oxidized and non-methyl-esterified DP-oligomer of HG.

When comparing all the ESI mass spectra (*m/z* 650-1000) in Fig. 3, it is seen that each sample had a unique MS oligosaccharide profile, being therefore PS structure-dependent. Thus, if a common condition based on periodate oxidation can be found among polysaccharides still generating the same MS oligosaccharide profiles, periodate oxidation of polysaccharides has good potential for polysaccharides fingerprinting by oligosaccharides.



3.4. ESI-MS/MS analysis of periodate-oxidized oligosaccharides

To reach a deeper understanding about the type of oxidized oligosaccharides observed in Fig. 3, and to study if their structures are solely due to the mechanisms proposed in scheme 1, tandem MS (ESI-MS/MS) was performed on the most abundant oligosaccharides of each sub-oligosaccharide cluster present in the first **ox-DP_n**-cluster. The fragmentation patterns of the oxidized oligosaccharides obtained for pOx-AX will be discussed in detail below. As the oxidized oligosaccharides of pOx-BWX, pOx-GM, pOx-XG, and pOx-HG were found by MS/MS to be formed by the mechanisms proposed for pOx-AX, their fragmentation patterns will be briefly discussed and summarized.

Oligosaccharides from pOx-AX

Based on the fragmentation spectrum of the ion m/z 769 ($[M+Na]^+$, Fig. 4A) of pOx-AX, this ion was tentatively identified as an oligosaccharide with a DP 6 comprising three pentose (Xyl) units, two dialdehyde pentose (Ara) units, and a reducing end originating fragment comprising -O-CHCH₂OHCHO. This was deduced from the presence of fragment ions differing 132 Da (anhydro-pentose), 148 Da (dialdehyde pentose), and 72 Da (Fig. 4A). Considering that this pOx-AX was fully oxidized (Fig. 2A), the Δ 132 Da fragment most likely indicates the presence of a substituted Xyl unit. The Δ 72 Da fragment shows that the C1-C2 bond of a dialdehyde Xyl at the reducing end can be cleaved off as C₂H₄O₂ [36-38], and that this Xyl unit was unsubstituted. Similar fragmentation losses were observed for the parent ion m/z 785 ($[M+Na]^+$, Fig. 4B). This ion was tentatively identified as containing two pentose (Xyl) units, two dialdehyde pentoses (Xyl and Ara; 130 Da), one hemialdal pentose (Xyl; anhydro-hemialdal 148 Da) and a reducing end originating fragment with -O-CHCH₂OHCHO (Δ 72 Da). The Δ 148 Da fragment should be derived from an hemialdal pentose instead of a pentose since no other isomer combinations fit m/z 785. Hemialdal structures upon periodate oxidation of other polysaccharides, such as GM and cellulose, have already been reported [20, 21, 23].

The m/z 753 and 803 ions (Fig. 4) of pOx-AX were tentatively characterized as containing C₂H₃O₂ and C₃H₅O₃ at the non-reducing end, respectively, in addition to pentoses, dialdehyde pentoses, and hemialdal pentoses. The C₂H₃O₂ and C₃H₅O₃ remnants indicate intra-molecular cleavage of a dialdehyde pentose and of a non-oxidized pentose, respectively, which is indicative for the presence of an unsubstituted Xyl unit. To the best of our knowledge, the intra-molecular cleavage of a non-oxidized pentose, highlighted by the presence of a fragment ion with a Δ m/z 90 (Fig. 4D), has never been reported during periodate oxidation. Hence, these results indicate that besides dialdehyde formation (the mechanisms proposed in scheme 1) and the formation of hemialdals [20, 21, 23], periodate oxidation can be accompanied by intra-molecular cleavages of non-oxidized sugar units. The oxidized sugar components identified by ESI-MS/MS are summarized in Table 2.

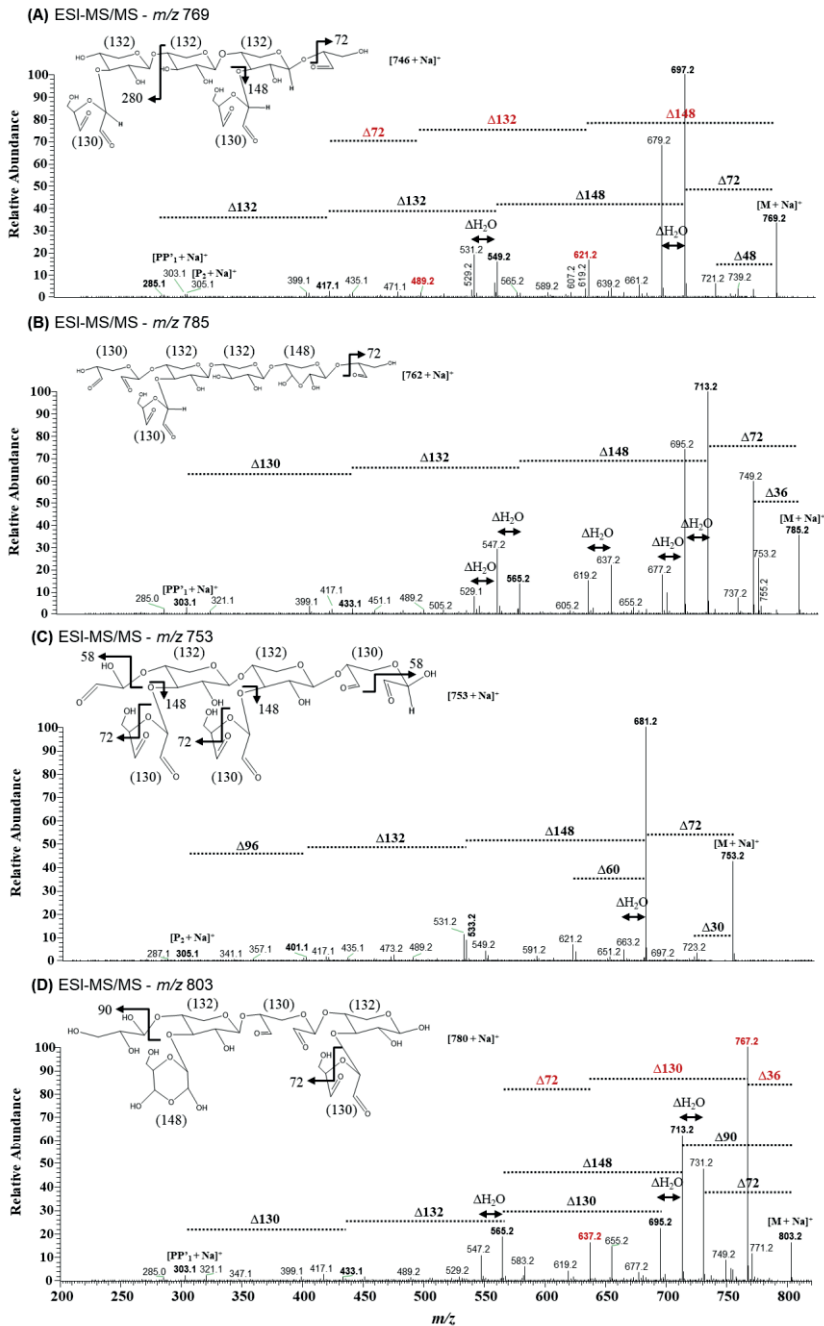


Figure 4. ESI-MS/MS spectra of $[M+Na]^+$ ions m/z 769 (A), m/z 785 (B), m/z 753 (C), and m/z 803 (D) identified in Fig. 3 for pOx-AX. Potential ion structures and respective fragmentation pathways are depicted. P_n – oligomer with n pentoses; P'_n – oligomer with n dialdehyde pentoses. Number in parentheses (#) corresponds to the molecular weight of the dehydrated sugar form. Red numbers indicate a possible second fragmentation pathway.



Although tandem MS provided insights in the structure of the released oxidized oligosaccharides and allowed us to speculate about the composition of the native AX, detailed AX characterization is difficult to achieve. This is due to the high complexity of the oxidized oligosaccharides and the impossibility to distinguish isomers by ESI-MS *via* direct infusion, which hinders precise location of the substituents along the polymer backbone and/or of the (oxidized) sugar units.

Table 2. Overview of the type of oxidized sugar units generated upon periodate oxidation of pOx-AX, pOx-BWX, pOx-GM, pOx-XG, and pOx-HG, as based on the ESI-MS/MS experiments.

	Oxidized sugar units identified				
Reaction type	pOx-AX	pOx-BWX	pOx-GM	pOx-XG	pOx-HG
Oxidation	 Ara 130/148 Xyl 130/148	 Xyl 130/148	 Man 160/178	 Glc 160/178	 GalA 174/192
Oxidation + Release of formic acid from C3					 GalA 88/106
Double oxidation			 Gal 130/148	 Xyl 100/118 Gal 130/148	
Hemialdal formation	 Ara 148/166 Xyl 148/166	 Xyl 148/166	 Gal 148/166	 Glc 178/196	
Decarboxylation					 GalA 132/150
Oxidation + -C5O-C1- cleavage	 Xyl 58/76 Xyl 72/90	 Xyl 72/90	 Man 102/120	 Xyl 58/76 Glc 102/120	
Hydrated aldehyde + -C5O-C1- cleavage				 Glc 120/138	
Intra-molecular cleavage of a non-oxidized sugar unit	 Xyl 72/90		 Man 104/122		

Name of the derived non-oxidized sugar unit is given below the depicted oxidized sugar unit. The molecular mass of the oxidized sugar unit in a non-hydrated and hydrated form (#-H₂O/#) is given under each structure, and the $\Delta m/z$ for this fragment observed in the ESI mass spectrum is highlighted in bold.



Oligosaccharides from pOx-BWX, pOx-GM, pOx-XG, and pOx-HG

ESI-MS(/MS) analysis of the oxidized oligosaccharides of pOx-BWX, pOx-GM, pOx-XG, and pOx-HG samples allowed us to identify **1)** dialdehyde sugar units; **2)** double oxidized sugar units, **3)** hemialdals; **4)** oligosaccharides containing fragments originating from dialdehyde formation followed by cleavage of the C5-O-C1 bond at both reducing and/or non-reducing sugar ends; and **5)** intramolecular cleavages of non-oxidized sugar units. Additionally, decarboxylation of the sugar units was exclusively found for pOx-HG. A summary of these oxidized sugar components identified by ESI-MS/MS for each pOx-PS sample is shown in Table 2.

Fig. 5 illustrates the presence of these oligosaccharide oxidation products in the ESI-MS² spectra of the parental ions (m/z 787 of pOx-BWX, m/z 757 of pOx-GM, m/z 683 of pOx-XG, and m/z 703 of pOx-HG) that were present in the original spectra shown in Fig. 3. ESI-MS² spectra of the other major m/z values corresponding to oxidized oligosaccharides present in the first cluster of each sample in Fig. 3 are shown in Fig. S6, S7, S8 and S9.

The tentatively assigned structures for the ions m/z 757 (Fig. 5B) and 761 (Fig. S7) of pOx-GM, and for the m/z 683 of pOx-XG (Fig. 5C) had only one modified sugar unit side chain per four (oxidized) sugar moieties in the backbone. As mentioned before, precise positioning of the substituents along the backbone and of the oxidized units in the backbone is not possible due to the presence of isomers. Nevertheless, the tentatively assigned structures suggest that debranching of GM and XG occurred during periodate oxidation at 70 °C for 24 h using a NaIO₄/PS ratio of 6.0. This can be substantiated since guar GM has a Gal:Man ratio of ~1:2 and a structure with repeating blocks typical of [α -Gal(1→6)- β -Man(1→4)- β -Man(1→4)[α -Gal(1→6)]- β -Man(1→)]_n [40, 41]. XG is made up of repeating substituted backbone units composed of X-(L/X)-(L/X)-G [42]. Therefore, although the released oligosaccharides from GM and XG (70 °C, 24 h, NaIO₄/PS ratio of 6.0), and from HG (70 °C, 24 h, NaIO₄/PS ratio of 12.0) were not diagnostic due to partial debranching and removal of non-sugar substituents, unique MS profiles could be formed per PS sample (Fig. 3). Furthermore, these oligosaccharides were indicative of the type of the PS class, showing that periodate oxidation has potential to identify PS classes based on the oxidized oligosaccharide profiles.

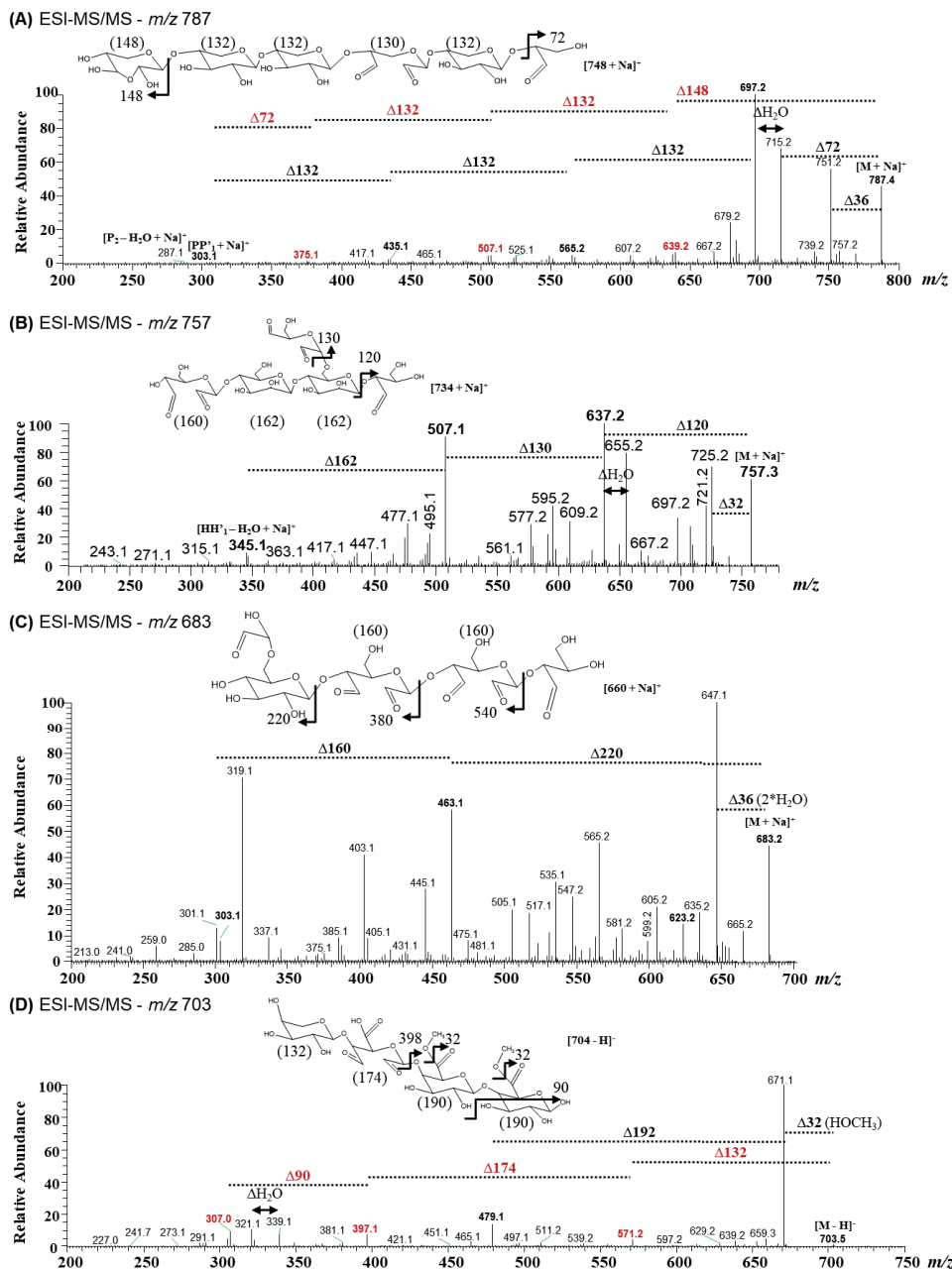


Figure 5. ESI-MS/MS spectra of $[M+Na]^+$ ions m/z 787 (A), m/z 757 (B), and m/z 683 (C) identified in Fig. 3 for pOx-BWX, pOx-GM, and pOx-XG, respectively. ESI-MS/MS spectrum of the m/z 703 $[M-H]^-$ ion (D) identified in Fig. 3 for pOx-HG. Potential ion structures and respective fragmentation pathways are depicted. P_n or H_n – oligomer with n pentoses or hexoses; P'_n or H'_n – oligomer with n dialdehyde pentoses or hexoses. Number in parentheses (#) corresponds to the molecular weight of the dehydrated sugar form. Red numbers indicate a possible second fragmentation pathway.



4. Conclusions

In this study, we demonstrated that structurally different polysaccharides require different periodate oxidation conditions to be depolymerized to oligosaccharides. ESI-MS analyses showed characteristic oligosaccharide profiles, comprising polysaccharide (PS) structure-dependent oxidized oligosaccharide clusters. The oxidized oligosaccharide clusters had highly complex structures, comprising dialdehyde sugar units and other oxidized sugar structures, such as hemialdals and decarboxylated sugars. The high structural complexity of these oligosaccharides hampered detailed characterization of the native PS structure. In addition, especially for galactomannan, xyloglucan, and homogalacturonan, the released oligosaccharides suffered from partial debranching and removal of non-sugar substituents. However, although detailed characterization of the native PS structure based on the oxidized oligosaccharides formed could not be achieved, the oligosaccharides are indicative for the native PS structure, as clearly PS structure-dependent oligosaccharides are formed. Our results are a good demonstration that a more generic chemical-induced polysaccharide depolymerization method can be developed for the recognition of polysaccharides via chemical oligosaccharide fingerprinting. In this regard, periodate oxidation could be an interesting reaction to include in such a chemical method.



References

- [1] Harris, P.J. and B.G. Smith. Plant cell walls and cell-wall polysaccharides: Structures, properties and uses in food products. *International Journal of Food Science and Technology*. **2006**, 41, 129-143.
- [2] Saha, A., S. Tyagi, R.K. Gupta, and Y.K. Tyagi. Natural gums of plant origin as edible coatings for food industry applications. *Critical Reviews in Biotechnology*. **2017**, 37, 959-973.
- [3] De Ruiter, G.A., H.A. Schols, A.G.J. Voragen, and F.M. Rombouts. Carbohydrate analysis of water-soluble uronic acid-containing polysaccharides with high-performance anion-exchange chromatography using methanolysis combined with TFA hydrolysis is superior to four other methods. *Analytical Biochemistry*. **1992**, 207, 176-185.
- [4] De Souza, A.C., T. Rietkerk, C.G.M. Selin, and P.P. Lankhorst. A robust and universal NMR method for the compositional analysis of polysaccharides. *Carbohydrate Polymers*. **2013**, 95, 657-663.
- [5] Peterson, G. Gas-chromatographic analysis of sugars and related hydroxy acids as acyclic oxime and ester trimethylsilyl derivatives. *Carbohydrate Research*. **1974**, 33, 47-61.
- [6] Ruiz-Matute, A.I., O. Hernández-Hernández, S. Rodríguez-Sánchez, M.L. Sanz, and I. Martínez-Castro. Derivatization of carbohydrates for GC and GC-MS analyses. *Journal of Chromatography B: Analytical Technologies in the Biomedical and Life Sciences*. **2011**, 879, 1226-1240.
- [7] Sims, I.M., S.M. Carnachan, T.J. Bell, and S.F.R. Hinkley. Methylation analysis of polysaccharides: Technical advice. *Carbohydrate Polymers*. **2018**, 188, 1-7.
- [8] Beaugrand, J., G. Chambat, V.W.K. Wong, F. Goubet, C. Rémond, G. Paës, S. Benamrouche, P. Debeire, M. O'Donohue, and B. Chabbert. Impact and efficiency of GH10 and GH11 thermostable endoxylanases on wheat bran and alkali-extractable arabinoxylans. *Carbohydrate Research*. **2004**, 339, 2529-2540.
- [9] Huisman, M.M.H., A. Oosterveld, and H.A. Schols. Fast determination of the degree of methyl esterification of pectins by head-space GC. *Food Hydrocolloids*. **2004**, 18, 665-668.
- [10] Bauer, S. Mass Spectrometry for Characterizing Plant Cell Wall Polysaccharides. *Frontiers in Plant Science*. **2012**, 3.
- [11] Westphal, Y., H.A. Schols, A.G.J. Voragen, and H. Gruppen. MALDI-TOF MS and CE-LIF fingerprinting of plant cell wall polysaccharide digests as a screening tool for arabidopsis cell wall mutants. *Journal of Agricultural and Food Chemistry*. **2010**, 58, 4644-4652.
- [12] Jermendi, É., M. Beukema, M.A. van den Berg, P. de Vos, and H.A. Schols. Revealing methylation patterns of pectins by enzymatic fingerprinting: Beyond the degree of blockiness. *Carbohydrate Polymers*. **2022**, 277, 118813.
- [13] Lombard, V., H. Golaconda Ramulu, E. Drula, P.M. Coutinho, and B. Henrissat. The carbohydrate-active enzymes database (CAZy) in 2013. *Nucleic Acids Research*. **2014**, 42, D490-D495.
- [14] Kristiansen, K.A., A. Potthast, and B.E. Christensen. Periodate oxidation of polysaccharides for modification of chemical and physical properties. *Carbohydrate Research*. **2010**, 345, 1264-1271.
- [15] Chemin, M., A. Rakotoveloa, F. Ham-Pichavant, G. Chollet, D. Da Silva Perez, M. Petit-Conil, H. Cramail, and S. Grelier. Periodate oxidation of 4-O-methylglucuronoxylans: Influence of the reaction conditions. *Carbohydrate Polymers*. **2016**, 142, 45-50.
- [16] Ding, W., J. Zhou, Y. Zeng, Y.N. Wang, and B. Shi. Preparation of oxidized sodium alginate with different molecular weights and its application for crosslinking collagen fiber. *Carbohydrate Polymers*. **2017**, 157, 1650-1656.
- [17] Gupta, B., M. Tummalapalli, B.L. Deopura, and M.S. Alam. Functionalization of pectin by periodate oxidation. *Carbohydrate Polymers*. **2013**, 98, 1160-1165.
- [18] Kholiya, F., J.P. Chaudhary, N. Vadodariya, and R. Meena. Synthesis of bio-based aldehyde from seaweed polysaccharide and its interaction with bovine serum albumin. *Carbohydrate Polymers*. **2016**, 150, 278-285.
- [19] Kochumalayil, J.J., Q. Zhou, W. Kasai, and L.A. Berglund. Regioselective modification of a xyloglucan hemicellulose for high-performance biopolymer barrier films. *Carbohydrate Polymers*. **2013**, 93, 466-472.
- [20] da Silva, L.M., L.F.S. Araújo, R.C. Alvez, L. Ono, D.A.T. Sá, P.L.R. da Cunha, R.C. Monteiro de Paula, and J.S. Maciel. Promising alternative gum: Extraction, characterization, and oxidation of the galactomannan of *Cassia fistula*. *International Journal of Biological Macromolecules*. **2020**, 165, 436-444.
- [21] Sirviö, J.A., H. Liimatainen, M. Visanko, and J. Niinimäki. Optimization of dicarboxylic acid cellulose synthesis: Reaction stoichiometry and role of hypochlorite scavengers. *Carbohydrate Polymers*. **2014**, 114, 73-77.
- [22] Spedding, H. 628. Infrared spectra of periodate-oxidised cellulose. *Journal of the Chemical Society (Resumed)*. **1960**, 3147-3152.
- [23] Nypelö, T., B. Berke, S. Spirk, and J.A. Sirviö. Review: Periodate oxidation of wood polysaccharides—Modulation of hierarchies. *Carbohydrate Polymers*. **2021**, 252, 117105.



- [24] Aspinall, G.O. and K.M. Ross. The degradation of two periodate-oxidised arabinoxylans. *Journal of the Chemical Society (Resumed)*. **1963**, 1676-1680.
- [25] Åman, P. and S. Bengtsson. Periodate oxidation and degradation studies on the major water-soluble arabinoxylan in rye grain. *Carbohydrate Polymers*. **1991**, 15, 405-414.
- [26] Pandeirada, C.O., D.W.H. Merx, H.-G. Janssen, Y. Westphal, and H.A. Schols. TEMPO/NaClO₂/NaOCl oxidation of arabinoxylans. *Carbohydrate Polymers*. **2021**, 259, 117781.
- [27] Blumenkrantz, N. and G. Asboe-Hansen. New method for quantitative determination of uronic acids. *Analytical Biochemistry*. **1973**, 54, 484-489.
- [28] Thibault, J. and T. JF. Automatisation du dosage des substances pectiques par la méthode au méthahydroxydiphényl. **1979**.
- [29] Deckers, H.A., C. Olieman, F.M. Rombouts, and W. Pilnik. Calibration and application of high-performance size exclusion columns for molecular weight distribution of pectins. *Carbohydrate Polymers*. **1986**, 6, 361-378.
- [30] Chetouani, A., N. Follain, S. Marais, C. Rihouey, M. Elkolli, M. Bounekhel, D. Benachour, and D. Le Cerf. Physicochemical properties and biological activities of novel blend films using oxidized pectin/chitosan. *International Journal of Biological Macromolecules*. **2017**, 97, 348-356.
- [31] Sirvio, J., U. Hyvakkko, H. Liimatainen, J. Niinimäki, and O. Hormi. Periodate oxidation of cellulose at elevated temperatures using metal salts as cellulose activators. *Carbohydrate Polymers*. **2011**, 83, 1293-1297.
- [32] Izydorczyk, M.S. and C.G. Biliaderis. Cereal arabinoxylans: advances in structure and physicochemical properties. *Carbohydrate Polymers*. **1995**, 28, 33-48.
- [33] Gupta, D.S., B. Jann, K.S. Bajpai, and S.C. Sharma. Structure of a galactomannan from *Cassia alata* seed. *Carbohydrate Research*. **1987**, 162, 271-276.
- [34] Kochumalayil, J.J., S. Morimune, T. Nishino, O. Ikkala, A. Walther, and L.A. Berglund. Nacre-mimetic clay/xyloglucan bionanocomposites: A chemical modification route for hygro-mechanical performance at high humidity. *Biomacromolecules*. **2013**, 14, 3842-3849.
- [35] Halsall, T.G., E.L. Hirst, and J.K.N. Jones. Oxidation of carbohydrates by the periodate ion. *Journal of the Chemical Society (Resumed)*. **1947**, 1427-1432.
- [36] Pereira, I., J. Simões, D.V. Evtyugin, S. Rouif, M.A. Coimbra, M.R.M. Domingues, and M. Gama. Effects of gamma irradiation and periodate oxidation on the structure of dextrin assessed by mass spectrometry. *European Polymer Journal*. **2018**, 103, 158-169.
- [37] Perlin, A.S. Glycol-Cleavage Oxidation. *Advances in Carbohydrate Chemistry and Biochemistry*. **2006**, 60, 183-250.
- [38] Hough, L., T.J. Taylor, G.H.S. Thomas, and B.M. Woods. 239. The oxidation of monosaccharides by periodate with reference to the formation of intermediary esters. *Journal of the Chemical Society (Resumed)*. **1958**, 1212-1217.
- [39] Simões, J., A.S.P. Moreira, E. da Costa, D. Evtyugin, P. Domingues, F.M. Nunes, M.A. Coimbra, and M.R.M. Domingues. Oxidation of amylose and amylopectin by hydroxyl radicals assessed by electrospray ionisation mass spectrometry. *Carbohydrate Polymers*. **2016**, 148, 290-299.
- [40] Daas, P.J.H., H.A. Schols, and H.H.J. de Jongh. On the galactosyl distribution of commercial galactomannans. *Carbohydrate Research*. **2000**, 329, 609-619.
- [41] Prajapati, V.D., G.K. Jani, N.G. Moradiya, N.P. Randeria, B.J. Nagar, N.N. Naikwadi, and B.C. Variya. Galactomannan: A versatile biodegradable seed polysaccharide. *International Journal of Biological Macromolecules*. **2013**, 60, 83-92.
- [42] Mishra, A. and A.V. Malhotra. Tamarind xyloglucan: A polysaccharide with versatile application potential. *Journal of Materials Chemistry*. **2009**, 19, 8528-8536.



Supplementary data

Effect of periodate oxidation on the Mw distribution of polysaccharides

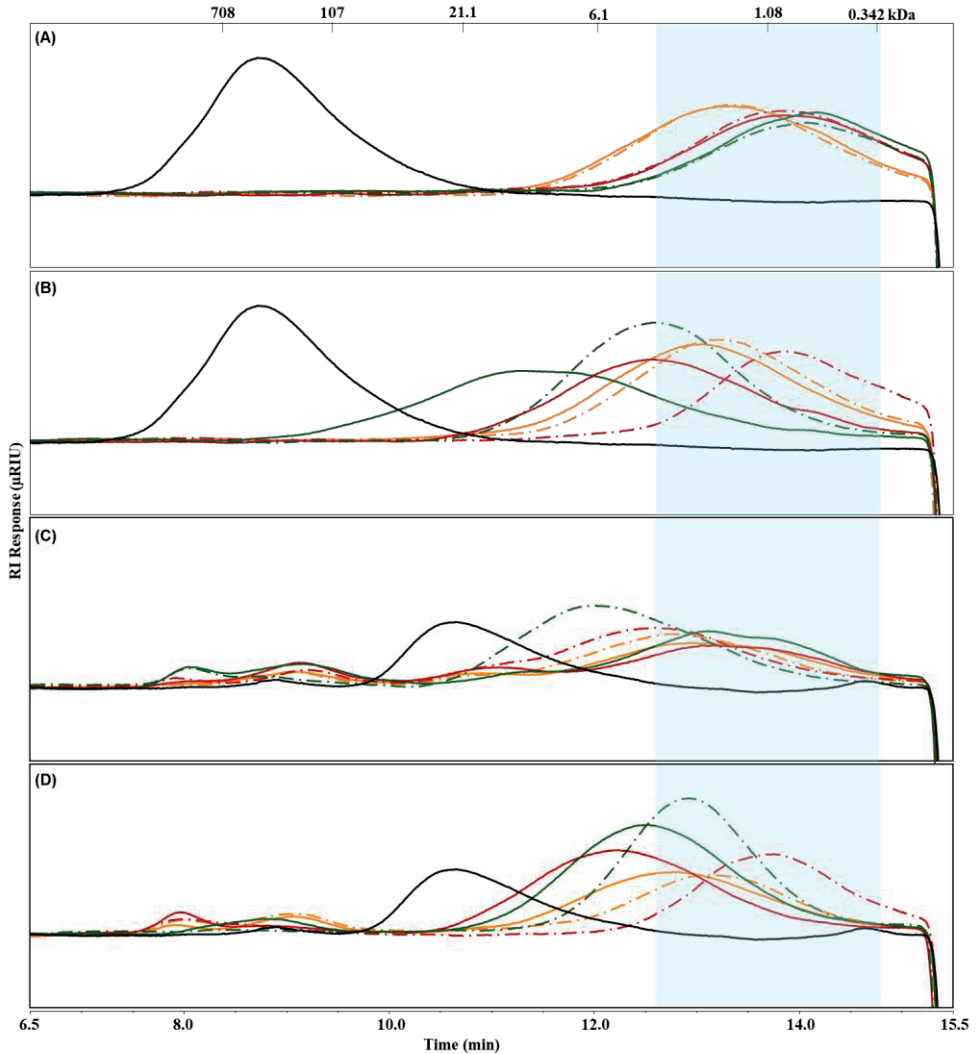


Figure S 1. HPSEC elution patterns of the periodate-oxidized AX samples at room temperature (A) and 70 °C (B), and of the periodate-oxidized BWX samples at RT (C) and 70 °C (D). Native AX and BWX are shown in black lines, and periodate-oxidized samples with 3.0, 6.0 and 12.0 NaIO₄/PS are shown in orange, red, and green lines, respectively. (—) 6 h reaction; (---) 24 h reaction. Pullulan standards were used to calibrate the system. Blue boxes indicate the time range corresponding to an apparent degree of polymerization between 2 and 20.

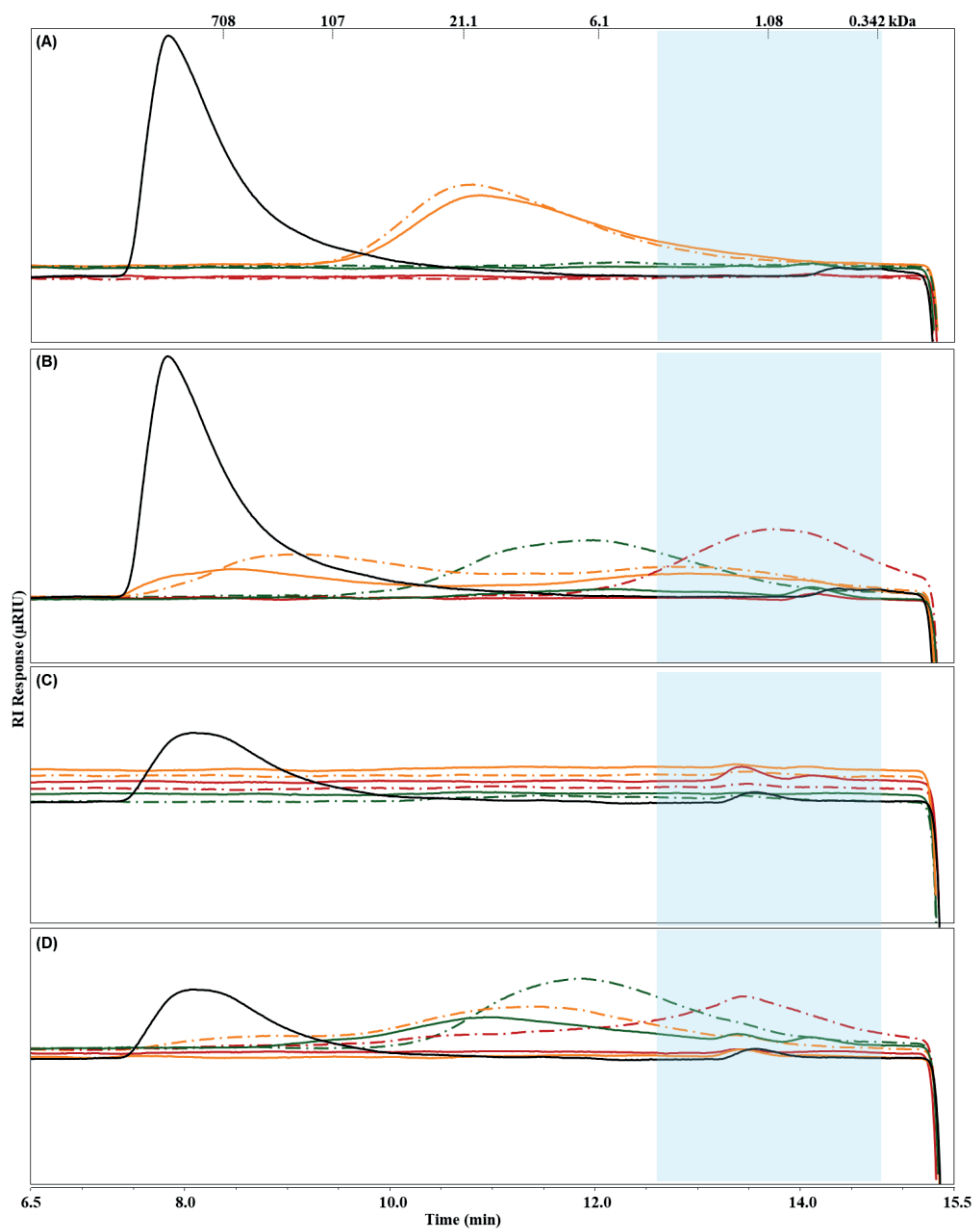


Figure S 2. HPSEC elution patterns of the periodate-oxidized GM samples at room temperature (A) and 70 °C (B), and of the periodate-oxidized XG samples at RT (C) and 70 °C (D). Native GM and XG are shown in black lines, and periodate-oxidized samples with 3.0, 6.0 and 12.0 NaIO₄/PS are shown in orange, red, and green lines, respectively. (—) 6 h reaction; (- · - · - · -) 24 h reaction. Pullulan standards were used to calibrate the system. Blue boxes indicate the time range corresponding to an apparent degree of polymerization between 2 and 20.

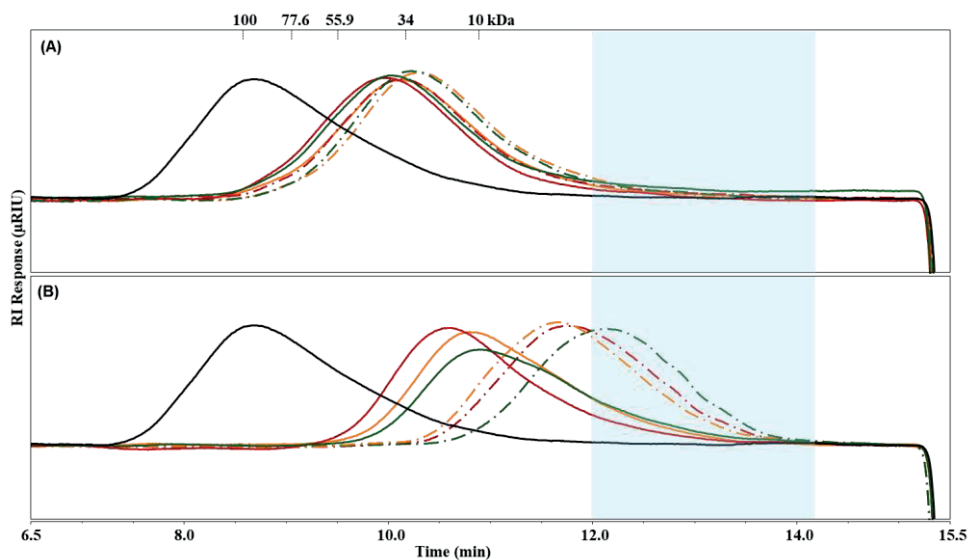


Figure S 3. HPSEC elution patterns of the periodate-oxidized HG samples at room temperature (A) and 70 °C (B). Native HG is shown in black lines, and periodate-oxidized samples with 3.0, 6.0 and 12.0 NaIO₄/PS are shown in orange, red, and green lines, respectively. (—) 6 h reaction; (---) 24 h reaction. Pectin standards were used to calibrate the system. Blue boxes indicate the time range corresponding to an apparent degree of polymerization between 2 and 20.



Yield, sugar recovery and degrees of oxidation (DO) of periodate-oxidized samples

Table S 1. Yield, sugar recovery yield, and degree of oxidation (DO) of the periodate-oxidized (pOx-)polysaccharide samples derived from various periodate oxidation conditions (room temperature (RT) and 70°C; 6 and 24 h; 3.0, 6.0 and 12.0 $\mu\text{mol NaIO}_4$ / mg polysaccharide) tested on AX, BWX, GM, XG, and HG samples.

Sample	Yield (%, w/w) ^a	Relative Sugar Recovery (%, w/w) ^b	DO ^c (DO _{rel}) ^d	Sample	Yield (%, w/w) ^a	Relative Sugar Recovery (%, w/w) ^b	DO ^c (DO _{rel}) ^d
AX	100	100.0	0 (77)	BWX	100	100.0	0 (93)
pOx-AX, RT, 6h,	61.5	38.0 ± 0.8	62 ± 1	pOx-BWX, RT, 6h,	71.0	59.4 ± 0.9	40 ± 1
3.0 NaIO ₄			(81 ± 1) ^d	3.0 NaIO ₄			(43 ± 1) ^d
pOx-AX, RT, 24h,	57.7	32.1 ± 0.7	68 ± 1	pOx-BWX, RT, 24h,	76.2	67.1 ± 3.4	33 ± 3
3.0 NaIO ₄			(88 ± 1) ^d	3.0 NaIO ₄			(35 ± 3) ^d
pOx-AX, RT, 6h,	47.2	20.5 ± 0.0	79 ± 0	pOx-BWX, RT, 6h,	71.0	58.9 ± 0.5	41 ± 1
6.0 NaIO ₄			(103 ± 0) ^d	6.0 NaIO ₄			(44 ± 1) ^d
pOx-AX, RT, 24h,	45.2	13.2 ± 0.1	87 ± 0	pOx-BWX, RT, 24h,	71.2	44.3 ± 0.1	56 ± 0
6.0 NaIO ₄			(113 ± 0) ^d	6.0 NaIO ₄			(60 ± 0) ^d
pOx-AX, RT, 6h,	45.9	10.7 ± 0.5	89 ± 0	pOx-BWX, RT, 6h,	63.9	42.2 ± 0.6	58 ± 1
12.0 NaIO ₄			(116 ± 0) ^d	12.0 NaIO ₄			(62 ± 1) ^d
pOx-AX, RT, 24h,	43.7	9.7 ± 0.3	90 ± 0	pOx-BWX, RT, 24h,	86.6	16.3 ± 6.1	84 ± 6
12.0 NaIO ₄			(117 ± 0) ^d	12.0 NaIO ₄			(90 ± 6) ^d
pOx-AX, 70°C,	56.6	37.9 ± 0.3	62 ± 0	pOx-BWX, 70°C, 6h,	73.3	75.2 ± 3.0	25 ± 3
6h, 3.0 NaIO ₄			(81 ± 0) ^d	3.0 NaIO ₄			(27 ± 3) ^d
pOx-AX, 70°C,	47.4	28.7 ± 0.7	71 ± 1	pOx-BWX, 70°C,	49.4	38.4 ± 2.9	62 ± 3
24h, 3.0 NaIO ₄			(92 ± 1) ^d	24h, 3.0 NaIO ₄			(67 ± 3) ^d
pOx-AX, 70°C,	80.0	23.9 ± 1.8	76 ± 2	pOx-BWX, 70°C, 6h,	77.0	28.8 ± 1.1	71 ± 1
6h, 6.0 NaIO ₄			(99 ± 3) ^d	6.0 NaIO ₄			(76 ± 1) ^d
pOx-AX, 70°C,	21.6	5.9 ± 0.0	94 ± 0	pOx-BWX, 70°C,	23.0	12.3 ± 0.2	88 ± 0
24h, 6.0 NaIO ₄			(122 ± 0) ^d	24h, 6.0 NaIO ₄			(95 ± 0) ^d
pOx-AX, 70°C,	91.4	18.9 ± 1.0	81 ± 1	pOx-BWX, 70°C, 6h,	68.3	16.4 ± 0.5	84 ± 1
6h, 12.0 NaIO ₄			(105 ± 1) ^d	12.0 NaIO ₄			(90 ± 1) ^d
pOx-AX, 70°C,	72.8	12.5 ± 0.6	88 ± 1	pOx-BWX, 70°C,	45.6	2.4 ± 0.0	98 ± 0
24h, 12.0 NaIO ₄			(114 ± 1) ^d	24h, 12.0 NaIO ₄			(105 ± 0) ^d



Table S 1. Continuation.

Sample	Yield (%, w/w) ^a	Relative Sugar Recovery (%, w/w) ^b	DO ^c (DO _{rel}) ^d	Sample	Yield (%, w/w) ^a	Relative Sugar Recovery (%, w/w) ^b	DO ^c (DO _{rel}) ^d
GM	100	100.0	0 (100)	XG	100.0	100.0	0 (90)
pOx-GM, RT, 6h, 3.0 NaIO ₄	65.9	22.2 ± 0.8	78 ± 1 ^d	pOx-XG, RT, 6h, 3.0 NaIO ₄	86.1	59.8 ± 6.5	41 ± 6 (46 ± 7) ^d
pOx-GM, RT, 24h, 3.0 NaIO ₄	86.2	31.0 ± 1.6	69 ± 2 ^d	pOx-XG, RT, 24h, 3.0 NaIO ₄	81.9	59.3 ± 5.7	42 ± 6 (47 ± 7) ^d
pOx-GM, RT, 6h, 6.0 NaIO ₄	86.6	5.3 ± 0.0	95 ± 0 ^d	pOx-XG, RT, 6h, 6.0 NaIO ₄	83.7	34.4 ± 2.2	68 ± 2 (76 ± 2) ^d
pOx-GM, RT, 24h, 6.0 NaIO ₄	85.1	5.8 ± 0.3	94 ± 0 ^d	pOx-XG, RT, 24h, 6.0 NaIO ₄	84.9	32.5 ± 0.2	70 ± 0 (78 ± 0) ^d
pOx-GM, RT, 6h, 12.0 NaIO ₄	82.7	0.0 ± 0.0	100 ± 0 ^d	pOx-XG, RT, 6h, 12.0 NaIO ₄	81.8	17.4 ± 5.3	84 ± 5 (93 ± 6) ^d
pOx-GM, RT, 24h, 12.0 NaIO ₄	86.2	0.0 ± 0.0	100 ± 0 ^d	pOx-XG, RT, 24h, 12.0 NaIO ₄	83.8	9.6 ± 2.9	91 ± 3 (101 ± 3) ^d
pOx-GM, 70°C, 6h, 3.0 NaIO ₄	81.0	27.5 ± 0.2	73 ± 0 ^d	pOx-XG, 70°C, 6h, 3.0 NaIO ₄	88.4	48.6 ± 14.9	53 ± 15 (59 ± 17) ^d
pOx-GM, 70°C, 24h, 3.0 NaIO ₄	73.6	20.9 ± 3.8	79 ± 4 ^d	pOx-XG, 70°C, 24h, 3.0 NaIO ₄	67.2	34.7 ± 9.1	66 ± 9 (73 ± 10) ^d
pOx-GM, 70°C, 6h, 6.0 NaIO ₄	81.2	4.8 ± 0.4	95 ± 0 ^d	pOx-XG, 70°C, 6h, 6.0 NaIO ₄	85.3	29.6 ± 1.2	72 ± 1 (80 ± 1) ^d
pOx-GM, 70°C, 24h, 6.0 NaIO ₄	45.0	5.5 ± 0.5	95 ± 0 ^d	pOx-XG, 70°C, 24h, 6.0 NaIO ₄	43.6	12.9 ± 0.9	88 ± 1 (98 ± 1) ^d
pOx-GM, 70°C, 6h, 12.0 NaIO ₄	84.1	3.1 ± 0.4	97 ± 0 ^d	pOx-XG, 70°C, 6h, 12.0 NaIO ₄	84.9	10.6 ± 1.1	90 ± 1 (100 ± 1) ^d
pOx-GM, 70°C, 24h, 12.0 NaIO ₄	80.0	3.5 ± 0.2	97 ± 0 ^d	pOx-XG, 70°C, 24h, 12.0 NaIO ₄	76.9	5.4 ± 0.4	95 ± 0 (106 ± 0) ^d



Table S 1. Continuation.

Sample	Yield (%, w/w) ^a	Relative Sugar Recovery (% w/w) ^b	DO ^c (DO _{rel}) ^d
HG	100	100.0*	0 (100)
pOx-HG, RT, 6h, 3.0 NaIO ₄	93.4	47.1 ± 0.9*	53 ± 1 ^d
pOx-HG, RT, 24h, 3.0 NaIO ₄	88.6	40.4 ± 1.1*	60 ± 1 ^d
pOx-HG, RT, 6h, 6.0 NaIO ₄	93.2	38.6 ± 0.4*	61 ± 0 ^d
pOx-HG, RT, 24h, 6.0 NaIO ₄	84.5	33.1 ± 0.3*	67 ± 0 ^d
pOx-HG, RT, 6h, 12.0 NaIO ₄	90.1	33.0 ± 1.9*	67 ± 2 ^d
pOx-HG, RT, 24h, 12.0 NaIO ₄	93.5	30.8 ± 0.1*	69 ± 0 ^d
pOx-HG, 70°C, 6h, 3.0 NaIO ₄	89.2	35.7 ± 0.2*	64 ± 0 ^d
pOx-HG, 70°C, 24h, 3.0 NaIO ₄	79.8	37.9 ± 0.6*	62 ± 1 ^d
pOx-HG, 70°C, 6h, 6.0 NaIO ₄	89.0	26.4 ± 0.5*	74 ± 1 ^d
pOx-HG, 70°C, 24h, 6.0 NaIO ₄	70.0	20.8 ± 0.0*	79 ± 0 ^d
pOx-HG, 70°C, 6h, 12.0 NaIO ₄	86.9	20.7 ± 0.0*	79 ± 0 ^d
pOx-HG, 70°C, 24h, 12.0 NaIO ₄	52.9	10.8 ± 0.2*	89 ± 0 ^d
NaIO ₄			

^a Yield in weight % relative to the native polysaccharide (PS) sample.

^b Relative sugar recovery relatively to the total sugar content of the native polysaccharide, expressed as average (n=2) weight %. * Relative sugar recovery relatively to the total UA content of the native polysaccharide, expressed as average (n=2) weight %.

^c DO based on the sugar recovery decrease or UA recovery decrease (for HG) relative the respective native PS samples. (#) is the maximum DO that can theoretically (DO_{Theo}) be obtained per polysaccharide.

^d Relative degree of oxidation (DO_{rel}) in % was calculated as follows:

$$DO_{Rel} (\%, w/w) = \frac{DO}{DO_{Theo}} \times 100$$



Methyl content and relative recovery of pOx-HG

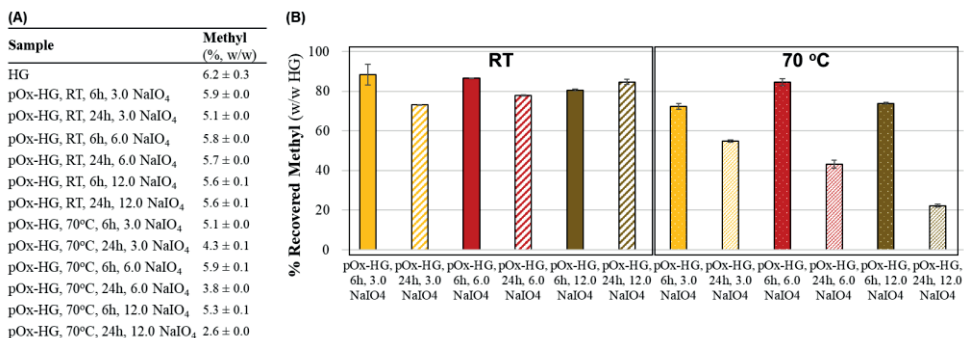


Figure S 4. Methyl-ester content (% w/w) (A) and relative methyl-ester recovery (B) of the periodate-oxidized (pOx-) homogalacturonan (HG) samples relatively to the native HG.

Variable levels of dialdehydes present in oxidized oligosaccharides

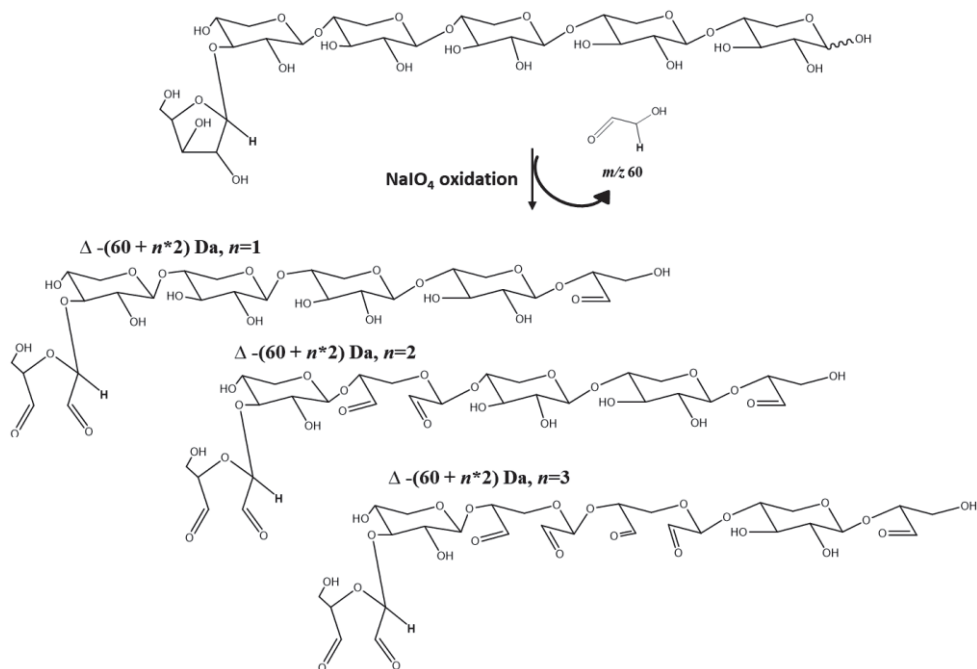


Figure S 5. Example of the sub-oligosaccharide cluster that is $\Delta-(60 + n \cdot 2)$ Da, with $n = 1, 2,$ and 3 , relative to the corresponding non-oxidized oligomer composed of six pentoses (DP=6). n indicates the level of dialdehydes present.



Oligosaccharides characterization by ESI-MS/MS

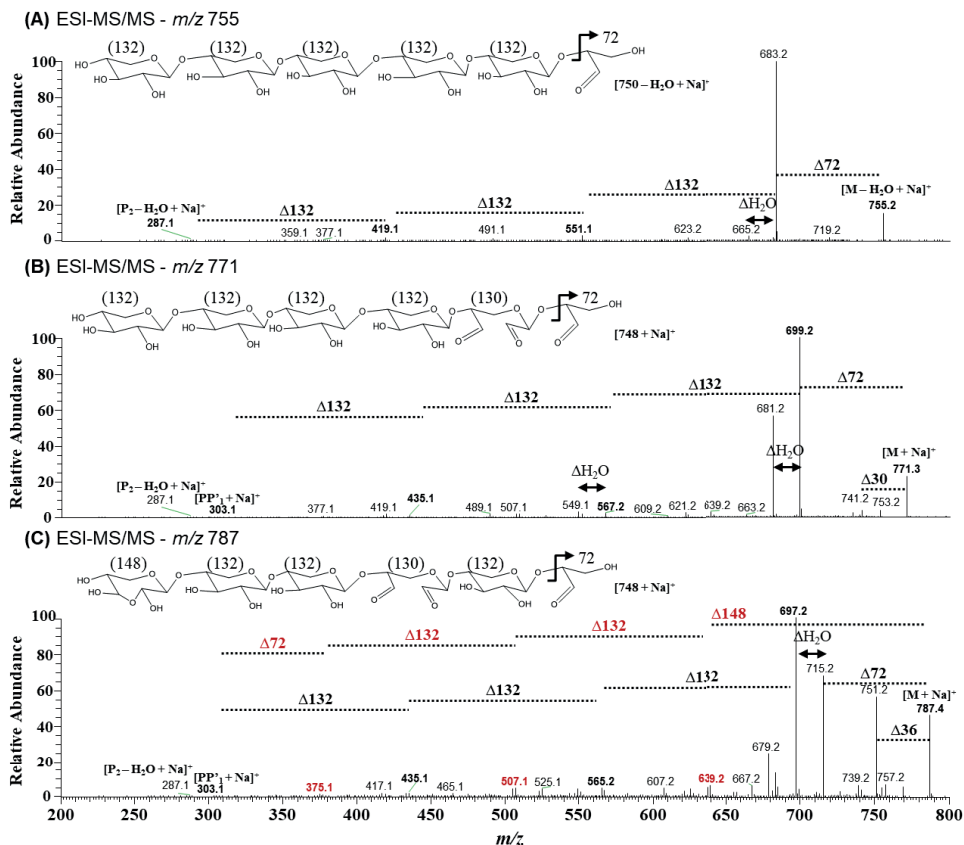


Figure S 6. ESI-MS/MS spectra of the m/z 755 (A), m/z 771 (B) and m/z 787 (C) ions identified in BWX after 6 h oxidation at RT using 3.0 $\mu\text{mol NaIO}_4$ / mg BWX. Potential ion structures and respective fragmentation pathways are depicted. P_n – oligomer with n pentoses; P_n^* – oligomer with n dialdehyde pentoses. Number in parentheses (#) corresponds to the molecular weight of the dehydrated sugar form. Red numbers indicate a possible second fragmentation pathway.

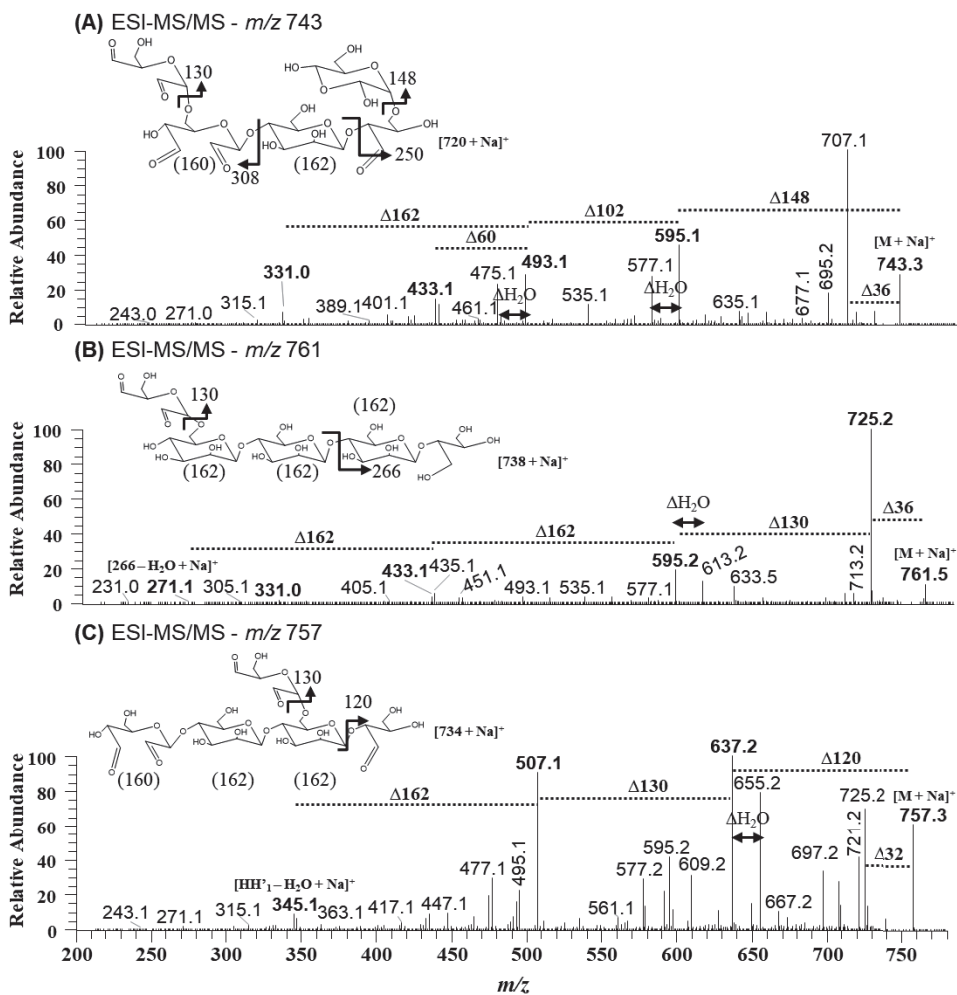


Figure S 7. ESI-MS/MS spectra of the m/z 743 (A), m/z 761 (B) and m/z 757 (C) ions identified in GM after 24 h oxidation at 70 °C using 6.0 $\mu\text{mol NaIO}_4$ / mg GM. Potential ion structures and respective fragmentation pathways are depicted. **H** – hexose; **H'** – dialdehyde hexose. Number in parentheses (#) corresponds to the molecular weight of the dehydrated sugar form.

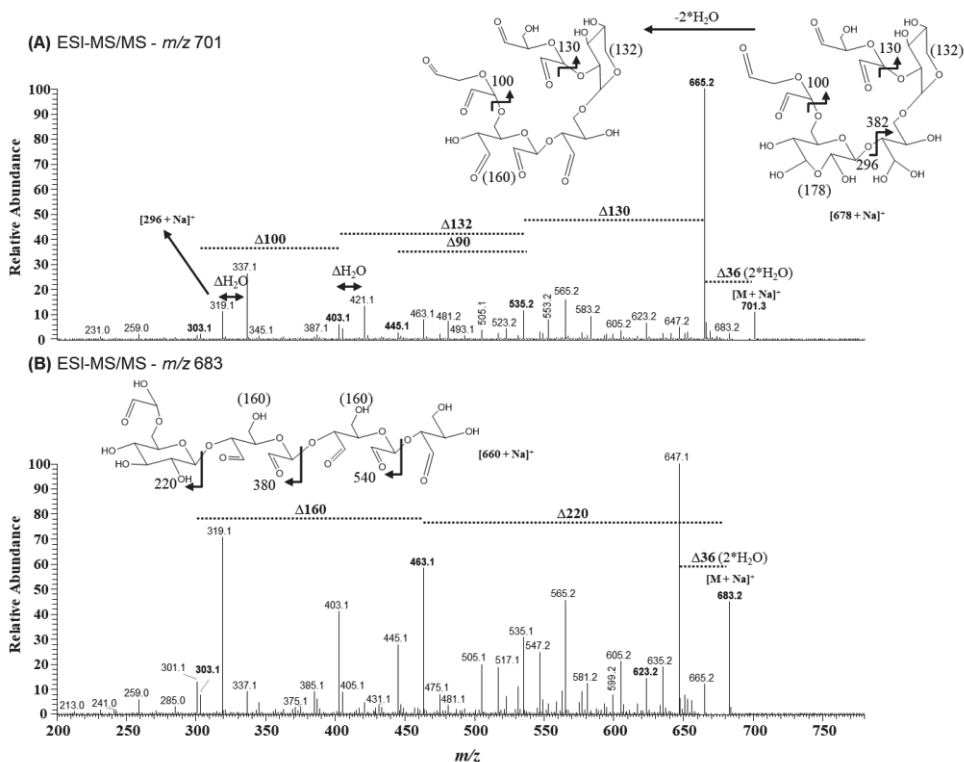


Figure S 8. ESI-MS/MS spectra of the m/z 701 (A) and m/z 683 (B) ions identified in XG after 24 h oxidation at 70 °C using 6.0 $\mu\text{mol NaIO}_4$ / mg XG. Potential ion structures and respective fragmentation pathways are depicted. Number in parentheses (#) corresponds to the molecular weight of the dehydrated sugar form.

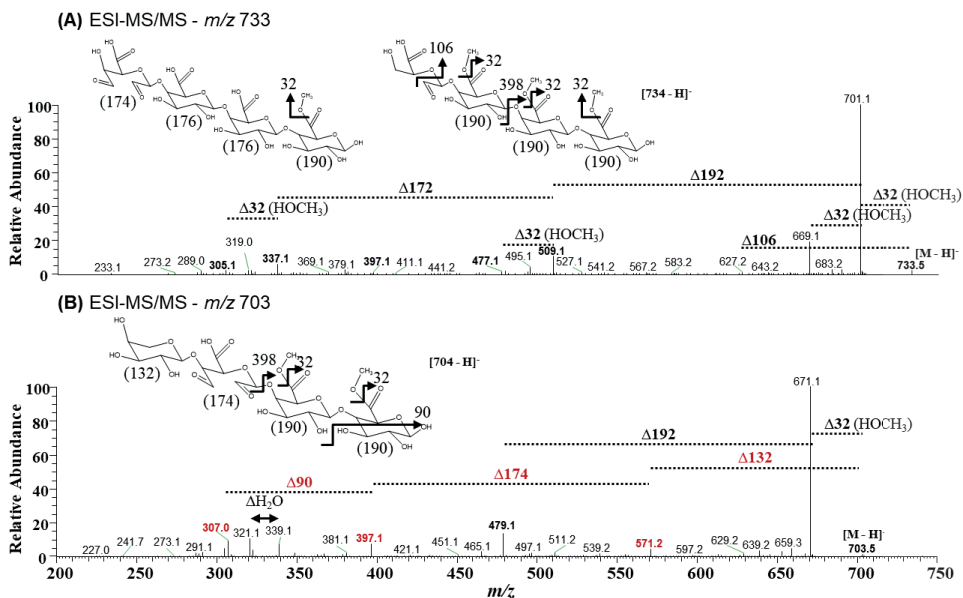


Figure S 9. ESI-MS/MS spectra of the m/z 733 (A) and m/z 703 (B) ions identified in HG after 24 h oxidation at 70 °C using 12.0 $\mu\text{mol NaIO}_4$ / mg HG. Potential ion structures and respective fragmentation pathways are depicted. Number in parentheses (#) corresponds to the molecular weight of the dehydrated sugar form. Red numbers indicate a possible second fragmentation pathway.

Chapter 5

Recognition of plant polysaccharides through MALDI-TOF MS fingerprinting after periodate oxidation and thermal depolymerization

Submitted for publication as: Recognition of plant polysaccharides by MALDI-TOF MS fingerprinting after periodate oxidation and thermal hydrolysis. Carolina O. Pandeirada, Jos A. Hageman, Hans-Gerd Janssen, Yvonne Westphal, and Henk A. Schols.



Abstract

An autoclave treatment at 121 °C on periodate-oxidized plant polysaccharides and mixes thereof was investigated for the release of oligosaccharides to obtain a generic polysaccharide depolymerization method for polysaccharides fingerprinting. Matrix-Assisted Laser Desorption Ionization Time-Of-Flight Mass Spectrometry (MALDI-TOF MS) analysis of the oligosaccharides released showed that polysaccharide structure-dependent oligosaccharide profiles were obtained, even for the same type of polysaccharide derived from different sources and/or having different fine structures (e.g. class of (arabino)xylans, galactomannans, glucans, or pectic materials). Various polysaccharide classes present in a polysaccharide mix could be identified based on significantly different ($p < 0.05$) marker m/z values present in the mass spectrum. Principal component analysis and hierarchical cluster analysis of the obtained MALDI-TOF MS data highlighted the structural heterogeneity of the polysaccharides studied, and clustered polysaccharide samples with resembling oligosaccharide profiles. Our approach represents a step further towards a generic and accessible recognition of plant polysaccharides individually or in a mixture.



1. Introduction

Although plant polysaccharides are the most abundant biomacromolecules found in nature and are frequently used in foods [1, 2], polysaccharide analysis remains slow and laborious. Most approaches currently used to characterize and identify polysaccharides are based on the enzymatic digestion of polysaccharides into structure-informative (diagnostic) oligosaccharides, followed by analysis of the released oligosaccharides [3-5]. Such an approach makes use of for example liquid chromatography coupled to mass spectrometry (LC-MS) [5] and Matrix-Assisted Laser Desorption Ionization Time-Of-Flight Mass Spectrometry (MALDI-TOF MS) to distinguish polysaccharide samples based on their oligosaccharide profiles [3, 6, 7]. Even though enzymatic digestion of polysaccharides is a powerful strategy to obtain diagnostic oligosaccharides, there is not a universal enzyme (mixture) able to release oligosaccharides from all polysaccharides, since enzymes are polysaccharide structure-specific [8]. Additionally, enzymatic digestion of polysaccharides composed of isomeric sugar units results in oligosaccharides with isomeric structures, which cannot easily be distinguished by MS [9, 10].

Periodate (IO_4^-) oxidation is a potential alternative approach for generating oligosaccharides and overcoming some of the enzymatic digestion limitations. Periodate oxidation of polysaccharides leads to specific oxidation of free vicinal diols to aldehydes with cleavage of the carbon chain [11]. In aqueous systems, the aldehyde groups of periodate-oxidized polysaccharides can also be present in masked forms (e.g. as hydrates, hemiacetals and hemialdals) [12]. An attractive feature of periodate oxidation of polysaccharides is that it can also lead to polysaccharide depolymerization, which allows the formation of oligosaccharides. Recently, we demonstrated by using electrospray ionization (ESI-)MS that periodate oxidation of plant polysaccharides releases oligosaccharides that are polysaccharide structure-dependent [13]. These oligosaccharides comprised dialdehyde, hemialdal, and hydrated aldehyde structural components, forming highly complex, and highly informative, periodate-oxidized oligosaccharide structures. Unfortunately, it was shown that the optimum conditions for periodate oxidation of plant polysaccharides into oligosaccharides differ per polysaccharide structure [13]. This prevented to have a single approach to release oligosaccharides from polysaccharides. A possible solution to reach a polysaccharide depolymerization method based on periodate oxidation that is common to a broad range of polysaccharides could be the inclusion of a subsequent thermal depolymerization treatment. Veelaert et al. [14] observed an extensive decrease in the molecular weight of a periodate-oxidized starch upon heating (90 °C) in acidic (pH 3 and 5) and neutral conditions. This indicates that subjecting periodate-oxidized polysaccharides to a thermal treatment in an aqueous solution might yield sufficient levels of oligosaccharides that are polysaccharide structure-dependent due to the high specificity of IO_4^- to oxidize vicinal diols [15].

In this study, we investigate the use of a thermal treatment to depolymerize periodate-oxidized plant polysaccharides into oligosaccharides in a more generic manner than by using enzymes. The thermally depolymerized periodate-oxidized polysaccharides were analyzed by MALDI-TOF MS for polysaccharides fingerprinting based on the MS oligosaccharide profiles. Additionally, MALDI-TOF MS data was subjected to principal component analysis (PCA) and hierarchical cluster analysis (HCA) as complementary techniques to substantiate variations among samples and to cluster polysaccharide samples based on the oligosaccharide profiles.



2. Materials and methods

2.1. Materials

Birch wood xylan (BWX) and microcrystalline cellulose (Cel) were obtained from Sigma (Darmstadt, Germany). Wheat flour arabinoxylan (WAX; Ara:Xyl=38:62, purity > 95 %, medium viscosity), rye flour arabinoxylan (RAX; Ara:Xyl=38:62, purity ~ 90 %), barley mixed-linked β -glucan (MLG; purity ~ 95 %, low viscosity), potato rhamnogalacturonan type I (RG-I; Purity > 90 %; GalA:Rha:Ara:Xyl:Gal:Other sugars (%) = 61.0: 6.2: 2.5: 0.5: 23.1: 6.7), and sugar beet arabinan (ABN; purity ~ 95 %; Ara:Gal:Rha:GalA:Other sugars (%) = 69:18.7:1.4:10.2:0.7) were obtained from Megazyme (Wicklow, Ireland). Guar galactomannan (GGM, Man:Gal=2:1) was from BFGoodrich Diamalt GmbH (Munich, Germany), locust bean galactomannan (LBGM, Man:Gal=4:1) from Unipektin (Eschenz, Switzerland), tamarind seed xyloglucan (XG; Gal:Glc:Xyl (%) = 7.9:58.9:33.1 (Table S1)) from Dainippon Sumitomo Pharma Co. Ltd., (Osaka, Japan), and lemon pectin (homogalacturonan - HG with a high degree of methyl-esterification) was from Copenhagen Pectin A/S (Lille Skensved, Denmark). Wheat starch (WS) was obtained from Fluka (Buchs, Switzerland). Sodium metaperiodate (NaIO_4 , 98 %) was purchased from Alfa Aesar (Thermo Fisher, Kandel, Germany). Ethylene glycol was from Merck (Darmstadt, Germany). LC-MS water was of UHPLC-grade (Biosolve, Valkenswaard, The Netherlands). 2,5-dihydroxybenzoic acid (DHB) was from Bruker Daltonics (Bremen, Germany). All water was purified in a Milli-Q system from Millipore (Molsheim, France), unless otherwise mentioned.

2.2. Periodate oxidation of polysaccharides

Various arabinoxylan (AX):glucan mixes composed of WAX:MLG (93:7 %, w/w), WAX:MLG:WS (65:5:30 %, w/w), RAX:MLG (86:14 %, w/w), and RAX:MLG:WS (30:5:65 %, w/w) were prepared. These mixtures were prepared in the ratio that is commonly found in wheat and rye brans, respectively [16]. Another polysaccharide mix (PS mix) was composed of WAX:MLG:GGM:HG:RG-I:ABN (1:1:1:1:1 %, w/w). Mixes and individual polysaccharides (BWX, WAX, RAX, MLG, WS, XG, Cel, GGM, LBGM, HG, RG-I, and ABN) were periodate-oxidized in duplicate. The reaction volume was set at 40 mL, and 200 mg of PS powder was used in all experiments. Polysaccharides were solubilized in (37.6 mL) water **1**) under magnetic stirring overnight (xylans, XG, HG, RG-I, ABN), or **2**) under vigorous magnetic stirring of the slurry covered with aluminium foil on a hot-plate at 120 °C until boiling, followed by stirring without heat until the PS was fully dissolved (MLG, GMs, and PS mix), or **3**) by autoclaving at 121 °C for 20 min (WS, Cel and AX mixes). After PS solubilization, a freshly prepared 250 $\mu\text{mol/mL}$ NaIO_4 solution (2.4 mL) was added to the PS solution to reach a 3.0 $\mu\text{mol NaIO}_4/\text{mg PS}$ ratio. The glass reaction flask was protected from light with aluminium foil, and the reaction was carried out at room temperature (RT) for 6 h, as previously described [13]. Periodate-oxidized (pOx-) PS samples were characterized and subjected to a thermal treatment using an autoclave (section 2.4).



2.3. Sugar composition analysis by HPAEC-PAD

Sugar composition of the pOx-PS samples (BWx, AXs, MLG, LBGM, WS, HG, RG-I, ABN, and AX:glucan mixes (2.0 mg)) was determined after methanolysis (3.0 M HCl in dried methanol, 16 h, 80 °C) and TFA acid hydrolysis (2.0 M, 1 h, 121 °C) as described elsewhere [17]. Hydrolysates were diluted in water to about 25 µg/mL before analysis. Sugar composition of (pOx-) GGM, XG, Cel and PS mix samples (10 mg) was accessed after pre-hydrolysis for 10 min, or for 1 h for Cel samples, at 30 °C in 72 % (w/w) H₂SO₄ followed by hydrolysis for 3 h at 100 °C in 1.0 M H₂SO₄. Sulphuric acid hydrolysates were 100 times diluted with water before analysis. The monosaccharides released were analyzed by High-Performance Anion-Exchange Chromatography with Pulsed Amperometric Detection (HPAEC-PAD). An ICS-5000 HPLC system (Dionex, Sunnyvale, CA, USA) equipped with a CarboPac PA1 guard column (2 mm ID × 50 mm) and a CarboPac PA-1 column (2 mm × 250 mm) (Dionex) was used for this analysis. Detection of the eluted compounds was performed by an ED40 EC-detector running in the PAD mode (Dionex). 10 µL of the diluted hydrolysates was injected into the system and compounds were eluted as described previously [17]. All samples were analyzed in duplicate. Monosaccharide standards in a concentration range of 1.0-150 µg/mL were used for quantification. The collected data were analyzed using Chromeleon 7.2 software (Dionex). The degree of oxidation (DO) (equation (1)) of samples was calculated based on the decrease in the sugar recovery relative to the respective native PS or PS mixes. The relative DO (DO_{Rel}) (equation (2)) was calculated using the theoretical maximum DO (DO_{Theo}) that each PS can reach, and the calculated DO. DO_{Theo} was calculated based on the expected total remaining sugar content, if all sugar units containing vicinal diols are oxidized.

$$(1) \text{ DO } (\%, w/w) = 100 - \text{Relative sugar recovery of pOx} - \text{PS}$$

$$(2) \text{ DO}_{\text{Rel}} (\%, w/w) = \frac{\text{DO}}{\text{DO}_{\text{Theo}}} \times 100$$

2.4. Thermal depolymerization of periodate oxidized polysaccharides

Two reaction temperatures, 121 and 134 °C, were initially tested for their ability to degrade native and periodate-oxidized BWx, WAX, GGM, XG and HG samples in aqueous solution (1.0 mg/mL). A temperature of 121 °C was selected to further depolymerize all native and periodate-oxidized plant polysaccharides investigated in this study. All native polysaccharides and one replica of each pOx-PS (individuals and mixes) were solubilized in water (1.0 mg/mL) and thermally degraded at 121 °C (in duplicate) in an autoclave (AC) device (Zirbus Technology Benelux B.V., Tiel, the Netherlands) for 20 min at 2300 mbar, yielding AC121-pOx-PS. After AC treatment, part of the AC121(-pOx-)HG/RG-I samples was freeze-dried and analyzed for methyl-ester and acetyl content.



2.5. Uronic acid, methyl and acetyl content

(Periodate-oxidized) BWX, HG, RG-I, ABN and PS mix were sulphuric acid-hydrolysed as described in section 2.3., and the total uronic acid content was determined using an automated colorimetric *m*-hydroxydiphenyl method [18, 19].

(Periodate-oxidized) HG/RG-I samples before and after AC treatment were saponified in duplicate at 5.0 mg/mL in 0.1 M NaOH for 24 h (1 h at 4 °C followed by 23 h at RT) to hydrolyse methyl-esters. The methanol released was quantified by headspace gas chromatography (GC) analysis as described elsewhere [20]. The collected data were analyzed using Xcalibur 4.1 software (Thermo Scientific). After GC analysis, samples were centrifuged (16.1 x 1000 g, 10 min) and analyzed by HPLC on an Ultimate 3000 system (Dionex) coupled to a Shodex RI-101 detector (Showa Denko K.K., Tokyo, Japan) to determine the acetyl content. The HPLC was equipped with an Aminex HPX-87H Ion exclusion column (300 mm x 7.8 mm) with guard column, both from BIO-RAD (Hercules, CA, USA). The column oven temperature was maintained at 40 °C during analysis. 20 µL of standards (acetic acid 0.005-2.0 mg/mL) and samples were injected onto the system and eluted with 5.0 mM H₂SO₄ solution at a flow rate of 0.6 mL/min for 30 min. Collected data were analyzed using Chromeleon 7.2 software (Dionex).

2.6. Molecular weight distribution by HPSEC-RI

The average molecular weight (Mw) was determined by high performance size exclusion chromatography (HPSEC) on an Ultimate 3000 system (Dionex) coupled to Shodex RI-101 detector (Showa Denko K.K.) as described elsewhere [17]. Columns were calibrated with pullulan (0.180–708 kDa; Polymer Laboratories, UK) and pectin standards (10-100 kDa, as estimated by viscometry [21]). Standards and samples were analyzed at 1.0 mg/mL. Collected data were analyzed using Chromeleon 7.2 software (Dionex). The extent of polysaccharide depolymerization after AC treatment into various degree of polymerization (DP; DP<2, 2<DP<20, DP>20; as % released per DP_x) was calculated as percentage of the total area of the native PS. For DP<2, the area under the peak with a retention time (Rt)>14.7, >14.5, or >14.3 min was used for the treated pentosans, hexosans, or polymers containing uronic acids (HG and RG-I), respectively. For 2<DP<20, the area between 12.7 min<Rt<14.7 min, 12.6 min<Rt<14.5 min, or 12.0 min<Rt<14.3 min was used for pentosans, hexosans, or HG and RG-I, respectively. For DP>20, the area with a Rt<12.7 min, <12.6 min, or <12.0 min was used for pentosans, hexosans, or HG and RG-I, respectively.

2.7. Screening of oligosaccharides by MALDI-TOF MS

1.0 µL of DHB matrix solution (25 mg/mL DHB in 50 % (v/v) acetonitrile/water) was mixed with 1.0 µL of AC121-pOx-PS (1.0 mg/mL) on a Matrix-Assisted Laser Desorption Ionization (MALDI) plate (Bruker Daltonics, Bremen, Germany). Then, the MALDI plate was dried under a stream of air. Each AC121-pOx-PS replica was applied onto the MALDI plate at two different spots, giving a total of 4 replicas per AC121-pOx-PS sample. For MALDI-Time-Of-Flight (TOF) MS analysis, a Bruker - Ultraflextreme MALDI-TOF/TOF-MS (Bruker Daltonics, Bremen, Germany) equipped with a 337 nm laser was used. The mass spectrometer was operated in the positive mode and



calibrated with a mixture of maltodextrins (AVEBE, Veendam, The Netherlands; mass range 500–3500 Da). After a delayed extraction time of 120 ns, the ions were accelerated with a 25 kV voltage and subsequently detected using the reflector mode. Measurements were performed in the m/z 500–2500 range. The lowest laser intensity that allowed us to obtain a clear spectrum was used, and in total 4 times 250 shots were taken per spot to exclude interferences due to local differences in crystallization. The resulting MALDI-TOF mass spectra from all replicas of each AC121-pOx-PS sample displayed identical magnitude signals. Collected MALDI-TOF MS data were analyzed using flexAnalysis 3.3 software (Bruker Daltonics). Repetitive series of oxidized oligosaccharide clusters were observed in the whole MALDI-TOF mass spectrum range analyzed, as observed by ESI-MS analysis of periodate-oxidized oligosaccharides in our previous work [13]. Therefore, a zoom-in of the m/z 800–1200 range of the MALDI-TOF mass spectra of all AC121-pOx-PS and -mixes is shown and discussed in this paper.

2.8. Statistical analysis of MALDI-TOF MS data

The generated MALDI-TOF MS data (the exact m/z values and their intensities) were analyzed using the R statistical software package [22]. The m/z range between 800–1200 was used. The AC121-pOx-XG and AC121-pOx-RG-I samples were not subjected to statistical analysis since their MALDI-TOF mass spectra (m/z 800–1200) had a low overall signal intensity (<500). Principal component analysis (PCA) was performed (using the R package FactoMineR [23]) to emphasize the most important variation and create a low dimensional overview of the data in the form of score plots. Hierarchical cluster analysis (HCA), an unsupervised clustering method, will put similar spectra in the same clusters, highlighting samples that display similar oligosaccharide profiles. Prior to PCA and HCA, replicates of MALDI-TOF mass spectra were averaged.

For PCA, all (averaged) spectra were mean centred and unit variance scaled. HCA used Ward's linkage method and a distance criterium based on Pearson's correlation coefficient, which was applied on the MALDI-TOF mass spectra.

A series of two independent sample t-tests (using an alpha of 0.05) were used to find significantly different m/z values between any two polysaccharide classes of xylans (BWX, WAX, and RAX), glucans (WS and MLG), galactomannans (GGM and LBGm) or pectins (HG and ABN). Furthermore, two independent sample t-tests were also used to find significantly different m/z values within each of the following polysaccharide classes: **1**) xylans (AC121-pOx-BWX, AC121-pOx-WAX), (AC121-pOx-BWX, AC121-pOx-RAX), and (AC121-pOx-WAX, AC121-pOx-RAX); **2**) glucans (AC121-pOx-WS, AC121-pOx-MLG); **3**) galactomannans (AC121-pOx-GGM, AC121-pOx-LBGm); and **4**) pectins (AC121-pOx-HG, AC121-pOx-ABN). Significances ("P-values") were adjusted according to the method of Benjamini & Hochberg [24] to reduce the risk of false positives.

3. Results and discussion

A single polysaccharide (PS) depolymerization approach based on a combination of periodate oxidation and autoclave (AC) treatment was investigated to obtain PS structure-dependent oligosaccharides in a generic manner. The present approach was applied to a broad range of plant polysaccharides that were divided into the following classes: xylans (BWX and AXs), glucans (MLG,



WS, XG, and Cel), galactomannans (GMs), and pectic polysaccharides (HG, RG-I, and ABN). Furthermore, AX:MLG(:WS) PS mixes, and a PS mix composed of WAX:MLG:GGM:HG:RG-I:ABN (1:1:1:1:1:1 ratio (w/w)) were also subjected to the above approach in order to validate our approach for complex mixtures of polysaccharides. The oligosaccharides released were analyzed by MALDI-TOF MS to investigate if PS structure-dependent MALDI-TOF MS oligosaccharide profiles are obtained for recognition of the parental polysaccharides.

3.1. Degree of oxidation of periodate-oxidized polysaccharides based on the sugar recovery

All individual plant polysaccharides, AX:MLG(:WS) mixes and the PS mix were periodate-oxidized at room temperature (RT) for 6 h using a 3.0 $\mu\text{mol NaIO}_4/\text{mg PS}$ ratio. This periodate oxidation condition was selected since it allows the formation of soluble periodate-oxidized (pOx-) plant polysaccharides with minimal loss of non-sugar substituents and sugar side chains. In addition, under this periodate oxidation condition, pOx-polysaccharides are expected to be obtained with a relative degree of oxidation (DO_{rel}) $40 < \text{DO}_{\text{rel}} < 80$ % and low formation of side oxidation products [13]. In addition, this oxidation condition was selected because partial PS oxidation already allows the formation of oligosaccharides that are PS structure-dependent.

Regarding individual pOx-PS samples, xylans were obtained with a DO_{rel} of 39, 74, and 93 % (w/w) for pOx-BWX, pOx-RAX, and pOx-WAX, respectively (Table S1). This shows that AXs are more easily oxidized than BWX, as previously reported [13], and that although WAX and RAX have an identical Ara:Xyl ratio, pOx-WAX had a higher DO_{rel} than pOx-RAX. This might be due to the lower degree of branching of WAX compared to RAX [25]. For glucans, pOx-MLG and pOx-WS had a $\text{DO}_{\text{rel}} > 90$ %, whereas pOx-XG displayed a $\text{DO}_{\text{rel}} \sim 35$ %, which was due to (almost) complete oxidation/degradation of the Gal and Xyl side chains. Cel did not undergo oxidation at all, most likely due to its insolubility hindering any noticeable periodate oxidation [15].

pOx-GGM and pOx-LBGM samples had a DO_{rel} of 80 and 72 %, respectively, with all the Gal side chains of both GMs completely oxidized and/or partially removed. This shows that the side chains are more readily oxidized than the Man units in the backbone, in accordance with literature [13, 26]. Regarding pectic polysaccharides, pOx-HG, pOx-RG-I, and pOx-ABN displayed a DO_{rel} of 39, 76, and 98 %, respectively. pOx-ABN and pOx-RG-I did not recover any Rha and Glc units from the respective native ABN and RG-I samples, indicating that these sugar units were fully oxidized and/or degraded, whereas some Ara, Gal, and uronic acid (UA) units initially present in ABN were recovered in pOx-ABN, and some Gal and UA units of RG-I were recovered in pOx-RG-I. Altogether, these results show that overoxidation ($\text{DO}_{\text{rel}} > 100\%$) of individual polysaccharides did not occur, which is important to preserve a structure still closely related to the native PS structure.

Regarding PS mixes, pOx-WAX:MLG and pOx-WAX:MLG:WS had a DO_{rel} of 80 and 72 %, respectively, and pOx-RAX:MLG and pOx-RAX:MLG:WS had a DO_{rel} of 71 and 77 %, respectively. The pOx-PS mix had a DO_{rel} of 68 %. In all pOx-AX:glucan mixes, Ara, Xyl and Glc units were still detected (Table S1), confirming that full or overoxidation of the polysaccharides present in the mix also did not occur. Furthermore, the DO_{rel} obtained for the studied PS mixes were overall lower than the DO_{rel} obtained for each individual PS when oxidized separately. This suggests that periodate oxidation of individual polysaccharides is influenced by the presence of other polysaccharides. Yet, a



DO_{Rel} between 68-80% could be obtained for PS mixes, indicating that at least partial oxidation of all polysaccharides has occurred, which is important to further release PS-specific oligosaccharides.

3.2. Preliminary thermal treatment of periodate-oxidized polysaccharides

pOx-BWX, pOx-WAX, pOx-GGM, pOx-XG, and pOx-HG were thermally treated at 121 and 134 °C for 20 min using AC, resulting in AC121-pOx-PS and AC134-pOx-PS samples, respectively. All samples were analyzed for oligomers released using HPSEC (results only shown for 121 °C treatment in the following paragraph). AC121-pOx-PS samples displayed molecules with a degree of polymerization (DP) from 2-20, except AC121-pOx-XG, which still exhibited a high molecular weight (Mw). Increasing the AC temperature to 134 °C boosted the release of the remaining non-oxidized Ara side chains of pOx-WAX (HPAEC data not shown), and it did not further increase the degradation of pOx-GGM and pOx-XG as judged from HPSEC. For pOx-HG, AC treatment at 134 °C increased the degradation comparatively to the treatment at 121 °C, and mainly released additional monomers and enhanced the release of methyl-esters. AC121-pOx-HG recovered approx. 54 % (w/w native HG) methyl-esters, whereas AC134-pOx-HG only recovered approx. 27 % methyl-esters.

Based on these preliminary results, an AC treatment at 121 °C was selected to study the degradation of all the different pOx-PS samples and pOx-PS mixes. At this temperature it is expected that all studied pOx-plant polysaccharides, except (pOx-)XG, will be depolymerized to oligosaccharides with minimal loss of structural features. As Cel did not undergo oxidation and due to its insolubility, (pOx-)Cel was not further subjected to AC treatment.

3.3. Molecular weight distribution of thermally treated pOx-PS samples

The Mw distribution of the native and pOx-PS samples before and after AC treatment at 121 °C was analyzed by HPSEC (Fig. S1, Xylans; Fig. S2, Glucans; Fig. S3, AX-Glucan mixes; Fig. S4, GMs; Fig. S5, Pectins; and Fig. S6, PS mix), and the extent of PS depolymerization is shown in Table 1. None or only minor changes in the Mw distribution were observed for all native polysaccharides and mixes after AC treatment. On the contrary, all AC121-pOx-PS and -mixes had molecular weights lower than the respective pOx-PS, corroborating that the Mw of pOx-PS samples in aqueous solutions decreases upon heating [14]. Furthermore, all AC121-pOx-PS samples, except AC121-pOx-XG, comprised oligosaccharides (35 to 79 %; 2<DP<20; Table 1). This result highlights that periodate oxidation of plant polysaccharides at RT for 6 h using a 3.0 μNaIO₄/mg PS followed by an AC treatment at 121 °C is a promising approach to depolymerize plant polysaccharides into oligosaccharides in a generic manner. This overcomes the requirement to have specific enzymes per structurally different PS when using an enzymatic depolymerization approach.



Table 1. Percentage of periodate-oxidized (pOx-) polysaccharide (PS) depolymerized into the various degree of polymerization (DP) segments DP<2, 2<DP<20 (oligosaccharide range), and DP>20, before and after autoclave (AC) treatment at 121 °C (AC121).

Sample	Percentage ^a of depolymerized polymer into various DP		
	DP<2	2<DP<20	DP>20
pOx-BWX*	1.2	26.8	44.3
AC121-pOx-BWX	5.3 ± 0.6	41.8 ± 1.1	65.0 ± 2.7
pOx-WAX*	2.0	49.6	38.5
AC121-pOx-WAX	4.4 ± 0.0	49.9 ± 2.2	14.5 ± 2.0
pOx-RAX*	2.1	36.1	53.0
AC121-pOx-RAX	4.3 ± 0.7	40.2 ± 1.1	24.2 ± 2.3
pOx-MLG*	0.7	37.2	22.5
AC121-pOx-MLG	2.1 ± 0.5	37.2 ± 1.8	15.4 ± 0.5
pOx-WS ^{b*}	31.1	148.7	11.6
AC121-pOx-WS ^b	49.3 ± 0.4	74.0 ± 1.2	33.9 ± 0.1
pOx-XG ^c	Insoluble sample		
AC121-pOx-XG ^d	0.0 ± 0.0	2.9 ± 0.4	27.6 ± 3.3
pOx-WAX:MLG*	1.7	44.6	47.3
AC121-pOx-WAX:MLG	5.2 ± 1.4	59.6 ± 0.1	36.3 ± 9.9
pOx-WAX:MLG:WS*	3.4	49.7	61.0
AC121-pOx-WAX:MLG:WS	5.7 ± 1.6	55.2 ± 5.7	34.0 ± 0.4
pOx-RAX:MLG*	1.6	28.7	53.4
AC121-pOx-RAX:MLG	4.2 ± 0.3	41.8 ± 0.5	29.7 ± 0.3
pOx-RAX:MLG:WS ^{b*}	4.9	65.7	165.7 ^b
AC121-pOx-RAX:MLG:WS ^b	12.9 ± 2.3	79.1 ± 7.4	144.1 ± 4.0 ^b
pOx-GGM*	2.8	24.6	62.4
AC121-pOx-GGM	10.7 ± 0.1	35.8 ± 0.9	32.9 ± 0.4
pOx-LBGM*	9.9	63.5	31.4
AC121-pOx-LBGM	17.7 ± 0.3	43.5 ± 0.1	4.4 ± 0.3
pOx-HG*	0.0	2.4	93.2
AC121-pOx-HG	7.5 ± 0.4	67.0 ± 1.8	4.8 ± 0.2
pOx-RG-I*	0.0	21.2	51.9
AC121-pOx-RG-I	5.2 ± 0.2	45.2 ± 3.1	15.4 ± 2.2
pOx-ABN*	0.0	4.6	90.1
AC121-pOx-ABN	3.6 ± 0.5	44.5 ± 3.2	27.6 ± 1.4
pOx-PS mix*	0.0	11.1	88.8
AC121-pOx-PS mix	4.8 ± 0.1	51.6 ± 0.8	38.8 ± 2.9

^a Results are expressed as average (n=2) of the area percentage (%) relative to the total area of the respective untreated native polysaccharide as described in section 2.6.

^b Samples solubility increased after AC treatment and/or periodate oxidation.

^c Sample became insoluble after periodate oxidation.

^d Sample contained some insoluble material.

* Single sample used to perform the AC121 treatment is shown.

3.4. MALDI-TOF MS analysis of thermally treated pOx-PS samples

The Mw distribution results showed that all AC121-pOx-PS, except AC121-pOx-XG, and -mixes released oligosaccharides. Particularly for AC121-pOx-HG and AC121-pOx-RG-I, some loss of ester groups (methyl-esters and acetyl groups; Fig. S7) occurred during periodate oxidation and AC



treatment. Despite this, the oligosaccharide profiles of the AC121-pOx-PS samples and -mixes might still be sufficiently PS structure-dependent.

All individual AC121-pOx-PS samples that contained oligosaccharides comprised clusters of oxidized oligosaccharides, except AC121-pOx-RG-I (Fig. 1-5), confirming our previous work on the ESI-MS analysis of periodate-oxidized plant polysaccharides [13]. Clusters of oxidized oligosaccharide fragments are marked as **ox-DP_n** (oxidized oligosaccharide cluster region potentially with a DP *n*) in the MALDI-TOF mass spectra (Fig. 1-5). Each **ox-DP_n** region is composed of various sub-oligosaccharide clusters that comprise various *m/z* values that were $\Delta -(x + n*2)$ Da relative to the corresponding DP-oligomer or, particularly for AC121-pOx-WS and AC121-pOx-HG, relative to the corresponding highest DP-oxidized oligomer within the **ox-DP_n** cluster, where $x = 12 - 214$ and $n = 0 - 4$. The $n*2$ is due to variable levels (*n*) of dialdehydes. The *x* is due to various oxidation reactions that can take place during periodate oxidation, such as double oxidations, intra-molecular cleavages of an (oxidized) sugar unit, and hemialdals formation, or even due to a combination of these reactions, as reported before [13]. In principle this high variety of oxidized oligosaccharide structures is attractive as it would increase the likelihood of obtaining unique patterns for identification. Below, the MALDI-TOF mass spectra (*m/z* 800-1200) of the various AC121-pOx-PS and -mixes will be compared and discussed.

Xylans

The MALDI-TOF mass spectrum of AC121-pOx-BWX (Fig. 1A) showed that each **ox-DP_n** region comprised the following sub-oligosaccharide clusters: $\Delta -(18 + n*2)$, $\Delta -(60 + n*2)$, and $\Delta -(76 + n*2)$ Da, with $n = 0, 1$ and 2 , relative to the corresponding pentose-oligomer (*P_n*). The sub-oligosaccharide cluster *P_n* $\Delta -(76 + n*2)$ Da was always the major sub-oligosaccharide cluster of each **ox-DP_n** in AC121-pOx-BWX.

Both AXs, AC121-pOx-WAX and AC121-pOx-RAX, comprised the same **ox-DP_n** regions, which were formed by the sub-oligosaccharide clusters $\Delta -(44 + n*2)$, $\Delta -(60 + n*2)$, and $\Delta -(76 + n*2)$, with $n = 0 - 4$, relative to *P_n* (Fig. 1B and C). Notably, the sub-cluster *P_n* $\Delta -(18 + n*2)$ Da present in AC121-pOx-BWX was absent in the spectra of both AC121-pOx-AXs, while the latter displayed the sub-cluster *P_n* $\Delta -(44 + n*2)$ Da as an additional sub-oligosaccharide cluster. This highlights that a moderately substituted xylan with UA (<10 %, w/w; Table S1) (BWX) and AXs generate oxidized oligosaccharide profiles that are PS structure-dependent after periodate oxidation and AC treatment. Remarkably, the ions *m/z* 919 and 1051 of the sub-clusters *P_n* $\Delta -(44 + n*2)$ Da of AC121-pOx-AXs (Fig. 1B and C) were significantly different from AC121-pOx-BWX ($p < 0.05$). Hence, these *m/z* values can be considered marker oligosaccharides for AXs, allowing us to distinguish them from BWX.

Although the **ox-DP_n** regions of AC121-pOx-WAX and AC121-pOx-RAX comprised the same sub-oligosaccharide clusters (Fig. 1B and C), their proportion within each **ox-DP_n** region varied between WAX and RAX. For AC121-pOx-WAX, the sub-oligosaccharide cluster *P_n* $\Delta -(60 + n*2)$ Da was the principal sub-oligosaccharide cluster in each **ox-DP_n** cluster, followed by the sub-oligosaccharide cluster *P_n* $\Delta -(76 + n*2)$ Da (Fig. 1B). While for AC121-pOx-RAX (Fig. 1C), both sub-oligosaccharide clusters *P_n* $\Delta -(60 + n*2)$ Da and *P_n* $\Delta -(76 + n*2)$ Da were similarly present in each **ox-DP_n**. These results highlight that although both WAX and RAX display an identical Ara:Xyl ratio, their differences in the Ara distribution along the xylan backbone [25] leads to differences in the



proportion of oxidized oligosaccharides released from pOx-AXs after AC treatment at 121 °C. This result is highly relevant because it shows that even the same type of PS derived from different sources having only slightly different structures can be distinguished using our approach.

Glucans

Regarding glucans, two **ox-DP_n** regions (ox-DP₆ and ox-DP₇) could be well-defined for AC121-pOx-MLG (Fig. 1D). For AC121-pOx-WS, only one **ox-DP_n** region (ox-DP_{6/7}) that comprised oxidized oligosaccharides derived from a DP 6 and/or DP 7 was defined (Fig. 1E). The given **ox-DP_n** cluster for AC121-pOx-WS was considered as one cluster since repetitive throughout the entire MALDI-TOF MS range (m/z 500-2500) analyzed (data not shown). Notably, none of the sub-oligosaccharide clusters present in the MALDI-TOF mass spectra of both glucans coincided, showing that different oligosaccharide profiles are obtained between samples. Hence, various significantly different ($p < 0.05$) m/z values were found for MLG (m/z 1097, 1115, and 1157) and for WS (m/z 913, 931, 949, 965, 991, 1015, 1039, 1075, 1093, 1109, 1127, and 1169), acting as marker oligosaccharides for the corresponding glucan.

AX:MLG(:WS) mixes

To investigate whether the main cereal hemicellulose components (AXs and MLG) can be identified when present in a mix based on the MALDI-TOF MS oligosaccharide profiles derived from AC121-pOx-PS samples, AX:MLG mixes were prepared in the proportion that are found in wheat and rye brans [16]. An AX:MLG:WS mix was also prepared because starch is also present in cereal bran preparations. While the oligosaccharide pattern of AC121-pOx-WAX:MLG (93:7 %, w/w) (Fig. 2A) was the same as AC121-pOx-WAX (Fig. 1B), the one of AC121-pOx-WAX:MLG:WS (65:5:30 %, w/w) (Fig. 2B) additionally comprised minor levels of WS-oxidized oligosaccharides. This shows that the mass spectra of AC121-pOx-WAX:MLG(:WS) ‘bran’ mixes are dominated by AX-oxidized oligosaccharides.

The AC121-pOx-RAX:MLG (86:14 %, w/w) (Fig. 2C) also displayed an oligosaccharide pattern identical to the individual AC121-pOx-RAX (Fig. 1C), with negligible amounts of MLG-oxidized oligosaccharides. On the contrary, AC121-pOx-RAX:MLG:WS (30:5:65 %, w/w) comprised RAX- and WS-oxidized oligosaccharides (Fig. 2D). In this RAX:MLG:WS mix, WS accounted for 65 % of the mix, whereas in the WAX:MLG:WS mix, WS represented 30 %. The higher proportion of WS in the rye mix compared to the wheat mix might explain the additional presence of WS-oxidized oligosaccharides in the MALDI-TOF mass spectrum of AC121-pOx-RAX:MLG:WS mix besides AX-oxidized oligosaccharides. This suggests that the release of periodate-oxidized oligosaccharides derived from specific polysaccharides present in a mix depends on the proportion of each PS in the mix. This can explain why MLG-oxidized oligosaccharides were hardly detected in the mass spectra of the AC121-pOx-AX:MLG(:WS) mixes, since MLG is present in low proportions. Yet, these results highlight that periodate oxidation/AC treatment of products containing wheat and/or rye bran hemicellulose components, followed by analysis of the oligosaccharides released by MALDI-TOF MS, has potential to identify AXs, regardless the presence of MLG and/or WS.

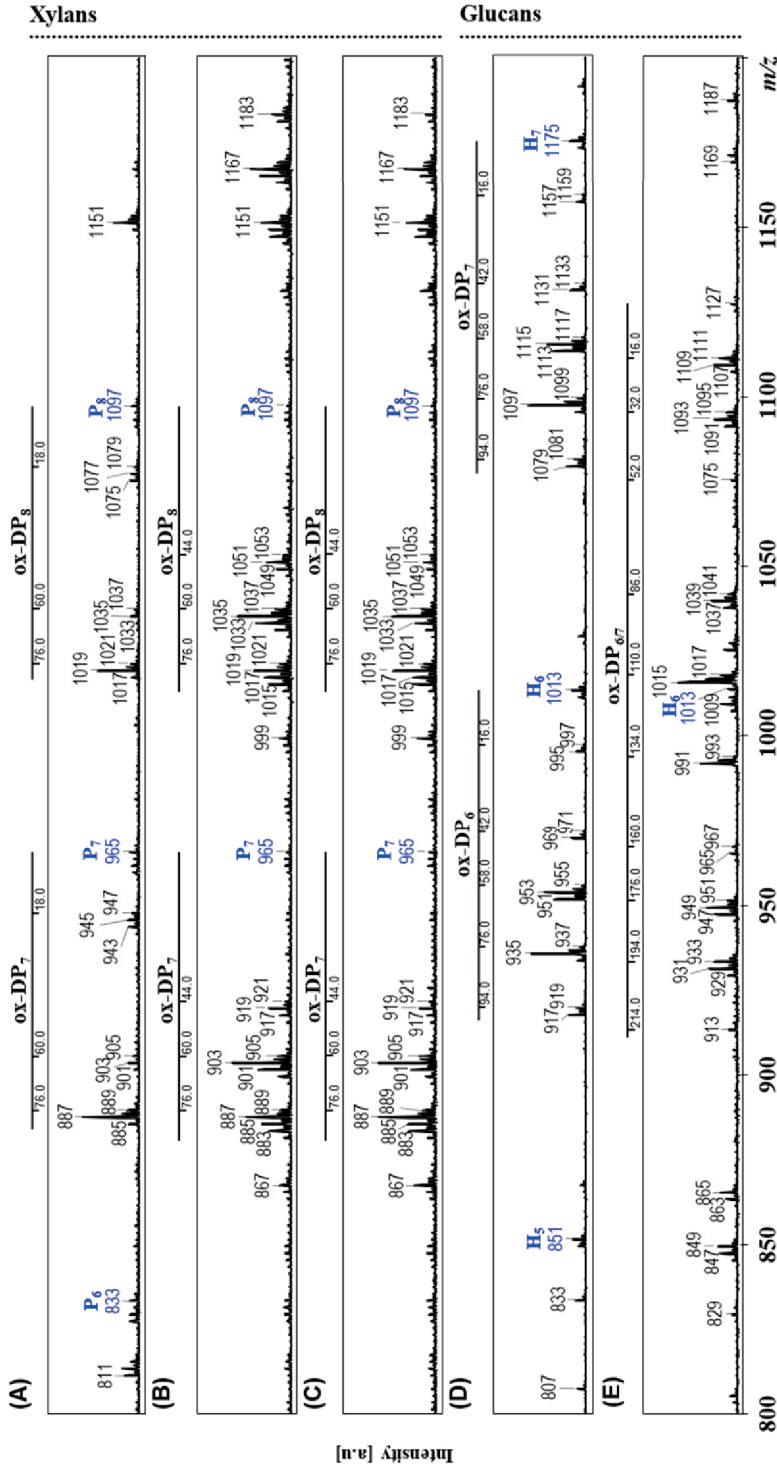


Figure 1. MALDI-TOF mass spectra (m/z 800–1200 range) of the AC121 treated periodate-oxidized BWX (A), WAX (B), RAX (C), MLG (D), and WS (E). P_n or $H_n - Na^+$ adduct of an oligomer composed of n pentoses (Ara or Xyl) or hexoses (Glc). ox-DP_n - m/z region of a cluster of oxidized oligosaccharides potentially with a n DP. m/z differences from each sub-oligosaccharide cluster with $\Delta - (x + n * 2)$ Da, $n = 0 - 4$, to the corresponding non-oxidized DP-oligomer are depicted in (A-D). In (E), m/z differences from each sub-oligosaccharide cluster with $\Delta - (x + n * 2)$ Da, $n = 0 - 3$, are given in relation to the highest oxidized m/z value detected within the ox-DP_n cluster. Detected non-oxidized oligomers are highlighted in blue.

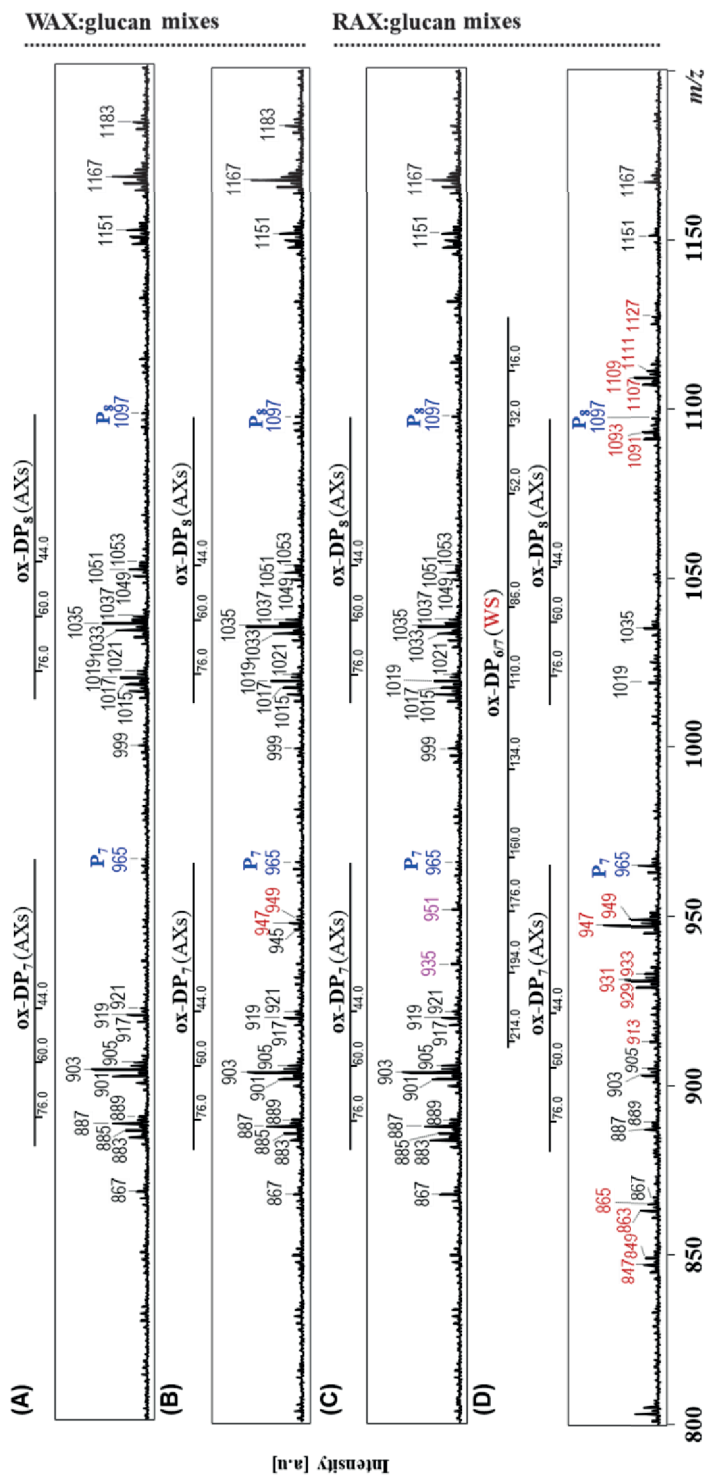


Figure 2. MALDI-TOF mass spectra (m/z 800–1200 range) of the AC121 treated periodate-oxidized WAX:MLG (93:7 %, w/w; **A**), WAX:MLG:WS (65:5:30 %, w/w; **B**), RAX:MLG (86:14 %, w/w; **C**), and RAX:MLG:WS (30:5:65 %, w/w; **D**). P_n or $H_n + Na^+$ adduct of an oligomer composed of n pentoses (Aa or Xyl) or hexoses (Glc). **ox-DP_n** (AXs) – m/z region of a cluster of oxidized oligosaccharides derived from AXs potentially with a n DP. **ox-DP_n** (WS) – m/z region of a cluster of oxidized oligosaccharides derived from WS potentially with a n DP. Detected non-oxidized oligomers are highlighted in blue, and oxidized oligomers derived from AXs, MLG, and WS are highlighted in black, pink, and red, respectively.



Galactomannans

The MALDI-TOF mass spectra of both AC121-pOx-GGM and AC121-pOx-LBGM (Fig. 3A and B) displayed the same oxidized oligosaccharide clusters. However, the proportion of sub-oligosaccharide clusters that formed the **ox-DP_n** region of each AC121-pOx-GM differed. 4 sub-oligosaccharide clusters, namely $H_n \Delta -(64 + n*2)$, $H_n \Delta -(78 + n*2)$, $H_n \Delta -(94 + n*2)$, and $H_n \Delta -(108 + n*2)$ Da, were predominantly present in each **ox-DP_n** region of AC121-pOx-GGM (Fig. 3A). In AC121-pOx-LBGM, the last 2 sub-oligosaccharide clusters of each **ox-DP_n** ($H_n \Delta -(108 + n*2)$ and $H_n \Delta -(94 + n*2)$) were present in much lower abundance than the precedent 2 sub-oligosaccharide clusters ($H_n \Delta -(64 + n*2)$ and $H_n \Delta -(78 + n*2)$; Fig. 3B). In addition, the ions m/z 899, 917, 1061 and 1077 were significantly more abundant ($p < 0.05$) in AC121-pOx-GGM than in AC121-pOx-LBGM. Therefore, these m/z values were considered marker oligosaccharides of GGM, allowing us to distinguish GGM from LBGM. The MALDI-TOF MS results obtained for galactomannans, glucans, and (arabino)xylans are particularly interesting because they show that periodate oxidation/AC treatment of structurally different polysaccharides composed of isomeric sugar units generates unique oligosaccharide profiles.

Pectins

Regarding pectic polysaccharides (Fig. 4A-C), AC121-pOx-HG displayed two **ox-DP_n** regions in the m/z 800-1200 range (Fig. 4A). Within these **ox-DP_n** regions, HG-oxidized and methyl-esterified unsaturated GalA-oligomers (uHexA_n^m) were identified. This result highlights that some contiguous GalA segments that were partially methyl-esterified resisted periodate oxidation and were further cleaved by AC treatment. Additionally, the presence of unsaturated sugar units indicates that an AC treatment degrades a pOx-HG via a β -elimination reaction [14].

For AC121-pOx-RG-I, many oligosaccharides were obtained (Fig. 4B). However, these oligosaccharides had a very low signal abundance throughout the entire mass spectrum range shown, not exhibiting any clear pattern of clusters of oxidized oligosaccharides. In contrast, AC121-pOx-ABN comprised three **ox-DP_n** clusters (Fig. 4C) that were totally different from the **ox-DP_n** regions of AC121-pOx-HG (Fig. 4A). Therefore, some significantly ($p < 0.05$) different m/z values were found for AC121-pOx-ABN (m/z 849, 865, 981, 995, 1113, and 1129) and for AC121-pOx-HG (m/z 883, 915, 1057, and 1089), and were considered marker oligosaccharides between both these samples. These results show that also AC121-pOx-pectic elements generate PS structure-dependent MS oligosaccharide profiles. Remarkably, MALDI-TOF MS oligosaccharide profiles of Ara-based polymer AC121-pOx-ABN (Fig. 4C) was also different from the ones obtained for the xylans investigated (Fig. 1A-C).

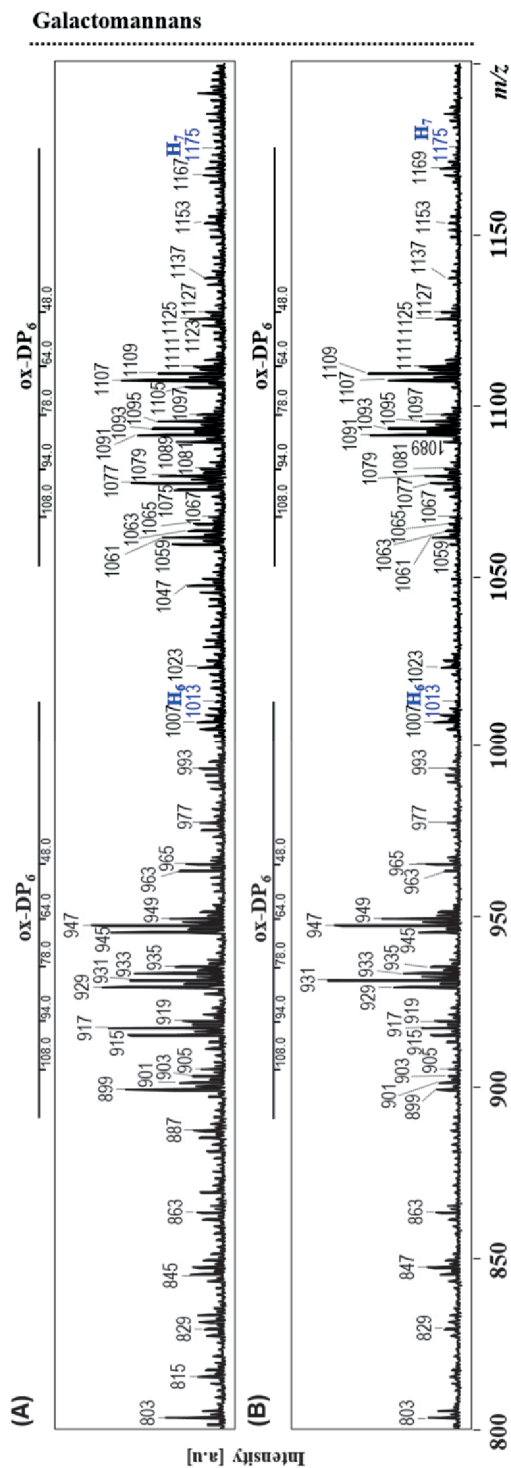


Figure 3. MALDI-TOF mass spectra (m/z 800–1200 range) of the AC121 treated periodate-oxidized GGM (A) and LBG (B). $H_n - Na^+$ adduct of an oligomer composed of n hexoses (Gal and/or Man), $ox-DP_n - m/z$ region of a cluster of oxidized oligosaccharides potentially with a n DP. m/z differences from each sub-oligosaccharide cluster with $\Delta - (x + n \cdot 2)$ Da, $n = 0 - 4$, to the corresponding non-oxidized DP-oligomer are depicted. Detected non-oxidized oligomers are highlighted in blue.



Pectins

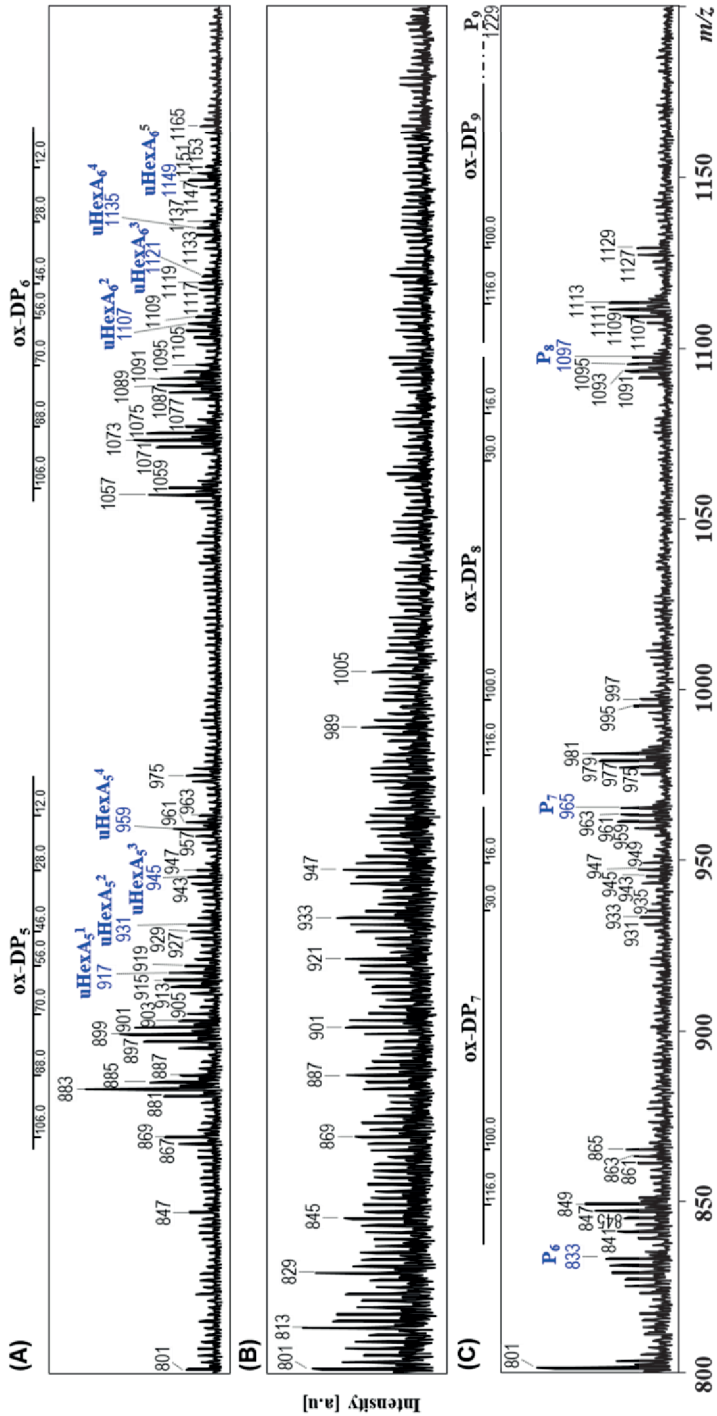


Figure 4. MALDI-TOF mass spectra (m/z 800-1200 range) of the AC121 treated periodate-oxidized HG (A), RG-I (B), and ABN (C). $uHexA_n^m$ - Oligomer composed of n GalA units from which one is unsaturated and m methyl-esters. $P_n - Na^+$ adduct of an oligomer composed of n pentoses (Ara). $ox-DP_n$ m/z region of a cluster of oxidized oligosaccharides potentially with a n DP. In (A), m/z differences from each sub-oligosaccharide cluster with $\Delta -(x + n*2)$ Da, $n = 0 - 5$, are given in relation the highest oxidized m/z value detected within the $ox-DP_n$ cluster. In (B), $ox-DP_n$ regions could not be defined for RG-I. In (C), m/z differences from each sub-oligosaccharide cluster with $\Delta -(x + n*2)$ Da, $n = 0 - 4$, to the corresponding non-oxidized DP-oligomer are depicted. Detected non-oxidized oligomers are highlighted in blue.



PS mix (WAX:MLG:GGM:HG:RG-I:ABN)

A PS mix composed of WAX:MLG:GGM:HG:RG-I:ABN in an 1:1:1:1:1:1 ratio (w/w) was also periodate-oxidized and AC treated to investigate if different PS classes can be identified when present in a complex mixture of polysaccharides. The MALDI-TOF mass spectrum of the AC121-pOx-PS mix (Fig. 5) exhibited m/z values derived from all individual AC121-pOx-PS samples (Fig. 1B, 1D, 3A, 4A-C). Despite being rather complex, the mass spectrum of AC121-pOx-PS mix still allowed us to get hints on the type of polysaccharides present in the mixture. Statistical analysis of the spectra between the various (AC121-pOx-)PS classes using a t-test with $p < 0.05$ showed that **1)** the oligosaccharides with m/z 887 and 1019 were significantly more abundant in the xylan class than in all the other studied PS classes; **2)** the oligosaccharides with m/z 931, 947, 1091 and 1107 were significantly more abundant in GMs than in xylans and pectic polysaccharides; **3)** the ion m/z 935 was significantly more abundant in glucans than in xylans and pectic polysaccharides, whereas the oligosaccharides with m/z 1013 and 1175 were more significantly abundant in glucans than in GMs; and **4)** the ion m/z 801 was most significantly abundant in pectic polysaccharides. Detection of some of these marker m/z values per PS class in the MALDI-TOF mass spectrum of the AC121-pOx-PS mix (Fig. 5) allowed us to unambiguously recognize the presence of pectic (m/z 801), GM (m/z 931 and 1091), glucan (m/z 935), and xylan components (m/z 887 and 1019).

Our results show that periodate oxidation/AC treatment of plant polysaccharides and -mixes is a potential approach to depolymerize polysaccharides in a generic manner, releasing oligosaccharides that are PS structure-dependent. This result is of the utmost importance since it highlights that purified plant polysaccharides and plant polysaccharides present in complex mixes can be identified based on their unique MALDI-TOF MS oligosaccharide profiles.

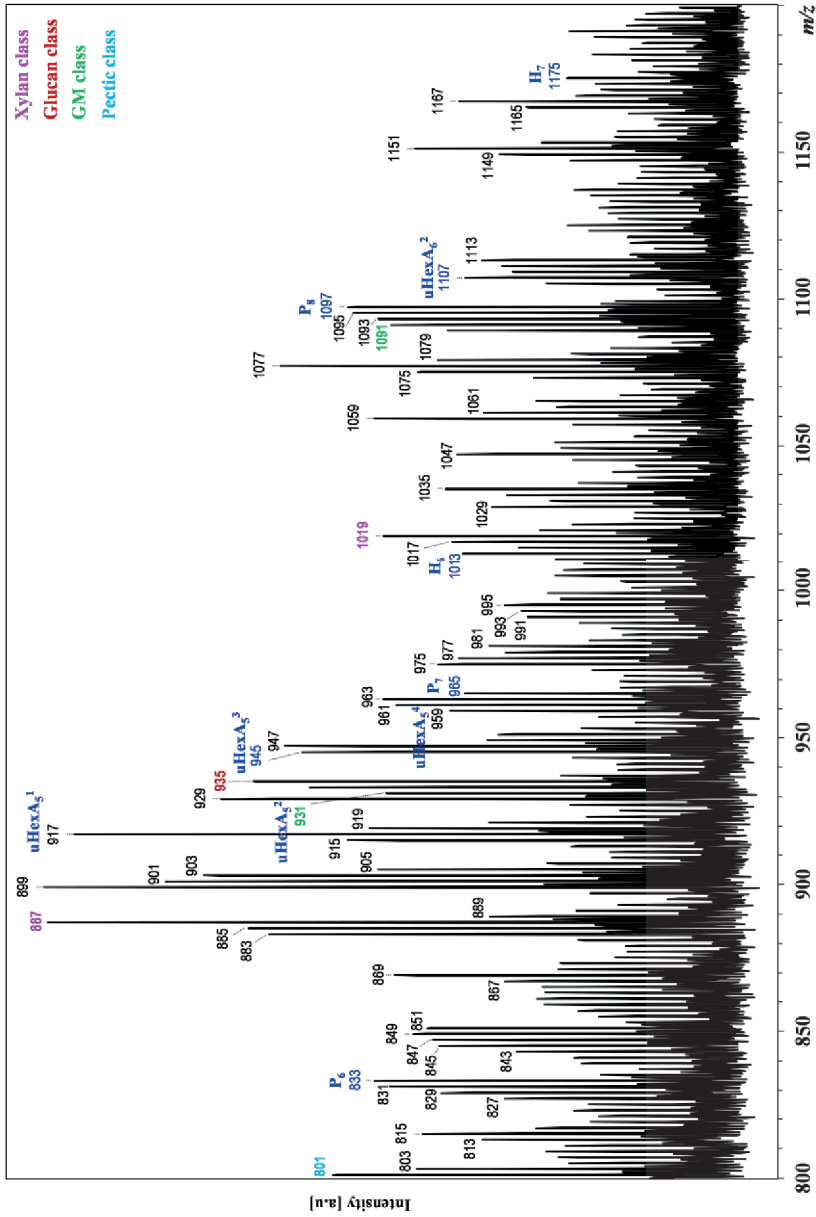


Figure 5. MALDI-TOF mass spectra (m/z 800–1200 range) of the AC121 treated periodate-oxidized PS mix (WAX:MLG:GGM:HG:RD-I:ABN 1:1:1:1:1 ratio (w/w)). P_n or $H_n - Na^+$ adduct of an oligomer composed of n pentoses (Ara or Xyl) or hexoses (Gal, and/or Man); $uHexA_m$ – Oligomer composed of n GalA units from which one is unsaturated and m methyl-esters. Detected non-oxidized oligomers are highlighted in dark blue. Significantly different ($p < 0.05$) m/z values found for the xylan, glucan, GM, and pectic polysaccharides class between PS classes are highlighted in pink, red, green, and light blue, respectively.



3.5. Exploratory PCA and HCA analysis of MALDI-TOF mass spectra of thermally treated pOx-PS samples

To illustrate and emphasize sources of variations among MALDI-TOF MS oligosaccharide profiles of AC121-pOx-PS and -mixes, and to cluster PS samples with similar oligosaccharide profiles, principal component analysis (PCA) and hierarchical cluster analysis (HCA) were performed.

The first two principal components (PC1 and PC2) of the PCA (Fig. 6A) accounted for 71.4 % of the total variance, with PC1 explaining most of the variation (57.9 %). AC121-pOx-MLG and AC121-pOx-WS samples were separated along PC1, which might be due to completely different MS oligosaccharide profiles for these samples (Fig. 1). Individual polysaccharides within the xylan-, GM- and pectin classes were separated along PC2. Notably, PCA also confirmed that the Ara-based polymer (AC121-pOx-)ABN was not closely related to any other pentose-based xylan polymer. Hence, PCA of the MALDI-TOF MS data clearly stressed the structural differences of all polysaccharides investigated in this study, even between the same type of polysaccharides (e.g. AXs and GMs).

MALDI-TOF MS results indicated that the oligosaccharide profiles of AC121-pOx-WAX:MLG(:WS) and AC121-pOx-RAX:MLG were comparable to the respective AC121-pOx-AX, whereas the mass spectrum of AC121-pOx-RAX:MLG:WS displayed both RAX- and WS-oxidized oligosaccharides. Although AC121-pOx-AX:MLG and AC121-pOx-AX:MLG:WS mixes were grouped together in the PCA (Fig. 6A), these samples were separated from AC121-pOx-AX and AC121-pOx-WS. This was not obvious from the MALDI-TOF MS results, indicating that there is distinct difference between AC121-pOx-AX:glucan mixes and the individual AC121-pOx-polysaccharides.

The correlation-based distance dendrogram obtained from HCA (Fig. 6B) clustered xylians in branch **a2** and GMs in branch **b5** (Fig. 6B), whereas the other PS classes (glucans and pectins) were not clustered. AC121-pOx-WAX and AC121-pOx-RAX were closer to each other than to AC121-pOx-BWX. In addition, the dendrogram highlighted that AC121-pOx-RAX:MLG:WS was more intimately correlated to AC121-pOx-WS (branch **b**, Fig. 6B) than to AC121-pOx-RAX (branch **a**, Fig. 6B), confirming the MALDI-TOF MS results (Fig. 2D). Altogether, MALDI-TOF MS analysis of the AC121-pOx-PS samples studied combined with advanced data sciences methods such as PCA and HCA unambiguously enabled us to recognize different PS classes in a mixture and, at the same time, to distinguish PS within a specific PS class. In addition, it allowed us to cluster polysaccharides with resembling MALDI-TOF MS oligosaccharide profiles.

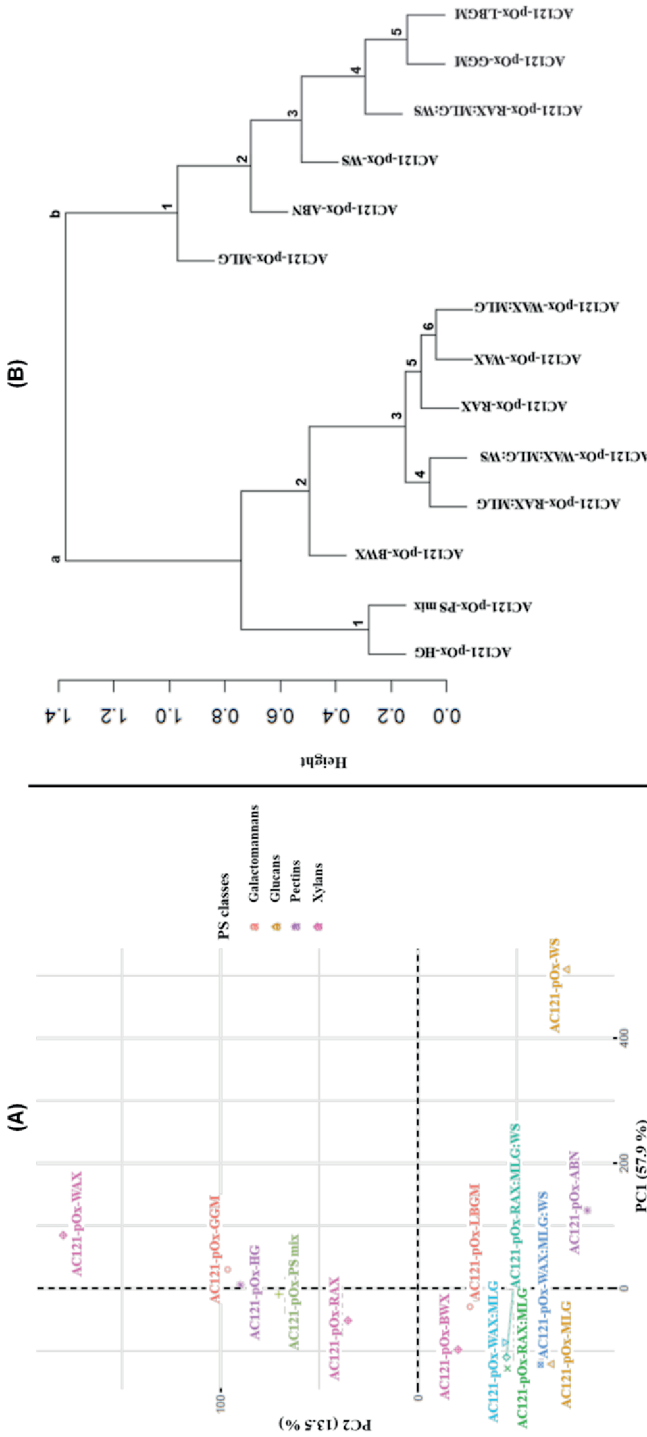


Figure 6. (A) Principal component analysis (PCA) biplot, and (B) Hierarchical cluster analysis (HCA) represented as a correlation-based distance dendrogram constructed with the MALDI-TOF mass spectra data (m/z 800-1200) of the various periodate-oxidized (pOx-) samples degraded using an AC treatment at 121 °C (AC121-pOx-BWX, AC121-pOx-WAX, AC121-pOx-RAX, AC121-pOx-MLG, AC121-pOx-GGM, AC121-pOx-LBGM, AC121-pOx-HG, AC121-pOx-ABN, AC121-pOx-AX:MLG(:WS), and AC121-pOx-PS mix). The PCA scores were plotted for PC1 and PC2, and the amount of variance explained by each PC is shown in parentheses.



4. Conclusions

In this study, depolymerization of periodate-oxidized plant polysaccharides and polysaccharide (PS) mixes using an autoclave (AC) treatment at 121 °C was an approach investigated to release oligosaccharides for polysaccharides fingerprinting. All investigated plant polysaccharides were depolymerized releasing oligosaccharides, except xyloglucan. MALDI-TOF MS analysis of the oligosaccharides released showed that structure-dependent oligosaccharide profiles were obtained per PS. This allowed us to distinguish even between polysaccharides with resembling structures, such as xylans (birch wood xylan, and wheat and rye arabinoxylans) and galactomannans (from guar and locust bean). Furthermore, based on significantly different ($p < 0.05$) marker m/z values identified per PS class, also different PS classes could be detected in the MALDI-TOF mass spectrum of a complex PS mix. These results bring us a step closer to recognize different polysaccharides and/or PS classes using a single PS depolymerization approach. The approach proposed could be extended to other food polysaccharides with the creation of a MALDI-TOF MS data library to recognize individual polysaccharides in a food product more easily. In addition, to clearly demonstrate the heterogeneity within and between PS classes, and cluster polysaccharides with resembling MS oligosaccharide profiles, performing PCA and HCA on the MALDI-TOF MS data is a nice complementary approach. Thus, periodate oxidation of plant PS followed by an AC treatment and MALDI-TOF MS analysis is a promising approach to depolymerize polysaccharides into PS-specific oligosaccharides in a more generic manner than by using enzymes.



References

- [1] Harris, P.J. and B.G. Smith. Plant cell walls and cell-wall polysaccharides: Structures, properties and uses in food products. *International Journal of Food Science and Technology*. **2006**, 41, 129-143.
- [2] Saha, A., S. Tyagi, R.K. Gupta, and Y.K. Tyagi. Natural gums of plant origin as edible coatings for food industry applications. *Critical Reviews in Biotechnology*. **2017**, 37, 959-973.
- [3] Broxterman, S.E., P. Picouet, and H.A. Schols. Acetylated pectins in raw and heat processed carrots. *Carbohydrate Polymers*. **2017**, 177, 58-66.
- [4] Leijdekkers, A.G.M., J.H. Huang, E.J. Bakx, H. Gruppen, and H.A. Schols. Identification of novel isomeric pectic oligosaccharides using hydrophilic interaction chromatography coupled to traveling-wave ion mobility mass spectrometry. *Carbohydrate Research*. **2015**, 404, 1-8.
- [5] Remorosa, C., S. Broxterman, H. Gruppen, and H.A. Schols. Two-step enzymatic fingerprinting of sugar beet pectin. *Carbohydrate Polymers*. **2014**, 108, 338-347.
- [6] Lerouxel, O., T. Siang Choo, M. Séveno, B. Usadel, L. Faye, P. Lerouge, and M. Pauly. Rapid structural phenotyping of plant cell wall mutants by enzymatic oligosaccharide fingerprinting. *Plant Physiology*. **2002**, 130, 1754-1763.
- [7] Westphal, Y., H.A. Schols, A.G.J. Voragen, and H. Gruppen. MALDI-TOF MS and CE-LIF fingerprinting of plant cell wall polysaccharide digests as a screening tool for arabidopsis cell wall mutants. *Journal of Agricultural and Food Chemistry*. **2010**, 58, 4644-4652.
- [8] Lombard, V., H. Golaconda Ramulu, E. Drula, P.M. Coutinho, and B. Henrissat. The carbohydrate-active enzymes database (CAZy) in 2013. *Nucleic Acids Research*. **2014**, 42, D490-D495.
- [9] Bauer, S. Mass Spectrometry for Characterizing Plant Cell Wall Polysaccharides. *Frontiers in Plant Science*. **2012**, 3.
- [10] Kailemia, M.J., L.R. Ruhaak, C.B. Lebrilla, and I.J. Amster. Oligosaccharide analysis by mass spectrometry: a review of recent developments. *Analytical chemistry*. **2014**, 86, 196-212.
- [11] Kristiansen, K.A., A. Pothast, and B.E. Christensen. Periodate oxidation of polysaccharides for modification of chemical and physical properties. *Carbohydrate Research*. **2010**, 345, 1264-1271.
- [12] Nypelö, T., B. Berke, S. Spirk, and J.A. Sirviö. Review: Periodate oxidation of wood polysaccharides—Modulation of hierarchies. *Carbohydrate Polymers*. **2021**, 252, 117105.
- [13] Pandeirada, C.O., M. Achterweust, H.-G. Janssen, Y. Westphal, and H.A. Schols. *Periodate oxidation of plant polysaccharides provides polysaccharide-specific oligosaccharides*. 2022, Submitted for publication.
- [14] Veelaert, S., D. de Wit, K.F. Gotlieb, and R. Verhé. Chemical and physical transitions of periodate oxidized potato starch in water. *Carbohydrate Polymers*. **1997**, 33, 153-162.
- [15] Perlin, A.S. Glycol-Cleavage Oxidation. *Advances in Carbohydrate Chemistry and Biochemistry*. **2006**, 60, 183-250.
- [16] Roye, C., K. Bulckaen, Y. De Bondt, I. Liberloo, D. Van De Walle, K. Dewettinck, and C.M. Courtin. Side-by-side comparison of composition and structural properties of wheat, rye, oat, and maize bran and their impact on in vitro fermentability. *Cereal Chemistry*. **2020**, 97, 20-33.
- [17] Pandeirada, C.O., D.W.H. Merckx, H.-G. Janssen, Y. Westphal, and H.A. Schols. TEMPO/NaClO₂/NaOCl oxidation of arabinoxylans. *Carbohydrate Polymers*. **2021**, 259, 117781.
- [18] Blumenkrantz, N. and G. Asboe-Hansen. New method for quantitative determination of uronic acids. *Analytical Biochemistry*. **1973**, 54, 484-489.
- [19] Thibault, J. and T. J.F. Automatisation du dosage des substances pectiques par la méthode au méthahydroxydiphényl. **1979**.
- [20] Huisman, M.M.H., A. Oosterveld, and H.A. Schols. Fast determination of the degree of methyl esterification of pectins by head-space GC. *Food Hydrocolloids*. **2004**, 18, 665-668.
- [21] Deckers, H.A., C. Olieman, F.M. Rombouts, and W. Pilnik. Calibration and application of high-performance size exclusion columns for molecular weight distribution of pectins. *Carbohydrate Polymers*. **1986**, 6, 361-378.
- [22] Team, R.C. *R: A language and environment for statistical computing*. 2017. Available from: <https://www.R-project.org/>.
- [23] Lê, S., J. Josse, and F. Husson. FactoMineR: An R Package for Multivariate Analysis. *Journal of Statistical Software*. **2008**, 25, 1 - 18.
- [24] Benjamini, Y. and Y. Hochberg. Controlling the False Discovery Rate: A Practical and Powerful Approach to Multiple Testing. *Journal of the Royal Statistical Society: Series B (Methodological)*. **1995**, 57, 289-300.
- [25] Pandeirada, C.O., S. Speranza, E. Bakx, Y. Westphal, H.-G. Janssen, and H.A. Schols. Partial acid-hydrolysis of TEMPO-oxidized arabinoxylans generates arabinoxylan-structure resembling oligosaccharides. *Carbohydrate Polymers*. **2022**, 276, 118795.



[26] da Silva, L.M., L.F.S. Araújo, R.C. Alvez, L. Ono, D.A.T. Sá, P.L.R. da Cunha, R.C. Monteiro de Paula, and J.S. Maciel. Promising alternative gum: Extraction, characterization, and oxidation of the galactomannan of *Cassia fistula*. *International Journal of Biological Macromolecules*. **2020**, 165, 436-444.



Supplementary data

Sugar composition of periodate oxidized samples

Table S 1. Yield, sugar composition and recovery, uronic acid (UA) recovery, and degree of oxidation (DO) of the periodate-oxidized (pOx-)polysaccharide (PS) samples derived from periodate oxidation (room temperature (RT), 6 h, 3.0 $\mu\text{mol NaIO}_4$ / mg PS) of various PS samples.

Sample	Yield (%, w/w) ^a	Sugar composition (% w/w) ^b					Total	UA recovery (%, w/w) ^c	Sugar Recovery yield (%, w/w) ^d	DO ^e (DO _{Rel}) ^f
		Ara	Gal	Glc	Xyl	Xyl				
BWX	100			0.4 ± 0.0	78.6 ± 0.9		79.0 ± 0.9	10.4 ± 0.2	100.0	0 (93)
pOx-BWX	79.2 ± 0.7			0	64.1 ± 1.9		64.1 ± 1.9	3.6 ± 0.0	63.9 ± 1.9	36.1 ± 3.2 (38.8 ± 3.5) ^f
WAX	100	34.4 ± 0.7		0.5 ± 0.1	63.3 ± 1.5		98.2 ± 2.1		100	0 (77)
pOx-WAX	44.8 ± 1.6	15.9 ± 0.2		0.2 ± 0.0	46.9 ± 0.6		63.0 ± 0.7		28.7 ± 0.3	71.3 ± 0.4 (92.6 ± 0.6) ^f
RAX	100	30.1 ± 0.9	0.6 ± 0.1	0.6 ± 0.1	46.3 ± 0.7		77.0 ± 1.6		100	0 (82)
pOx-RAX	57.3 ± 1.0	14.6 ± 0.1	0.6 ± 0.0	0.1 ± 0.0	37.3 ± 0.2		52.5 ± 0.3		39.1 ± 0.2	60.9 ± 0.4 (74.2 ± 0.5) ^f
MLG	100			100.1 ± 0.9			100.1 ± 0.9		100	0 (80)
pOx-MLG	29.3 ± 0.6			76.7 ± 2.5			76.7 ± 2.5		22.5 ± 0.7	77.5 ± 0.3 (96.8 ± 0.4) ^f
WS	100			87.7 ± 19.7			87.7 ± 19.7		100	0 (100)
pOx-WS	18.6 ± 1.3			45.3 ± 0.3			45.3 ± 0.3		10.3 ± 0.1	91.5 ± 1.8 (91.5 ± 1.8) ^f
XG*	100		5.4 ± 1.4	40.2 ± 0.8	22.6 ± 2.1		68.2 ± 4.2		100	0 (90)
pOx-XG*	89.2 ± 1.9		0	47.8 ± 6.6	4.6 ± 2.1		52.5 ± 8.8		68.6 ± 11.6	31.4 ± 0.9 (34.9 ± 1.0) ^f
Cel*	100			81.0 ± 0.7			81.0 ± 0.7		100	0 (100)
pOx-Cel*	99.0 ± 1.2			89.0 ± 2.3			89.0 ± 2.3		108.8 ± 2.8	0 (0)



Table S 1. Continuation.

Sample	Yield (%, w/w) ^a	Sugar composition (%, w/w) ^b						Total	Sugar Recovery yield (%, w/w) ^d	DO ^e (DO _{Rel}) ^f
		Ara	Gal	Glc	Xyl	Man				
WAX:MLG	100	29.3 ± 1.3		5.9 ± 0.2	51.9 ± 3.2		87.1 ± 4.7	100	0 (77)	
pOx-	54.6 ± 0.7	13.5 ± 0.2		7.7 ± 0.1	40.1 ± 0.5		61.2 ± 0.7	38.4 ± 0.5	61.6 ± 2.4 (79.8 ± 3.1) ^f	
WAX:MLG:W	100	21.5 ± 0.2		36.9 ± 0.6	38.7 ± 0.3		97.1 ± 0.2	100	0 (84)	
S										
pOx-	48.0 ± 2.6	23.2 ± 0.2		8.4 ± 0.3	48.2 ± 0.3		79.8 ± 0.4	39.1 ± 0.2	60.9 ± 5.3 (72.4 ± 6.3) ^f	
WAX:MLG:W										
S										
RAX:MLG	100	27.8 ± 0.9	0.5 ± 0.0	13.5 ± 0.4	42.5 ± 1.9		84.3 ± 2.5	100	0 (82)	
pOx-	63.5 ± 1.5	11.8 ± 0.3	0.4 ± 0.0	12.4 ± 0.2	31.4 ± 0.6		55.9 ± 1.1	42.1 ± 0.9	57.9 ± 1.0 (70.8 ± 1.2) ^f	
RAX:MLG										
RAX:MLG:WS	100	8.4 ± 0.4		63.0 ± 5.6	15.4 ± 0.4		86.8 ± 6.4	100	0 (94)	
pOx-	37.0 ± 0.6	13.9 ± 0.0		22.9 ± 0.9	28.3 ± 0.1		65.2 ± 0.9	27.8 ± 0.4	72.2 ± 0.4 (77.1 ± 0.4) ^f	
RAX:MLG:WS										
GGM*	100		35.5 ± 2.1				104.4 ± 5.9	100	0 (100)	
pOx-GGM*	82.8 ± 1.0		0				24.9 ± 5.0	19.7 ± 3.9	80.3 ± 0.8 (80.3 ± 0.8) ^f	
LBGM	100		15.2 ± 0.2	1.1 ± 0.0			70.3 ± 0.5	100	0 (100)	
pOx-LBGM	64.6 ± 0.6		0.2 ± 0.1	0.1 ± 0.0			30.4 ± 0.3	27.9 ± 0.3	72.1 ± 0.6 (72.1 ± 0.6) ^f	



Table S 1. Continuation.

Sample	Yield (%, w/w) ^a	Sugar composition (%, w/w) ^b							Total	UA recovery (%, w/w) ^c	Sugar Recovery yield (%, w/w) ^d	DO ^e (DO _{Rel}) ^f
		Ara	Rha	Gal	Glc	Man	GalA					
HG	100	0.3 ± 0.0		3.1 ± 0.2	0.7 ± 0.0			65.5 ± 2.8	70.5 ± 0.9	100**	0 (100)	
pOx-HG	98.2 ± 1.2	0		0.2 ± 0.1	0			16.2 ± 0.9	43.2 ± 1.2	61.3 ± 1.6*	38.7 ± 0.8*	
ABN	100	63.4 ± 0.8	1.8 ± 0.1	11.5 ± 0.1	2.6 ± 0.1			4.7 ± 0.3	10.5 ± 0.0	100	0 (62)	
pOx-ABN	59.6 ± 25.8	52.6 ± 3.2	0	4.7 ± 0.3	0			2.7 ± 0.0	4.0 ± 0.0	39.2 ± 1.9	60.8 ± 13.2 (98.1 ± 21.3) ^f	
RG-I	100		1.7 ± 0.1	9.0 ± 0.4	0.1 ± 0.0			39.1 ± 1.6	56.4 ± 0.2	100***	0 (66)	
pOx-RG-I	83.4 ± 0.6		0	1.8 ± 0.1	0			18.4 ± 1.1	31.9 ± 0.6	49.8 ± 1.5*	50.2 ± 1.5*	
PS mix*	100	5.1 ± 0.5		1.2 ± 0.6	2.9 ± 1.1	2.0 ± 0.0		10.2 ± 3.1	28.0 ± 2.4	100	0 (81)	
pOx-PS mix*	92.9 ± 0.4	1.7 ± 0.0		0	4.1 ± 0.0	0		5.0 ± 0.0	17.3 ± 0.2	45.3 ± 0.0	54.7 ± 15.6 (67.7 ± 19.3) ^f	

^a Average (n=2) yield in weight % relative to the native polysaccharide (PS) sample.

^b Results are expressed as average weight % of sample (n=2 for native PS and n=4 for pOx-PS). * Results are obtained after hydrolysis to monosaccharides by sulphuric acid hydrolysis. Remaining samples were hydrolysed using a methanolysis procedure.

^c Results are expressed as average weight % of native polysaccharide (n=2 for native PS and n=4 for pOx-PS).

^d Relative sugar recovery relatively to the total sugar content of the native polysaccharide, expressed as average (n=2 for native PS and n=4 for pOx-PS) weight %.

^e ** Relative sugar recovery relatively to the total UA content of the native polysaccharide, expressed as average (n=4 for pOx-PS) weight %.

^f *** Sugar recovery yield considering Rha, Gal, Glc and UA content.

^g DO based on the sugar recovery decrease relative to the respective native PS samples. (#) is the maximum DO that can theoretically (DO_{Theo}) be obtained per polysaccharide.

^h Relative degree of oxidation (DO_{Rel}) in % was calculated as follows:

$$DO_{Rel} (\%, w/w) = \frac{DO}{DO_{Theo}} \times 100$$



Effect of periodate oxidation and AC121 treatment on the Mw distribution of polysaccharides

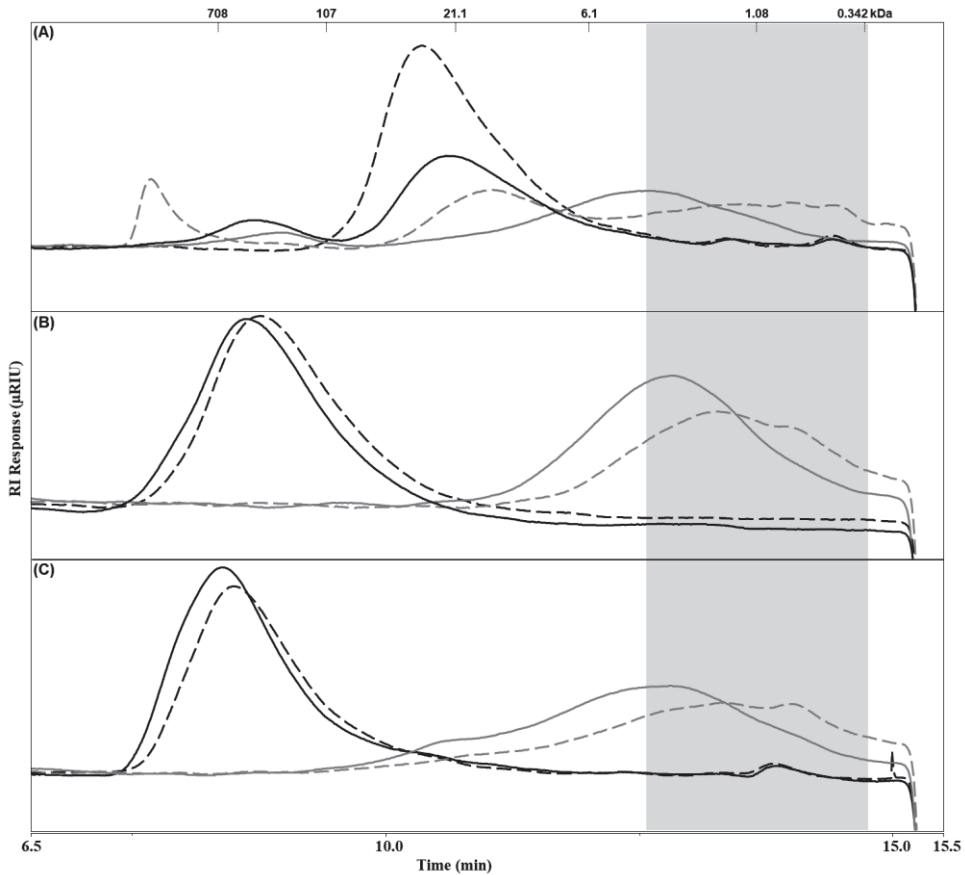


Figure S 1. HPSEC elution patterns of BWX (A), WAX (B), and RAX (C) derived samples. Native polysaccharide (PS) samples before and after AC121 treatment are shown in black full and dashed lines, respectively. Periodate-oxidized PS samples before and after AC121 treatment are shown in grey full and dashed lines, respectively. Pullulan standards were used to calibrate the system. Grey boxes indicate the time range corresponding to an apparent degree of polymerization between 2 and 20.

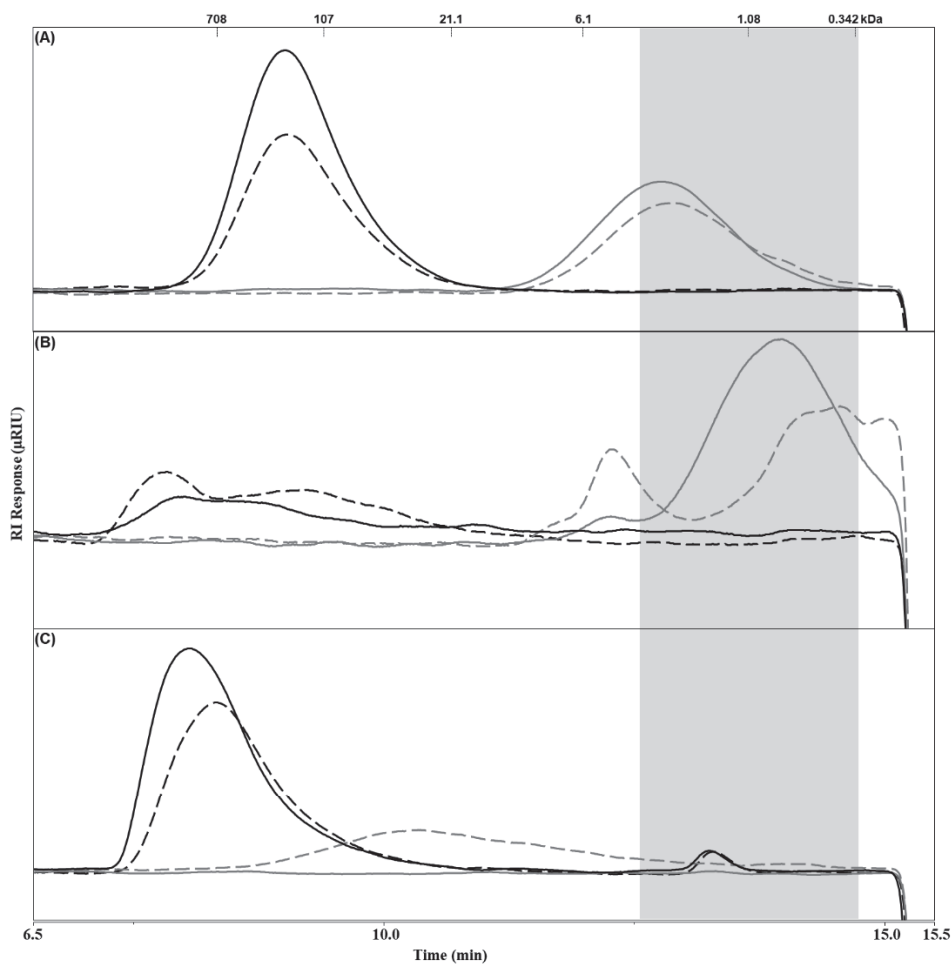


Figure S 2. HPSEC elution patterns of MLG (A), WS (B), and XG (C) derived samples. Native polysaccharide (PS) samples before and after AC121 treatment are shown in black full and dashed lines, respectively. Periodate-oxidized PS samples before and after AC121 treatment are shown in grey full and dashed lines, respectively. Pullulan standards were used to calibrate the system. Grey boxes indicate the time range corresponding to an apparent degree of polymerization between 2 and 20.

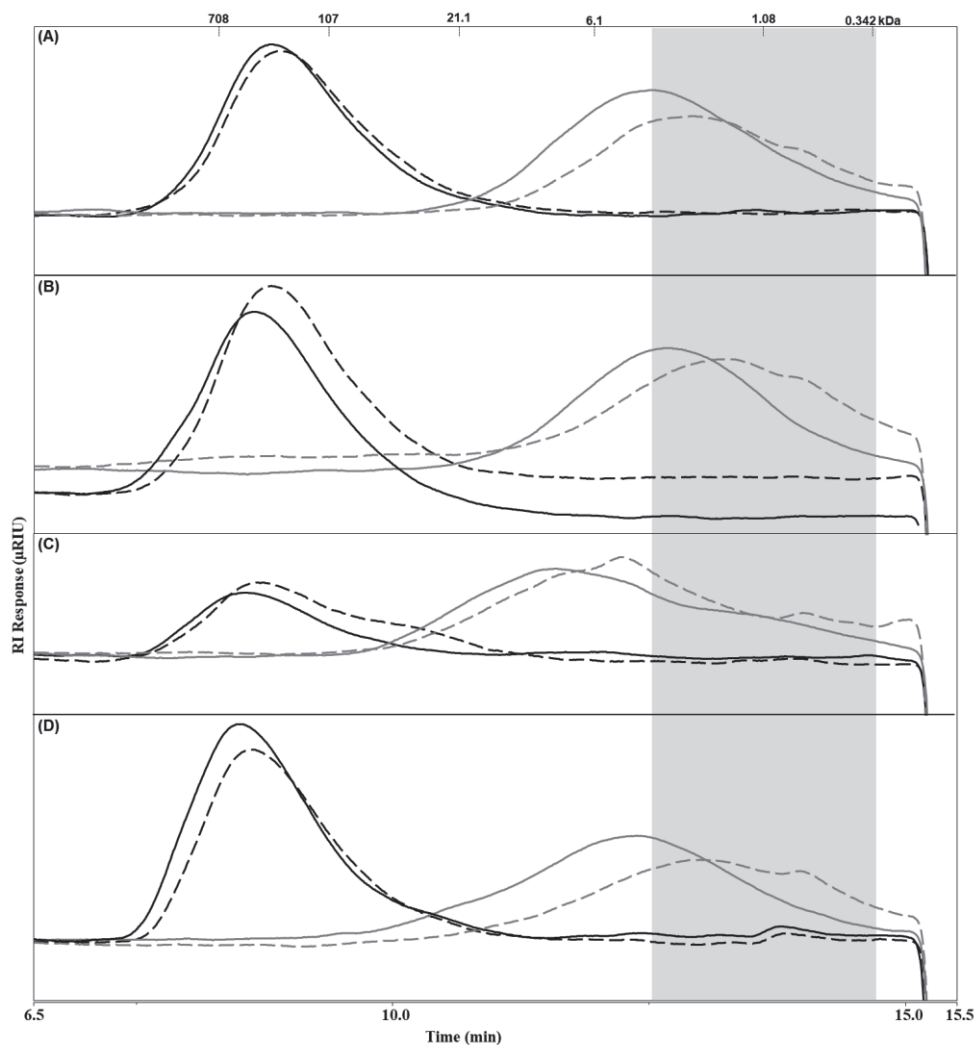


Figure S 3. HPSEC elution patterns of WAX:MLG (A), WAX:MLG:WS (B), RAX:MLG (C), and RAX:MLG:WS (D) derived samples. Native polysaccharide (PS) sample mixtures before and after AC121 treatment are shown in black full and dashed lines, respectively. Periodate-oxidized PS sample mixtures before and after AC121 treatment are shown in grey full and dashed lines, respectively. Pullulan standards were used to calibrate the system. Grey boxes indicate the time range corresponding to an apparent degree of polymerization between 2 and 20.

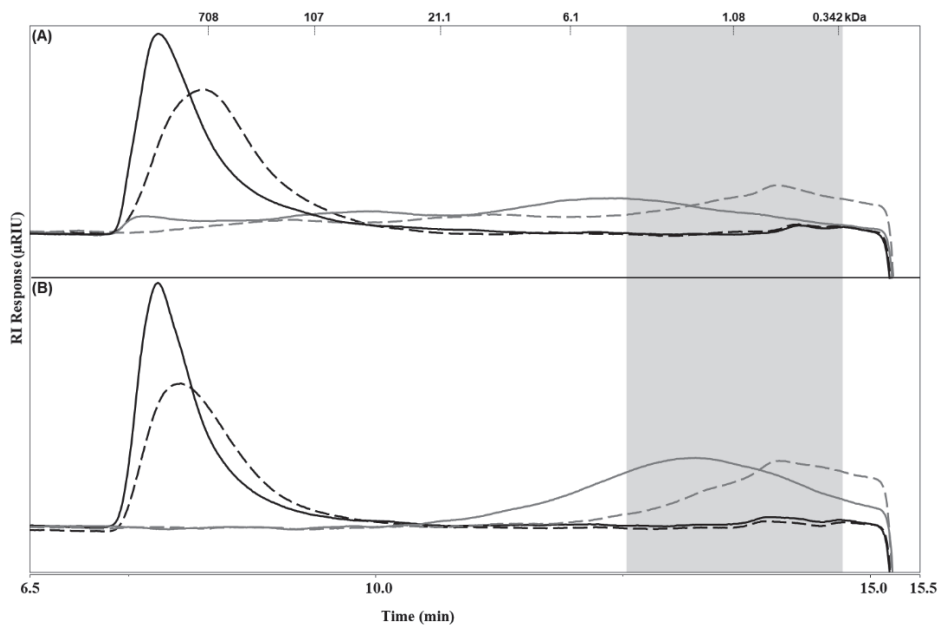


Figure S 4. HPSEC elution patterns of GGM (A), and LBGM (B) derived samples. Native polysaccharide (PS) samples before and after AC121 treatment are shown in black full and dashed lines, respectively. Periodate-oxidized PS samples before and after AC121 treatment are shown in grey full and dashed lines, respectively. Pullulan standards were used to calibrate the system. Grey boxes indicate the time range corresponding to an apparent degree of polymerization between 2 and 20.

5

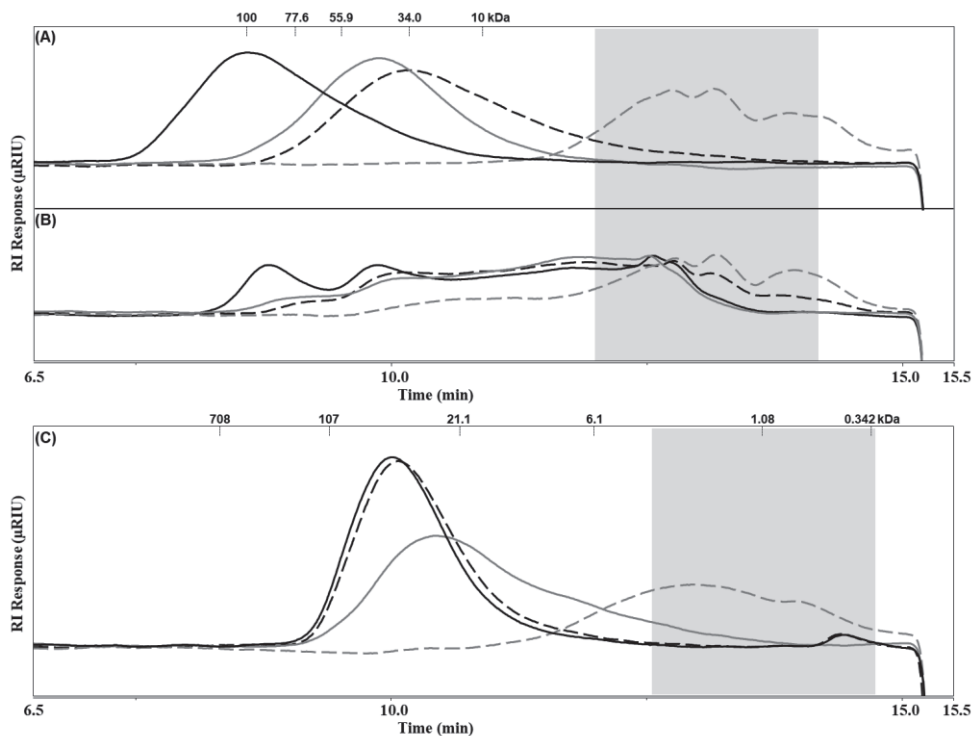


Figure S 5. HPSEC elution patterns of HG (A), RG-I (B) and ABN (C) derived samples. Native polysaccharide (PS) samples before and after AC121 treatment are shown in black full and dashed lines, respectively. Periodate-oxidized PS samples before and after AC121 treatment are shown in grey full and dashed lines, respectively. Pectin standards were used to calibrate the system for HG and RG-I samples, and pullulan standards were used to calibrate the system for ABN samples. Grey boxes indicate the time range corresponding to an apparent degree of polymerization between 2 and 20.

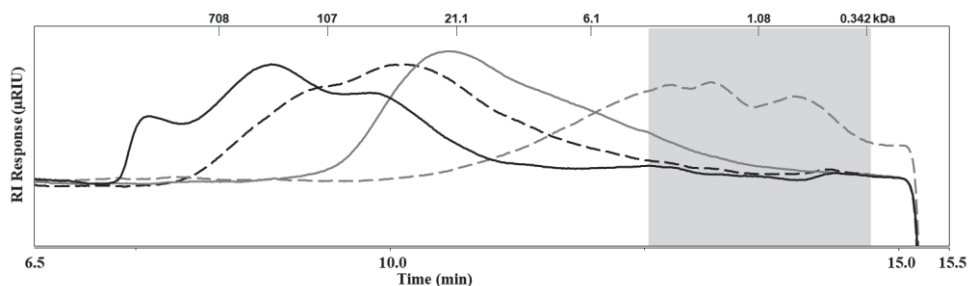


Figure S 6. HPSEC elution patterns of PS mix (WAX:MLG:GGM:HG:RG-I:ABN) and derived samples. Native PS mix samples before and after AC121 treatment are shown in black full and dashed lines, respectively. Periodate-oxidized PS mix samples before and after AC121 treatment are shown in grey full and dashed lines, respectively. Pullulan standards were used to calibrate the system. Grey boxes indicate the time range corresponding to an apparent degree of polymerization between 2 and 20.



Influence of the autoclave treatment at 121 °C on the methyl- and acetyl-content of periodate-oxidized HG and RG-I samples

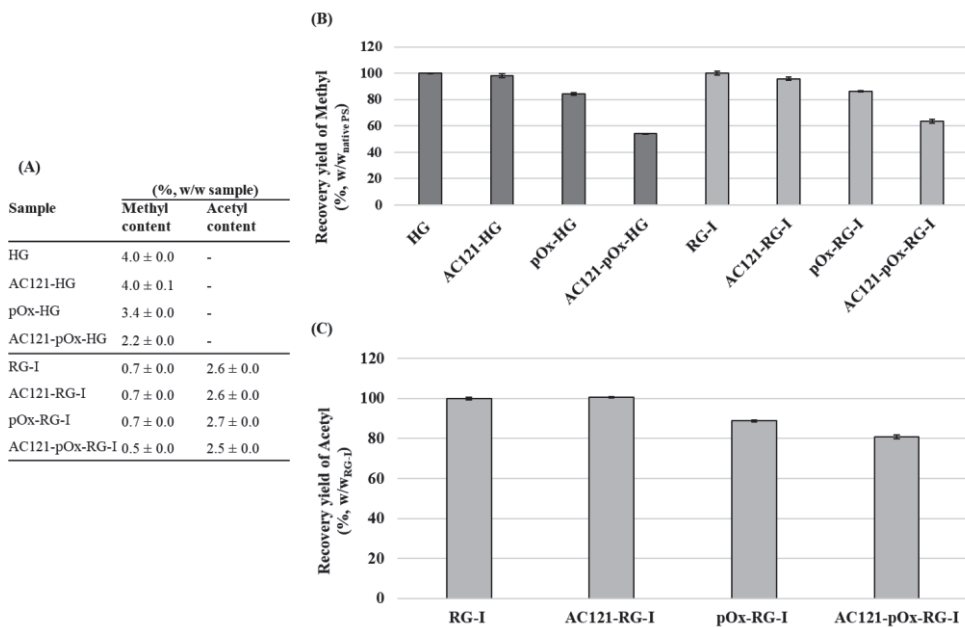


Figure S 7. Methyl-ester and acetyl content (% w/w) (A), methyl-ester recovery yield (B), and acetyl recovery yield (C) of the homogalacturonan (HG) and rhamnogalacturonan-I (RG-I) samples before and after AC121 treatment, and of the periodate-oxidized (pOx-)HG and RG-I samples before and after AC121 treatment. Recovery yield relatively to the native PS sample.

Chapter 6

General Discussion



1. Motivation and aim of the research

Recognition and structural characterization of polysaccharides of food products is of high interest for food industry since polysaccharides, especially from plant origin, are added to foods as functional ingredients with the purpose to modulate food texture and physical properties and/or as dietary fibres to provide health benefits [1, 2]. Thus, a fast and generic recognition and characterization of polysaccharides is desirable to optimize the utilization of food polysaccharides and/or food raw materials. Detailed characterization of polysaccharide (PS) chemical structures can be performed by depolymerization of polysaccharides to structure-informative (diagnostic) oligosaccharides [3, 4], followed by analysis of the oligosaccharides released by advanced analytical techniques such as liquid chromatography (LC) and mass spectrometry (MS) [5, 6]. MS analysis of these diagnostic oligosaccharides allows recognition and characterization of the chemical structure of the parental PS. To find a generic and accessible PS depolymerization method to obtain diagnostic oligosaccharides that allow us to structurally recognize and/or characterize plant polysaccharides, this PhD research investigated various chemical-induced PS depolymerization approaches. In this chapter, the main findings obtained in this PhD thesis will be discussed and reflected upon. In addition, the chemical-induced depolymerization methods studied in this research will be compared against the traditional enzymatic PS depolymerization method and against recent developed non-enzymatic depolymerization approaches. Lastly, potential application and exploitation of the chemical reactions investigated in this research will be put into perspective.

2. Promising chemical-induced polysaccharide depolymerization approaches to obtain oligosaccharides

In this PhD thesis, two chemical approaches were investigated for a defined depolymerization of various plant polysaccharides: TEMPO-oxidation of arabinoxylans (AXs) followed by partial acid-hydrolysis, and periodate oxidation with and without thermal treatment for several polysaccharides (Fig.1).

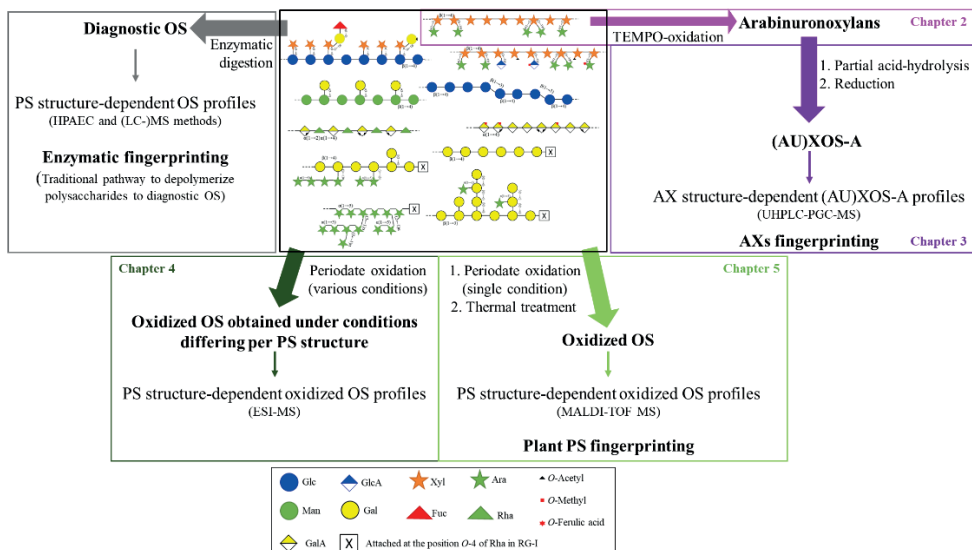


Figure 1. Summary of the chemical polysaccharide (PS) depolymerization approaches investigated in this PhD thesis (colored boxes). Traditional enzymatic PS depolymerization approach is included in the grey box. AX, arabinoxylan; (AU)XOS-A, (arabinurono-)xylo-oligomer alditols; OS, oligosaccharides.

TEMPO-oxidation based depolymerization approach for arabinoxylans

Diagnostic xylo-oligosaccharides (XOS) carrying Ara side chains cannot be obtained directly from partial acid-hydrolysis of AXs due to the low stability of the Ara substituents to acid treatment. TEMPO-oxidation of AXs was performed to selectively oxidize Ara side chains into its uronic acid form (arabinuronic acid, AraA) (**Chapters 2 and 3**). This reaction was performed to increase the stability of the Ara side chains to acid hydrolysis, since the glycosidic linkage between a uronic acid and a neutral sugar is more resistant to acid hydrolysis than the linkage between neutral sugars [7]. After TEMPO-oxidizing a wheat AX using various TEMPO:NaClO₂:NaOCl ratios, it was found that using a TEMPO:NaClO₂:NaOCl ratio of 1.0:2.6:0.4 per mol of Ara allows us to obtain a high molecular weight (Mw) oxidized arabinoxylan (ox-)AX (arabinuronoxylan) with a xylan backbone mainly substituted with AraA residues (Fig. 2). This arabinuronoxylan, named ox-AX^{1.0:2.6:0.4} (**Chapter 2**), had an AraA distribution over the xylan backbone intimately related to its parental AX structure. This result is highly important to trustworthily determine the structure of the parental PS.

After successful oxidation of wheat AX to arabinuronoxylan, various structurally different AXs (wheat, partially-debranched wheat and rye AXs) were TEMPO-oxidized using the above TEMPO:NaClO₂:NaOCl system and subsequently partially acid-hydrolyzed and NaBD₄-reduced (**Chapter 3**). To analyze the oligosaccharides formed, a UHPLC-PGC-MS method was developed. The UHPLC-PGC-MS profiles showed the presence of linear XOS alditols (XOS-A) and substituted XOS with AraA units (arabinurono-xylo-oligomer alditols, AUXOS-A) (Fig. 2). This result highlighted that the AraA→Xyl linkage is more resistant to acid hydrolysis by 0.2 M TFA at 90 °C for 2 h than the Ara→Xyl linkage, and that substituted XOS can successfully be obtained. AUXOS-A could be easily

identified and distinguished from linear XOS-A because AraA is no longer an isomer of Xyl and Ara (Fig. 2). This allows us to overcome a limitation of MS to distinguish compounds comprising isomers e.g., XOS from arabino-xylo-oligomers (AXOS). Additionally, the developed UHPLC-PGC-MS method allowed separation of isomeric AUXOS-A with a degree of polymerization (DP) from 2-5, comprising one and two AraA substituents (Fig. 2). This result demonstrated the ability of the PGC column to efficiently separate neutral and acidic oligosaccharides [8-11]. More importantly, due to efficient separation of AUXOS-A isomers, AX structure-dependent UHPLC-PGC-MS oligosaccharide profiles could successfully be obtained for structurally different AXs investigated in this PhD thesis (**Chapter 3**; Fig. 2 and 5). Some Ara(A) was lost during TEMPO-oxidation and/or partial acid-hydrolysis of the arabinuroxylans, not allowing us to obtain AUXOS-A fully representing the native AX structure. However, the clear differences in the PGC-MS oligosaccharide profiles allowed us to assign various marker AUXOS-A per AX. This remarkable finding indicates that the different level and distribution of substituents of the AXs are reflected in the oligosaccharides formed, proving their diagnostic character. Therefore, the UHPLC-PGC-MS AUXOS-A profiles can be used for AXs fingerprinting to recognize different AXs.

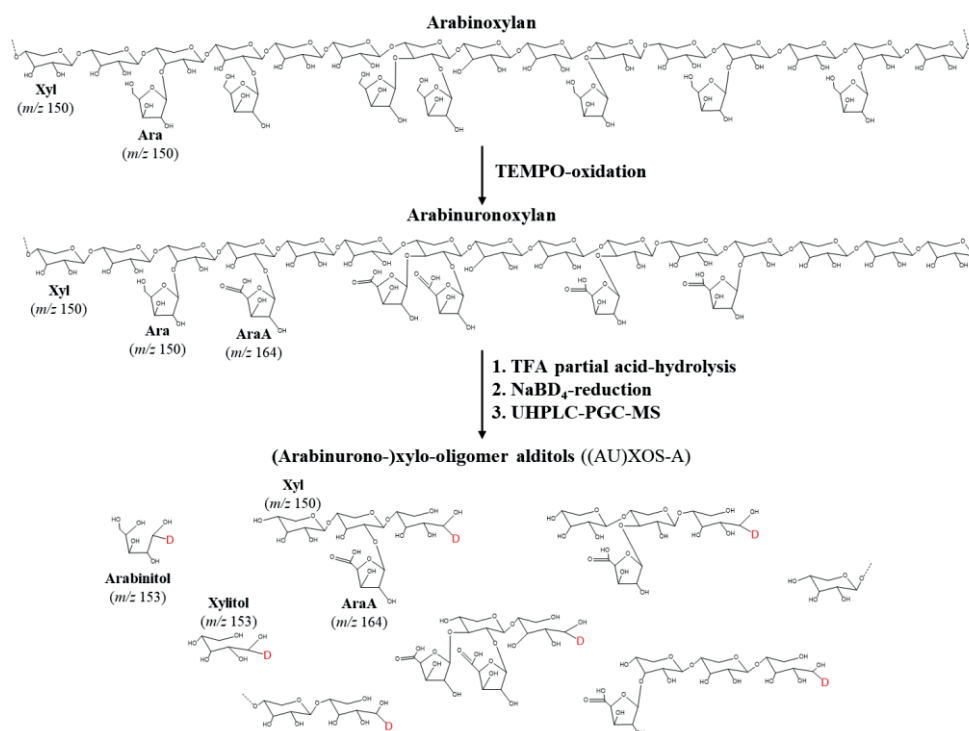


Figure 2. Illustration of the arabinoxylan depolymerization approach studied in this PhD thesis consisting of TEMPO-oxidation of arabinoxylans followed by partial acid-hydrolysis (0.2 M TFA, 90 °C, 2 h), NaBD₄-reduction, and analysis of the (AU)XOS-A by UHPLC-PGC-MS. Molecular masses of xylose (Xyl), arabinose (Ara), arabinuronic acid (AraA), arabinitol, and xylitol are given in parentheses.

Conclusive and tentative characterization of isomeric AUXOS-A structures could be reached by combining tandem MS analysis of AUXOS-A with sugar and linkages analyses of the intact PS (**Chapter 3**). Various isomeric AUXOS-A structures could be successfully assigned, e.g., AUXOS-A DP 4 containing a double AraA substituted Xyl unit, and an isomeric AUXOS-A DP 4 containing one Xyl unit substituted with Ara at position *O*-3 (**Chapter 3**; Table 2 isomer **d**₂) or at position *O*-2 (**Chapter 3**; Table 2 isomer **d**_s). Characterization of the AUXOS-A structures also reflected the structural differences among AXs, confirming that wheat AX was more double substituted with Ara(A) units than the partially-debranched wheat AX and the rye AX. In addition, it was confirmed that single-substitution of the Xyl unit preferably occurred at position *O*-3 of these AX samples. Therefore, the findings obtained in **Chapter 3** give us confidence to extend the proposed method to other types of AXs to recognize different AXs by AUXOS-A fingerprinting, and to study their main structural differences.

Periodate oxidation based depolymerization approaches for plant polysaccharides

Given the high specificity of the periodate oxidation towards vicinal hydroxyl groups and the noticeable decrease in the Mw of polysaccharides after periodate oxidation [12-15], various plant polysaccharides (birch wood xylan – BWX; wheat - WAX; guar galactomannan – GGM; xyloglucan – XG; and homogalacturonan – HG) were periodate-oxidized using various conditions to investigate if polysaccharides are depolymerized to oligosaccharides (**Chapter 4**). By testing different NaIO₄ concentrations, reaction temperatures and times, it was shown that each PS could be depolymerized to oligosaccharides, albeit under different periodate oxidation conditions, as shown by the HPSEC results (**Chapter 4**; Fig. 1). Direct infusion electrospray (ESI-)MS analysis of the oligosaccharides released showed characteristic clusters of oxidized oligosaccharide profiles, which comprised sub-clusters of oxidized oligosaccharides (**Chapter 4**; Fig. 3). Remarkably, even when polysaccharides were only partially oxidized, clusters of (oxidized) oligosaccharides were formed. These clusters of oxidized oligosaccharides had very complex structures, as found by ESI-MS/MS analyses. Besides non-oxidized sugar units, the oxidized oligosaccharides comprised oxidized sugar units in the form of e.g., dialdehydes, hemialdals, and remnants of sugars (Fig. 3). To the best of our knowledge this was the first time that ESI-MS/MS was used to unravel structural features of the type of oxidized oligosaccharides exclusively resulting from the periodate oxidation of plant polysaccharides. Due to the formation of all these oxidized sugar products, independent clusters of oxidized oligosaccharides were formed per structurally different PS which was reflected in PS-dependent ESI-MS oligosaccharide profiles (**Chapter 4**; Fig. 3). Remarkably, even polysaccharides composed of isomeric sugar units (BWX vs WAX) exhibited independent clusters of oxidized oligosaccharides. Although some of the oxidized oligosaccharides derived from GGM and XG were partially debranched, and from HG were partially de-(methyl-) esterified, the PS structure-dependent MS oligosaccharide profiles outlined the potential of periodate oxidation of polysaccharides to release oligosaccharides for PS fingerprinting. Hence, finding a single PS depolymerization condition based on periodate oxidation will potentially enable plant polysaccharides recognition in a generic manner.

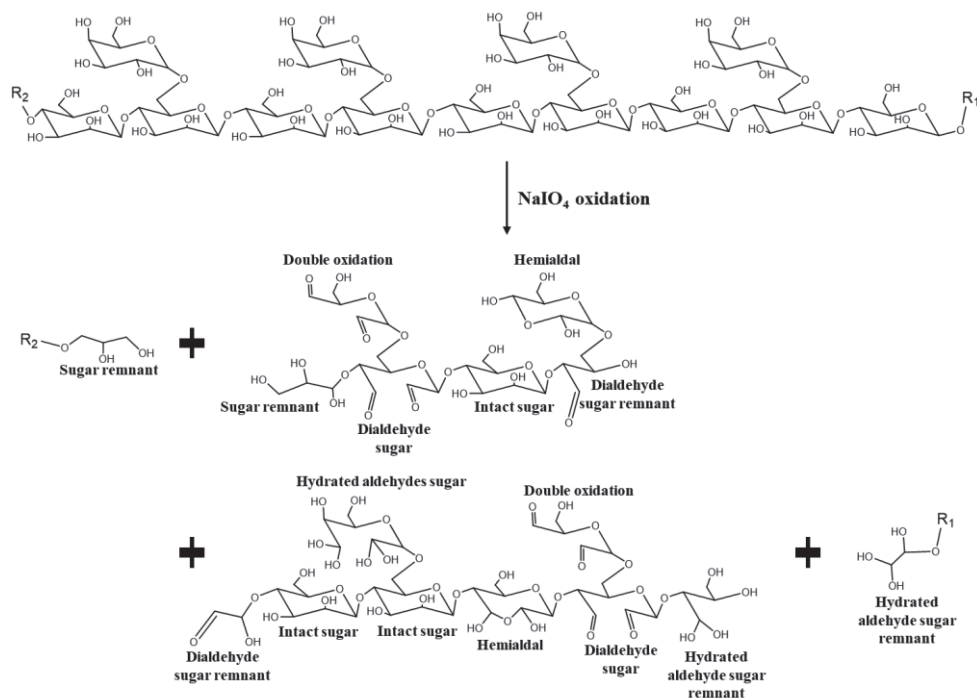


Figure 3. Overview of the possible structures present in oxidized oligosaccharides derived from periodate oxidation of a polysaccharide in aqueous systems, using guar galactomannan as example. The oxidized compounds depicted were based on the ESI-MS/MS experiments described in **Chapter 4**. R_1 and R_2 are the remaining polysaccharide chains comprising the reducing end and non-reducing end, respectively.

To have a single PS depolymerization method based on periodate oxidation for various plant polysaccharides, periodate oxidation of polysaccharides followed by a thermal treatment was chosen as approach, since periodate-oxidized polysaccharides are quite sensitive to subsequent degradation reactions [16]. A broad range of plant polysaccharides, including xylans (BW_X, W_X, rye AX – RAX), glucans (cellulose – Cel, wheat starch – WS, mixed linked-glucan – MLG, and XG), galactomannans (GGM and locust bean GM – LBGM), pectic polysaccharides (HG, rhamnogalacturonan I – RG-I, and arabinan – ABN), and PS mixes ((R/W)AX:MLG, (R/W)AX:MLG:WS, and W_X:MLG:GGM:HG:RG-I:ABN (1:1:1:1:1:1 ratio (w/w)) were periodate-oxidized using a single set of periodate oxidation conditions. The conditions used led to partial oxidation of polysaccharides and allowed us to keep most of the structural features of the original polysaccharides, which is essential to reliably identify/characterize the parental PS. These periodate-oxidized (pOx-) polysaccharides and mixes thereof were thermally depolymerized using an autoclave (AC) treatment at 121 °C, giving AC121-pOx-PS samples. Our results showed that all AC121-pOx-PS samples contained oligosaccharides, except XG (**Chapter 5**; Table 1). This result highlighted the potential of the proposed approach to depolymerize plant polysaccharides into oligosaccharides in a generic manner, even when they are present in a PS mix.

Considering that MALDI-TOF MS is a quicker and a more straight forward technique than direct infusion ESI-MS, MALDI-TOF MS was the technique chosen to quickly screen the oligosaccharides

released from periodate-oxidized polysaccharides after AC treatment. PS structure-dependent MALDI-TOF MS oligosaccharide profiles were obtained per AC121-pOx-PS (**Chapter 5**). These oligosaccharide profiles contain clusters of oxidized oligosaccharides, as found in **Chapter 4**. Importantly, the MALDI-TOF MS results emphasized that even polysaccharides composed of isomeric sugar units that are structurally different, e.g., BWX, AXs, and ABN (Fig. 4); or MLG and WS; or GGM and LBGM, generate unique oxidized oligosaccharide MS profiles. This structural heterogeneity of polysaccharides was clearly illustrated by principal cluster analysis (PCA) of the MALDI-TOF MS data obtained (Fig. 4). Although the MALDI-TOF mass spectra of AC121-pOx-WAX and AC121-pOx-RAX showed that both AXs were composed of the same clusters of oxidized oligosaccharides only slightly differing in the proportion of the sub-clusters of oligosaccharides, PCA really highlighted their structural variation (Fig. 2). Therefore, when closely related MALDI-TOF MS oligosaccharide profiles are obtained between samples, it is highly recommended to perform PCA in order to emphasize the structural differences of samples. Furthermore, based on significantly different ($p < 0.05$) marker m/z values identified for each AC121-pOx-PS class in the MALDI-TOF mass spectrum, recognition of different PS classes present in a PS mix could be accomplished. These findings were highly relevant since they show that periodate oxidation of polysaccharides followed by a thermal treatment and analysis of the oligosaccharides released by MALDI-TOF MS can possibly be used as a fingerprinting approach to recognize plant polysaccharides (Fig. 1). Furthermore, these results offer the possibility to extend this approach to other food polysaccharides, such as alginate, to create a MALDI-TOF MS oligosaccharide library to recognize food polysaccharides. Importantly, the proposed approach also shows potential to screen for PS-types present in a food product.

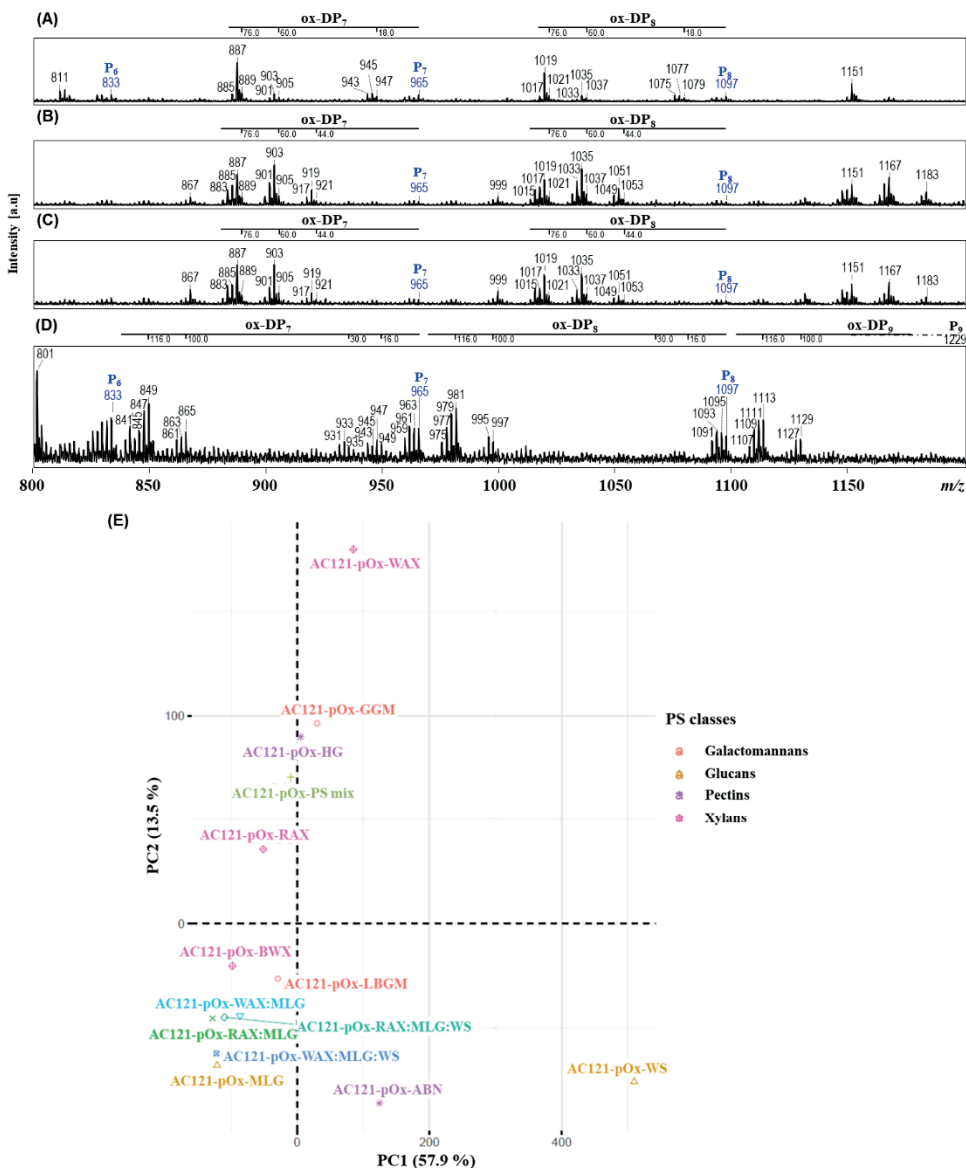


Figure 4. MALDI-TOF mass spectra (m/z 800-1200 range) of the AC121 treated periodate-oxidized BWX (A), WAX (B), RAX (C), and ABN (D). Principal component analysis (PCA) biplot (E) constructed with the MALDI-TOF mass spectra data (m/z 800-1200) of the various AC121 treated periodate-oxidized BWX, WAX, RAX, MLG, WS, GGM, LBGM, HG, ABN, AX:MLG(:WS), and PS mix samples. The PCA scores were plotted for PC1 and PC2, and the amount of variance explained by each PC is shown in parentheses. P_n – Na⁺ adduct of an oligomer composed of n pentoses (Ara or Xyl). ox-DP_n – m/z region of a cluster of oxidized oligosaccharides potentially with a n DP. m/z differences from each sub-oligosaccharide cluster with $\Delta -(x + n*2)$ Da, $n = 0-4$, to the corresponding non-oxidized DP-oligomer are depicted in (A-D). Detected non-oxidized oligomers are highlighted in blue in (A-D).

3. Challenges and promising methods to quantify and characterize oxidized saccharide structures

Chemical modification with simultaneous degradation of polysaccharides are promising approaches to depolymerize polysaccharides to oligosaccharides. However, when using chemical approaches to depolymerize polysaccharides sugar units can be modified in such a way that quantification and characterization of modified sugar units gets really challenging. In this section, remaining questions regarding quantification and characterization of the chemical modified saccharide fragments generated in the previous chapters of this PhD thesis will be discussed and reflected upon. In addition, approaches to potentially reach a more accurate quantification and characterization of these modified saccharide fragments will be put into prospect.

Quantification of arabinuronic acid (AraA)

In **Chapters 2** and **3**, the Ara side chains of AXs were selectively oxidized using TEMPO to AraA (Fig. 2), which was confirmed by 1D- and 2D-NMR, by glycosidic linkage analysis, and by UHPLC-PGC-MS analysis. Nonetheless, accurate AraA quantification could not be attained in our study. Quantification of AraA by HPAEC-PAD analysis of the hydrolysate of the ox-AXs was hampered by the absence of a commercially available AraA standard. Quantification of AraA could not be performed neither using e.g. galacturonic acid (GalA) nor Ara standards because the response factor of the sugars is sugar-dependent, as demonstrated e.g., for aldaric acids in comparison to neutral sugars [17].

Although NMR can be used to quantify monomeric components after complete hydrolysis of polysaccharides without using monosaccharide standards [18, 19], AraA quantification using NMR so far was not possible. This was because the ^1H -NMR spectrum of the ox-AX^{1.0:2.6:0.4} hydrolysate besides having chemical shifts derived from AraA, also had chemical shifts derived from modification of some AraA units during full acid hydrolysis of ox-AX^{1.0:2.6:0.4}. (**Chapter 2**; Fig. 3). Additionally, the α -AraA chemical shifts present in the ^1H -NMR spectrum of the intact ox-AX^{1.0:2.6:0.4} (**Chapter 2**; Fig. 4) could also not be used to estimate the AraA content because the arabinuronoxylan solution was much more viscous than the parental AX solution, and high viscosities negatively affect NMR resolution [20].

During this PhD research, quantification of AraA was also attempted by using the meta-hydroxydiphenyl (*m*-HDP) colorimetric method [21]. However, after subjecting arabinuronoxylans to this method, no color was developed. The *m*-HDP method is based on the concentrated sulfuric acid hydrolysis of polysaccharides, releasing dehydrated monosaccharides in various furan structures [22] that will react with *m*-HDP [23]. Unfortunately, dehydration of AraA will likely not result in a furan structure due to the presence of a carboxyl group at C5, which might have hindered AraA quantification.

A method that can lead to a more accurate quantification of AraA is based on gas chromatography (GC) – MS analysis of open-chain trimethylsilyl (TMS) derivatives [24-27]. Although this method was not investigated in this PhD thesis, it is worth investigating in the future. Alternatively, synthesizing an AraA standard might be a solution to quantify AraA using HPAEC-PAD analysis. This could be done e.g., by oxidation of Ara f to Ara A_f via methyl glycosidation of Ara f , followed by oxidation of the



methyl Ara f to methyl AraA f using platinum oxide, and hydrolysis of the methyl AraA f to AraA f [28]. To note, attention must be paid to the Ara furanose-pyranose ratios in solution [29, 30], as a furanose ring for Ara is required to obtain a penturonic acid.

Quantification of periodate-oxidized sugars

In **Chapters 4** and **5**, the periodate-oxidized polysaccharides had a poor total sugar recovery in comparison to the native PS samples. This was due to modification of the sugar structures in the oxidation process, leading to underestimation of the total carbohydrate-derived content of a pOx-PS by HPAEC-PAD analysis of the pOx-PS hydrolysates. The modified sugar units formed (Fig. 3) are rather challenging to be quantified. An approach to better quantify the total carbohydrate-derived content of a pOx-PS could be by measuring the total organic carbon (TOC) of each sample [17]. This would allow us to derive a carbon mass balance and it would provide information about the recovery of the isolated periodate-oxidized material. Additionally, determining both the sugar composition and the TOC of each pOx-PS would allow to determine the total non-oxidized and oxidized sugars content.

Characterization of TEMPO-oxidized AXs and AUXOS-A

Although GC-MS analysis of the carbodiimide/NaBD₄ carboxyl-reduced and partially methylated alditol acetates derived from ox-AX^{1.0:2.6:0.4} allowed us to identify AraA, accurate glycosidic linkage results were not obtained due to incomplete reduction of AraA to Ara (**Chapter 2**). Recently, Galermo et al. [31] have developed an UHPLC/ triple quadrupole (QqQ) MS method to analyze the glycosidic linkages of polysaccharides. This method consists of per-methylation of the polysaccharide, acetylation, acid hydrolysis and 1-phenyl-3-methyl-5-pyrazolone (PMP) derivatization, followed by analysis of the partially methylated PMP-labeled monosaccharides using reverse-phase (RP-)UHPLC/QqQ MS. It allowed determination of both neutral and acidic partially-methylated PMP-labeled monosaccharide residues. This method could be worth investigating to attempt a more complete characterization of the TEMPO-oxidized AXs.

The UHPLC-PGC-MS method described in **Chapter 3** allowed us to detect and characterize AUXOS-A in a DP 2-5 range, but from the HPSEC elution patterns of the TFA partially acid-hydrolyzed ox-AX samples (**Chapter 3**; Fig. 1), longer AUXOS(-A) would be expected. Characterization of longer AUXOS-A would provide more insights on the PS chemical structure. From literature, oxidized cello-oligosaccharides longer than DP 5 could also not be successfully eluted from a PGC material even at high elution strengths [32, 33]. HILIC is an alternative/complementary technique that can successfully elute (AU)XOS with longer DPs [34] with appropriate separation of isomeric structures [35].

Although UHPLC-PGC-MS analysis of AUXOS-A was effective in separating isomeric AUXOS-A structures and conclusively assigning various isomeric AUXOS-A structures by tandem MS analysis (**Chapter 3**), some distinct isomeric AUXOS-A structures could only be tentatively assigned. This was due to rather similar MS/MS spectra. An emerging method to characterize isomeric oligosaccharide structures is ion mobility spectrometry (IMS) [36]. IMS separates gas-phase ions based on their 3D shape and size, in addition to the conventional MS separation by mass and charge [37]. IMS can be coupled to LC to analyze complex oligosaccharides in mixtures [38]. A new-generation of

IMS instruments that allows analysis of precursor and/or fragment ions has recently been developed, including CID-travelling wave ion mobility spectrometry-tandem mass spectrometry (CID-TWIMS-MS/MS), cyclic IM-MS (cIM-MS) and IMS-CID-IMS-MS [39-44]. Juvonen et al. [41] demonstrated that CID-TWIMS-MS/MS could separate most of the isomeric fragment ions produced from (A)XOS, and it allowed differentiation between most of the isomeric fragment ions. Hence, IMS, particularly CID-TWIMS-MS of AUXOS-A could also provide more insights into the AUXOS-A structures.

Characterization of periodate-oxidized oligosaccharides

Direct infusion ESI-MS/MS analysis of periodate-oxidized oligosaccharides unraveled their structural features (Fig. 3 and **Chapter 4**). Although isomeric oligosaccharides cannot be distinguished by (MALDI-TOF- or ESI-)MS (**Chapters 4 and 5**), which hinders precise elucidation of the oligosaccharide chemical structures, IMS could be a promising method to separate and characterize isomeric oligosaccharides.

In order to separate isomers prior to MS, the AC121-pOx-WAX, -BWx, -GGM, and -HG samples were analyzed by LC-MS in a preliminary experiment using an HILIC BEH amide column as stationary phases under various elution conditions. Elution and detection of oxidized oligosaccharides was achieved by UHPLC-HILIC-MS (Box 1, Fig. 5). The double shape of the peaks in the UHPLC-HILIC-MS profile reflected the presence of the α - and β -configurations of oligosaccharides. Unfortunately, separation was not optimal especially for AC121-pOx-WAX and AC121-pOx-GGM (Fig. 5A and 5C), and only two major peaks were observed for AC121-pOx-HG (Fig. 5D). Despite this, especially for AC121-pOx-WAX and AC121-pOx-GGM, various peaks with the same m/z value could be identified at various retention times in the UHPLC-HILIC-MS profile, for example the ions m/z 618, 712, 844, and 976 of AC121-pOx-WAX, and the ions m/z 447 and 449 of AC121-pOx-GGM (Fig. 5A and 5C). This result indicates successful separation of isomeric periodate-oxidized oligosaccharides. Moreover, the UHPLC-HILIC-MS oligosaccharide profiles obtained particularly for AC121-pOx-WAX, AC121-pOx-BWx, and AC121-pOx-GGM were completely different. Even though optimization of the HILIC-UHPLC-MS method is still needed, these preliminary results show the potential use of UHPLC-HILIC-MS to obtain PS structure-dependent periodate-oxidized oligosaccharide profiles for recognition of polysaccharides and to characterize different isomeric periodate-oxidized oligosaccharides.

Box 1 - Materials and methods

Autoclave (AC) treated periodate-oxidized WAX, BWX, GGM, and HG samples (0.5 mg/mL) were analyzed by LC-MS. LC was carried out on a Vanquish UHPLC system (Thermo Scientific, Waltham, MA, USA) equipped with an Acquity UPLC BEH Amide column (Waters, Millford, MA, USA; 1.7 μm , 2.1 mm ID \times 150 mm) and a VanGuard pre-column (Waters; 1.7 μm , 2.1 mm ID \times 150 mm). The column oven temperature was set at 35 $^{\circ}\text{C}$ and the flow rate at 0.4 mL/min; injection volume was 5.0 μL . Water (A) and acetonitrile (B), both containing 0.01 % (v/v) NH_4OH were used as mobile phases. The following gradient was used: 0–2.0 min, 85 % B; 2.0–42 min, 85–55 % B; 42–49 min, 55 % B; 49–50 min, 55–85 % B; and 50–60 min, 85 % B. The m/z of the separated oligosaccharides was detected by a LTQ-VelosPro mass spectrometer (Thermo Scientific) equipped with a heated ESI probe. MS data were obtained in positive ion mode with the following settings: source heater temperature 425 $^{\circ}\text{C}$, capillary temperature 263 $^{\circ}\text{C}$, sheath gas flow 50 units, source voltage 3.5 kV and m/z range 110–2000. Mass spectrometric data were processed using Xcalibur 4.1 software (Thermo Scientific).

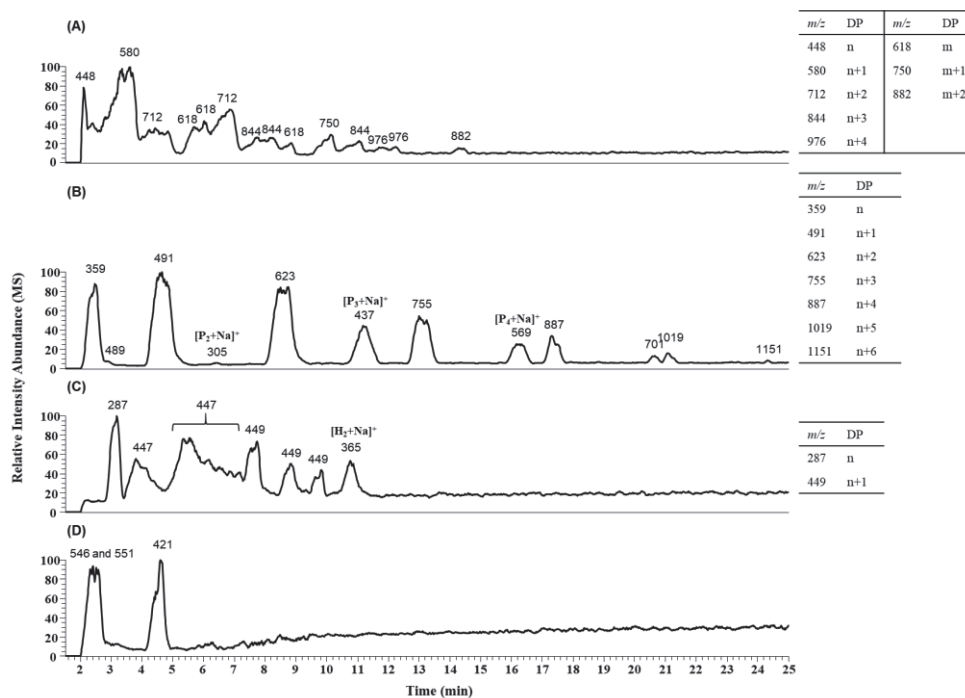


Figure 5. UHPLC-HILIC-MS base peak elution patterns of the thermally hydrolyzed periodate-oxidized WAX (A), BWX (B), GGM (C), and HG (D) at 121 $^{\circ}\text{C}$. Several isomeric products were obtained for m/z 618, 712, 844, and 976 of WAX (A), and for m/z 447 and 449 of GGM (C). Inserted tables for each PS provide the m/z values of periodate-oxidized oligosaccharides differing in 1 or more non-oxidized sugar units. **DP**, degree of polymerization; **P_n** or **H_m** – Na^+ adduct of an oligomer composed of n pentoses (Ara or Xyl) or m hexoses (Gal or Man), respectively.

4. Chemical vs enzymatic polysaccharide fingerprinting

In this section, the *pros*, and *cons* of the chemical depolymerization methods developed in this PhD research will be compared and discussed against the traditional enzymatic depolymerization approaches used for polysaccharides fingerprinting. This comparison will be focused on AXs in particular, and plant polysaccharides in general.

Arabinoxylan fingerprinting

In **Chapter 3**, the UHPLC-PGC-MS AUXOS-A profiles, and characterization of AUXOS-A structures allowed us to verify structural differences among three different AXs. Nonetheless, some Ara(A) debranching occurred during TEMPO-oxidation and/or partial acid-hydrolysis (Fig. 2; **Chapters 2** and **3**). This hindered the precise structural AXs characterization using our method. In this regard, enzymatic digestion of AXs using endo-xylanases is advantageous since AXs depolymerization will only occur in the xylan backbone, allowing to obtain AXOS fully representing the native AX structure.

Enzymatic digestion of AXs using endo-xylanases (glycoside hydrolases (GHs) of family 10 and 11) has frequently been used as enzymatic fingerprinting due to the enzyme's substrate specificity [45-49], forming AX structure-dependent (A)XOS profiles. However, determination of the (A)XOS composition by MS is challenging since Ara and Xyl are isomers [50, 51]. This limitation was overcome in this PhD thesis by selectively oxidizing the Ara side chains of AX to AraA, and subsequently releasing AUXOS from arabinuronoxylans (Fig. 2), allowing us to easily differentiate Xyl from Ara(A) units using MS.

Depolymerization of AXs by endo-xylanases is limited when having highly branched AXs [52], or more complex AX structures, e.g. glucuronoAX, acetylated AX, and feruloylated AX [53]. This is especially applicable to GH11 xylanases, since these enzymes require a higher number of contiguous unsubstituted β -(1 \rightarrow 4)-Xyl p units in the backbone to act than GH10 xylanases [54]. In addition, more complex AXs often require additional accessory enzymes to release substituents to make the xylan backbone more accessible to xylanases [52, 55], resulting in the loss of PS structural features. Furthermore, highly pure, and well-characterized enzymes are needed to have adequate depolymerization, and the isolation of such pure enzymes is quite difficult and time-consuming [56]. Hence, although some debranching might occur during TEMPO-oxidation of AXs followed by partial acid-hydrolysis, the chemical-induced depolymerization method described in **Chapter 3** represents a nicely accessible and general approach to depolymerize and recognize different AXs by oligosaccharides fingerprinting. Considering the selectivity of TEMPO towards primary hydroxyl groups [57], it is expected that more complex AXs are also solely TEMPO-oxidized at the unsubstituted Ara side chains, since the other sugar units do not contain primary hydroxyl groups. These structurally complex TEMPO-oxidized AXs might also generate AX structure-dependent UHPLC-PGC-MS AUXOS-A profiles due to differences in the degree of branching and the presence of substituents besides AraA units, which will induce a different retention behavior of the oligosaccharides onto the PGC column [58]. Yet, further research is needed to prove that partial acid-hydrolysis of structurally

complex TEMPO-oxidized AXs will generate AX structure-dependent UHPL-PGC-MS AUXOS-A profiles.

Arabinoxylan fingerprinting in polysaccharide mixes

AXs are the main hemicellulose component of cereals, and they are often together in a matrix with MLG and cellulose [59]. Characterization of AXs requires their isolation and purification from the matrix [60, 61], which can be a quite laborious process. As these cereal polysaccharides are considered dietary fibres, a single PS depolymerization method that would allow identification and quantification of these polysaccharides in cereals is of high interest for the food industry. In a preliminary experiment, WAX, MLG, a mix of WAX:MLG 50:50 (% w/w), and a mix of WAX:MLG:Cellulose 75:21:5 (% w/w) were TEMPO-oxidized. These TEMPO-oxidized samples and mixes were partially acid-hydrolyzed and reduced, and the oligosaccharides released were analyzed by UHPLC-PGC-MS (Box 2, Fig. 6). The individual partially acid-hydrolyzed TEMPO-oxidized WAX (Fig. 6A) and MLG (Fig. 6B) comprised (AU)XOS-A and (glucurono-)gluco-oligomer alditols ((GU)GlcOS-A), respectively. While 19 AUXOS-A were identified in the UHPLC-PGC-MS profile of the partially acid-hydrolyzed TEMPO-oxidized WAX, only four GUGlcOS-A were observed for the partially acid-hydrolyzed TEMPO-oxidized MLG. This indicates that WAX was more completely TEMPO-oxidized and depolymerized to oligosaccharides than MLG. The partially acid-hydrolyzed and TEMPO-oxidized WAX:MLG 50:50 (% w/w) mix (Fig. 6C) comprised both (AU)XOS-A and (GU)GlcOS-A, showing that TEMPO-oxidation of both hemicelluloses has occurred. The TEMPO-oxidized WAX:MLG 50:50 (% w/w) mix had a higher proportion of AUXOS-A than GUGlcOS-A, in conformity with the UHPLC-PGC-MS profiles obtained for the individual partially acid-hydrolyzed TEMPO-oxidized WAX and MLG (Fig. 6A and 6B). This indicates that in a WAX:MLG mixed in a 50:50 ratio both WAX and MLG are identically TEMPO-oxidized and partially acid-hydrolyzed than when individually. This allows recognition of WAX and MLG polysaccharides when present in a 50:50 mix by using a single depolymerization method, which would be complicated to obtain by enzymatic fingerprinting since besides xylanases, also an enzyme able to digest MLG like e.g. lichenase [62] would be required.

The partially acid-hydrolyzed TEMPO-oxidized WAX:MLG:Cellulose 75:21:5 (% w/w) (Fig. 6D) mainly comprised (AU)XOS-A and negligible levels of GUGlcOS-A. This shows that oligosaccharides derived from (TEMPO-oxidized) cellulose were not formed using 0.2 M TFA (90 °C, 2 h), which was likely due to (TEMPO-oxidized) cellulose insolubility. In addition, the high level of AUXOS-A in comparison to GUGlcOS-A in the UHPLC-PGC-MS profile of this PS mix indicates that increasing the proportion of WAX:MLG from 1:1 to ~ 3.5:1 mainly allows identification of an AX type structure. This shows that the proportion of polysaccharides in a mix does have an influence in the oligosaccharides released. Nonetheless, considering that AXs are the main hemicellulose components of cereals, TEMPO-oxidation of extracted cereal PS fractions followed by partial acid-hydrolysis, reduction, and analysis of the oligosaccharides released by UHPLC-PGC-MS using the conditions described in **Chapter 3** might be a promising approach for AXs fingerprinting.

Box 2 - Materials and methods

WAX, MLG, a mixture of WAX:MLG 50:50 (% w/w) and a mixture of WAX:MLG:Cellulose 75:21:5 (% w/w) were TEMPO-oxidized, TFA partially acid-hydrolyzed, NaBD₄-reduced, and the NaBD₄-reduced oligosaccharides were purified by SPE as described in **Chapter 3**. NaBD₄-reduced oligosaccharides were analyzed by UHPLC-PGC-MS as described in **Chapter 3** with a small adaptation to the elution gradient. Water (A) and 50 % (v/v) acetonitrile:isopropanol (B), both containing 0.1 % (v/v) formic acid were used as mobile phases. The following gradient was used: 0–2 min, 3 % B; 2–15.3 min, 3–15 % B; 15.3–42 min, 15–40 % B; 42–43 min, 40–100 % B; 43–48.3 min, 100 % B; 48.3–49.3 min, 100–3 % B, and 49.3–55.3 min, 3 % B.

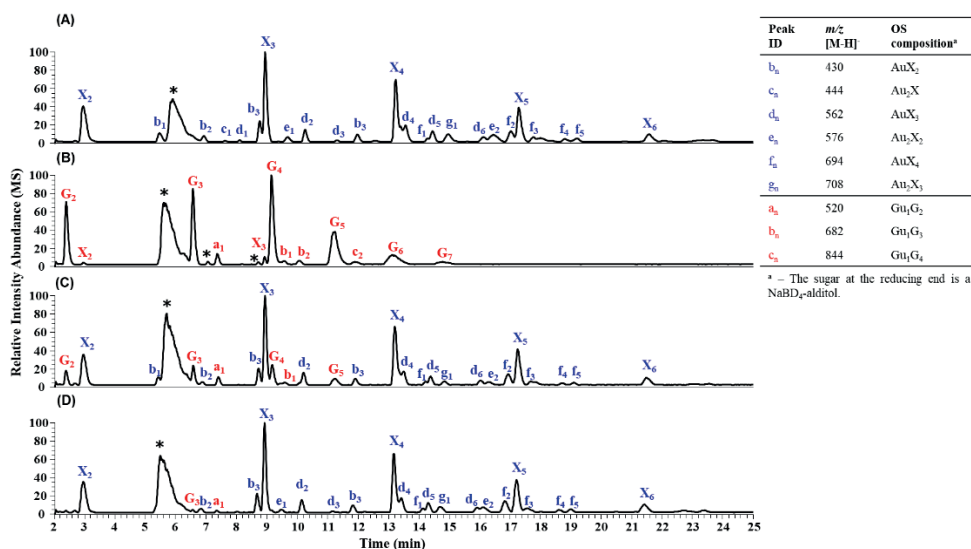


Figure 6. UHPLC-PGC-MS base peak elution patterns of the NaBD₄-reduced (0.2 M) TFA partially acid-hydrolysed (90 °C, 2 h) TEMPO-oxidized (A) WAX, (B) MLG, (C) WAX:MLG 50:50 (% w/w) and (D) WAX:MLG:Cellulose 75:21:5 (% w/w) samples. Oxidized oligosaccharides (OS) are coded by alphabet letters in blue for WAX derived-OS (b–g), and in red for MLG derived-OS (a–c), identical letters with different subscript numbers are isomers. AUXOS-A and GUGlcOS-A compositions are respectively given in the table as Au_mX_n: m - number of AraA; n - number of Xyl units from which one is a terminal xylitol, and Gu_mG_n: m - number of GlcA; n - number of Glc; one of the GlcA or Glc is a terminal alditol. * Background peaks.

General fingerprinting of plant polysaccharides

Fingerprinting of plant polysaccharides by MALDI-TOF MS analysis of thermally depolymerized periodate-oxidized plant polysaccharides (AC121-pOx-PS) is described in **Chapter 5**. All AC121-pOx-PS samples contained oligosaccharides, except XG. The pOx-XG (RT, 6 h, NaIO₄/PS 3.0) obtained did not contain Gal and only small amounts of f₅ Xyl were found in its composition but recovering all the Glc (**Chapters 4 and 5**). This indicates that the Gal and Xyl side chains of XG were completely modified during periodate oxidation, whereas Glc resisted oxidation likely due to the presence of side chains and *trans*-hydroxyl groups in the Glc units, which are less favorable for



oxidation [63-65]. The presence of dialdehyde sugar units in the backbone are essential to obtain PS depolymerization using thermal treatments. Hence, the absence of dialdehyde sugar units in the cellulose-like backbone of pOx-XG might explain the absence of oligosaccharides in AC121-pOx-XG, contrary to the other AC121-pOx-plant polysaccharides investigated in this PhD thesis. Therefore, the periodate oxidation reaction should still be optimized to oxidize the XG backbone. Based on the results described in **Chapter 4**, a periodate oxidation condition that could lead to oxidation of the XG backbone uses a NaIO_4/PS ratio of 6.0 ($\mu\text{mol}/\text{mg}$) for 6 h at RT. This condition also neither leads to overoxidation of the other polysaccharides investigated in this PhD research nor to substantial removal of PS structural features.

Apart from XG, PS structure-dependent MALDI-TOF MS oligosaccharide profiles were obtained for all investigated AC121-pOx-PS samples including pectins (**Chapter 5**). However, it was found that some methyl-esters and acetyl groups were lost for pectic polysaccharides (HG and RG-I) during periodate oxidation and/or thermal treatment. This indicates that the HG- and RG-I-derived oligosaccharides cannot be used for full-detail PS structure elucidation. In addition, the type of oxidized oligosaccharides formed for all investigated polysaccharides in this PhD research are so diverse and structurally complex (Fig. 3) that characterization of the native PS structure is further hampered. In this regard, although being PS-specific, enzymes are advantageous because they depolymerize polysaccharides into oligosaccharides with unique structures, allowing an easier structural elucidation/characterization.

Although the oligosaccharides formed by AC thermal treatment of pOx-polysaccharides might not be suitable for characterization of the parental PS structure, all investigated AC121-pOx-polysaccharides, except (pOx-)XG, had unique MALDI-TOF MS oligosaccharide profiles, even AC121-pOx-polysaccharides composed of isomeric sugar units (**Chapter 5**). This allowed us to distinguish polysaccharides belonging to different PS classes, for example AXs versus glucans, and within the same PS class, for example galactomannans (GGM versus LGBM). Furthermore, identification of significantly different ($p < 0.05$) marker m/z values in the MALDI-TOF mass spectrum of a PS mix corresponding to a specific PS class allowed us to verify the PS classes present in the PS mix. These findings overcome the limitations of the enzymatic digestion of polysaccharides composed of isomers, which would release oligosaccharides with isomeric structures that cannot be distinguish by MS, and the use of specific enzymes per PS, either single or in a mix. Thus, MALDI-TOF MS analysis of AC121-pOx-PS samples is a promising approach to reach a generic fingerprinting of plant polysaccharides by oligosaccharides, and it might be a good initial approach to recognize (unknown) PS classes extracted from a food product.

5. Recent alternative polysaccharide depolymerization approaches for polysaccharides fingerprinting

Recently, other researchers have also been seeking for alternative non-enzymatic PS depolymerization approaches in order to find a unique method capable of generating oligosaccharides from all polysaccharides, which will represent an enormous step forward for carbohydrate research. Nandita et al. [66] and Amicucci et al. [67] have depolymerized various food (standard)

polysaccharides (galactan, amylopectin, amylose, MLG, ABN, XG, curdlan, AX, lichenan, glucomannan, mannan, GM, arabinogalactan, xylan, and cellulose) using a Fenton reaction in the presence of iron ions and hydrogen peroxide (H_2O_2) to generate oligosaccharides for polysaccharide fingerprinting. A single Fenton reaction condition could release oligosaccharides from all investigated food polysaccharides. The oligosaccharides released were reduced and analyzed by HPLC-PGC-Q-TOF MS. Afterwards, the oligosaccharide products were compiled in order to generate an oligosaccharide reference library to identify the respective parental PS. Unique HPLC-PGC-Q-TOF MS oligosaccharide profiles were obtained for each Fenton depolymerized PS [66, 67]. This allowed distinction of polysaccharides, and even distinction of homopolysaccharides, for example starch and cellulose. These authors made use of the ability of the PGC material to separate isomeric oligosaccharides, as also seen in **Chapter 3** of this PhD thesis, where we could separate isomeric AUXOS-A structures. Nandita et al. [66] also applied the Fenton reaction to a mix of polysaccharides (amylopectin, AX and XG). By comparing the HPLC-PGC-Q-TOF MS oligosaccharide profile of the mix with the oligosaccharide profile of the individual PS, they could successfully identify the polysaccharides present in the mix, as we described in **Chapter 5** but based on the MALDI-TOF mass spectra. In comparison to our **Chapter 5**, Nandita et al. [66] and Amicucci et al. [67] went one step further and applied the Fenton depolymerization reaction also to food samples (e.g., wheat and oat brans, yellow corn meal, various fleshes and leaves, and spent coffee grounds). By comparing the LC-MS oligosaccharide profiles derived from the food samples with their oligosaccharide reference library, they could identify the PS components of each food sample. These authors have not yet included HG- and RG-I-derived oligosaccharides in their oligosaccharides library and consequent PS recognition. Hence, the method developed by Nandita et al. [66] and Amicucci et al. [67] cannot yet be applied to identify these polysaccharides in food samples, contrary to the method described in **Chapter 5**, which includes both HG and RG-I. Some other research groups have subjected pectins to a Fenton reaction using iron or copper ions together with H_2O_2 , and pectic oligosaccharides could be obtained [68-70]. This allowed e.g., to demonstrate the presence of HG and RG-I pectic components in citrus canning processing water [68]. Thus, depending on the Fenton reaction conditions, it might also be possible to generate diagnostic oligosaccharides from Fenton depolymerized pectin samples, allowing fingerprinting of polysaccharides in mixes.

Comparing the non-enzymatic depolymerization method described in **Chapter 5** with the Fenton reaction method described by Nandita et al. [66] and Amicucci et al. [67], the Fenton reaction is faster (max. 1 h reaction). However, the data acquisition in our method is rather fast. For example, within 5 min we acquire MALDI-TOF MS data for one AC121-pOx-PS, whereas for one Fenton depolymerized PS, HPLC-PGC-Q-TOF MS data are obtained only after 45 min. Additionally, we could obtain oligosaccharides for HG and RG-I in addition to the other plant polysaccharides investigated in **Chapter 5**. Furthermore, our study also showed that polysaccharides composed of isomeric sugar units can be successfully distinguished based on the MALDI-TOF MS oligosaccharide profiles, and that even the same type of polysaccharides derived from different sources can be differentiated, for example wheat and rye AXs, and guar and locust bean GMs. This, unfortunately, was not investigated by Nandita et al. [66] and Amicucci et al. [67]. Thus, both the Fenton reaction and the method described in **Chapter 5** seem to be promising alternative methods to enzymatic depolymerization of polysaccharides to recognize PS components of food products more generically.



Various studies have still wisely used mild acid-hydrolysis to **1) identify** polysaccharides in a mix from the edible bivalve mollusk, *Cyclina sinensis*, by depolymerization of polysaccharides into disaccharides followed by reverse phase (RP-)HPLC-ESI-MS analysis [71]; and **2) characterize** PS structures by combination with sugar and linkage analyses, for example of maize mucilage polysaccharides (highly fucosylated and xylosylated galactose backbone with arabinan and mannoglucuronan branches) [72]. Nonetheless, finding a unique (mild) acid-hydrolysis condition able to depolymerize all plant polysaccharides without losing structural information is difficult to accomplish due to the different resistance to acid of the glycosidic linkage of various monosaccharides [73].

6. Future Perspectives

Ultimately, the chemical-induced PS depolymerization approaches developed in this PhD research (Fig. 1) were aimed to be applicable to carbohydrate fractions extracted from food products to contribute for a more generic recognition of the PS composition of a food product. In this section, some perspectives on how these PS depolymerization methods could be extended to other polysaccharides and foods will be provided. Additionally, some thoughts about the potential use of the generated (oxidized) polysaccharides regarding their potential new/improved functionalities will be put forward.

Potential application of the chemical-induced polysaccharide depolymerization methods in food products

TEMPO-oxidation of AXs followed by partial acid-hydrolysis, and analysis of the oligosaccharides released by UHPLC-PGC-MS showed potential to characterize and recognize AXs from different sources (wheat and rye) based on the UHPLC-PGC-MS oligosaccharide profiles (**Chapter 3**). To verify the suitability of the method for AXs fingerprinting, this method should be applied to an even broader range and more complex AXs, e.g., from barley, maize, oats, and rice [74]. Similarly, it would be interesting to extend the AC treatment of periodate-oxidized polysaccharides followed by analysis of the oligosaccharides released by MALDI-TOF MS method (**Chapter 5**) to a wider range of AXs, GMs, and HGs with different substitution levels and patterns to validate that the same type of polysaccharides with different structural features generate unique MALDI-TOF MS oligosaccharide profiles. Moreover, as besides plant polysaccharides also non-plant polysaccharides are added to food products, the method described in **Chapter 5** should also be extended to non-plant polysaccharides used in the food industry, for example alginate and xanthan [75, 76]. Finally, construction of an oligosaccharide reference library based on the UHPLC-PGC-MS profiles of partially acid-hydrolyzed TEMPO-oxidized AXs and another one based on the MALDI-TOF MS oligosaccharide profiles of the thermally treated periodate-oxidized polysaccharides would be highly valuable. An oligosaccharide reference library would allow an easier PS assignment based on marker oligosaccharides.

Considering that AXs are mainly found in cereals, a next step would be applying both methods described in **Chapters 3** and **5** to cereal raw materials (e.g., wheat and rye brans), or food products enriched with AXs or with cereal-derived polysaccharides. Particularly, the method described in

Chapter 5 could also be extended to food raw materials or more complex food systems containing plant polysaccharides as food ingredients/additives, as done for example by Nandita et al. [66] and Amicucci et al. [67] but using a Fenton reaction. It is worth mentioning that other food components or biomolecules may interfere with the depolymerization of polysaccharides into oligosaccharides. For example, the aldehyde groups of periodate-oxidized polysaccharides can easily react with compounds containing amino groups, which are abundantly present in proteins, via Schiff base crosslinking [77]. Therefore, isolation of the PS fraction from a food product matrix [19, 66, 78] before performing the PS depolymerization method is needed to reliably recognize the polysaccharides composition of a food product. Depending on the food product, defatting, deproteination, and desalting might be needed to obtain a PS enriched fraction [78].

In the future, once UHPLC-PGC-MS and MALDI-TOF MS oligosaccharide reference libraries for AXs and for food (standard) polysaccharides, respectively, are developed, and the proposed approaches in **Chapters 3** and **5** are validated in PS extracts from food products, it really would be interesting to build a reactor and incorporate these PS depolymerization reactions in this reactor. This would allow automation, making these PS depolymerization methods less laborious, and even more reproducible. Afterwards, coupling the developed reactor(s) to an LC-MS and/or MALDI-TOF MS system would enable a quick data acquisition, making the PS fingerprinting and structural characterization processes faster. Moreover, when successfully incorporated the reactor in an LC-MS system, one may even consider connecting another type of LC separation, e.g. HPSEC or Ion-Exchange LC, *before* the reactor. This would allow separation of distinct populations of the parental polymer(s) prior to the PS depolymerization reaction in the reactor, enabling the separation and identification of oligosaccharides derived from a single PS population present in the parental PS preparation in the next LC(-MS) system at a time. The future automation of these PS depolymerization methods would be of high interest not only for the food industry, but also for nutrition and health, and plant sciences, to quickly recognize different populations of one single PS preparation or to recognize the PS composition of a food product by analyzing an individual PS from a crude PS food extract.

Potential exploitation of oxidized polysaccharides

The PS depolymerization methods investigated in this PhD thesis chemically modified polysaccharides by using TEMPO-oxidation or periodate oxidation reactions. This chemical functionalization of polysaccharides can be of high interest since it may create polysaccharides with new/improved functionalities, which is valuable for further exploitation. An advantage of functionalizing polysaccharides for new applications is that polysaccharides are widely spread in nature, are biodegradable, and are non-toxic [79].

TEMPO-oxidation of neutral polysaccharides has raised the interest of the scientific community to obtain new polyuronides due to their valuable properties [57]. Some studies have shown the importance of TEMPO-oxidized polysaccharides for biomedical applications. For example, **1**) TEMPO-oxidation of sacchachitin nanofibers (TOSCNF) have shown potential for tissue regeneration [80]; and **2**) TEMPO-oxidized starch nanoassemblies can be used as nanocarriers for drug delivery and for enhancing anti-cancer therapy [81]. Thus, considering that in this PhD research novel differently charged and substituted arabinuronoxylan structures (**Chapter 3**) comprising negatively charged



uronic acid residues in the side chains were produced, it would be interesting to investigate if these polyuronides display new/improved functional properties.

Periodate oxidation has also emerged as a PS modification approach to create materials with new/improved functionalities by introducing dialdehydes [12, 13, 64, 82]. The aldehyde groups can bring new functionalities to the PS as such, for example hydrogels formation [12, 64, 82-85]. Additionally, due to the reactivity of aldehydes, periodate-oxidized polysaccharides can react further with for example materials containing amino groups [86], and/or carbonyl/hydroxyl groups [87] to form new materials with e.g. potential biomedical applications. Thus, investigating potential new properties of the periodate-oxidized plant polysaccharides formed in this PhD research (**Chapters 4 and 5**) could be interesting since renewable plant polysaccharides are the most abundant biomacromolecules found in nature.

All in all, in addition to showing the potential use of chemical-induced PS depolymerization approaches based on oxidative reactions to form oligosaccharides for polysaccharide fingerprinting in a more generic manner than by using enzymes, this PhD thesis also outlines that the chemically modified polysaccharides can be further exploited for their potential new functionalities.



References

- [1] Harris, P.J. and B.G. Smith. Plant cell walls and cell-wall polysaccharides: Structures, properties and uses in food products. *International Journal of Food Science and Technology*. **2006**, 41, 129-143.
- [2] Saha, A., S. Tyagi, R.K. Gupta, and Y.K. Tyagi. Natural gums of plant origin as edible coatings for food industry applications. *Critical Reviews in Biotechnology*. **2017**, 37, 959-973.
- [3] Ralet, M.C., M.J. Crépeau, and E. Bonnin. Evidence for a blockwise distribution of acetyl groups onto homogalacturonans from a commercial sugar beet (*Beta vulgaris*) pectin. *Phytochemistry*. **2008**, 69, 1903-1909.
- [4] Westphal, Y., H.A. Schols, A.G.J. Voragen, and H. Gruppen. MALDI-TOF MS and CE-LIF fingerprinting of plant cell wall polysaccharide digests as a screening tool for arabidopsis cell wall mutants. *Journal of Agricultural and Food Chemistry*. **2010**, 58, 4644-4652.
- [5] Bauer, S. Mass Spectrometry for Characterizing Plant Cell Wall Polysaccharides. *Frontiers in Plant Science*. **2012**, 3.
- [6] Ruhaak, L.R., A.M. Deelder, and M. Wührer. Oligosaccharide analysis by graphitized carbon liquid chromatography-mass spectrometry. *Analytical and Bioanalytical Chemistry*. **2009**, 394, 163-174.
- [7] De, K.K. and T.E. Timell. The acid hydrolysis of glycosides: IV. Hydrolysis of aldobiouronic acids. *Carbohydrate Research*. **1967**, 4, 177-181.
- [8] Gu, F., S. Wang, R. Beijers, C. de Weerth, and H.A. Schols. Structure-Specific and Individual-Dependent Metabolization of Human Milk Oligosaccharides in Infants: A Longitudinal Birth Cohort Study. *Journal of Agricultural and Food Chemistry*. **2021**, 69, 6186-6199.
- [9] Veillon, L., Y. Huang, W. Peng, X. Dong, B.G. Cho, and Y. Mechref. Characterization of isomeric glycan structures by LC-MS/MS. *Electrophoresis*. **2017**, 38, 2100-2114.
- [10] Logtenberg, M.J., K.M.H. Donners, J.C.M. Vink, S.S. van Leeuwen, P. de Waard, P. de Vos, and H.A. Schols. Touching the High Complexity of Prebiotic Vivinal Galacto-oligosaccharides Using Porous Graphitic Carbon Ultra-High-Performance Liquid Chromatography Coupled to Mass Spectrometry. *Journal of Agricultural and Food Chemistry*. **2020**, 68, 7800-7808.
- [11] Westphal, Y., H.A. Schols, A.G.J. Voragen, and H. Gruppen. Introducing porous graphitized carbon liquid chromatography with evaporative light scattering and mass spectrometry detection into cell wall oligosaccharide analysis. *Journal of Chromatography A*. **2010**, 1217, 689-695.
- [12] Chetouani, A., N. Follain, S. Marais, C. Rihouey, M. Elkolli, M. Bounekhel, D. Benachour, and D. Le Cerf. Physicochemical properties and biological activities of novel blend films using oxidized pectin/chitosan. *International Journal of Biological Macromolecules*. **2017**, 97, 348-356.
- [13] Kristiansen, K.A., A. Potthast, and B.E. Christensen. Periodate oxidation of polysaccharides for modification of chemical and physical properties. *Carbohydrate Research*. **2010**, 345, 1264-1271.
- [14] Li, H., B. Wu, C. Mu, and W. Lin. Concomitant degradation in periodate oxidation of carboxymethyl cellulose. *Carbohydrate Polymers*. **2011**, 84, 881-886.
- [15] Marasca, E., S. Boulos, and L. Nyström. Bile acid-retention by native and modified oat and barley β -glucan. *Carbohydrate Polymers*. **2020**, 236, 116034.
- [16] Veelaert, S., D. de Wit, K.F. Gotlieb, and R. Verhé. Chemical and physical transitions of periodate oxidized potato starch in water. *Carbohydrate Polymers*. **1997**, 33, 153-162.
- [17] Derrien, E., M. Ahmar, E. Martin-Sisteron, G. Raffin, Y. Queneau, P. Marion, M. Beyerle, C. Pinel, and M. Besson. Oxidation of Aldoses Contained in Softwood Hemicellulose Acid Hydrolysates into Aldaric Acids under Alkaline or Noncontrolled pH Conditions. *Industrial and Engineering Chemistry Research*. **2018**, 57, 4543-4552.
- [18] De Souza, A.C., T. Rietkerk, C.G.M. Selin, and P.P. Lankhorst. A robust and universal NMR method for the compositional analysis of polysaccharides. *Carbohydrate Polymers*. **2013**, 95, 657-663.
- [19] Merckx, D.W.H., Y. Westphal, E.J.J. van Velzen, K.V. Thakoer, N. de Roo, and J.P.M. van Duynhoven. Quantification of food polysaccharide mixtures by ¹H NMR. *Carbohydrate Polymers*. **2018**, 179, 379-385.
- [20] Silva Elipe, M.V. Advantages and disadvantages of nuclear magnetic resonance spectroscopy as a hyphenated technique. *Analytica Chimica Acta*. **2003**, 497, 1-25.
- [21] Blumenkrantz, N. and G. Asboe-Hansen. New method for quantitative determination of uronic acids. *Analytical Biochemistry*. **1973**, 54, 484-489.
- [22] Li, J., K. Kisara, S. Danielsson, M.E. Lindström, and G. Gellerstedt. An improved methodology for the quantification of uronic acid units in xylans and other polysaccharides. *Carbohydr Res*. **2007**, 342, 1442-9.
- [23] Viel, M., F. Collet, and C. Lanos. Chemical and multi-physical characterization of agro-resources' by-product as a possible raw building material. *Industrial Crops and Products*. **2018**, 120, 214-237.
- [24] Kamerling, J.P. and G.J. Gerwig, 2.01 - Strategies for the Structural Analysis of Carbohydrates, in *Comprehensive Glycoscience*, H. Kamerling, Editor. **2007**, Elsevier: Oxford. 1-68.
- [25] Peterson, G. Gas-chromatographic analysis of sugars and related hydroxy acids as acyclic oxime and ester trimethylsilyl derivatives. *Carbohydrate Research*. **1974**, 33, 47-61.



- [26] Petersson, G. Mass spectrometry of hydroxy dicarboxylic acids as trimethylsilyl derivatives. Rearrangement fragmentations. *Organic Mass Spectrometry*. **1972**, 6, 565-576.
- [27] Ruiz-Matute, A.I., O. Hernández-Hernández, S. Rodríguez-Sánchez, M.L. Sanz, and I. Martínez-Castro. Derivatization of carbohydrates for GC and GC-MS analyses. *Journal of Chromatography B: Analytical Technologies in the Biomedical and Life Sciences*. **2011**, 879, 1226-1240.
- [28] Wu, J. and A.S. Serianni. d-Penturonic acids: solution studies of stable-isotopically enriched compounds by ¹H- and ¹³C-n.m.r. spectroscopy. *Carbohydrate Research*. **1991**, 210, 51-70.
- [29] Borges, M.R. and R.d.C. Balaban. L-Arabinose (pyranose and furanose rings)-branched poly(vinyl alcohol): Enzymatic synthesis of the sugar esters followed by free radical polymerization. *Journal of Biotechnology*. **2014**, 192, 42-49.
- [30] Mackie, W. and A.S. Perlin. PYRANOSE-FURANOSE AND ANOMERIC EQUILIBRIA: INFLUENCE OF SOLVENT AND OF PARTIAL METHYLATION. *Canadian Journal of Chemistry*. **1966**, 44, 2039-2049.
- [31] Galermo, A.G., E. Nandita, J.J. Castillo, M.J. Amicucci, and C.B. Lebrilla. Development of an Extensive Linkage Library for Characterization of Carbohydrates. *Analytical Chemistry*. **2019**, 91, 13022-13031.
- [32] Westereng, B., J.W. Agger, S.J. Horn, G. Vaaje-Kolstad, F.L. Aachmann, Y.H. Stenström, and V.G.H. Eijsink. Efficient separation of oxidized cello-oligosaccharides generated by cellulose degrading lytic polysaccharide monoxygenases. *Journal of Chromatography A*. **2013**, 1271, 144-152.
- [33] Westereng, B., M.Ø. Arntzen, F.L. Aachmann, A. Vármai, V.G.H. Eijsink, and J.W. Agger. Simultaneous analysis of C1 and C4 oxidized oligosaccharides, the products of lytic polysaccharide monoxygenases acting on cellulose. *Journal of Chromatography A*. **2016**, 1445, 46-54.
- [34] Bowman, M.J., B.S. Dien, P.J. O'Bryan, G. Sarath, and M.A. Cotta. Selective chemical oxidation and depolymerization of (*Panicum virgatum* L.) xylan with switchgrass oligosaccharide product analysis by mass spectrometry. *Rapid Communications in Mass Spectrometry*. **2011**, 25, 941-950.
- [35] Demuth, T., S. Boulos, and L. Nyström. Structural investigation of oxidized arabinoxylan oligosaccharides by negative ionization HILIC-qToF-MS. *Analyst*. **2020**, 145, 6691-6704.
- [36] Jin, C., D.J. Harvey, W.B. Struwe, and N.G. Karlsson. Separation of isomeric o-glycans by ion mobility and liquid chromatography-mass spectrometry. *Analytical Chemistry*. **2019**, 91, 10604-10613.
- [37] Gabelica, V. and E. Marklund. Fundamentals of ion mobility spectrometry. *Current Opinion in Chemical Biology*. **2018**, 42, 51-59.
- [38] Leijdekkers, A.G.M., J.-H. Huang, E.J. Bakx, H. Gruppen, and H.A. Schols. Identification of novel isomeric pectic oligosaccharides using hydrophilic interaction chromatography coupled to traveling-wave ion mobility mass spectrometry. *Carbohydrate Research*. **2015**, 404, 1-8.
- [39] Gaye, M.M., R. Kurulugama, and D.E. Clemmer. Investigating carbohydrate isomers by IMS-CID-IMS-MS: precursor and fragment ion cross-sections. *Analyst*. **2015**, 140, 6922-6932.
- [40] Hofmann, J., A. Stuckmann, M. Crispin, D.J. Harvey, K. Pagel, and W.B. Struwe. Identification of Lewis and Blood Group Carbohydrate Epitopes by Ion Mobility-Tandem-Mass Spectrometry Fingerprinting. *Analytical Chemistry*. **2017**, 89, 2318-2325.
- [41] Juvonen, M., E. Bakx, H. Schols, and M. Tenkanen. Separation of isomeric cereal-derived arabinoxylan-oligosaccharides by collision induced dissociation-travelling wave ion mobility spectrometry-tandem mass spectrometry (CID-TWIMS-MS/MS). *Food Chemistry*. **2022**, 366, 130544.
- [42] Peterson, L.T. and G. Nagy. Toward Sequencing the Human Milk Glycome: High-Resolution Cyclic Ion Mobility Separations of Core Human Milk Oligosaccharide Building Blocks. *Analytical Chemistry*. **2021**, 93, 9397-9407.
- [43] Ropartz, D., M. Fanuel, J. Ujma, M. Palmer, K. Giles, and H. Rogniaux. Structure Determination of Large Isomeric Oligosaccharides of Natural Origin through Multipass and Multistage Cyclic Traveling-Wave Ion Mobility Mass Spectrometry. *Analytical Chemistry*. **2019**, 91, 12030-12037.
- [44] Ollivier, S., L. Tarquis, M. Fanuel, A. Li, J. Durand, E. Laville, G. Potocki-Veronese, D. Ropartz, and H. Rogniaux. Anomeric Retention of Carbohydrates in Multistage Cyclic Ion Mobility (IMS n): De Novo Structural Elucidation of Enzymatically Produced Mannosides. *Analytical Chemistry*. **2021**, 93, 6254-6261.
- [45] Gruppen, H., R.A. Hoffmann, F.J.M. Kormelink, A.G.J. Voragen, J.P. Kamerling, and J.F.G. Vliegthart. Characterisation by ¹H NMR spectroscopy of enzymically derived oligosaccharides from alkali-extractable wheat-flour arabinoxylan. *Carbohydrate Research*. **1992**, 233, 45-64.
- [46] Kormelink, F.J.M., R.A. Hoffmann, H. Gruppen, A.G.J. Voragen, J.P. Kamerling, and J.F.G. Vliegthart. Characterisation by ¹H NMR spectroscopy of oligosaccharides derived from alkali-extractable wheat-flour arabinoxylan by digestion with endo-(1 → 4)-β-d-xylanase III from *Aspergillus awamori*. *Carbohydrate Research*. **1993**, 249, 369-382.
- [47] Ordaz-Ortiz, J.J., M.F. Devaux, and L. Saulnier. Classification of wheat varieties based on structural features of arabinoxylans as revealed by endoxylanase treatment of flour and grain. *Journal of Agricultural and Food Chemistry*. **2005**, 53, 8349-8356.

- [48] Rakha, A., L. Saulnier, P. Man, and R. Andersson. Enzymatic fingerprinting of arabinoxylan and β -glucan in triticale, barley and tritordeum grains. *Carbohydrate Polymers*. **2012**, 90, 1226-1234.
- [49] Tian, L., H. Gruppen, and H.A. Schols. Characterization of (Glucurono)arabinoxylans from Oats Using Enzymatic Fingerprinting. *Journal of Agricultural and Food Chemistry*. **2015**, 63, 10822-10830.
- [50] Juvonen, M., M. Kotiranta, J. Jokela, P. Tuomainen, and M. Tenkanen. Identification and structural analysis of cereal arabinoxylan-derived oligosaccharides by negative ionization HILIC-MS/MS. *Food Chemistry*. **2019**, 275, 176-185.
- [51] Kouzounis, D., P. Sun, E.J. Bakx, H.A. Schols, and M.A. Kabel, *Strategy to identify reduced arabinoxylo-oligosaccharides by HILIC-MSⁿ*. 2022, Submitted for publication.
- [52] Guilloux, K., I. Gaillard, J. Courtois, B. Courtois, and E. Petit. Production of arabinoxylan-oligosaccharides from flaxseed (*Linum usitatissimum*). *Journal of Agricultural and Food Chemistry*. **2009**, 57, 11308-11313.
- [53] Izydorczyk, M.S., 23 - Arabinoxylans, in *Handbook of Hydrocolloids (Second Edition)*, G.O. Phillips and P.A. Williams, Editors. **2009**, Woodhead Publishing. 653-692.
- [54] Biely, P., M. Vršanská, M. Tenkanen, and D. Kluepfel. Endo- β -1,4-xylanase families: Differences in catalytic properties. *Journal of Biotechnology*. **1997**, 57, 151-166.
- [55] Agger, J., A. Viksø-Nielsen, and A.S. Meyer. Enzymatic Xylose Release from Pretreated Corn Bran Arabinoxylan: Differential Effects of Deacetylation and Deferuloylation on Insoluble and Soluble Substrate Fractions. *Journal of Agricultural and Food Chemistry*. **2010**, 58, 6141-6148.
- [56] Kormelink, F.J.M., M.J.F. Searle-Van Leeuwen, T.M. Wood, and A.G.J. Voragen. Purification and characterization of three endo-(1,4)- β -xylanases and one β -xylosidase from *Aspergillus awamori*. *Journal of Biotechnology*. **1993**, 27, 249-265.
- [57] Pierre, G., C. Punta, C. Delattre, L. Melone, P. Dubessay, A. Fiorati, N. Pastori, Y.M. Galante, and P. Michaud. TEMPO-mediated oxidation of polysaccharides: An ongoing story. *Carbohydrate Polymers*. **2017**, 165, 71-85.
- [58] Pereira, L. Porous graphitic carbon as a stationary phase in HPLC: Theory and applications. *Journal of Liquid Chromatography and Related Technologies*. **2008**, 31, 1687-1731.
- [59] Cui, S.W. and Q. Wang. Cell wall polysaccharides in cereals: Chemical structures and functional properties. *Structural Chemistry*. **2009**, 20, 291-297.
- [60] Aguedo, M., C. Fougnes, M. Dermience, and A. Richel. Extraction by three processes of arabinoxylans from wheat bran and characterization of the fractions obtained. *Carbohydrate Polymers*. **2014**, 105, 317-324.
- [61] Schooneveld-Bergmans, M.E.F., A.M.C.P. Hopman, G. Beldman, and A.G.J. Voragen. Extraction and partial characterization of feruloylated glucuronarabinoxylans from wheat bran. *Carbohydrate Polymers*. **1998**, 35, 39-47.
- [62] Johansson, L., P. Tuomainen, M. Ylinen, P. Ekholm, and L. Virkki. Structural analysis of water-soluble and -insoluble β -glucans of whole-grain oats and barley. *Carbohydrate Polymers*. **2004**, 58, 267-274.
- [63] Kochumalayil, J.J., S. Morimune, T. Nishino, O. Ikkala, A. Walther, and L.A. Berglund. Nacre-mimetic clay/xyloglucan bionanocomposites: A chemical modification route for hygromechanical performance at high humidity. *Biomacromolecules*. **2013**, 14, 3842-3849.
- [64] Kochumalayil, J.J., Q. Zhou, W. Kasai, and L.A. Berglund. Regioselective modification of a xyloglucan hemicellulose for high-performance biopolymer barrier films. *Carbohydrate Polymers*. **2013**, 93, 466-472.
- [65] Halsall, T.G., E.L. Hirst, and J.K.N. Jones. Oxidation of carbohydrates by the periodate ion. *Journal of the Chemical Society (Resumed)*. **1947**. 1427-1432.
- [66] Nandita, E., N.P. Bacalzo, C.L. Ranque, M.J. Amicucci, A. Galermo, and C.B. Lebrilla. Polysaccharide Identification Through Oligosaccharide Fingerprinting. *Carbohydrate Polymers*. **2021**, 257, 117570.
- [67] Amicucci, M.J., E. Nandita, A.G. Galermo, J.J. Castillo, S. Chen, D. Park, J.T. Smilowitz, J.B. German, D.A. Mills, and C.B. Lebrilla. A nonenzymatic method for cleaving polysaccharides to yield oligosaccharides for structural analysis. *Nature Communications*. **2020**, 11, 3963.
- [68] Li, J., S. Li, S. Liu, C. Wei, L. Yan, T. Ding, R.J. Linhardt, D. Liu, X. Ye, and S. Chen. Pectic oligosaccharides hydrolyzed from citrus canning processing water by Fenton reaction and their antiproliferation potentials. *International Journal of Biological Macromolecules*. **2019**, 124, 1025-1032.
- [69] Martinov, J., M. Krstić, S. Spasić, S. Miletić, J. Stefanović-Kojić, A. Nikolić-Kokić, D. Blagojević, I. Spasojević, and M.B. Spasić. Apple pectin-derived oligosaccharides produce carbon dioxide radical anion in Fenton reaction and prevent growth of *Escherichia coli* and *Staphylococcus aureus*. *Food Research International*. **2017**, 100, 132-136.
- [70] Zhi, Z., J. Chen, S. Li, W. Wang, R. Huang, D. Liu, T. Ding, R.J. Linhardt, S. Chen, and X. Ye. Fast preparation of RG-I enriched ultra-low molecular weight pectin by an ultrasound accelerated Fenton process. *Scientific Reports*. **2017**, 7, 541.



- [71] Cao, C., L. Wang, L. Wang, Y. Gong, C. Ai, C. Wen, and S. Song. A strategy to identify mixed polysaccharides through analyzing the monosaccharide composition of disaccharides released by graded acid hydrolysis. *Carbohydrate Polymers*. **2019**, 223, 115046.
- [72] Amicucci, M.J., A.G. Galermo, A. Guerrero, G. Treves, E. Nandita, M.J. Kailemia, S.M. Higdon, T. Pozzo, J.M. Lavavitch, A.B. Bennett, and C.B. Lebrilla. Strategy for Structural Elucidation of Polysaccharides: Elucidation of a Maize Mucilage that Harbors Diazotrophic Bacteria. *Analytical Chemistry*. **2019**, 91, 7254-7265.
- [73] Rabemanantsoa, H., S. Ayada, and S. Saka, *Evaluation of different methods to determine monosaccharides in biomass*, in *Green Energy and Technology*. 2011, Springer Verlag. p. 123-128.
- [74] Bastos, R., E. Coelho, and M.A. Coimbra, Arabinoxylans from cereal by-products: Insights into structural features, recovery, and applications, in *Sustainable Recovery and Reutilization of Cereal Processing By-Products*. **2018**, Elsevier Inc. 227-251.
- [75] Habibi, H. and K. Khosravi-Darani. Effective variables on production and structure of xanthan gum and its food applications: A review. *Biocatalysis and Agricultural Biotechnology*. **2017**, 10, 130-140.
- [76] Liao, Y.C., C.C. Chang, D. Nagarajan, C.Y. Chen, and J.S. Chang. Algae-derived hydrocolloids in foods: applications and health-related issues. *Bioengineered*. **2021**, 12, 3787-3801.
- [77] Ding, W. and Y. Wu. Sustainable dialdehyde polysaccharides as versatile building blocks for fabricating functional materials: An overview. *Carbohydrate Polymers*. **2020**, 248, 116801.
- [78] Grün, C.H., P. Sanders, M. van der Burg, E. Schuurbiens, L. van Adrichem, E.J.J. van Velzen, N. de Roo, K. Brunt, Y. Westphal, and H.A. Schols. Strategy to identify and quantify polysaccharide gums in gelled food concentrates. *Food Chemistry*. **2015**, 166, 42-49.
- [79] Liu, J., S. Willför, and C. Xu. A review of bioactive plant polysaccharides: Biological activities, functionalization, and biomedical applications. *Bioactive Carbohydrates and Dietary Fibre*. **2015**, 5, 31-61.
- [80] Chao, F.-C., M.-H. Wu, L.-C. Chen, H.-L. Lin, D.-Z. Liu, H.-O. Ho, and M.-T. Sheu. Preparation and Characterization of Chemically TEMPO-oxidized and Mechanically Disintegrated Sacchachitin Nanofibers (SCNF) for Enhanced Diabetic Wound Healing. *Carbohydrate Polymers*. **2020**, 229, 115507.
- [81] Jiang, Y., T. Li, M. Lu, D. Li, F. Ren, H. Zhao, and Y. Li. TEMPO-oxidized starch nanoassemblies of negligible toxicity compared with polyacrylic acids for high performance anti-cancer therapy. *International Journal of Pharmaceutics*. **2018**, 547, 520-529.
- [82] Chemin, M., A. Rakotoveloa, F. Ham-Pichavant, G. Chollet, D. Da Silva Perez, M. Petit-Conil, H. Cramail, and S. Grelier. Synthesis and characterization of functionalized 4-O-methylglucuronoxylan derivatives. *Holzforschung*. **2015**, 69, 713-720.
- [83] Börjesson, M., A. Larsson, G. Westman, and A. Ström. Periodate oxidation of xylan-based hemicelluloses and its effect on their thermal properties. *Carbohydrate Polymers*. **2018**, 202, 280-287.
- [84] Chetouani, A., M. Elkolli, M. Bounekhel, and D. Benachour. Synthesis and properties of novel hydrogels from oxidized pectin crosslinked gelatin for biomedical applications. *Polymer Bulletin*. **2014**, 71, 2303-2316.
- [85] Li, N., F. Xue, H. Zhang, H.J. Sanyour, A.P. Rickel, A. Uttecht, B. Fanta, J. Hu, and Z. Hong. Fabrication and Characterization of Pectin Hydrogel Nanofiber Scaffolds for Differentiation of Mesenchymal Stem Cells into Vascular Cells. *ACS Biomaterials Science and Engineering*. **2019**, 5, 6511-6519.
- [86] Ren, J., M. Li, R. Yuan, A. Pang, Z. Lu, and L. Ge. Adherent self-healing chitosan/dialdehyde starch coating. *Colloids and Surfaces A: Physicochemical and Engineering Aspects*. **2020**, 586, 124203.
- [87] Chen, Y., G. Dai, and Q. Gao. Starch Nanoparticles-Graphene Aerogels with High Supercapacitor Performance and Efficient Adsorption. *ACS Sustainable Chemistry and Engineering*. **2019**, 7, 14064-14073.

Summary
Resumo



Plant polysaccharides are amongst the most abundant biomacromolecules found in nature and are frequently used in foods. These polysaccharides are of interest for food industry since they can be added to foods to modulate their physical properties and/or as dietary fibres to provide health benefits. These functionalities of polysaccharides are highly dependent on their chemical structures. However, characterization and/or recognition of polysaccharides in a rapid and generic manner remains a challenge due to their high diversity and complexity.

The chemical features of plant polysaccharides, as well as the traditional methods used to characterize their structures is described in the **first chapter** of this thesis. **Chapter 1** also describes the traditional enzymatic approach including the depolymerization of polysaccharides into diagnostic oligosaccharides for structural characterization. Due to the enzyme polysaccharide-specificity, enzymatic digestion of polysaccharides has limited use as a generic approach to obtain oligosaccharides for structural characterization. To seek for an alternative polysaccharide depolymerization method that allows to generically depolymerize plant polysaccharides to oligosaccharides, various chemical-induced polysaccharide depolymerization approaches reported in literature are discussed in **Chapter 1** in detail. Based on the literature discussed, the most promising chemical approaches to generate polysaccharide structure-informative oligosaccharides for recognition and/or structural characterization of polysaccharides rely on partial acid-hydrolysis of TEMPO-oxidized arabinoxylans (AXs) in particular, and on periodate oxidation of polysaccharides in general with and/or without a subsequent thermal treatment.

Chapter 2 describes a method to selectively oxidize the arabinose (Ara) side chains of a wheat AX into its uronic acid form (arabinuronic acid - AraA) to create an arabinuronoxylan with increased resistance to acid hydrolysis. In addition, this selective oxidation of Ara was performed to create an arabinuronoxylan with a xylan backbone with a substitution pattern closely related to the parental AX. This method consisted of the TEMPO/NaClO₂/NaOCl oxidation of AXs using various TEMPO:NaClO₂:NaOCl ratios. The most suitable reaction condition yielded a high molecular weight TEMPO-oxidized AX with minimal xylan backbone degradation and comprising AraA side chains, as proven by 1D- and 2D-NMR. Although accurate AraA quantification was not attained in this PhD research, glycosidic linkage analysis of the TEMPO-oxidized AX under the most ideal TEMPO-oxidation condition showed that the xylan backbone was mainly single-substituted at position *O*-3 of the xylose (Xyl) (> 75%), similarly to the parental AX. These results indicated that TEMPO-oxidation of AXs creates an arabinuronoxylan mostly resembling its parental AX.

The most suitable TEMPO:NaClO₂:NaOCl oxidation condition found for wheat AX (**Chapter 2**) was further used to oxidize three structurally different AXs, as described in **Chapter 3**. The resulting TEMPO-oxidized AXs were subjected to partial acid-hydrolysis to obtain oligosaccharides. A UHPLC-PGC-MS method was developed to analyze the oligosaccharides released, which allowed us to separate and identify various arabinurono-xylo-oligomer alditol (AUXOS-A) isomers with degree of polymerization between 2 and 5, comprising one and two AraA residues located at different positions of the Xyl residue(s). Successful separation of isomeric AUXOS-A resulted in UHPLC-PGC-MS profiles of AUXOS-A that were AX structure-dependent. This was a remarkable finding as it enabled recognition of different AXs by oligosaccharides fingerprinting. Moreover, tandem MS analyses of AUXOS-A highlighted the

main structural differences among the (TEMPO-oxidized) AXs studied. Therefore, TEMPO-oxidation of AXs followed by analysis of the AUXOS-A by UHPLC-PGC-MS was considered to be a promising approach to recognize different AXs and obtain insights into their structures.

Chapter 4 describes the potential of periodate oxidation of plant polysaccharides as a generic polysaccharide depolymerization approach. By testing different NaIO_4 concentrations, reaction temperatures and times, we found that harsher periodate oxidation conditions led to an increased loss of the structural features of the original polysaccharide. Additionally, it was found that oligosaccharides were formed under periodate oxidation conditions that differed per polysaccharide structure. ESI-MS analysis of the oligosaccharides released showed that these oligosaccharides were highly diverse and complex, forming clusters of oxidized oligosaccharides in the mass spectrum, even when samples were only partially oxidized. The structural complexity of these oligosaccharides was highlighted by ESI-MS/MS analysis, unveiling that periodate-oxidized oligosaccharides besides containing dialdehyde sugar units also comprised e.g., hemialdals, remnants of oxidized and non-oxidized sugar units. Importantly, unique clusters of oxidized oligosaccharides were formed per polysaccharide structure, which was reflected in polysaccharide-specific (ESI-)MS oligosaccharide profiles.

A single periodate oxidation condition could not be found to depolymerize all plant polysaccharides investigated in **Chapter 4**. Hence, the mildest periodate oxidation condition tested was selected to oxidize a wider range of plant polysaccharides and mixes thereof to create partially periodate-oxidized polysaccharides keeping most of structural features of the original polysaccharide (**Chapter 5**). These periodate-oxidized samples were further subjected to a thermal hydrolysis. By doing this, a single approach to depolymerize a wide range of plant polysaccharides and mixes thereof to oligosaccharides could be found. MALDI-TOF MS oligosaccharide profiles that were polysaccharide structure-dependent were obtained (**Chapter 5**), which allowed us not only to distinguish polysaccharides from different classes, e.g. xylans and glucans, but also within the same class, e.g. arabinan and homogalacturonan, and the same type of polysaccharide but from different sources, e.g. wheat and rye AXs. Moreover, based on the MALDI-TOF MS oligosaccharide profiles and on statistical analysis of the MALDI-TOF MS data, it was possible to recognize different polysaccharides when analyzed alone and when present in a complex mix of polysaccharides. These results highlighted that periodate oxidation of plant polysaccharides followed by a thermal hydrolysis is a promising approach to recognize polysaccharides in a faster and more generic manner than by using enzymes.

The PS depolymerization methods investigated in this PhD thesis, especially the TEMPO-oxidation of AXs and the thermal depolymerization of plant polysaccharides bring us a step closer in reaching a generic recognition of AXs and plant polysaccharides, respectively, by oligosaccharides fingerprinting. This is of high interest for food industry to study the polysaccharides composition of a food product more quickly. In **Chapter 6**, the main findings of this PhD thesis are discussed and reflected upon, as are the remaining challenges faced in this thesis and promising approaches to solve them. Additionally, the chemical depolymerization methods presented in this thesis are compared and discussed against the traditional enzymatic depolymerization approach used frequently, and against other recent non-enzymatic polysaccharide depolymerization approaches. Future perspectives on the application of the polysaccharide depolymerization methods developed in this PhD thesis on other polysaccharides



and on extracted polysaccharide fractions from food matrices are discussed. Lastly, the potential exploitation of the oxidized polysaccharides obtained in this PhD thesis is put into perspective.

Os polissacarídeos de plantas são uma das biomacromoléculas mais abundantes encontradas na natureza e são frequentemente usados em alimentos. Estes polissacarídeos têm interesse para a indústria alimentar porque podem ser adicionados a alimentos para modular as propriedades físicas de produtos alimentares e/ou como fibras dietéticas para fornecer benefícios para a saúde. Estas funcionalidades dos polissacarídeos são extremamente dependentes das suas estruturas químicas. Contudo, caracterização e/ou reconhecimento de polissacarídeos de uma forma rápida e genérica é ainda desafiante devido à elevada diversidade e complexidade dos polissacarídeos.

A características químicas dos polissacarídeos de plantas, assim como os métodos tradicionais usados para caracterizar as suas estruturas químicas são descritos no **primeiro capítulo** desta tese. O **Capítulo 1** também descreve a tradicional abordagem enzimática para despolimerizar polissacarídeos em oligossacarídeos diagnósticos que são adequados para caracterizar a estrutura dos polissacarídeos. Devido à especificidade da enzima para cada polissacarídeo, a digestão de polissacarídeos com enzimas não é uma abordagem adequada para obter oligossacarídeos de uma forma genérica para caracterizar a estrutura dos polissacarídeos. Com vista a encontrar um método de despolimerização de polissacarídeos que nos permite despolimerizar polissacarídeos em oligossacarídeos genericamente, várias abordagens de despolimerização de polissacarídeos com base em reações químicas reportadas na literatura são discutidas em detalhe no **Capítulo 1**. Com base na literatura discutida, as abordagens químicas mais promissoras para formar oligossacarídeos contendo informação estrutural dos polissacarídeos que permitam reconhecimento e/ou caracterização estrutural dos polissacarídeos são baseadas na hidrólise parcial ácida de arabinoxilanas (AXs) oxidadas com TEMPO em particular, e na oxidação de polissacarídeos com periodato em geral com e/ou sem um tratamento térmico subsequente.

O **Capítulo 2** descreve um método para seletivamente oxidar as cadeias laterais de arabinose (Ara) de uma AX de aveia no seu correspondente ácido urónico (ácido arabinurónico – AraA) para criar uma arabinuronoxilana mais resistente à hidrólise ácida. Adicionalmente, a oxidação seletiva de Ara foi feita para criar uma arabinuronoxilana com uma cadeia principal de xilana contendo um padrão de substituição intimamente relacionado com a AX nativa. Este método consistiu na oxidação de AXs usando várias proporções de TEMPO/NaClO₂/NaOCl. A condição da reação de oxidação mais adequada originou uma AX oxidada com TEMPO contendo um elevado peso molecular com degradação mínima da cadeia principal de xilana e contendo cadeias laterais de AraA, o que foi provado com 1D- and 2D-NMR. Embora quantificação precisa de AraA não foi conseguida nesta pesquisa de doutoramento, a análise de ligações glicosídicas da AX oxidada com TEMPO usando a condição mais adequada da oxidação com TEMPO mostrou que a cadeia principal de xilana foi principalmente mono-substituída na posição O-3 da xilose (Xyl) (> 75%), semelhantemente à AX original. Estes resultados indicam que a oxidação de AXs com TEMPO cria uma arabinuronoxilana parecida à sua AX nativa.

A condição mais adequada da oxidação usando TEMPO/NaClO₂/NaOCl encontrada para a AX de aveia (**Capítulo 2**) foi posteriormente usada para oxidar três AXs estruturalmente diferentes, o que é descrito no **Capítulo 3**. As AXs resultantes da oxidação com TEMPO foram sujeitas a hidrólise parcial ácida para obter oligossacarídeos. Para analisar os oligossacarídeos formados foi desenvolvido um método usando UHPLC-PGC-MS, o qual nos permitiu separar e identificar vários isómeros de arabinurono-xilo-oligómero alditols (AUXOS-A) com um grau de

polimerização entre 2 e 5, contendo um e dois resíduos de AraA localizados em posições diferentes das unidades de Xyl. A boa separação dos isômeros de AUXOS-A resultou em perfis de UHPLC-PGC-MS de AUXOS-A que foram dependentes da estrutura de cada AX. Isto foi uma descoberta notável porque permitiu reconhecer AXs diferentes através fingerprinting de oligossacarídeos. Além disso, as análises de AUXOS-A usando tandem MS realçou as principais diferenças estruturais entre as AXs estudadas oxidadas com TEMPO. Portanto, a oxidação de AXs com TEMPO seguido da análise dos AUXOS-A com UHPLC-PGC-MS pode ser considerado uma abordagem promissora para reconhecer AXs diferentes e obter conhecimento das suas estruturas.

O **Capítulo 4** descreve o potencial da oxidação de polissacarídeos de plantas com periodato como uma abordagem de despolimerização de polissacarídeos genérica. Várias concentrações de NaIO₄, temperaturas e tempos de reação foram testadas. Com base nisto, foi verificado que condições mais drásticas de oxidação com periodato promovem a perda de características estruturais do polissacarídeo original. Adicionalmente, foi verificado que os oligossacarídeos foram obtidos sobre condições de oxidação que diferiram por cada polissacarídeo. Análises dos oligossacarídeos formados usando ESI-MS mostrou que os oligossacarídeos eram extremamente diversos e complexos, formando grupos de oligossacarídeos oxidados no espectro de massa, mesmo quando as amostras foram apenas oxidadas parcialmente. A complexidade estrutural destes oligossacarídeos foi verificada através de análises usando ESI-MS/MS, o que revelou que estes oligossacarídeos além de conterem unidades de açúcar na forma de dialdeídos também tinham e.g., hemialdais, “pedaços” de unidades de açúcares oxidados e não oxidados. É importante referir que grupos de oligossacarídeos únicos foram formados por cada polissacarídeo, o que foi refletido em perfis de (ESI-)MS de oligossacarídeos que eram específicos de cada polissacarídeo.

Uma única condição de oxidação com periodato não foi encontrada para despolimerizar todos os polissacarídeos de plantas investigados no **Capítulo 4**. Consequentemente, a condição de oxidação com periodato mais suave testada foi selecionada para oxidar uma gama mais abrangente de polissacarídeos de plantas e misturas destes para criar polissacarídeos parcialmente oxidados mantendo a maioria das características estruturais do polissacarídeo original (**Capítulo 5**). Estas amostras de polissacarídeos oxidados foram posteriormente sujeitas a uma hidrólise térmica. Através deste tratamento, foi possível encontrar-se uma única abordagem de despolimerização comum a uma ampla gama de polissacarídeos de plantas. Os perfis de oligossacarídeos gerados com MALDI-TOF MS foram dependentes da estrutura de cada polissacarídeo (**Capítulo 5**), isto permitiu-nos não só distinguir polissacarídeos de diferentes classes, e.g. xilans e glucanas, mas também dentro da mesma classe, e.g. arabinana e homogalacturononana, e o mesmo tipo de polissacarídeo, mas derivado de fontes diferentes, e.g. AXs de aveia e centeio. Além disso, com base nos perfis de oligossacarídeos de MALDI-TOF MS e na análise estatística dos dados obtidos com MALDI-TOF MS foi possível reconhecer polissacarídeos diferentes quando analisados sozinhos e quando presentes numa mistura complexa de polissacarídeos. Estes resultados destacaram que a oxidação de polissacarídeos de plantas com periodato seguida de um tratamento térmico é uma abordagem promissora para reconhecer polissacarídeos de uma forma mais rápida e genérica do que usando enzimas.

Os métodos de despolimerização de polissacarídeos investigados nesta tese de doutoramento, especialmente a oxidação de AXs usando TEMPO e a despolimerização de polissacarídeos de plantas usando uma despolimerização térmica trazem-nos um passo mais perto



de alcançar um reconhecimento genérico de AXs e de polissacarídeos de plantas, respetivamente, através de fingerprinting de oligossacarídeos. Isto é altamente relevante para a indústria alimentar com vista a estudar a composição em polissacarídeos de um produto alimentar mais rapidamente. No **Capítulo 6**, as principais descobertas desta tese de doutoramento são discutidas e refletidas, assim como desafios que perduraram ao longo desta tese e possíveis abordagens para resolver estes desafios. Adicionalmente, os métodos de despolimerização químicos apresentados nesta tese são comparados e discutidos contra a tradicional abordagem de despolimerização de polissacarídeos usando enzimas e contra outras abordagens de despolimerização de polissacarídeos que não são baseadas no uso de enzimas. Perspetivas futuras sobre a aplicação dos métodos de despolimerização de polissacarídeos desenvolvidos nesta tese de doutoramento noutros polissacarídeos e em frações de polissacarídeos extraídas de produtos alimentares são discutidas. Por fim, a potencial exploração dos polissacarídeos oxidados nesta tese de doutoramento é colocada em perspetiva.

Acknowledgements



And in a blink of the eyes, four years have just passed. In these four years, I have had the opportunity to get to know so many people that supported me and accompanied me during this PhD journey. Without them, this PhD thesis would not have come together. Therefore, I would like to express my gratitude and acknowledge all the people that contribute to make this work possible.

(PT: E num piscar de olhos quatro anos se passaram. Ao longo destes quatro anos tive a oportunidade de conhecer tantas pessoas que me apoiaram e acompanharam ao longo desta jornada de doutoramento. Sem estas pessoas este doutoramento não teria dado certo. Portanto, eu gostaria de expressar a minha gratidão e reconhecer todas as pessoas que de certa forma contribuíram para tornar este trabalho possível.)

Henk, thank you for giving me the opportunity to engage in a challenge that turned out to be extremely enriching. Thank you for your critical view on my work, and above all, thank you for all the wisdom that you shared with me. I must also thank you for your patience while reading my very long manuscripts, which in the end were almost half the length without losing a bit 😊 I really had a good supervisor! Henk, thank you for all your support during this PhD journey!

This work would not have been possible without our collaboration with Unilever. **Yvonne**, special thanks for all your support, guidance, and integration at FCH, especially in the first year of my PhD. It was essential for my development. I also want to thank you for all the feedback and discussions that we had about my (our) project. Special thanks also to **Hans-Gerd** for the (co-) supervision. Hans-Gerd, you really helped me to narrow down my thoughts and to see things in a more positive manner. I really appreciated your critical view on my results and writing, and I also enjoyed very much our fruitful discussions during our meetings. **Hans-Gerd, Yvonne, and Henk**, the three of you really made my project to step forward. Dank u wel!

I would also like to thank all the members from the TNI group (Sylvia, Donny, Carla, Marie, Jean-Paul, Peter W., John Duynhoven, Peter Haring, John Chapman, and Jan-Willem Sanders) for the useful meetings and insights. It is always nice to have an opinion coming from someone outside our field, specially from a company's point of view. Especial thanks to **Donny** for all your support during my NMR experiments!

Jos Hageman, thank you for your contribution to my chemometric experiments, as well as for being always available to answer my questions and to share your statistical knowledge.

I also need to acknowledge my BSc (**Hanna and Wouter**) and MSc (**Sofia, Meijing, Max, and Luuk**) students for their contribution to the development of my work. I really enjoyed working in a team to solve a challenge. Thank you!

FCH staff & colleagues

Jolanda, there are no words to thank you, you are just there for everything. Even when we think that something does not have a solution, you find one! Thanks a lot for all your patience in dealing with all the (annoying) bureaucracies.

Jean-Paul, Henk, Mirjam, Willem, Marie, Peter, Julia, Wouter, Carla, and Roelant, thanks for teaching, supervising, and taking care, in such a beautiful way, of all the BSc, MSc, PhD, and Post-docs that have the opportunity to pass by FCH! I would also like to thank you for



all the useful and nice feedback on my work throughout the past years. A particular thank you to **Jean-Paul**, who has been carrying a great work as Chair of the FCH group!

Edwin, many thanks for all the nice and interesting discussions about MS, you really were of enormous help with MS! **René**, I could not have asked for a nicer lab head (sorry to the other technicians 😊), you were always there when needed and even when not needed, you were tireless! **Margaret**, your support with all the HPLC systems was amazing, I really learnt a lot from you! **Peter**, I could not thank you more for all the help with my (few) GC analyses, and especially with the filling up the nitrogen tank, thank you! **Mark**, your help with the UHPLC systems while I was a supervisor of it really gave me some insights about the machine, thank you! Talking about UHPLC systems, I also must thank **Sylvia**, **Roelant**, **Wouter**, **Sarah**, **Madelon**, and **Judith** for being of help when I had to do some troubleshooting! **Wouter** and **Giovanni**, I did not interact much with the two of you, but as you contribute for the good function of FCH, you do contribute for my work as well, thank you!

Thank you also to all the **carbohydrate/C₆O₇ members** (Henk, Mirjam, Willem, Margaret, Edwin, Peter, Melliana, Suzanne, Bianca, Christianne, Moheb, Matthias, Eva, Madelon, Peicheng, Dimitris, Gijs, Katharina, Cynthia, Romy, Krishna, Anne, Jan Willem, Caifang, Carol, Bram, Luis, Pim, and Theo) for all the nice discussions and input on my work.

I would like to thank to all my **officemates** Tibo, Hugo, Fangjie, Judith, Jianli, Caifang, Pim, Matthijs, and Abel for the nice work environment that we always had. I would particularly like to thank **Judith** for being such a wonderful buddy in the office and in the lab during basically my entire PhD journey. Judith, thanks for all the talks, laughs, help, support, for some gossiping, and for being such a good listener. Unburdening with you some of my PhD frustrations/challenges/sorrows/achievements/... was very much appreciated! Without you, my PhD would not have been the same. For me, you are an incredible scientist and person. You are extremely well-organized, motivated, and always ready for a new adventure. Undoubtedly, there is a great future waiting for you after your PhD. Thanks again for everything, Judith!

Talking about mates, it is time to also thank my **labmates** René, Maud, Yuxi, Claire, Judith, Gijs, Tibo, Madelon, and more recently Luana and Abel, for creating a very nice and fun atmosphere in the lab, especially during the great “Guilty pleasure” hour. Also, thanks for being so tidy 😊

I am getting to the point that names are going to get lost, therefore, to not hurt any feelings, I want to in general thank **all FCH’s colleagues**. Without you, working at FCH would have been much less pleasant. I would like to express my gratitude to all the **FCH activity committees** for always having so nice ideas and making FCH more interactive. Especially during Covid times, you guys were extremely active and never left FCH disintegrate. Thanks to you, FCH is always very unite! I also want to thank the **PhD trip committees** for organizing a nice trip to Italy and Vienna, and even during Covid times, to have managed to organize a memorable PhD trip in the Netherlands!

Andrji, **Ellen**, **Sibrean**, **Fred**, **Jorick** and **Seville**, thanks for always welcoming me in your “crew” in such a joyful manner.

Sylvia, I have to thank you for your help with the thesis formatting and for letting me annoy you so many times. Thanks a lot!



Matthias, thank you for all the help and knowledge transmitted to me during my PhD. More importantly, I want to thank you for all the talks, coffee walks, laughs, and so many funny moments during my PhD. You really were a great colleague inside and outside work, and you are now a friend for life!

Natalia, I must have a word to you, “retarded”, kidding!! Natalia, I want to thank you for step by step reaching out to me and entering in my life. You certainly helped me in this journey with all the chocolates, the laughs, the talks, and the help with equipment. Thank you!

Madelon and **Eva**, thanks for all the nice talks, laughs, dinners, and more importantly for all the gossiping. We really could keep each other updated 😊

Dear paranympths Madelon and **Alice**, thank you so much for sitting next to me in one of the most important days of my life! Thank you for all the care and support!

Beloved ones / Essenciais

Alice, thank you so much for all the four years that we have lived together. You really were a pillar of support for me. You made my end of the afternoons, evenings, and weekends much more pleasant. I never felt alone in the Netherlands thanks to you! Without you, this journey would have had way more downs. You really helped me to enjoy every single up as if it would have been the last. Those ups were always extremely energizing. Alice, I do not have words to express all my gratitude to you. Grazie amore mio!

Cláudia, não poderia não ter uma palavra para si, é a minha primeira mãe científica. O meu gosto por polissacarídeos foi-me transmitido por si e pelo Prof. Manuel António. Graças a vocês adquiri o conhecimento básico (e bem mais do que o básico) sobre polissacarídeos, e tive a oportunidade de ingressar neste doutoramento (louco 😊). Muito obrigada Cláudia por me ter dado suporte e confiança para ingressar neste doutoramento, o qual não só me deu a oportunidade de crescer como cientista, mas também como pessoa. Obrigada!

Rita, Cris, Catarina, Sofia, Catarina, João, Joana, Élia, Pedro, Calados, Ana, Marco, Sofia, Lisandra, Lino, Lara e Tânia, todos vocês são amigos para o resto da vida. Mesmo longe, vocês conseguem dar suporte. Quando perto, fazem-me esquecer todos os problemas. Convosco não consigo não deixar de sorrir e ser uma pessoa feliz. Vocês realmente são e sempre serão essenciais. Sem vocês esta jornada teria sido intolerável. De quem vos ama, obrigada!

Mã, Pai, Nanã, Vó e Vô, como sempre me ensinaram, primeiro as obrigações e depois o lazer e diversão. Isto é o que tenho sempre tentado aplicar na minha vida. Este trabalho é o reflexo disso mesmo, muito trabalho que só pôde ser concretizado com momentos de lazer e amor dados por vocês! Sei que não vos foi (e é) fácil ter-me visto sair de Portugal para trabalhar. Contudo, vocês nunca se impuseram e deram-me muito apoio. Não podia estar mais grata por isso. Vocês foram e sempre serão o pilar mais importante da minha vida estejam perto ou longe de mim. Por isso, este trabalho é sem dúvida dedicado a vocês. Amo-vos, cada dia um pouco mais!

Huguinho, sei que esperas um agradecimento da minha parte, mas penso que te tenho vindo a agradecer todos os dias um bocadinho mais e mais ao longo destes 4 anos. O meu agradecimento pelo teu apoio e amor não cabe nestas páginas. Espero que o meu agradecimento por ti possa continuar a crescer cada dia mais e mais para o resto da minha vida e que isso possa ser demonstrado com carinho, resiliência e harmonia. De quem te ama, obrigada!

About the author



Curriculum vitae

Carolina Pandeirada was born on October 21st, 1993 in Aveiro, Portugal. After graduating from high school (Escola Secundária Dr. Mário Sacramento, Aveiro, Portugal) in 2012, she started her bachelor in Biochemistry at the University of Aveiro (Portugal). Her bachelor study was completed with a thesis on the *biochemical characterization of two marine microalgae, Isochrysis galbana and Phaeodactylum tricorutum*, within the Laboratory of Food Biochemistry. In 2015, she started her master in Food Biochemistry at the University of Aveiro. Her master thesis was performed at the Laboratory of Food Biochemistry at the University of Aveiro in collaboration with the NOVA School of Science and Technology (Lisbon), within the Glycolab and X-tal groups. Her MSc thesis focused on the *Characterization of carbohydrates from Nannochloropsis oculata and their use in microarrays*. In 2017, she obtained her MSc degree in Food Biochemistry with the distinction of “Best student” on her master’s degree. In 2017, she started as PhD candidate at the Laboratory of Food Chemistry under the supervision of Prof. Dr H.A. Schols, in a cooperative project with Unilever called ‘Tapping into Nature’s Ingenuity (TNI)’. The results of her PhD research are presented in this thesis. Carolina continues to work at the Laboratory of Food Chemistry as a postdoctoral researcher.



Contact: copand93@hotmail.com



List of publications

This thesis:

Pandeirada, C.O., M. Achterweust, H.-G. Janssen, Y. Westphal, and H.A. Schols. Periodate oxidation of plant polysaccharides provides polysaccharide-specific oligosaccharides. *Carbohydrate Polymers*. **2022**, 291, 119540.

Pandeirada, C.O., S. Speranza, E. Bakx, Y. Westphal, H.-G. Janssen, and H.A. Schols. Partial acid-hydrolysis of TEMPO-oxidized arabinoxylans generates arabinoxylan-structure resembling oligosaccharides. *Carbohydrate Polymers*. **2022**, 276, 118795.

Pandeirada, C.O., D.W.H. Merckx, H.-G. Janssen, Y. Westphal, and H.A. Schols. TEMPO/NaClO₂/NaOCl oxidation of arabinoxylans. *Carbohydrate Polymers*. **2021**, 259, 117781.

Other publications:

Mota, R., R. Vidal, **C. Pandeirada**, C. Flores, A. Adessi, R. De Philippis, C. Nunes, M.A. Coimbra, and P. Tamagnini. Cyanoflan: a cyanobacterial sulfated carbohydrate polymer with emulsifying properties. *Carbohydrate Polymers*. **2020**. 115525.

Pandeirada, C.O., É. Maricato, S.S. Ferreira, V.G. Correia, B.A. Pinheiro, D.V. Evtuguin, A.S. Palma, A. Correia, M. Vilanova, M.A. Coimbra, and C. Nunes. Structural analysis and potential immunostimulatory activity of *Nannochloropsis oculata* polysaccharides. *Carbohydrate Polymers*. **2019**, 222, 114962.



Overview of completed training activities

Discipline specific activities

Courses

Summer Course Glycosciences ^a	VLAG, Wageningen, 2018
Advanced Food Analysis ^a	VLAG, Wageningen, 2019

Conferences and meetings

6 th EPNOE ^b	UA, Aveiro (Portugal), 2019
Chains 2020 ^a	NWO, online, 2020
CCC Spring Symposium	CCC, online, 2021
7 th EPNOE ^b	INRAE, Nantes (France), 2021
23 th International Conference on Carbohydrate 2021 ^b	IRC, online, 2021

General Courses

41 st VLAG PhD week	VLAG, Baarlo, 2018
Supervising BSc and MSc thesis students	WUR Education Support, Wageningen, 2018
Information Literacy including EndNote Introduction	WUR Library, Wageningen, 2018
14 th Philosophy and Ethics of Food Science and Technology	WGS, Wageningen, 2019
Project and Time management	VLAG, Wageningen, 2019
The Essentials of Scientific Writing and Presenting	WGS, Wageningen, 2019
Chromleon 7 CDS User Days	ThermoFisher Scientific, Breda, 2019
Career orientation	WGS, Wageningen, 2021

Optional Courses and Activities

Preparation of research proposal	FCH, Wageningen, 2018
PhD Study Trip 2018 ^{a,b}	FCH, Italy and Austria, 2018
PhD Study Trip 2021 ^{a,b}	FCH, The Netherlands, 2021
BSc/MSc thesis students supervision, presentations, and colloquia	FCH, Wageningen, 2017-2021
PhD presentations	FCH, Wageningen, 2017-2021
TNI Project meetings	FCH/Unilever, Wageningen/Vlaardinggen, 2017-2021

^aPoster presentation, ^bOral presentation.

Abbreviations: VLAG, Graduate School for Advanced studies in Food Technology, Agrobiotechnology, Nutrition and Health Sciences; UA, University of Aveiro; NWO, Dutch Research Council; CCC, Carbohydrate Competence Center; INRAE, French National Research Institute for Agriculture, Food and Environment; IRC, International Research Conference; WUR, Wageningen University and Research; WGS, Wageningen Graduate School; FCH, Food Chemistry; TNI, Tapping into Nature's Ingenuity.

The research described in this thesis was performed at the Laboratory of Food Chemistry, Wageningen University & Research, the Netherlands.

Funding for this work was (partly) provided by Unilever's global Foods Innovation Centre in Wageningen, the Netherlands. This work was part of the project Tapping into Nature's Ingenuity (TNI).

Financial support from Wageningen University for printing this thesis is gratefully acknowledged.

Cover design by Carolina Correia

Printed by ProefschriftMaken, the Netherlands

Edition: 170 copies

Carolina O. Pandeirada, 2022

